Genetics of Relapse and Treatment Resistance in Multiple Myeloma

James Croft
Institute of Cancer Research

Thesis submitted to the University of London for the Degree of Doctor of Medicine (Research)

2021

Declaration

This thesis is submitted for consideration of the degree of MD(Res) at The University of London. It is all my own work except where stated in the text. Part of this work has been published, but has not been previously submitted for a degree at this or any other institution.

Dr James Croft Date 01/12/2021

Publications

The following manuscript came from work presented in this thesis:

Croft, J., Ellis, S., Sherborne, A.L. et al. Copy number evolution and its relationship with patient outcome—an analysis of 178 matched presentation-relapse tumor pairs from the Myeloma XI trial. Leukemia 35, 2043–2053 (2021). https://doi.org/10.1038/s41375-020-01096-y

Acknowledgments

I would like to start by thanking Ralph Stockwell, his generous donation to the ICR helped fund this research. I am extremely grateful for his support and hope this project fulfils his expectations.

This project would not have been possible without the tireless work of the ICR myeloma biobank team. In particular Amy Sherborne, Sidra Ellis, Amy Price and Kim Sharp who completed all wet laboratory work, I will be forever grateful.

Finally I would like to thank Martin Kaiser. He has been incredibly supportive throughout this project, showing me patience to kindness. He has taught me a great deal and had an extremely positive influence on my career as a haematologist.

Abstract

Better understanding of the mechanisms of relapse and treatment resistance in myeloma could improve clinical outcomes. Copy number aberrations (CNA) are a major feature of multiple myeloma, however their evolution over time in the context of modern biological therapy is not well characterised. To investigate acquisition of CNA and their prognostic relevance in the context of first-line therapy, I have profiled paired tumour samples at diagnosis–relapse from NCRI Myeloma XI (ISRCTN49407852) trial patients using digital multiplex ligation-dependent probe amplification. To facilitate identification of driver genes and molecular pathways associated with CNA evolution at relapse, sequential gene expression profiles were also analysed using the affymetrix HGU133 plus 2.0 array.

CNA profiles acquired at relapse differed substantially between myeloma subtypes: hyperdiploid (HRD) tumors evolved predominantly in branching pattern vs. linear pattern in t(4;14) vs. stable pattern in t(11;14). CNA acquisition also differed between subtypes based on cyclin D expression, with a marked enrichment of acquired del(17p) in *CCND2* over *CCND1* tumors. Acquired CNA were not influenced by high-dose melphalan or lenalidomide maintenance randomisation. A branching evolution pattern was associated with a significantly inferior overall survival. Acquisition of gain(1q) at relapse was the most common new CNA to evolve at relapse and associated with significantly shorter OS, independent of other risk factors or time of relapse.

High risk signatures increased at relapse in the majority of tumours. Gene set enrichment analysis highlighted mechanisms of tumour proliferation and leading edge analysis highlighted the role of XPO1 inhibition in treating relapsed myeloma. No significant gene set enrichment at relapse in relation to high-dose melphalan or lenalidomide maintenance randomization was identified.

There is an increasing need for rational therapy sequencing in myeloma. This data supports the value of repeat molecular profiling to characterise disease evolution and inform management of relapsing myeloma.

Contents

Figures

Tables

Chapter 1: Introduction

1.1 Multiple Myeloma

1.1.1 Epidemiology

Multiple myeloma is a malignant condition of plasma cells. There are approximately 6000 new cases diagnosed per year in the UK, accounting for 2% of all new cancer diagnoses. Incidence increases with age, median age at diagnosis is 72 years in Europe[1]. While survival has improved in the last 40 years myeloma remains incurable, with a median survival 5-10 years[2].

1.1.2 Clinical features

Myeloma is characterised by the malignant proliferation of plasma cells in the bone marrow which results in the clonal production of immunoglobulin (Ig); manifesting as paraprotein and free light chains in the serum and urine. The direct effect of plasma cell proliferation within the bone marrow leads to cytopenias, bone lysis with hypercalcaemia and immunosuppression. Paraprotein and free light chain production also causes end organ damage, a common example being renal failure. The International Myeloma Working Group (IMWG) specifies clinical features that are considered to be myeloma defining events **Table 1-1**[3].

End organ damage associated with PC proliferation	
Hypercalcaemia	• Serum calcium >2.75mmol/L
Renal insufficiency	• Creatinine clearance <40ml/min or • Creatinine >177umol/L
Anaemia	• Hb >20g/L below lower limit of normal or • Hb <100g/L
Bone Lesions	• ≥1osteolytic lesion
Biomarkers of malignancy associated with PC proliferation	
Clonal bone marrow PC	• ≥60%
Involved:uninvolved SFLC ratio	• ≥100
Focal bone lesion on MRI	• >1

Table 1-1 Myeloma defining events as per the International Myeloma Working Group (IMWG) [3]. PC: plasma cell; SFLC: serum free light chain; MRI: magnetic resonance imaging.

1.1.3 Pre-clinical stages

Plasma cell proliferation constitutes a spectrum of disorders defined by their abundance within the bone marrow bone marrow and presence or absence of clinical symptoms (**Table 1-2, Figure 1-1)**. Hence myeloma is always preceded by monoclonal gammanopathy of unknown significance (MGUS)[4]; affecting 3% of people over 50 years of age, the risk of progression to myeloma is 1% per year. A small proportion of MGUS will progress to asymptomatic myeloma where risk of progression increases to 10% per year for the first 5 years, interestingly this rate then becomes lower; similar to that of MGUS [3-5]. Both conditions are defined by lack of clinical symptoms and as a consequence many patients are diagnosed after these stages. At present there is not enough evidence to support treatment prior to transformation into symptomatic myeloma; both are currently managed with active surveillance.

1.1.4 Pathophysiology

The fundamental principle in the development of myeloma is the accumulation of multiple genetic aberrations which dysregulate pathways of plasma cell biology. Examination of normal plasma cell development in conjunction with genetic aberrations observed in myeloma has provided insight into pathophysiology of the disease.

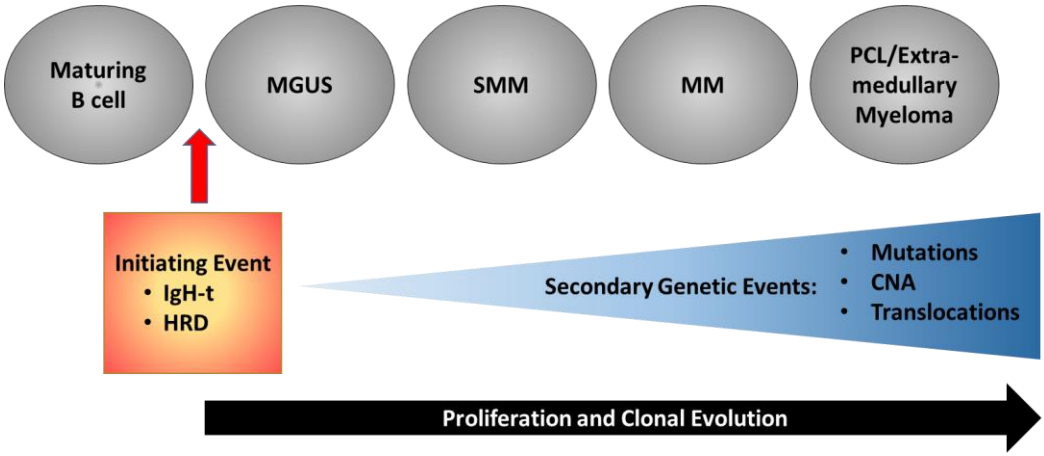

Figure 1-1 Stages of plasma cell dyscrasia; MGUS: monoclonal gammanopathy of unknown significance; SMM: smouldering myeloma; MM: multiple myeloma; PCL: plasma cell leukaemia; IgH-t: IgH translocation; HRD: Hyperdiploid; CNA: copy number aberration.

Disorder	Definition
Non IgM MGUS	All criteria must be met: • Paraprotein < 30 g/L • Clonal bone marrow PC <10% • Absence of PC associated end organ damage
Light chain MGUS	All criteria must be met: • Abnormal SFLC ratio (<0.26 or >1.65) • No immunoglobulin heavy chain expression on immunofixation • Absence of PC associated end organ damage • Clonal bone marrow PC <10% • Urinary BJP <500mg/24hr
Asymptomatic or smouldering myeloma	• PP >30g/L or • Urinary BJP ≥500mg/24hr or • Clonal bone marrow PC >10% AND • Absence of PC associated end organ damage
Multiple myeloma	Both criteria must be met: • Clonal bone marrow PC ≥10% or biopsy proven bony or extra medullary plasmacytoma • Any one or more myeloma defining event (Table1-1)

Table 1-2 Disorders associated with plasma cell proliferation. Table modified from Rajkumar 2018 [6]. MGUS: monoclonal gammanopathy of unknown significance; PC: plasma cell; PP: paraprotein; BJP: Bence-Jones protein.

1.1.4.1 Normal Plasma cell biology

Plasma cells are terminally differentiated B-lymphocytes that secrete Ig that act as antibodies for recognition of pathogens, playing an integral role in the body's humoral immune system. In order to produce diverse antibodies with high affinity, plasma cells undertake multiple stages of DNA rearrangement, providing ample opportunity for the introduction of genetic aberrations [7, 8].

Starting life in the bone marrow B cells undergo rearrangement of Ig genes, in a process termed VD(J) recombination, to create a functional B cell receptor precursor [8, 9]. They then leave the bone marrow as virgin B cells where they can be activated by their cognate antigen. At this point the B cell can differentiate into a low affinity IgM /IgD secreting PC or migrate to the lymph node germinal centre for affinity maturation [9]. Within the germinal centre, B cell DNA encoding the hypervariable region of the Ig heavy chain (IgH), undergoes somatic hypermutation (SMH) facilitating the production of a highly

specific and avid antibody. This is followed by class switch recombination (CSR) a process involving deletion and recombination of IgH gene switch regions. This results in a change of Ig isotype to increase antibody utility [8, 9]. SHM and CSR are mediated via the expression of activation-induced deaminase (AID) which generates double strand DNA breaks to allow rearrangement. When these breaks are repaired they can be aberrantly joined to double stranded DNA breaks elsewhere in the genome causing the formation of chromosomal translocation involving the IgH gene on chromosome 14. Through double strand DNA breaks, AID has also been shown to cause mutations and translocations in other areas of the plasma cell genome [8, 9].

Differentiation into a mature antibody secreting plasma cell requires cell cycle arrest, with downregulation of unnecessary cellular functions to allow upregulation of those involved in Ig production and secretion [8]. The process involves a complex molecular network, disruption of which can lead to malignant transformation. For example failure to arrest the cell cycle would result in uncontrolled proliferation.

On leaving the germinal centre plasma cells migrate to the bone marrow where they either undergo apoptosis or remain as long lived plasma cells to provide serological immune memory. This requires a specialised niche within the bone marrow where PC survival is dependent on cellular interactions of with bone marrow stroma. Malignant plasma cells utilise these cellular interactions obtaining survival advantage over others allowing accumulation within the bone marrow and as a consequence reduction in normal plasma cell populations; resulting in an immuneparesis [8].

1.1.4.2 Myeloma genetics

Like other cancers the molecular landscape of myeloma is heterogeneous. Abnormalities are acquired over time and facilitate proliferation and progression through each stage of the plasma cell dyscrasia spectrum. Examination of MGUS, SMM and myeloma has provided insight into the temporal acquisition of genetic aberrations providing evidence of their hierarchy in pathogenesis [10, 11]. Common genetic events are summarised in **Table1-3.**

	Aberration	**Potential genes involved**	**~Frequency***
Initiating events			
IgH translocation	t(4;14)	*FGFR3/MMSET*	16%
	t(6;14)	*CCND3*	1%
	t(11;14)	*CCND1*	17%
	t(14;16)	*MAF*	4%
	t(14;20)	*MAFB*	1%
CNA	HRD		50%
Secondary events			
Translocation	Involving *MYC*	*MYC*	20%
CNA	gain(1q)	*CKS1B/MCL1/ANP32E*	35%
	gain(6p)		12%
	gain(8q)	*MYC*	4%
	del(1p)	*CDKN2C/FAF1*	10%
	del(12p)	*CD27*	15%
	del(14q)	*TRAF3*	8%
	del(16q)	*CYLD/WWOX*	17%
	del(17p)	*TP53*	9%
	Del(13q)	*DIS3/RB1*	45%
Mutations	MAPK pathway	*KRAS/NRAS/BRAF*	30%
	NF-kB pathway	*CYLD/TRAF3/BIRC2/BIRC3*	20%
	DNA repair pathway	*TP53/ATM/ATR*	10%

Table 1-3: Summary of common genetic aberrations in myeloma. *Approximate frequency in newly diagnosed multiple myeloma. HRD defined as ≥2 trisomies in chromosomes 3,5,7,9,11,15,19 or 21. [7, 8, 11, 12]. CNA; copy number aberration.

1.1.4.2.1 Initiating Events

Genetic aberrations common to and stable throughout all stages of the plasma cell disorders have been termed initiating events, they are thought to be the first aberration to facilitate clonal proliferation of a PC and provide potential for later malignant transformation. They can be divided into two distinct groups; Immunoglobulin heavy chain (IgH) translocations and hyperdiploidy (HRD). They are mutually exclusive in the majority of cases [8, 10, 11].

1.1.4.2.1.1 IgH Translocations

IgH translocations are likely caused by aberrant CSR or SHM as previously discussed in section 1.1.4.1 [7, 8]. Of the IgH translocations, approximately 40% involve 5 recurrent chromosomal partners which hold oncogenes (shown in brackets): 11q13(*CCND1*), 4p16(*FGFR3* and *MMSET*), 16q23(*MAF*), 6p21*(CCND3*) and 20q11(*MAFB*) at frequencies of 17%, 16%, 4%, 1% and 1% respectively [12, 13]. Translocation places the oncogenes close to the strong IgH enhancer region leading to increased expression [7, 8, 11].

1.1.4.2.1.2 Hyperdiploidy (HRD)

The majority of myeloma without IgH translocations are HRD, defined by ≥2 trisomies found in odd chromosomes 3, 5, 7, 9, 11, 15, 19 or 21 [13]. The mechanism leading to HRD remains unknown however it is postulated to result from a single catastrophic event during mitosis [13].

1.1.4.2.2 Secondary Events

Aberrations with increasing prevalence at later stages of the disease spectrum or those unique to symptomatic myeloma are termed secondary or progression events. They provide survival benefit assisting further proliferation and malignant transformation from MGUS [10]. The repertoire of secondary events is diverse including non IgH translocations, copy number aberrations (CNA) and somatic mutations[11].

1.1.4.2.2.1 Translocations

Translocations involving *MYC* occur in 3-4% of MGUS patients and 15-20% of newly diagnosed myeloma, thus clearly demonstrating a secondary genetic event. Partner loci vary but commonly involve IgH, IgL, IgK and non Ig genes

such as *FAM46C*. All lead to overexpression of the *MYC* gene highlighting its role as an oncogene in myeloma [7, 8, 11].

1.1.4.2.2.2 Copy Number Aberration (CNA)

Recurrent CNA are the most common secondary genetic events found in newly diagnosed myeloma highlighting their importance in myeloma pathogenesis. They result in the gain or loss of DNA which can be focal, interstitial or involve the whole chromosomes, as seen in HRD. Common areas of focal deletion highlight potential tumour suppressor genes, loss of which facilitates tumour progression. Conversely common copy number gain results in overexpression of genes, indicating possible oncogenes to drive tumour progression [8, 11]. The most frequently observed CNA are more likely to harbour driver events, for example gain(1q), which occurs in approximately 35% of newly diagnosed patients[7, 8, 11]. While its precise role in oncogenesis has not been identified numerous candidate oncogenes are located here including *CKS1B, ANP32E, MCL1, BCL9* and *PDZK1* [8, 11]. Another example is del(17p) occurring in approximately 10% of newly diagnosed myeloma patients [7, 12]. This CNA involves deletion of the tumour suppressor gene *TP53* which influences cell cycle arrest, DNA repair and apoptosis in response to DNA damage [11]. Deletion and or mutation of this gene is common to many cancers.

1.1.4.2.2.3 Mutations

The average number of non-synonymous mutations in myeloma is intermediate when compared to other cancers [7, 11, 14]. The frequency of recurrently mutated genes is relatively low compared to CNA in myeloma [7]. However convergence of mutations within specific cellular pathways highlights areas of interest. For example mutations within the MAPK pathway are seen in approximately 30% of patients due to mutations of *KRAS, NRAS* and *BRAF* genes. Similarly mutations of the NF-kB pathway occur in approximately 20%; involving *TRAF3, CYLD, BIRC2* and *BIRC3* [11]. Mutations are found to be sub-clonal in the majority of cases highlighting their role as secondary progression events [11]. None have yet been clearly demonstrated to effect prognosis.

1.1.4.2.3 Co-occurrence of genetic events

While I have described a heterogeneous molecular landscape within myeloma, discrete subgroups can be defined by initiating events. This distinction highlights common associations of specific genetic events, for example the co-occurrence of t(4;14) with del(13) and gain(1q) [12]. Frequent patterns of co-occurring aberrations suggests a reciprocal relationship that provides survival benefit for malignant transformation/progression and highlights the differences in disease biology between each subgroup.

Frequent bi-allelic aberrations also signifies a gene's importance in tumour genesis; for example the homozygous deletion or combinations of mutation and heterozygous deletion in tumour suppressor gene *TP53* [8, 15].

Specific genetic events have been associated with worse outcome in myeloma, the co-occurrence of which appears to have a cumulative effect leading to ultra-high risk patients [12]. I will discuss these lesions and their prognosis in more detail in a later section.

1.1.4.2.4 Gene expression

Transcriptome studies have also provided information regarding myeloma pathogenesis. Upregulation of D group cyclins; cyclin D1 (*CCND1*), D2 (*CCND2*) or D3 (*CCND3*) has been identified as a universal characteristic of myeloma [7, 13]. D group cyclins interact with cyclin dependent kinase (*CDK*) 4 and 6 leading to phosphorylation of *RB*. Phosphorylation causes dissociation of *RB* from transcription factor *E2F*, liberating *E2F* from inhibition. Allowing *E2F* to promote transcription of genes required to push the cell through the G1/S cell cycle check point, facilitating plasma cell proliferation [7].

Despite the molecular heterogeneity described earlier, this process of convergent evolution can be linked back to common cytogenetic features described in section 1.1.4.2: *CCND1* is upregulated in t(11;14) and HRD with gain(11), *CCND2* in t(4;14), t(14,16), t(14;20) and HRD without gain(11) and *CCND3* in t(6;14) [7, 12, 13]. Secondary molecular events also play a role, for example gain(1q) and *MYC* translocations cause upregulation of *CKS1B* and *MYC* respectively, which increases the CDK-Cyclin D interaction. Whereas

del(1p) causes down regulation of *CDKN2C* which normally acts to inhibit the activity of CDK-Cyclin D [7].

Expression of D group cyclins was therefore utilised to define subgroups within the Translocation Cyclin-D (TC) GEP classification system. 8 distinct subgroups of myeloma were identified using expression levels of *CCND1, CCND2, CCND3, FGFR3, MMSET, MAF, ITGB7* and *CX3CR1* [13]. This approach is reflected in the design of the Taqman translocation assay used in this project, detailed in section 2.3.

1.1.4.3 Risk stratification

The molecular heterogeneity of myeloma is reflected by varied clinical outcomes despite uniform treatment. Prognosis can be assessed using disease burden, response to treatment and disease biology. Durie-Salmon staging and the international staging system (ISS) (**Table 1-5)** aid evaluation of disease burden[6]. Whereas molecular events help define high risk disease biology; t(4;14), t(14;16), t(14;20), gain(1q), del(17p) and del(1p) are associated with a significantly worse progression free survival (PFS) and overall survival (OS)[7, 12]. Co-occurrence of these high risk lesions also has clinical impact, with more than one hit shown to have significantly worse PFS and OS compared to single hit [12]. Plasma cell leukaemia, defined by the number of plasma cells on peripheral blood, and elevated lactate dehydrogenase (LDH) also reflect high risk disease biology regardless of cytogenetics [6].

Current IMWG consensus advises use of the revised ISS (**Table 1-6)** which incorporates disease burden and biology, of note it only considers high risk lesions t(4;14), t(14;16) and del(17p)[16]. Boyd et al used UK Myeloma IX data to produce a more detailed risk stratification system often used in UK practice **(Table 1-7)**[17]**.** It should also be noted that this scoring system considers newly diagnosed patients and has not been validated at relapse.

Survival data in conjunction with gene expression has also provided opportunity to define high risk signatures that can be used for prognostication. A number of high risk gene expression signatures have been described

including the EMC92, UAMS70, UAMS17, UAMS80, IFM15 and MRCIX6, details can be found in (**Table 1-4)**. Each signature has been produced from different trial cohorts, as a consequence baseline characteristics and anti-myeloma treatments differ. This is reflected by the variation of genes with little or no overlap between signatures. The marked difference suggests each signature may not identify all high risk patients within a given cohort. Currently gene expression prognostic signatures have not been incorporated into routine clinical practice[18]. However the EMC92 signature has now been developed into a commercially available test named MM profiler.

Signature	Number of genes	Trial Cohort	Reference
EMC92	92	HOVON-65/GMG-HD4	[19]
UAMS70	70	UARK 98-026	[20]
UAMS17	17	UARK 98-026	[20]
UAMS80	80	TT3	[21]
IFM15	15	IFM-99	[22]
MRCIX6	6	MRC Myeloma IX	[23]

Table 1-4 High risk gene expression signatures

Stage	Criteria	Median Survival
I	Serum β2m <3.5mg/L and serum albumin ≥35g/L	62 months
II	Neither I or III	45 months
III	Serum β2m ≥5.5mg/L	29 months

Table 1-5 The International Staging System (ISS) for myeloma [24]. β2m: beta2 macroglobulin.

Risk Group	Criteria
R-ISS I	ISS-I, no high risk cytogenetics (del(17p),t(4;14),t(14;16)), normal LDH
R-ISS II	Neither R-ISS-I or III
R-ISS III	ISS-III and 1 or more high risk cytogenetics (del(17p), t(4;14),t(14;16)) or high LDH

Table 1-6 The Revised International Staging System (R-ISS) for myeloma [16]. LDH; lactate dehydrogenase.

Risk Group	Criteria
Standard	None of below
Intermediate	≥1 of t(4;14), t(14;16), t(14;20), del(17p), gain(1q), del(1p) and β2m <5.5mg/L Or Blastic morphology
High	≥1 of t(4;14), t(14;16), t(14;20), del(17p), gain(1q), del(1p) and β2m ≥5.5mg/L
Ultra-high	>1 of t(4;14), t(14;16), t(14;20), del(17p), gain(1q), del(1p) Or GEP high risk Or Plasma cell leukaemia

Table 1-7 Myeloma IX risk stratification [17]. β2m: beta2 macroglobulin; GEP; gene expression profile.

1.1.5 Treatment

The aim of anti-myeloma therapy is to maximise depth of response to maximise progression free survival (PFS) and overall survival (OS), while keeping treatment related toxicity to a minimum. The introduction of immunomodulatory drugs (IMiDs) Thalidomide and Lenalidomide and Proteasome Inhibitor (PI) Bortezomib has improved outcomes in myeloma, in combination with steroids they form the backbone of treatment in the majority of regimes [6].

More recently novel IMiDs, PIs, monoclonal antibodies and a histone deacetylase inhibitors have been approved for use in relapsed MM increasing treatment options for patients. Current, FDA approved, novel anti myeloma drugs are detailed in **Table 1-8,** common regimes used internationally are listed in **Table 1-9.**

1.1.5.1 PI mechanism of action

The ubiquitin-proteasome pathway coordinates the degradation of cellular proteins, it is required for cellular signal transduction, transcription regulation, stress response and control of receptor functions. Bortezomib inhibits the proteasome pathway by binding to the 20S proteasome complex therefore blocking enzyme activity. This causes cell cycle arrest and apoptosis within the highly proliferative myeloma cells [25].

1.1.5.2 IMiD mechanism of action

The anti-myeloma effects of IMiDs include direct PC cytotoxicity, anti-angiogenesis and immune modulation[6]. IMiDs bind to cereblon (CRBN), which acts as a substrate adaptor of the CRL4^{CRBN}E3 ubiquitin ligase complex. The binding of IMiDs leads to the selective ubiquitination and therefore proteasome degradation of PC transcription factors Ikaros *(IKZF1)* and Aiolos (*IKZF3). IKZF1* and *IKZF3* regulate a transcriptional network that is essential for malignant PC survival[26]. For example, reduction in *IKZF3* results in down regulation of interferon regulatory factor 4 (*IRF4). IKZF3* is also known to repress interleukin 2 (*IL2)* expression. Through reduction of *IKZF3,* IMiDs increase interleukin-2 (*IL2)* expression which has been shown to increase

proliferation of natural killer and CD4+ T cells thus contributing to the drugs immune modulatory effects[26].

1.1.5.3 Management of newly diagnosed myeloma

Current UK practice recommends newly diagnosed, transplant eligible, patients to have 4-6 cycles of Bortezomib, Thalidomide and Dexamethasone (VTD) as induction followed by consolidation with high dose melphalan and autologous stem cell rescue. A patient's suitability for transplant is based on performance status, age, comorbidities, previous treatments and disease risk. Based on data recently published from the Myeloma XI trial, patients who receive transplant also have access to low dose lenalidomide maintenance[27]. For patient considered transplant ineligible a number of combination regimes are available and listed in **Table 1-9**.

1.1.5.4 Management of relapsed myeloma

Treatment options for relapsed disease are varied but should largely be determined by previous therapies received, response to said therapies and presence of related side effects. For patients who derived > 18months progression free survival from first transplant, re-induction followed by high dose consolidation and second autologous transplant is currently recommended. NICE has recently approved the use of Daratumamab, Bortezomib and dexamethasone (DVd) at first relapse; this regimen provides the opportunity for ongoing Daratumamab maintenance and therefore current UK practice appears to be changing at first relapse. Possible treatment regimens for relapsed disease are detailed in **Table 1-9.**

1.1.5.5 Management during the COVID pandemic

During the COVID pandemic access to myeloma treatments has temporarily changed in an attempt to minimise patient's exposure to the virus. As a result some information in **Table1-9** may not be up-to-date.

Class	**Drug**
IMiDs	Thalidomide
	Lenalidomide
	Pomalidomide
Proteasome Inhibitor	Bortezomib
	Carfilzomib
	Ixazomib
Monoclonal Antibody	Daratumumab (*CD38*)
	Elotuzumab (*SLAMF7*)
	Isatuximab (*CD38)*
Histone deacetylase inhibitor	Panobinostat
XPO1 inhibitor	Selinexor

Table 1-8 FDA approved novel anti-myeloma drugs. IMiDs: immunomodulatory drugs.

Regime		Available UK (line)
Cyclophosphamide, Thalidomide, Dexamethasone	CTd	Yes (any)
Lenalidomide, Dexamethasone	Rd	Yes (1st in transplant ineligible)
Bortezomib, Melphalan, Prednisolone	VMP	Yes (1st)
Bortezomib, thalidomide, Dexamethasone	VTd	Yes (1st)
Cyclophosphamide, Bortezomib, Dexamethasone	CVd	Yes (1st)
Daratumumab, Bortezomib, Dexamethasone	DVd	Yes (2nd)
Carfilzomib, Lenalidomide, Dexamethasone	KRd	Yes (2nd if previously treated with Bortezomib)
Carfilzomib, cyclophosphamide, Dexamethasone	KCd	Yes (2nd)
Ixazomib, Lenalidomide, Dexamethasone	IRd	Yes (3rd)
Isatuximab, pomalidomide, dexamethasone,	IsaPd	Yes(4th)
Pomalidomide, Dexamethasone	Pd	Yes (4th)
Daratumumab monotherapy	D	Yes (4th)
Panobinostat, Bortezomib		Yes (4th)
Bortezomib, Lenalidomide, Dexamethasone	VRd	No
Carfilzomib, Pomalidomide, Dexamethasone	KPd	No
Daratumumab, Pomalidomide, Dexamethasone	DPd	No
Elotuzumab, Lenalidomide, Dexamethasone	ERd	No

Table 1-9 Common anti myeloma drug regimens [6].

1.2 Relapsed Myeloma

1.2.1 Disease course

While the introduction of novel therapies has improved outcomes in myeloma [6] the condition remains incurable with multiple relapses common throughout the disease course. Typically the depth and length of response to each subsequent treatment reduces before reaching a state of refractory disease (**Figure 1-3).**

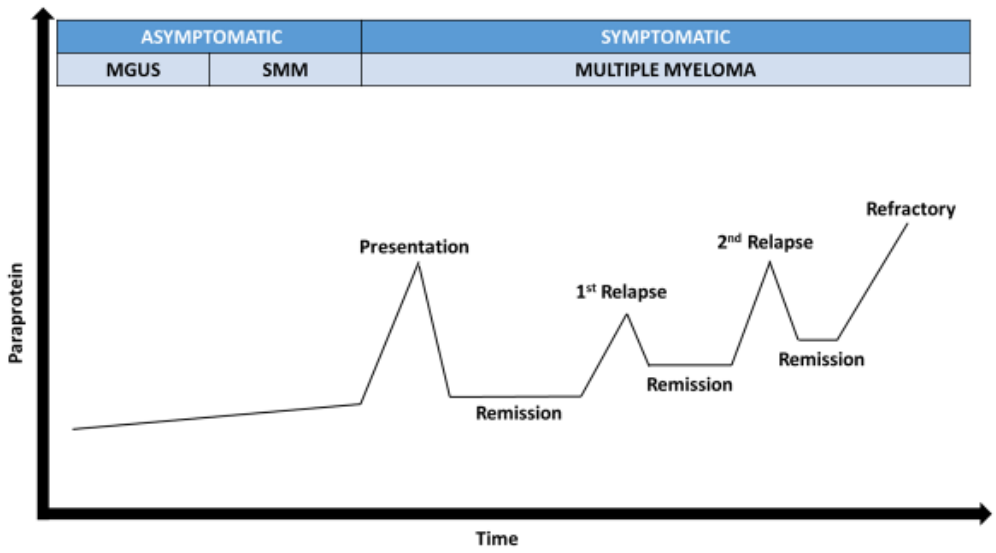

Figure 1-2 Disease course of myeloma, burden of disease reflected by paraprotein; MGUS: monoclonal gammanopathy of known significance; SMM smouldering myeloma.

1.2.2 Mechanism of relapse

Knowledge of myeloma biology is most commonly based on investigation of tumour samples from patients at diagnosis. This has provided insight into molecular events that lead to the development of myeloma, facilitated risk stratification and provided focus for drug development. However the use of samples from newly diagnosed patients does not provide a useful model to investigate mechanisms of relapse and treatment resistance; as a consequence they are less well understood.

To address this issue, attempts have been made to describe new molecular changes from presentation to relapse. Given the molecular heterogeneity of myeloma studies require sequential samples from the same patients to be able to identify true patterns of change, for which there are a limited number. Early studies using sequential samples lacked uniform treatment, had smaller cohorts and some compared different stages of relapse. If patterns of molecular change are to be correlated to specific mechanisms of treatment resistance, uniform treatment is required. I have therefore reviewed studies with sequential myeloma bone marrow sampling by those with non-uniform (**Table 1-11**) and uniform treatment (**Table 1-12**).

1.2.2.1 Sequential tumour genetic studies: non-uniform treatment

1.2.2.1.1 Keats et al

Keats et al used array comparative genomic hybridization (aCGH) to assess copy number of 28 patients with sequential samples at varying time-points of their disease. The median time between samples was 19.3 months; however the exact nature of each time-point was not specified. Treatments also varied between patients. They found the mean number of CNA per patient to significantly increase over time. They described three patterns of evolution in CNA: no change, linear and branching occurring in 35.7%, 21.4% and 42.9% of patients respectively. Linear defined as evolution of new CNA at relapse in addition to changes already observed at presentation, whereas branching involved the loss of initial CNA as well as evolution of new CNA. Interestingly, within the branching group, loss of CNA included regions with previous homozygous deletion. The authors reported this to unequivocally demonstrate the presence of unique clones at baseline which change in relative frequency over time. Patients with high risk cytogenetics t(4;14), t(14;16), t(14;20) and del(17p) had a significantly higher increase of CNA over time, suggesting their poor outcome could be related to higher levels of clonal heterogeneity and genome instability. A third sequential sample in 3 patients showed the pattern of evolution to also vary between each time-point [28].

1.2.2.1.2 Magrangeas et al

Magrangeas et al used single nucleotide polymorphism (SNP) arrays to investigate the change in CNA of 24 patients from presentation to first relapse. In agreement with Keats et al they also observed evolution of new CNA and loss of CNA at relapse, with an overall significant increase in the mean number of CNA between time points. Through unsupervised clustering sequential samples paired together demonstrating their clonal relationship despite molecular evolution [29]. Due to the diversity in CNA observed, the study focused on loci thought to be significant in myeloma pathogenesis; 1q21, *TP53*, *RB1* and the NF-kB pathway regulator genes; TRAF3, cIAP1/2, CYLD, CD40. Sequential comparison revealed 3 patterns of evolution. A third of patients had no change in clonal structure. A third of patients had evidence of major sub-clone evolution. The other third showed minor sub-clone evolution; demonstrating loss of presentation CNA and evolution of new CNA. For example one patient had bi-allelic *RB1* deletion at presentation which returned to diploid status at relapse indicating the predominance of a previously minor sub-clone which lacked the deletion [29]. The observation of evolution from major or minor sub-clone is synonymous to the linear or branching evolution respectively [28]. Interestingly the group also found evolution from minor sub-clones to be more common in patients treated with Bortezomib in comparison to conventional chemotherapy, also in those with deeper responses to treatment. It therefore appears that Bortezomib is more effective at clearing the dominant clone leaving potential for competing minor clones to flourish [29].

1.2.2.1.3 Bolli et al

Bolli et al used SNP arrays and whole exome sequencing (WES) to combine CNA and mutation data to investigate the clonal structure of 67 patients at diagnosis, however only 15 had sequential samples and time points were not uniform. They described 4 types of clonal evolution which again included no change, linear and branching patterns described by the Keats and Magrangeas groups. The fourth pattern was termed differential clonal response; in which all clones are identified at both time points however relative proportions changed [30]. Differential clonal response reflects the increased

depth of molecular assessment added by WES. Patterns of evolution were concordant between CNA and mutations per patient. The group did not show an association between pattern of evolution and treatment type or depth of response. However a higher proportion of t(11;14) patients (4 out of 5) showed no change, the authors suggest this to demonstrate potential differences in evolutionary trajectory of molecular subgroups [9]. This observation could help explain the prognostic differences observed between molecular subgroups in other studies. Interestingly 2 patients with the most extensive branching evolution had extramedullary disease at the second time point [30].

Focussing on known driver mutations in myeloma, 12 non silent mutations were found in KRAS, NRAS, *TP53*, BRAF and FAM46C. 50% were clonal at both time points. 30% appeared as new clones in the later sample and 20% were evident as sub-clonal on first sample, increasing in fraction in the later sample. Despite being labelled as driver mutations not all were found to be clonal at presentation, conversely none had a reduction in clonal fraction at relapse [30].

1.2.2.1.4 Weinhold et al.

Weinhold at al. also used SNP array and WES data to examine sequential samples from 33 patients treated on the Total Therapy protocol. While patients all had multi agent induction, transplant and maintenance, specific regimes varied between patients. Time point comparisons were uniform looking at presentation and first relapse only [15]. The study only focused on CNA with known prognostic significance including del(1p), gain(1q) and del(17p); consistent with previous studies their frequency increased at relapse. They also described 4 patients with gain(1q) at presentation who went on to acquire further copies at relapse and 2 patients where sub-clonal gain(1q) later became dominant [14]. While gain(1q) has already been identified as a prognostically significant progression event in the development of myeloma these findings suggest an ongoing process in chromosome 1 in relapse.

TP53 deletion as a consequence of del(17p) is associated with worse prognosis in myeloma and reported at a frequency of approximately 9% at presentation [7, 8, 12]. With the addition of WES, Weinhold reported 15 (45%)

of patients to have molecular alteration of *TP53* at relapse, abnormalities included non-silent SNV, indels and CNA [15]. While they were unable to demonstrate a significantly worse outcome in these patients, 4 patients had clonal bi-allelic events in the form of del(17p)/*TP53*mut or del(17p)/*TP53*del, which all promptly developed PCL or extramedullary disease. Another patient had 2 separate sub-clonal *TP53* abnormalities and died within one year of the relapse [15]. The authors suggest that poor outcome associated with bi-allelic *TP53* events, highlights the genes pivotal role in relapsed refractory (RR) disease. Furthermore disrupted *TP53* is a feasible mechanism of resistance to the cytotoxic/DNA damage intense total therapy protocol used to treat these patients [15].

The median frequency of non-silent SNV was significantly higher at relapse (60) compared to presentation (43). The most frequent non silent SNV at presentation involved NRAS, *DIS3*, KRAS, CYLD and BRAF. NRAS and *TP53* were the genes that most frequently evolved new mutations at relapse. Of sub-clonal mutations observed at presentation, NRAS was also the most frequent to be selected and expand to become clonal at relapse. Sub-clones containing KRAS, BRAF, *DIS3* and FAM46C also showed expansion at relapse. CYLD was the most common mutation to be lost at relapse, occurring in 2 patients [15]. Competing NRAS, KRAS and BRAF sub–clones were observed within 4 patients, with a switch in dominance at relapse. Similarly different clones with altered *TP53* were seen to compete within one patient; with the presenting dominant del(17p) clone being overtaken by a clone containing *TP53* mutation at relapse. Mutation status was also considered by networks identified in previous pan cancer analysis. The NOTCH, *TP53*, RTK and PI(3)K/RAS networks all acquired new mutations at relapse, of which the latter had a significant increase. There was no change in mutations known to be associated with IMiD and PI resistance [15].

Patterns of clonal evolution matched those previously described although the proportions differed with 22(67%) branching, 7(21%) linear, 3(9%) differential response and only 1(3%) patient showing no change, of note this patient was primary refractory showing no response to treatment[15].

1.2.2.1.5 Kortum et al.

Given the extensive cost and analysis time of WES Kortum et al. developed and validated a myeloma specific 47 gene panel to investigate 25 patients with sequential samples. Time points were not uniform across the group although the majority of sequential samples (22) were diagnosis and first relapse. The panel included genes known to be expressed in myeloma or those that have had a non-silent mutation frequency reported at >3%. It also included genes known to be targeted by IMiD, PI and steroids in which mutations have been associated with treatment resistance[31]. The mean number of variants per patient increased at second time point from 1.92 to 2.12 and more than 50% of patients showed a change in the clonal proportions. Evolution of new mutations and loss of initial mutations was observed, genes with mutation frequencies >10% at presentation and their relative change in frequency at subsequent time points can be seen in **Table 1-10**. Parallel clonal evolution of mutations found within the RAS/MAPK pathway was observed in 2 patients. Only 2 patients were found to have mutations relating to therapy, both involved XBP1, one of which reduced in proportion at time point 2[31].

Gene	Time point 1 (%)	Time point 2 (%)
KRAS	36	36
NRAS	20	16
TP53	20	24
DIS3	16	16
FAM46C	12	16
SP140	12	12

Table 1-10 Kortum et al. change in mutation frequency between time points [31]

1.2.2.1.6 Gene expression analysis

Magrangeas et al. conducted gene set enrichment analysis (GSEA) of presentation and relapse samples and found a significant up regulation of genes involved in the NF-kB pathway, confirming the importance and driver status of this pathway in disease progression [29]. Weinhold et al. used the GEP70 score to assess patient risk status between time points. They found GEP70 score to increase in the majority of patients at relapse, with a third of patients moving to an unfavourable risk group [15]. GESA found significant upregulation of genes involved in cell cycle and DNA replication. Accordingly

GEP based proliferation index was also seen to significantly increase at relapse. Increase in proliferation index was more common in those patients identified to be high risk by GEP70 score. High risk GEP70 was also associated with a higher rate of change in CNA at relapse (branching and linear) and frequency of bi allelic events [15]. Synonymous to Keats', these findings also suggest chromosome instability to be a key feature of high risk disease.

1.2.2.2 Sequential studies with Uniform treatment

1.2.2.2.1 Corre et al.

The first sequential study with uniform treatment was published by Corre et al. They looked at 43 patients with presentation and first relapse samples after 4 cycles of VTD and melphalan autologous stem cell transplant followed by 2 further cycles of VTD. This treatment therefore reflects standard UK practice in newly diagnosed myeloma. Using targeted sequencing they looked at 246 genes known to be recurrently mutated in myeloma and called CNA based on 2358 SNPs [32]. IgH translocations remained stable at relapse. Change in CNA profile at relapse was seen in 88% of patients. The most common new CNA to evolve at relapse was gain(1q) and del(1p) at 19% and 14% respectively. Evolution of new del(17p) was seen in 7% of patients one of which co-occurred with new *TP53* mutation. New mutations were seen in 42% of patients however there was no significant difference in mutational burden between time points. 30 new mutations were found at relapse involving 23 different genes; KRAS was the most frequent occurring in 3 patients (7%). Stable, linear and branching patterns of evolution were observed [32]. Importantly no specific mutation or CNA appeared more commonly at relapse to suggest enrichment from treatment. This contradicts the theory that treatment exerts a specific selective pressure on clonal dynamics. However the authors suggest it is not unexpected to have a heterogeneous result when applying a uniform pressure to an already heterogeneous population. Mutations associated with IMiD resistance were found in 16% of patients at presentation and remained stable at relapse, suggesting that thalidomide had no effect on their clonal selection within these patients. No mutations involved in proteasome inhibitor resistance were found [32].

1.2.2.2.2 Jones et al.

The most recent study of sequential samples came from Jones et al, who looked at presentation and first relapse samples from 56 patients treated on the Myeloma XI trial. Induction therapy was not strictly uniform as patients were randomised to different cyclophosphamide, IMiD and dexamethasone regimes and only received transplant if eligible. All patients had a second randomisation to maintenance Lenalidomide vs observation, hence allowing the investigation of the molecular evolution while on maintenance[14].

As with other studies branching and linear patterns of evolution were also seen at relapse. Gain(1q) was the most frequent new CNA to evolve at relapse, found in 13% of patients. Frequency of bi allelic inactivation involving *RB1*, TRAF3 and *TP53* increased at relapse. Focussing on genes known to be recurrently mutated in myeloma, 79% and 80% of patients had at least 1 non-synonymous mutation at presentation and relapse respectively. 37% of patients showed change at relapse with evolution of new and or loss of mutations. Evolution of new mutations (13%) was more common than loss of mutation (9%) and the majority of new mutations were clonal at relapse. KRAS and PRDM1 were the most frequent new mutations at relapse found in 5% of patients, followed by *TP53* and NRAS at 4%. KRAS and NRAS were also the most frequent mutations to be lost; in 5% and 4% of patients respectively[14].

Depth of response to therapy was associated with a significantly higher rate of new mutations at relapse. Patients achieving CR increased the median number of non-synonymous mutations at presentation from 40 to 59 at relapse, whereas patients achieving non-CR had no significant change. Focusing only on genes known to be commonly mutated in myeloma, 67% of patients achieving CR showed new change to mutational landscape compared to 25% of non CR patients. This finding was also mirrored in CNA with higher frequency of new gain(1q), del(1p), del(17p), del(13) and del(14) at relapse found in patients achieving CR[14].

No significant differences in molecular evolution were found between the Lenalidomide maintenance and observation patients. No common mutation or new copy number pattern was found in the maintenance patients at relapse to

suggest selection from treatment. Mutations associated with IMiD resistance were not increased in the maintenance arm at relapse. 1 patient who had received 8 months of Lenalidomide maintenance acquired new clonal *CRBN* mutation at relapse[14].

Patterns of evolution matched those previously described with 66% branching, 20% linear and 14% stable. Maintenance treatment appeared to have no effect on type of evolution. Depth of response was associated with pattern of evolution, with all patients achieving CR having linear or branching change. Whereas a significantly higher number of patients achieving non-CR had stable CNA at progression[14].

1.2.3 Conclusion

Myeloma is genetically diverse with a broad range of aberrations documented. It remains an incurable condition with evidence of continued molecular evolution at subsequent relapses in the majority of patients. Differing patterns of evolution have been observed including linear, branching, stable and differential response; which can been attributed to complex sub-clonal dynamics. Factors proposed to influence sub-clonal dynamics include anti-myeloma treatment, immune response and the bone marrow microenvironment [14, 15, 28-32]. While anti-myeloma therapies undoubtedly exert pressure on clonal selection, current evidence has been unable to define this process, with no common or unifying molecular changes noted, even in studies with uniform treatment.

A key feature previous studies lack, is adequate cohort size to investigate change within the molecular subgroups of the heterogeneous myeloma population. There is an association with worse outcome in patients with t(4;14), t(14;16) and t(14;20) which suggests different evolutionary trajectories within these tumour groups. Furthermore there are common patterns of aberration co-occurrence observed within these groups; for example the association of t(4;14), gain(1q) and del(13q) [12]. Differing evolutionary trajectories between molecular subgroups was also supported by Keats et al who noted a higher frequency of change in high risk patients and Bolli et al who saw stable evolution in t(11;14) [28, 30].

Investigation of sequential samples with uniform treatment, from a larger cohort, could help identify specific patterns of evolution within molecular subgroups. Identification could help to reveal mechanisms of myeloma relapse and treatment resistance. As recurrent CNA are the most common genetic aberration observed, sequential analysis of genome wide CNA evolution could provide clinically relevant insight.

Reference	Number of Sequential samples	Uniform time points	Uniform treatment	Genomic Analysis
Keats, J.J., et al., *Clonal competition with alternating dominance in multiple myeloma.* Blood, 2012.[28]	28	No	No	CGH, FISH: CNA. U133 plus 2.0: GEP.
Magrangeas, F., et al., *Minor clone provides a reservoir for relapse in multiple myeloma.* Leukemia, 2013. [29]	24	Yes	No	SNP: CNA. U133 plus 2.0: GEP.
Bolli, N., et al., *Heterogeneity of genomic evolution and mutational profiles in multiple myeloma.* Nat Commun, 2014. [30]	15	No	No	WES: SNV, CNA. SNP: CNA.
Weinhold, N., et al., *Clonal selection and double-hit events involving tumor suppressor genes underlie relapse in myeloma.* Blood, 2016 [15]	33	Yes	No	WES: SNV, CNA. SNP: CNA. U133 : GEP
Kortüm, K.M., et al., *Longitudinal analysis of 25 sequential sample-pairs using a custom multiple myeloma mutation sequencing panel (M(3)P).* Ann Hematol, 2015.[31]	25	No	No	Targeted sequencing: SNV. FISH: CNA, Translocations

Table 1-11 Sequential studies with non-uniform treatment. CGH: comparative genomic hybridisation array; FISH: fluorescence in situ hybridization; CNA: copy number aberration; GEP: gene expression profile; WES: whole exome sequencing; SNP: single nucleotide polymorphism; SNV: single nucleotide variation.

Reference	Number of Sequential samples	Uniform time points	Uniform treatment	Genomic Analysis
Corre, J., et al., Multiple myeloma clonal evolution in homogeneously treated patients. Leukemia, 2018 [32]	43	Yes	Yes	Targeted sequencing: SNV. SNP: CNA.
Jones, J.R., et al., Clonal evolution in myeloma: the impact of maintenance lenalidomide and depth of response on the genetics and sub-clonal structure of relapsed disease in uniformly treated newly diagnosed patients. Haematologica, 2019 [14]	56	Yes	Yes	WES: SNV MLPA: CNA

Table 1-12 Sequential studies with uniform treatment. CNA: copy number aberration; WES: whole exome sequencing; SNP: single nucleotide polymorphism; SNV: single nucleotide variation; MLPA: multiple ligation probe analysis.

1.3 Hypothesis and Aims

1.3.1 Hypothesis

Prognostic variation between the molecular sub-groups of myeloma likely constitutes different evolutionary trajectories. Changes to the molecular landscape of myeloma in response to therapy are central to emergence of disease progression and treatment resistance. By identifying and characterising the molecular evolution of specific pathogenetic subgroups at relapse, I hope to provide better understanding of mechanisms of relapse and treatment resistance to inform future translational research.

1.3.2 Aims

Using matched sequential tumour samples from the phase 3 Myeloma XI clinical trial I aim to address the following points:

- Describe new genetic changes associated with myeloma relapse.
- Compare genetic changes at relapse within specific pathogenetic subgroups of myeloma.
- Identify new genetic changes at relapse that are associated with high risk disease.
- Identify new genetic changes at relapse specifically associated with evolving resistance to treatment and immunomodulatory maintenance.
- Consider novel therapeutic targets for relapsed disease.

Chapter 2: Materials and Methods

2.1 Patients and treatment

All patients entered into the UK NCRI Myeloma XI (MXI) (ISRCTN49407852) trial were considered. Patients with sequential bone marrow aspirates taken at trial entry and first relapse, with adequate genetic material for CNA profiling were included. Relapse was defined as progressive disease using the International Myeloma Working Group (IMWG) response criteria [33].

All patients gave informed written consent for trial entry and for the use of genetic material in future research. The study was approved by the UK National Research Ethics Service, research ethics committees at participating centres and the UK Medicines and Healthcare Products Regulatory Agency. Research was conducted according to the Declaration of Helsinki and the principles of Good Clinical Practice as espoused in the Medicines for Human Use (Clinical Trials) Regulations.

2.1.1 Myeloma XI Trial

The MXI trial is a randomised, phase 3, parallel group, multi-centre trial. Induction randomisations differed between transplant eligible (TE) and non-eligible (TNE) patients. After induction treatment all patients then underwent maintenance randomisation.

2.1.1.1 Transplant eligible

TE patients were randomised to triplet induction with thalidomide (CTD), lenalidomide (CRD), or carfilzomib and lenalidomide (KCRD) in combination with cyclophosphamide and dexamethasone. Insufficient responders (partial or minimal response) were also randomised to cyclophosphamide, bortezomib and dexamethasone (CVD) vs no intensification. Non-responders (stable or progressive disease) received CVD. Induction +/- consolidation was followed by high dose melphalan ASCT.

2.1.1.2 Transplant non-eligible

TNE patients were randomised to attenuated triplet induction with thalidomide (CTDa) or lenalidomide (CRDa) in combination with cyclophosphamide and dexamethasone. Insufficient responders (partial or minimal response) were next randomised to cyclophosphamide, bortezomib and dexamethasone (CVD) vs no intensification. Non-responders (stable or progressive disease) received CVD.

2.1.1.3 Maintenance

Post induction all patients were randomised a second time between lenalidomide monotherapy, lenalidomide plus vorinostat or observation only. At physicians discretion some patients were not deemed fit to enter the maintenance randomisation.

2.2 Genetic Profiling

Samples were profiled for CNA, common IgH translocations and gene expression. All tumours had CNA profiling at presentation and relapse. Patients had IgH translocation assessed at baseline, where possible sequential tumour samples were profiled. A subset of patients also had gene expression profiling at presentation and relapse; those with adequate tumour RNA from both samples. I did not personally complete sample processing or molecular assays. All wet lab was completed by members of the ICR myeloma bio-banking team.

2.2.1 Sample Processing

Plasma cells were selected from bone marrow aspirates using CD138 immune-magnetic cell sorting (Miltenyi Biotec, Bergisch Gladbach, Germany) as previously described [34]. Purity of >95% was confirmed by cytospin. DNA and RNA were extracted using Allprep kits (QIAGEN) according to manufacturer's instructions.

2.2.2 Copy Number Assessment

2.2.2.1 dMLPA

Digital multiplex ligation-dependent probe amplification (dMLPA) is a PCR based technique used to assess relative copy number of sample DNA to normal reference DNA. The technique has been previously described and validated against normal MLPA and FISH in acute lymphoblastic leukaemia and more recently in myeloma [35, 36]. Digital MLPA utilises Illumina next generation sequencing (NGS) platforms to quantify amplicons. Thus multiplexed sequences of DNA of up to 96 samples can be tested simultaneously in one analysis.

The newly developed research version of D006-X2 Multiple Myeloma dMLPA probe-mix was used to assess CNA as previously described [36], designed specifically for assessment of targeted genome wide CNA in myeloma. The panel contains 282 target probes which interrogate regions recurrently affected by CNA in myeloma. Also 96 reference probes hybridizing to copy number stable regions, 45 input DNA and assay quality control probes, six X and Y chromosome-specific probes and 39 pairs of SNP probes for sample identification and detection of sample contamination. Reference probes were used for data normalization. A combination of reference and target probes (194 in total) were used to also provide a digital karyotype, capturing telomeric, centromeric, and mid-chromosome arm regions for all chromosomes. Details of the D006-X2 probes are listed in **Supplementary Tables 14-1.**

2.2.2.2 dMLPA principle:

Each dMLPA probe consists of a left and right oligonucleotide for specific target DNA sequence. Once left and right oligos have hybridised with target DNA they are ligated using Ligase-65, the ligation step also incorporates a barcode oligonucleotide (unique to the sample). The barcode oligos contain an Rd1 sequence which acts as the Illumina tag for quantification. Ligated probes are then amplified using PCR and products quantified using Illumina sequencer. Male DNA from healthy volunteers is used for controls. Raw results were analysed using Coffalyser software (MRC Holland). After quality assessment, results undergo intra sample then inter sample normalisation. For

intra sample normalisation the read number of each probe is normalised against the median read of reference probes within that sample. The relative read number generated for each probe is then compared to the read value of that probe in each reference sample to complete inter sample normalisation. This generates a final ratio per probe, which reflects copy number relative to normal DNA, a ratio of 1.0 considered normal. The ratio can be used to infer >3, 3, 2, 1 and 0 copies of DNA at a given probe, reflecting amplification, gain, normal, heterozygous and homozygous deletion respectively.

2.2.2.3 Defining CNA per probe

Specific cut-offs to determine CNA per probe from dMLPA final ratios have not yet been defined. Classical MLPA has been validated in myeloma against iFISH using probe mix P425 [37]. 63 probes are common between classical and digital MLPA. Leeds CTRU provided a “snap shot” cohort of 236 MXI patients thought to be clinically representative of the whole trial population. Presentation samples of the 236 patients were run on normal MLPA (probe mix P425) and dMLPA (probe mix D006-X2) for comparison. Taking normal MLPA as standard, I applied a series of different cut-offs incrementing by 0.05 to dMLPA data. Copy number call was compared to normal MLPA to calculate specificity and sensitivity. The most accurate cut-offs for dMLPA were used throughout my analysis and can be seen in **Table 2-1**.

CNA	Copies	Cut-off
Homozygous Deletion	0	≤0.25
Heterozygous Deletion	1	>0.25 ≤ 0.75
Diploid	2	>0.75 ≤1.20
Gain	3	>1.20 ≤1.7
Amplification	>3	>1.7

Table 2-1 Cut-offs to assign copy number per probe.

2.2.2.4 Defining focal and interstitial CNA

Using the cut-offs defined in section 2.2.2.3, I used a majority rule (CNA present in ≥50% of relevant probes) to determine CNA per gene, chromosome band, chromosome arm.

For example the *CKS1B* gene has 3 different probes (covering exons 1, 2 and 3). To call amplification of *CKS1B*, ≥ 2 probes are required to have ratios >1.7. To call gain of *CKS1B*, ≥ 2 probes are required to have ratios >1.2 and not meet the criteria of amplification. This step wise approach allows for cases where probes show a mixture of gain and amplification.

Whole chromosome CNA required both p and q arms to have said CNA after application of majority rule per arm. Hyperdiploidy was defined as gain in 2 or more of chromosomes 3,5,7,9,11,15,19 or 21.

For the purpose of this study I have defined interstitial CNA to involve a whole chromosome arm and focal CNA to involve ≥1 chromosome band as per the majority rule. CNAs involving sex chromosomes were not considered.

2.2.2.5 Defining evolution of CNA

Sequential CNA profile was compared per patient; CNA evolution at relapse was described as new CNA, loss of CNA or stable CNA. Frequency of CNA at relapse therefore reflects net change between time points. Assignment of CNA evolution is detailed in **Table 2-2**. Evolution pattern at relapse was described as branching, linear, linear loss and stable. Assignment of evolution pattern is detailed in **Table 2-3.**

2.2.2.6 CNA Analysis

Analysis was completed using R version 4.0.2. There are currently no packages available for analysis of dMLPA data. I wrote code to assign CNA using the “tidyr” and “dplyr” packages **(Table 2-4)**.

Presentation CNA	Relapse CNA	Evolution of CNA
Hom D	Hom D	Stable
Hom D	Het D	Loss Hom D
Hom D	Diploid	Loss Hom D
Hom D	Gain	New Gain
Hom D	Amp	New Amp
Het D	Hom D	New Hom D
Het D	Het D	Stable
Het D	Diploid	Loss Het D
Het D	Gain	New Gain
Het D	Amp	New Amp
Diploid	Hom D	New Hom D
Diploid	Het D	New Het D
Diploid	Diploid	Stable
Diploid	Gain	New Gain
Diploid	Amp	New Amp
Gain	Hom D	New Hom D
Gain	Het D	New Het D
Gain	Diploid	Loss Gain
Gain	Gain	Stable
Gain	Amp	New Amp
Amp	Hom D	New Hom D
Amp	Het D	New Het D
Amp	Diploid	Loss Amp
Amp	Gain	Loss Amp
Amp	Amp	Stable

Table 2-2 Assignment of CNA evolution. Hom D: Homozygous deletion; Het D: heterozygous deletion; Amp: amplification.

Pattern of Evolution	Definition
Branching	New CNA at relapse and loss of CNA at relapse.
Linear	New CNA at relapse.
Linear loss	Loss of CNA at relapse.
Stable	No change in CNA at relapse.

Table 2-3 Assignment of evolution pattern.

2.3 IgH translocation assessment

2.3.1 Taqman translocation assay

Common IgH translocations were assessed using a validated TaqMan multiplexed real-time quantitative reverse transcriptase-PCR (qRT-PCR) assay developed by Kaiser et al. Details of methods have previously been reported [34].

2.3.2 Taqman principle

Tumor RNA is transcribed to complementary DNA (cDNA) using reverse transcriptase. The cDNA acts as the template of the genes expressed by the tumor, PCR primers specific to the genes in question bind to initiate the PCR reaction leading to amplification of the genes DNA. TaqMan uses fluorophore-labelled hydrolysis probes which bind downstream to the primer to release florescent signal allowing real time quantification of DNA.

The Taqman translocation assay consists of 5 multiplexed assays using three different TaqMan fluroprobes each (NED, VIC, FAM). This allows measurement of 9 genes known to be overexpressed in myeloma; t(4;14), t(6;14), t(11;14),t(14;16) and t(14;20). Genes measured include *MMSET, FGFR3, CCND1, CCND3, ITGB7, MAF, MAFB, CCND2* and *CX3CR1. GAPDH* is used as a control. Details of primers for each gene can found in **Supplementary Table 14-2.**

2.3.3 Taqman analysis

The relative expression of each translocation target gene was used to assign translocation group using a previously validated algorithm [34] shown in **Figure 2-1**. The majority of samples had adequate RNA to provide assay results at both time-points. Where the assay was only successful at one time-point the result was assigned to both presentation and relapse. This decision was based on the fact that common IgH translocations are initiating events in myeloma and have been demonstrated to remain stable with time [10].

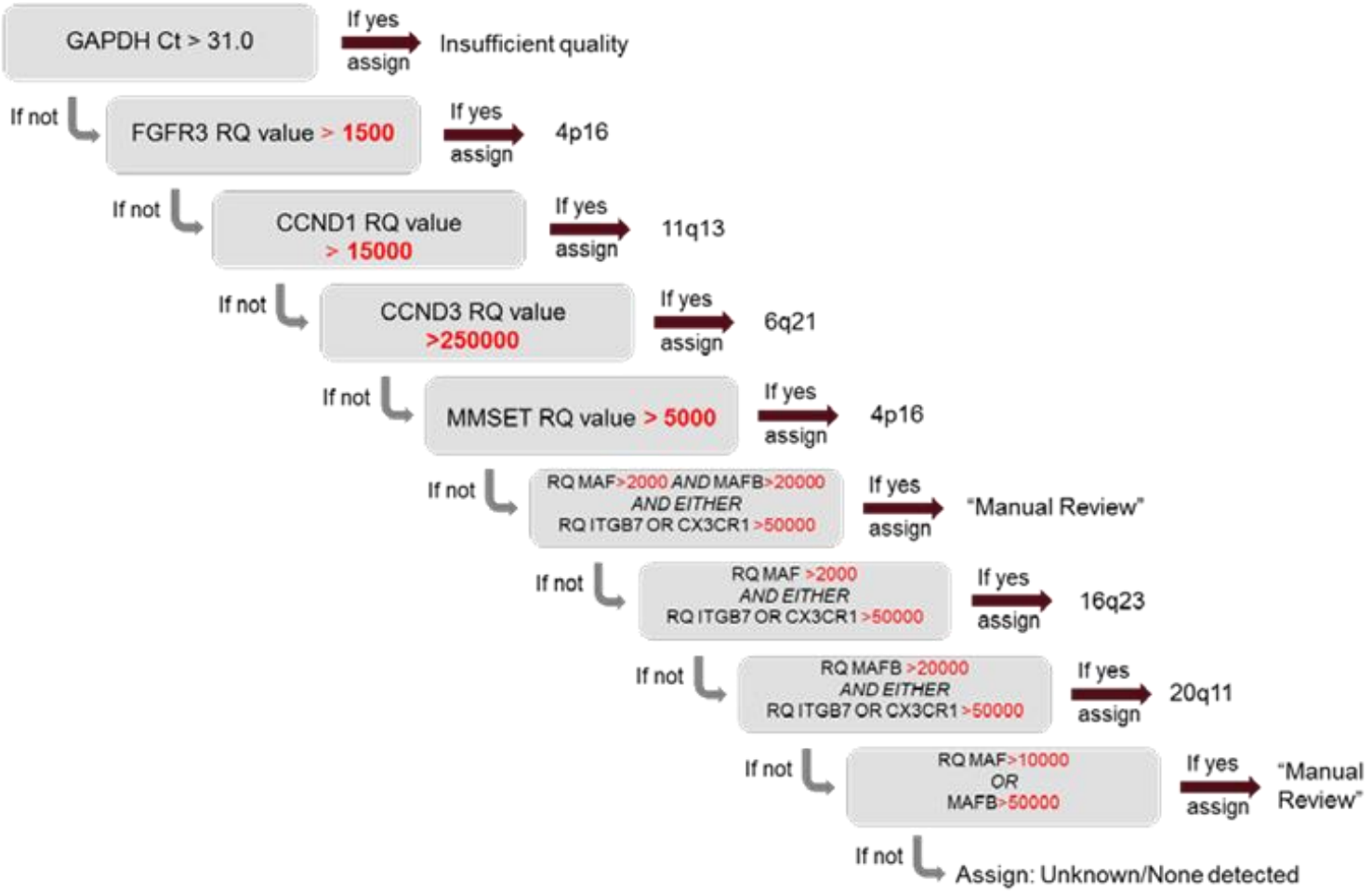

Figure 2-1 Algorithm to assign IgH translocation based on Taqman expression.

2.4 Gene Expression

2.4.1 U133 Plus 2.0 Array

Gene expression profiles were assessed using the Affymetrix U133 Plus 2.0 Array, as previously described [28]. Only patients with adequate quantity and quality of tumour RNA at both time points were assessed. The U133 plus 2.0 array is a single channel DNA microarray that can be used to measure expression of thousands of genes simultaneously. This array provides comprehensive coverage of the transcribed human genome; comprised of 54000 probe sets that cover 38500 genes. Arrays were run according to standard Affymetrix protocol.

2.4.2 U133 Plus 2.0 Array principle

The microarray consists of a solid surface chip with DNA oligonucleotide probes attached. Each probe cell on the chip contains multiple copies ($40x10^7$) of one probe. Probe cells combine to form probe sets. Probesets each contain 11 probe cell pairs made up of perfect match (PM) and Mis-Match (MM) probes, which are used to facilitate normalisation in down-stream analysis. Each probeset corresponds to a gene.

Complementary DNA (cDNA) is made from RNA using reverse transcriptase. In vitro transcription of cDNA with a biotin label produces biotinylated cRNA. Labelled cRNA is purified and fragmented before being added to the array for hybridisation. After hybridisation, the chip is washed to remove non hybridised cRNA, then stained. Stained microarrays are scanned to produce a basic DAT file which is processed to create a CEL file which provides an intensity value for each probe cell on the microarray.

2.4.3 Expression Analysis

All analysis was completed in R version 4.0.2; affyPLM, simpleaffy, affy, sva, panp, biobase, hgu133plus2.db, geneClassifiers and limma packages were used **(Table 2-3)**.

2.4.3.1 Quality control and data transformation

Normalised unscaled standard errors (NUSE) and Relative Log Expression (RLE) values were calculated and plotted using affyPLM. Samples with NUSE >1.05 and RLE >0.15 were considered poor quality and removed.

Affymetrix common metrics of quality control were reviewed using simpleaffy and standard recommendations followed for all chips; ensuring average background and percent of present calls were similar; scale factors were within 3 fold of each other, GAPDH and b-actin ratios were less than 1.25 and 3 respectively, and BioB spikes were present.

After quality control steps all remaining data was normalised using MAS5.0. Normalised data was log2 transformed for all subsequent analysis. Batch effect removed using ComBat. Biobase was used to create expression sets which includes probeset IDs, expression values and phenotype data. Probeset IDs were annotated using the hgu133plus2.db to provide gene symbol and chromosome locations.

2.4.3.2 Gene expression risk scores

MAS5.0 normalised, log2 transformed data was run through the geneClassifiers package to calculate EMC92 and UAMS 70 gene expression risk scores [19-23].

2.4.3.3 Differential gene expression

Differential gene expression was assessed using linear models within the limma package. Limma uses an empirical Bayes method to moderate the standard errors of estimated log fold change. For models that investigated change in sequential expression, unique trial ID was used as a block to ensure only matched samples were compared. Differential expression was considered significant in genes with a false discovery rate of <5%.

2.4.3.4 Gene set enrichment analysis

Significant differentially expressed genes were ranked according to t statistic. Ranked gene lists were analysed using the online Broad institute GSEA platform. Gene sets with an FDR of <25% were considered relevant as described by Subramanian et al. [38].

2.4.4 Other Statistical analysis

All analysis was completed in R version 4.0.2 using dplyr, tidyr, stats, survival, survminer, ComplexHeatmap and ggpubr packages **(Table 2-3)**.

Association between categorical variables was examined using Chi-square and Fishers exact test. Association between continuous variables was examined using Wilcoxon signed-rank test. A two-sided *P*-value of ≤0.05 was considered statistically significant. Hierarchical clustering was performed using ComplexHeatmap; Ward's method with Euclidean distance.

Progression-free survival (PFS) was defined as time from induction randomization to progression, according to International Myeloma Working Group (IMWG) criteria, or death of any cause. Overall survival (OS) was time from induction randomization to death of any cause. Cox proportional hazards regression was used to estimate univariate and multivariable hazard ratios (HRs) and 95% confidence intervals (CI). Differences between Kaplan–Meier survival curves was assessed using the log-rank test. A two-sided *P*-value of ≤0.05 was considered statistically significant.

To examine the predictive value of evolution in CNA, high risk CNA were considered as time dependent covariates within a multivariate model. The occurrence of high risk CNA per tumor were recorded at diagnosis and relapse. The "tmerge" function from survival package was used to record CNA status over two time intervals; months from induction randomisation to relapse (PFS) and months from relapse to death of any cause (difference between OS and PFS). The proportional hazards (PH) assumption was tested using 'cox.zph' function, requiring a non-significant relationship between Schoenfeld's residuals and time to be considered true. Cox.zph results were plotted to demonstrate log(HR) over time.

Package	Reference
tidyr	Hadley Wickham (2021). tidyr: Tidy Messy Data. R package version 1.1.3. https://CRAN.R-project.org/package=tidyr.
dplyr	Hadley Wickham, Romain François, Lionel Henry and Kirill Müller (2021). dplyr: A Grammar of Data Manipulation. R package version 1.0.5. https://CRAN.R-project.org/package=dplyr.
affyPLM	Bolstad BM, Collin F, Brettschneider J, Simpson K, Cope L, Irizarry RA, and Speed TP. (2005) Quality Assessment of Affymetrix GeneChip Data in Bioinformatics and Computational Biology Solutions Using R and Bioconductor. Gentleman R,Carey V, Huber W, Irizarry R, and Dudoit S. (Eds.), Springer, New York.
simpleaffy	Crispin J Miller (2020). simpleaffy: Very simple high level analysis of Affymetrix data. http://www.bioconductor.org, http://bioinformatics.picr.man.ac.uk/simpleaffy/.
affy	Gautier, L., Cope, L., Bolstad, B. M., and Irizarry, R. A. 2004. affy---analysis of Affymetrix GeneChip data at the probe level. Bioinformatics 20, 3 (Feb. 2004), 307-315.
panp	Peter Warren (2020). panp: Presence-Absence Calls from Negative Strand Matching Probesets. R package version 1.58.0.
Biobase	Orchestrating high-throughput genomic analysis with Bioconductor. W. Huber, V.J. Carey, R. Gentleman, ..., M. Morgan Nature Methods, 2015:12, 115.
hgu133plus2.db	Marc Carlson (2016). hgu133plus2.db: Affymetrix Human Genome U133 Plus 2.0 Array annotation data (chip hgu133plus2). R package version 3.2.3.
geneClassifiers	R Kuiper (2020). geneClassifiers: Application of gene classifiers. R package version 1.12.0. https://doi.org/doi:10.18129/B9.bioc.geneClassifiers
limma	Ritchie, M.E., Phipson, B., Wu, D., Hu, Y., Law, C.W., Shi, W., and Smyth, G.K. (2015). limma powers differential expression analyses for RNA-sequencing and microarray studies. Nucleic Acids Research 43(7), e47.
stats	R Core Team (2020). R: A language and environment for statistical computing. R Foundation for Statistical Computing, Vienna, Austria. URL https://www.R-project.org/.
survival	Therneau T (2021). _A Package for Survival Analysis in R_. R package version 3.2-10, <URL:https://CRAN.R-project.org/package=survival>.
survminer	Alboukadel Kassambara, Marcin Kosinski and Przemyslaw Biecek (2021). survminer: Drawing Survival Curves using 'ggplot2'. R package version 0.4.9. https://CRAN.R-project.org/package=survminer
ComplexHeatmap	Gu, Z. (2016) Complex heatmaps reveal patterns and correlations in multidimensional genomic data. Bioinformatics.
ggpubr	Alboukadel Kassambara (2020). ggpubr: 'ggplot2' Based Publication Ready Plots. R package version 0.4.0. https://CRAN.R-project.org/package=ggpubr

Table 2-4: R packages used for analysis.

Chapter 3: Pre analysis quality control checks

3.1 Introduction

Small differences in the quality of sequential tumour samples have the potential to produce false positive changes when comparing samples. To increase the validity of this sequential sample analysis I completed a number of quality control steps on the CNA data received back from the MRC Holland Coffalyser software.

3.2 Non-malignant CD138+ contamination

3.2.1 *IgHD* copy number

1 year into this project I completed an interim analysis, at that time there were 285 patients from the MXI trial with matched sequential samples and adequate DNA to complete dMLPA. When examining initiating molecular events I found a significant decrease in the frequency of HRD tumours at relapse; 185 (64.9%) at presentation vs 153 (53.7%) at relapse (*P*=0.0082). On closer inspection, relapse samples with loss of HRD appeared to have a dilution effect; with evidence of sub-clonal gain within the HRD chromosomes which had previously been clonal at presentation. As previously discussed HRD is an initiating event in myeloma that remains stable throughout disease evolution [10]. I therefore concluded that the decrease in frequency of HRD reflected contamination of samples with normal CD138+ plasma cells or other CD138+ bone marrow cells; their presumed normal copy number affecting normalisation of the sample and the ability to detect aberrations. While cell sorting ensures >95% purity for CD138+ cells it cannot ensure them to be malignant. Furthermore recurrence of a paraprotein as low as 5g/L can indicate relapse using the IMWG definition [33]. As a consequence the malignant plasma cell burden within the bone marrow at relapse is often lower than that of presentation which could lead to higher rates of contamination with non-malignant CD138+ cells at relapse.

While loss of HRD may highlight evidence of contamination, it is only relevant to approximately half the cohort. Removing these cases alone would cause bias. I therefore set out to find a robust biological based process to identify and remove contamination across all samples. The D006-X2 probe mix contains a probe for the *IgHD* gene. During normal plasma cell development the majority of activated B lymphocytes go through CSR, switching IgM or IgD production to IgG, E or A. The mechanism of CSR involves deletion of *IgHM* and *IgHD* genes from the DNA of the IgH constant region (as discussed in section 1.1.4.1) and illustrated in **Figure 3-1** [39].

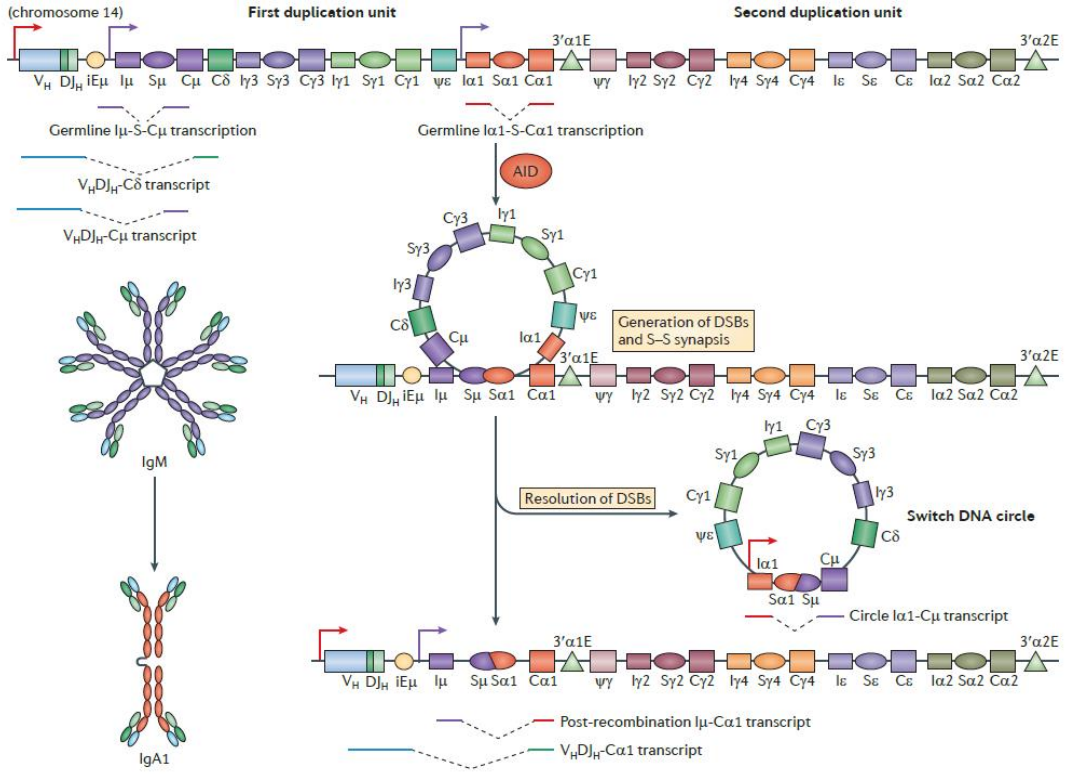

Figure 3-1 Class switch recombination (CSR) exchanges the gene encoding the immunoglobulin heavy chain constant region (CH) with one of a set of downstream CH genes (the figure depicts CSR between Sμ and Sα1 in the human immunoglobulin heavy chain locus). This deletion–recombination reaction requires activation-induced cytidine deaminase (AID) and involves the generation of DNA double-strand breaks (DSBs) in switch regions (which lie upstream of the CH gene) followed by DSB repair. This leads to the juxtaposition of rearranged heavy chain variable region with a downstream CH exon cluster and deletion of the intervening sequence between S regions as an extrachromosomal circle. (Figure taken from Xu et al, Immunoglobulin class-switch DNA recombination: induction, targeting and beyond. Nature 2012 [17]

Deletion of *IgHD* is an irreversible step and an initiating event in normal plasma cell development, therefore the majority of patients should have deletion of the *IgHD* probe used in dMLPA, furthermore the deletion should remain stable at sequential time points. An exception to this would be in IgD myeloma, of which I have 2 patients in my cohort. Consistent with this hypothesis my interim analysis found 95% of tumors to have IgHD deletion at presentation, however deletion decreased to 88% at relapse **(Table 3-1).** Synonymous to loss of HRD, loss of *IgHD* probe deletion at relapse suggests the presence of contamination. Although still classified as deletion (ratio ≤0.75) some patients showed an increase in IgHD ratio towards diploid at relapse, for example changing from homozygous deletion to heterozygous deletion; indicating contamination of non-malignant CD138+ cells at relapse.

Copy Number, n (%)	Presentation	Relapse
Homozygous deletion	163(59)	117 (42)
Heterozygous deletion	100 (36)	128 (46)
Diploid	11 (4)	29 (11)
Gain	2(1)	2 (1)

Table 3-1 Frequency of IgHD CNA at sequential time points.

As *IgHD* deletion is present in 95% of patients it provides useful tool to assess contamination between sequential samples across the whole cohort. I used the HRD patients as a test cohort. Cases of HRD from presentation were selected. The mean ratio of probes from chromosomes 3, 5, 7, 9, 11, 15, 19, and 21 calculated per patient. The presentation value was subtracted from relapse to provide mean difference in HRD; a negative value reflecting loss of HRD and therefore contamination. Presentation *IgHD* ratio was subtracted from relapse *IgHD* ratio; a positive value reflecting loss of deletion. Values were plotted against each other per patient, shown in **Figure 3-2**.

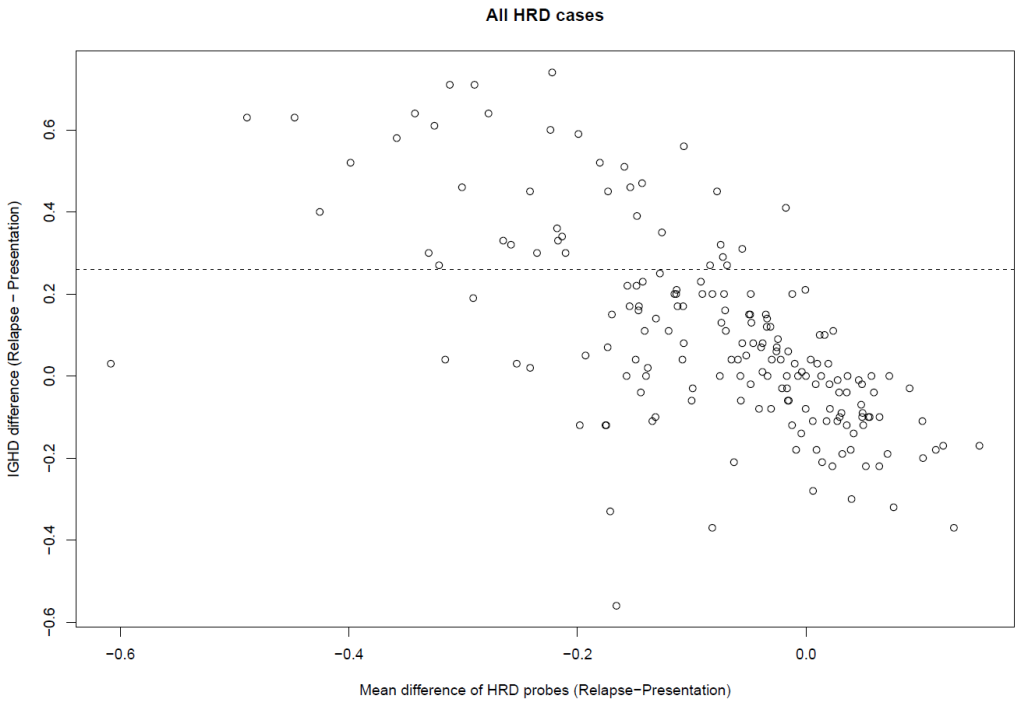

Figure 3-2 Change in mean HRD probe ratio versus change in IgHD probe ratio.

The difference in mean HRD probe ratio negatively correlates with difference in *IgHD* probe ratio. Removing cases with *IgHD* difference >0.26 (those above dotted line) takes out patients with the largest HRD loss but does not compromise those with stable HRD. Filtering this way leaves a proportion of patients who still show some loss of HRD, however their mean HRD difference is smaller suggesting lower levels of contamination and these smaller differences are less likely to affect HRD frequency using the discrete cut-offs. Applying this rule across the whole interim analysis, patients with an IgHD difference of >0.26 were removed leaving 210 patients. Within the 210, frequency of HRD did not significantly change between time points; 136 (64.8%) at presentation, 135 (64.3%) at relapse (P=1).

Patients with an IgHD difference of >0.26 were therefore removed from the final analysis, details of the final numbers of patients removed during pre-analysis quality control checks are summarised in section 3.5.

3.2.2 Ig Gene expression

Following the same principle of *IgHD* CNA change, the expression of the Ig genes was also used to identify signs of contamination with non-malignant CD138+ cells. This method has also been used in previous myeloma gene expression studies[13]. Using normalised log2 transformed values, I looked at change in *IgM* and *IgD* expression, removing patients where the log fold change (LFC) was greater than 5 at relapse. I also removed kappa restricted patients with a LFC of Ig lambda (*IgL*) >5 and Lambda restricted patients with a LFC of Ig kappa (*IgK*) >5.

3.3 DNA Concentration

The dMLPA protocol has been developed with technical advice from MRC Holland. The assay uses a dilution of 1.25-20 ng/µl DNA in a 4 µl volume (total 5-80 ng). Some samples with low concentrations of DNA had low count reads and therefore final ratios were variable and discordant within one region, for example showing deletion and gain within the same gene. The product description advices caution at low DNA concentration with possible effects on performance of the assay. Examining count reads and input DNA concentration, MRC Hollands QC flags were most often positive in samples with DNA concentrations <3ng/ul. While dMLPA may be able to perform at low concentrations to produce CNA data, this study relies on the identification of subtle change through comparison of sequential samples. Given the occasional variability at lower DNA concentration I was concerned regarding false positive results. I therefore decided to filter my samples to only include patients with sequential samples with DNA concentrations >3ng/ul.

3.4 Confirmation of sequential samples

To ensure sequential samples were from the same patient I used the dMLPA SNP probes. There are 39 pairs of SNP probes included in the D006-X2 mix. They have been designed to target DNA where small deletion SNPs occur in approximately 50% of people. Within each SNP probe pair, one probe targets the deletion and the other diploid status; allele A and B respectively. I calculated the ratio of count reads within each pair to determine if a patient was homozygous A, heterozygous AB or homozygous B and scored them 0,

1 or 2 respectively. SNP sequences of each sample were then compared per patient with discordance suggesting a possible mismatch due to sample processing error.

Ratios were calculated as follows and rounded to the nearest tenth:

- Allele A ratio = A/(A+B)
- Allele B ratio = B/(A+B)

Assignment of SNP zygosity by allele ratio is summarised in **Table 3-2**. Where the SNP sequences of sequential samples had <70% match, short tandem repeat (STR) typing was also completed. If STR typing confirmed a mismatch the samples were removed from the analysis.

Ratio A	Ratio B	Zygosity	Score
>0.7	≤0.3	Homozygous A	0
>0.3 ≤0.7	>0.3 ≤0.7	Heterozygous AB	1
≤0.3	>0.7	Homozygous B	2

Table 3-2: Cut offs for the assignment of SNP zygosity

3.5 Final cohort numbers

Before completing QC steps I had a cohort of 300 patients with sequential tumour samples from the MXI trial. 68 patients were removed due to an IgHD probe difference of >0.26. 14 patients were removed due to LFC >5 in expression of IgM, IgD, IgK or IgL. 36 patients were removed due to inadequate DNA concentrations of a sequential sample. 4 patients were removed after sequential sample mismatch was confirmed using SNP probes and STR typing. This left a final cohort of 178 patients with high quality sequential tumor samples taken at presentation and first relapse for CNA profiling **Figure 3-3**. Of the 178 patients, 67 patients had adequate RNA to also allow sequential gene expression profiling.

Therefore, in total 122 patients were removed during pre-analysis CNA quality control checks. Comparison of their demographics to the final 178 CNA evolution cohort did not find any significant differences. Outcomes were also

similar to those reported in chapter 4; overall median time to progression of the 122 removed patients was 23.7 months (range 1.3 to 82.1 months) and median follow up 48.1 months (range 1.3 to 83.9 months).

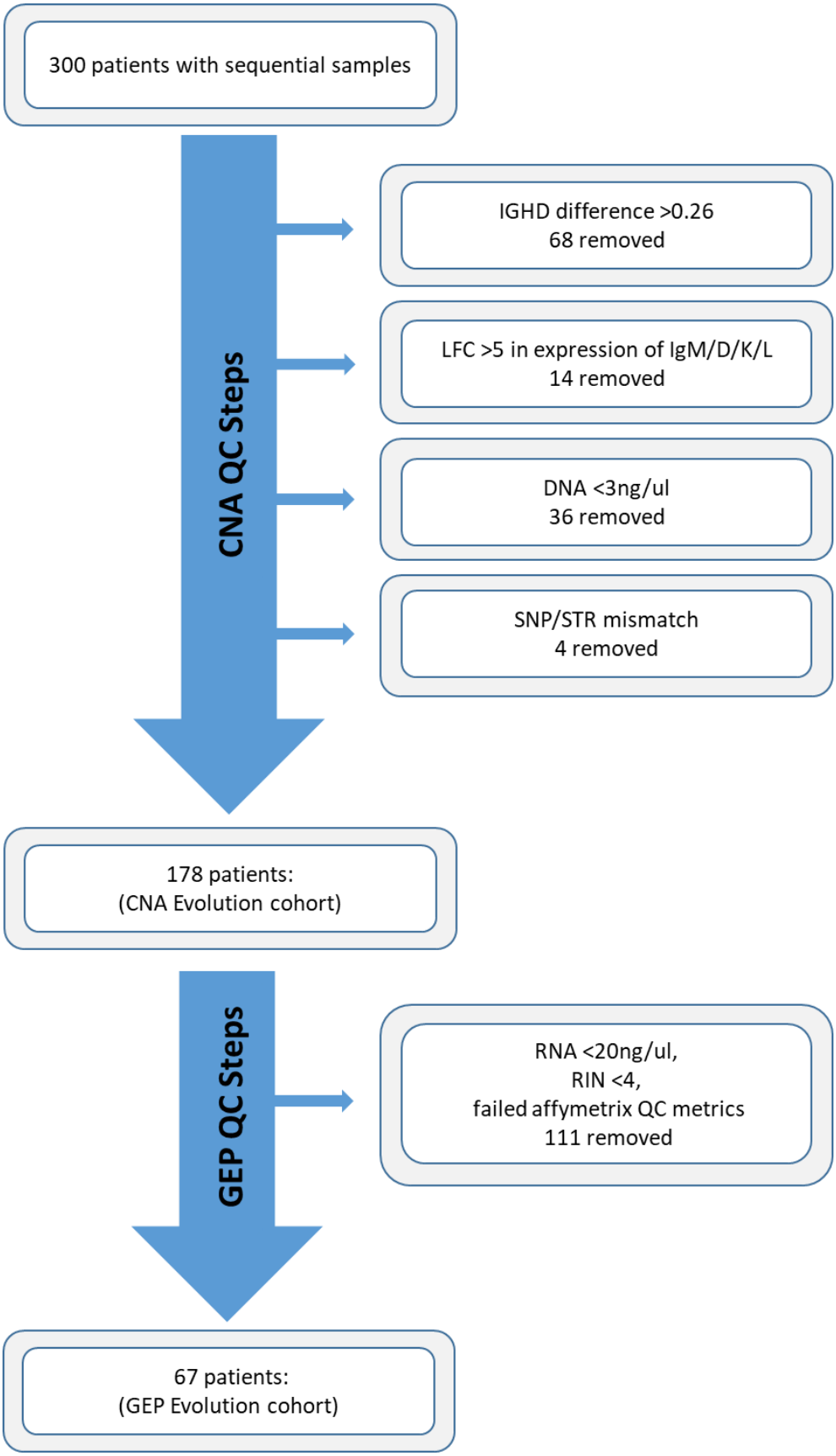

Figure 3-3 Summary of quality control steps and patients removed; QC: Quality Control; LFC: log fold change, SNP: single nuclear polymorphism; STR: Short tandem repeat; RIN: RNA integrity number.

Chapter 4: CNA evolution cohort- patient demographics

4.1 Introduction

The MXI trail was a large national study which recruited 4420 patients, many of which are yet to relapse and remain on trial. Patients who relapsed before the 31st of May 2019 with bone marrow aspirates at presentation and relapse were reviewed. 178 patients had adequate DNA for molecular profiling at each time point and passed the subsequent quality control checks discussed in chapter 3, thus forming the CNA evolution cohort.

Since a larger number of patients remain on active trial treatment without relapse, I compared baseline demographics to investigate for systematic bias (**Table 4-1**).

4.2 Baseline Demographics

Baseline demographics were similar between the CNA evolution cohort and the overall trial population (n=4242), with the exception of sex and age. The CNA evolution cohort had a significantly higher ratio of men to women; 73.6% men compared to 57.9% in the overall trial population (Chi-square =16.8; degree freedom =1; $P<0.001$). Whilst mean age was similar, the proportion of age categories differed significantly with a higher ratio of patients <75 years old in the CNA evolution cohort (Chi-square =8.6, degrees of freedom =2, $P=0.013$). There were no other significant differences seen between the CNA evolution cohort demographics and overall trial population.

		CNA evolution cohort (n=178)		Overall trial population (n=4242)	
Sex, n (%)	F	47.0	(26.4)	1788.0	(42.1)
	M	131.0	(73.6)	2454.0	(57.9)
Age, mean (SD)	mean	64.9	(9.7)	65.7	(10.3)
n (%)	≤75	160.0	(89.9)	3470.0	(81.8)
	76-80	15.0	(8.4)	530.0	(12.5)
	>80	3.0	(1.7)	242.0	(5.7)
PS, n (%)	0	58.0	(32.6)	1512.0	(35.6)
	1	72.0	(40.4)	1665.0	(39.3)
	2	27.0	(15.2)	630.0	(14.9)
	3	12.0	(6.7)	196.0	(4.6)
	NA	9.0	(5.1)	217.0	(5.1)
PP, n (%)	IgA	54.0	(30.3)	1034.0	(24.4)
	IgD	2.0	(1.1)	35.0	(0.8)
	IgG	98.0	(55.1)	2608.0	(61.5)
	IgM	1.0	(0.6)	15.0	(0.4)
	LCO	22.0	(12.4)	516.0	(12.2)
LC, n (%)	Kappa	118.0	(66.3)	2785.0	(65.7)
	Lambda	59.0	(33.1)	1410.0	(33.2)
Hb, mean (SD)		105.9	(19.4)	108.4	(19.4)
Creatinine mean (SD)		98.7	(52.3)	102.0	(58.3)
Calcium, mean (SD)		2.5	(0.3)	2.4	(0.3)
Albumin, mean (SD)		34.7	(6.6)	35.2	(6.7)
LDH, mean (SD)		326.7	(287.3)	302.4	(175.7)
B2M, mean (SD)		5.3	(6.6)	5.4	(5.0)
ISS, n (%)	I	40.0	(22.5)	1055.0	(24.9)
	II	85.0	(47.8)	1631.0	(38.4)
	III	46.0	(25.8)	1229.0	(29.0)
	NA	7.0	(3.9)	327.0	(7.7)
TE, n (%)		100.0	(56.2)	2468.0	(58.2)
Induction, n (%)	CRD	34.0	(34.0)	-	
	CTD	55.0	(55.0)	-	
	KCRD	11.0	(11.0)	-	
Maintenance, n (%)	Len	21.0	(21.0)	707.0	(28.6)
	Len + Vor	11.0	(11.0)	185.0	(7.5)
	Observation	31.0	(31.0)	489.0	(19.8)
	NR	37.0	(37.0)	1087.0	(44)
TNE, n (%)		78.0	(43.8)	1774.0	(41.8)
Induction, n (%)	CRDa	43.0	(55.1)	-	
	CTDa	35.0	(44.9)	-	
Maintenance, n (%)	Len	21.0	(26.9)	385.0	(21.7)
	Len + Vor	3.0	(3.8)	108	(6.1)
	Observation	26.0	(33.3)	292	(16.5)
	NR	28.0	(35.9)	989	(55.7)

Table 4-1: CNA evolution cohort baseline demographics; PS: performance status; PP: paraprotein; LC: light chain; LDH: lactate dehydrogenase; B2M: beta2 macroglobulin; ISS: International staging system; TE: transplant eligible; TNE: transplant non eligible; Len: Lenalidomide; Vor: Vorinostat; NR Not randomised.

4.3 Baseline cytogenetics

Frequency of baseline high risk cytogenetics were compared between the CNA evolution cohort and overall MXI population with complete cytogenetic profiles (**Table 4-2**)[12]. Frequencies were comparable in t(4;14), t(14;16), t(14;20) and Del(17p). The CNA evolution cohort had a significantly higher frequency of gain/amp(1q) at baseline; 44.4% versus 34.5% (*P*=0.014).

		CNA evolution cohort		**Overall trial population (Shah et al [12])**	
HR lesion, n (%)	t(4;14)	24	(13.5)	163	(15.7)
	t(14;16)	5	(2.8)	38	(3.7)
	t(14;20)	1	(0.6)	13	(1.3)
	Gain/Amp (1q)	79	(44.4)	357	(34.5)
	Del(1p)	27	(15.2)	107	(10.3)
	Del 17p	19	(10.7)	96	(9.3)

Table 4-2 CNA evolution cohort comparison of baseline high risk cytogenetics

4.4 Treatment

Treatment pathway and randomisations of the CNA evolution cohort are summarised in **Figure 4-1.** The proportion of treatment intensities reflected that of overall MXI population, with 100 (56.2%) patients TE and 78 (43.8%) TNE. Of these 113 (63.5%) completed maintenance randomisation; 42 (23.6%) to Lenalidomide, 14 (7.9%) to Lenalidomide plus vorinostat and 57 (32.0%) to observation. 65 (36.5%) of patients were deemed unsuitable for maintenance at the time of randomisation.

4.5 Follow up

Overall median time to progression was 20.7 months (range 3.7-71.9 months) and median follow up 47.0 months (range 5.2 -83.3 months).

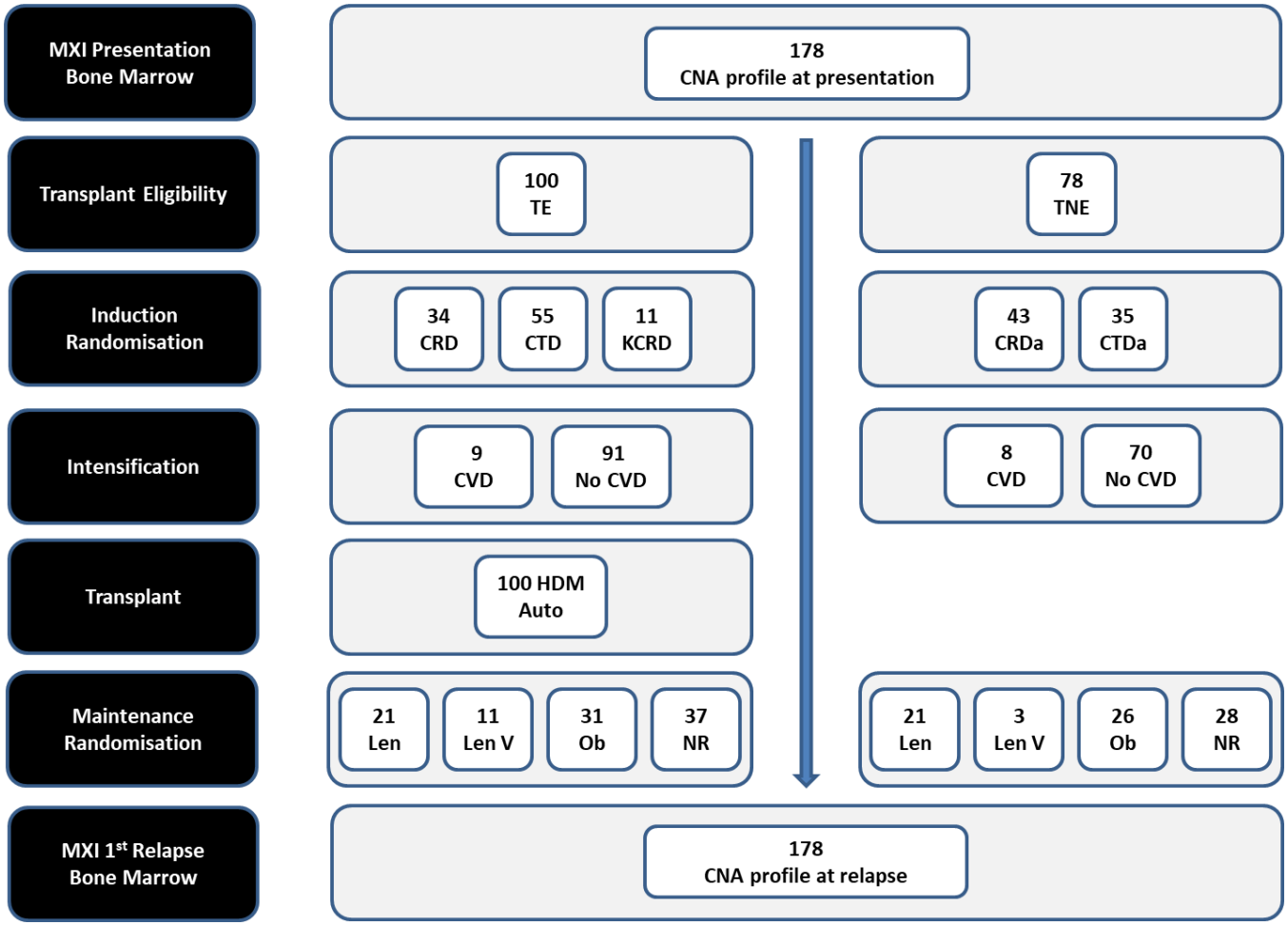

Figure 4-1 Summary of treatment randomisations in the CNA evolution cohort; MXI: Myeloma XI; TE: transplant eligible; TNE: Transplant non-eligible; C: Cyclophosphamide; R: lenalidomide; D: dexamethasone; T: thalidomide; K: carfilzomib; V: velcade; HDM: high dose melphalan; Len: lenalidomide; V: vorinostat; Ob: observation; NR; not randomised; a: attenuated.

Chapter 5: CNA evolution results- overall change

5.1 Introduction

Previous studies of myeloma using sequential tumour samples have demonstrated molecular evolution at relapse. Differing patterns of change have been observed including branching, linear, linear loss and stable; attributed to complex sub-clonal dynamics in a model of Darwinian evolution.

My hypothesis proposes that changes in molecular profile at relapse are significantly related to myeloma progression and treatment resistance. As the molecular landscape of myeloma is dominated by numerical and structural chromosome abnormalities, I have focused on CNA using dMLPA. The technique provides a digital karyotype (see section 2.2.2.1), by way of introduction to the data, I have summarised the frequency of chromosome arm CNA at presentation (**Figure 5-1).** The high frequency of gain and amplification in in odd chromosomes reflects HRD trisomies. Non HRD CNA observed in more than 10% of tumors are listed in **Table 5-1.** Gain/amp(1q) and del(13q) were the most common CNA, observed in 44% and 39% of cases, respectively.

In this chapter I will consider overall evolution of CNA at relapse; comparing cumulative frequency of CNA between time points and describing patterns of evolution. I will then consider the change in frequency of specific CNA, in the context of interstitial CNA (chromosome arm) and focal CNA (sub chromosomal). Due to branching evolution I will describe frequency at relapse by:

- New CNA (Acquisition of new CNA at relapse)
- Loss of CNA (Resolution of baseline CNA at relapse)
- Net change of CNA at relapse (New CNA - Loss CNA)

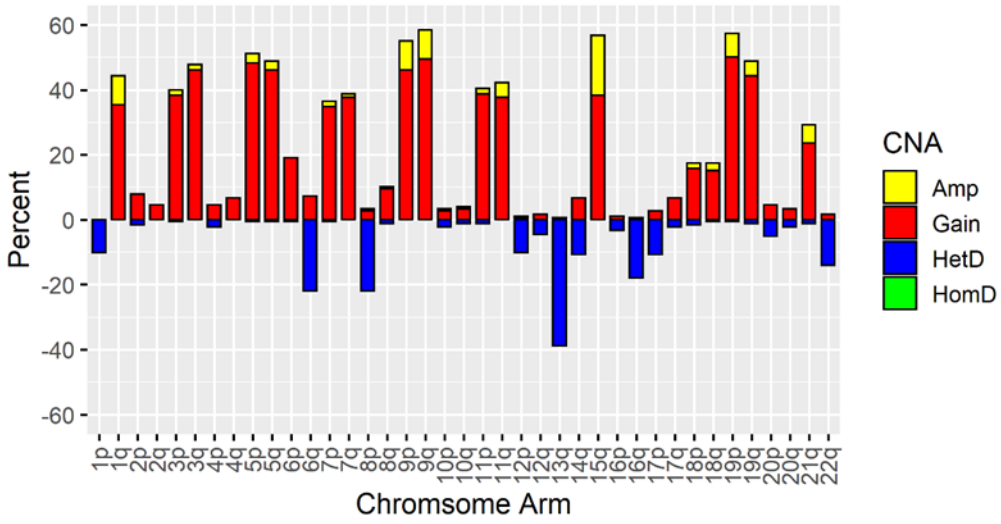

CNA	n	%
Gain/Amp(1q)	79	44
Del(13q)	69	39
Del(6q)	39	22
Del(8p)	38	22
Gain(6p)	34	19
Del(16q)	32	18
Gain(18p)	28	16
Gain(18q)	27	15
Del(22q)	25	14
Del(14q)	19	11
Del(17p)	19	11
Del(1p)	19	11
Gain(8q)	17	10

Figure 5-1 Overall frequency of interstitial CNA at presentation (Top). Table 5-1 Non HRD CNA occurring in ≥10% of patients at presentation (Bottom).

5.2 Evolution of CNA at relapse per patient

Overall there was a significant net increase in the average number of CNA per patient at relapse: 11.5 (range 0-34) at presentation vs. 12 (range 0-29) at relapse (Wilcoxon Signed-Ranked *P* = 0.0058).

There were clonal changes in CNA from presentation to relapse in the majority of tumors, with 87.1% showing an evolving pattern at relapse vs. 12.9% without change. The majority of CNA changes were interstitial (73.2%) compared to focal (26.8%).

Based on interstitial and focal CNA, I classified changes as per molecular evolution categories; branching, linear, linear loss and stable and found 45.5%, 22.5%, 19.1% and 12.9% of tumors to follow respective patterns (**Figure 5-2)**.

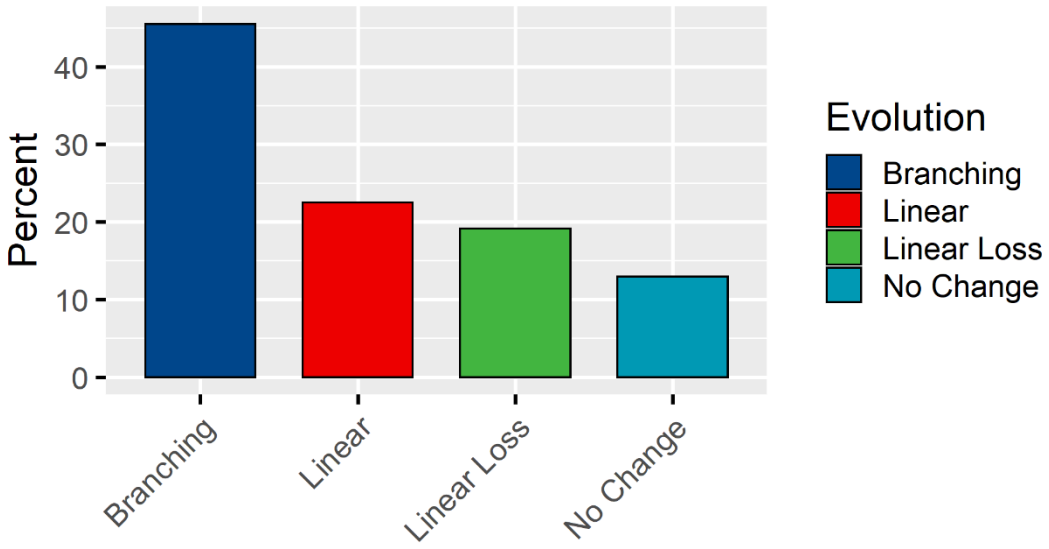

Figure 5-2 Frequency of evolutionary patterns across all patients.

5.3 Change in interstitial CNA

5.3.1 New CNA

Frequency of new interstitial CNA at relapse is summarised in **Figure 5-3** and **Table 5-2.** The most frequent new CNA to evolve at relapse were gain/amp(1q) observed in 34 (19%), del(13q) in 17 (10%), gain/amplification(11q) in 16 (9%) and del(17p)/*TP53* in 15 (9%) tumors. The high frequency of new gain/amp(1q) and new del(13) at relapse mirrors the high frequencies of each observed at presentation (**Figure 5-1, Table 5-1)**, suggesting a potential role as key driver events in disease progression.

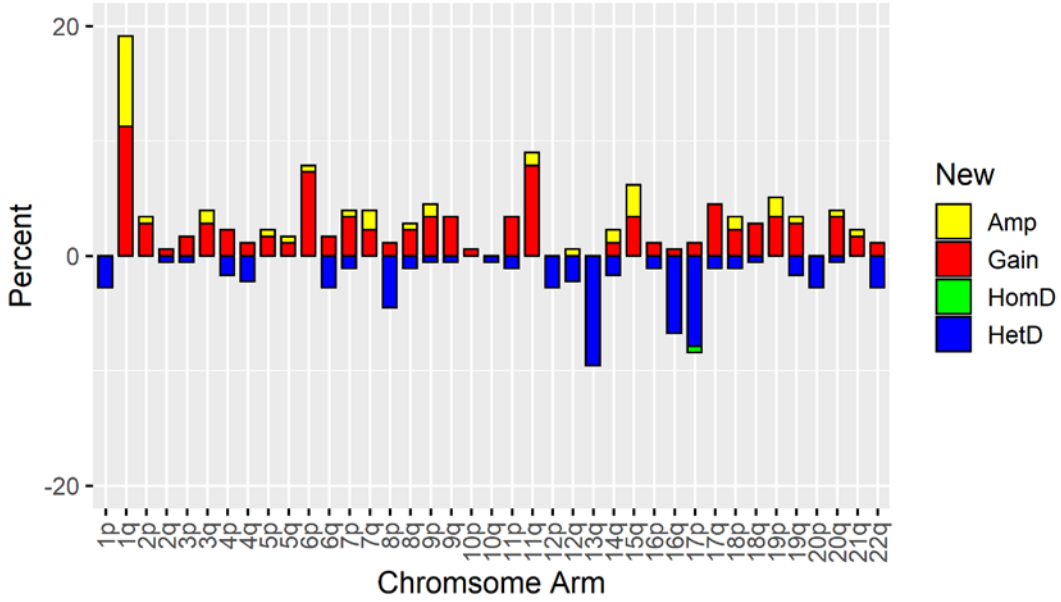

New CNA	n	%
Gain/Amp(1q)	34	19
Del(13q)	17	10
Gain/Amp(11q)	16	9
Del(17p)	15	9
Gain/Amp(6p)	14	8
Del(16q)	12	7
Gain/Amp(15q)	11	6
Gain/Amp(19p)	9	5

Figure 5-3 Frequency of new interstitial CNA at relapse (Top). Table 5-2 New interstitial CNA at relapse with a frequency of ≥5% (Bottom).

5.3.1.1 Evolution of CNA seen at presentation

Progressive evolution of CNA seen at presentation was also observed. This was most common in 1q, where 11 (17.5%) tumours with gain(1q) at presentation gained further copies resulting in amp(1q) at relapse. This was also observed for gain(15q) and gain(19p), with 3(4.4%) and 2 (2.3%) tumours respectively acquiring further copies resulting in amplification at relapse. There was 1 case of homozygous deleted 17p at relapse, which evolved from heterozygous deletion at presentation.

5.3.1.2 Evolution of sub-clonal driver CNA

The high CNA resolution of digitalMLPA has previously been demonstrated to enable detection of sub-clonal CNA [36, 40]. I therefore also looked for evidence of sub-clonal evolution; investigating samples with new CNA at relapse I looked back for evidence of sub-clonal CNA at presentation. I focused on driver events with prognostic significance; 1q and 17p.

Sub-clonal gain at presentation was assigned when the majority of 1q probes had dMLPA copy number ratios of 1.05 - 1.2. Sub-clonal deletion at presentation was assigned when the majority of 17p probes had ratios of 0.76-0.95. 6 tumours (30%) with new gain(1q) at relapse showed evidence of a possible minor sub-clone at presentation. This was more pronounced at 17p/*TP53*, where 7 tumours (50%) with new del(17p) at relapse had evidence of sub clonal aberration at presentation (**Figure 5-4**). While the dMLPA technique accepts the ratio of individual probes to vary up to 0.1 within normal diploid reference control samples, my detection of minor sub-clones was underpinned by concordant ratios of neighbouring probes within each chromosome arm per patient.

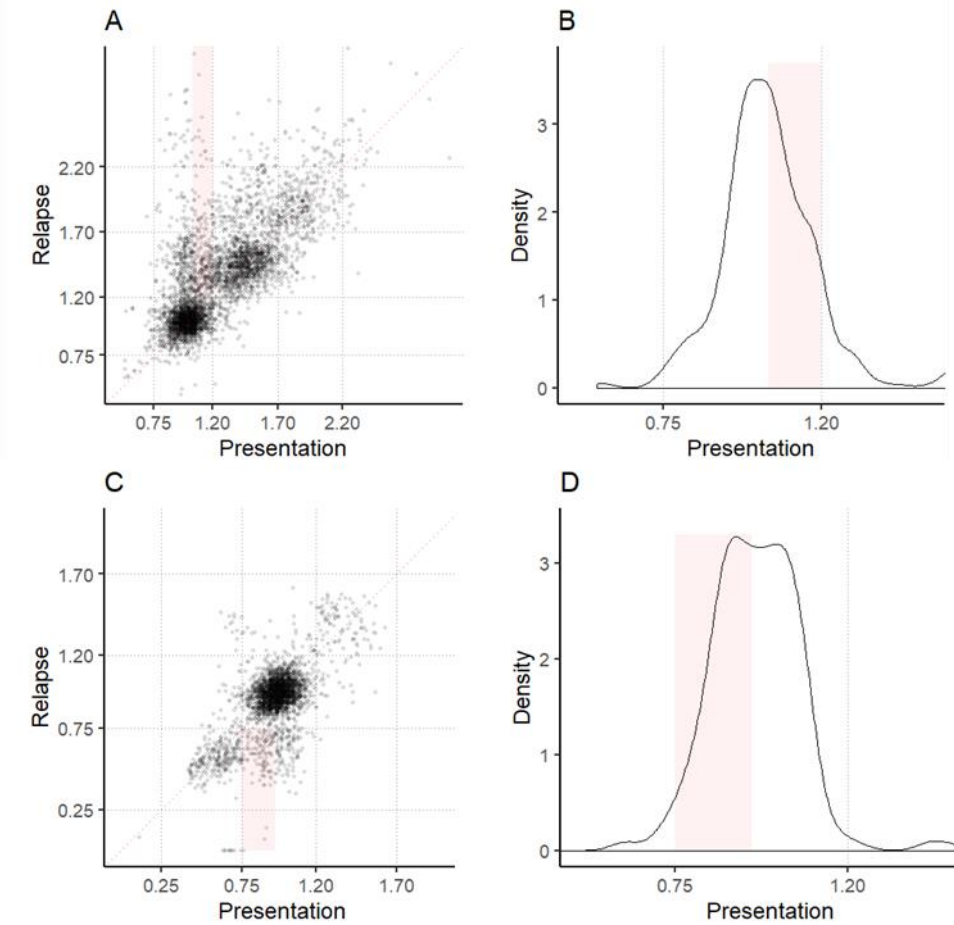

Figure 5-4 Emergence of sub-clonal to clonal CNA (A, B) gain(1q) and (C, D) del(17p). Clonal gain(1q) or del(17p) was considered in relapse tumors when the majority (>50%) of relevant dMLPA probes had normalised values of >1.2 or ≤0.75 respectively. The potential presence of sub-clonal aberrations in presentation tumors was considered when the majority of relevant dMLPA probes were >1.05 ≤1.20 for gain(1q) and >0.75 ≤0.95 for del(17p). Left hand side: scatter plots of normalised values of relevant dMLPA probes at presentation (x axis) and relapse (y axis). Right hand side: density plots of normalised values of relevant dMLPA probes at presentation. Pink shading indicates tumors with probes values sitting within sub-clonal range at presentation

5.3.2 Loss of CNA

Some regions with copy number gain at baseline were recurrently found to revert to diploid status at relapse, specifically gain/amp of 19q in 32 (18%) tumours. Chromosome arm CNA that revert to diploid status at relapse in >5% of tumors are summarised in **Figure 5-5** and **Table 5-3.**

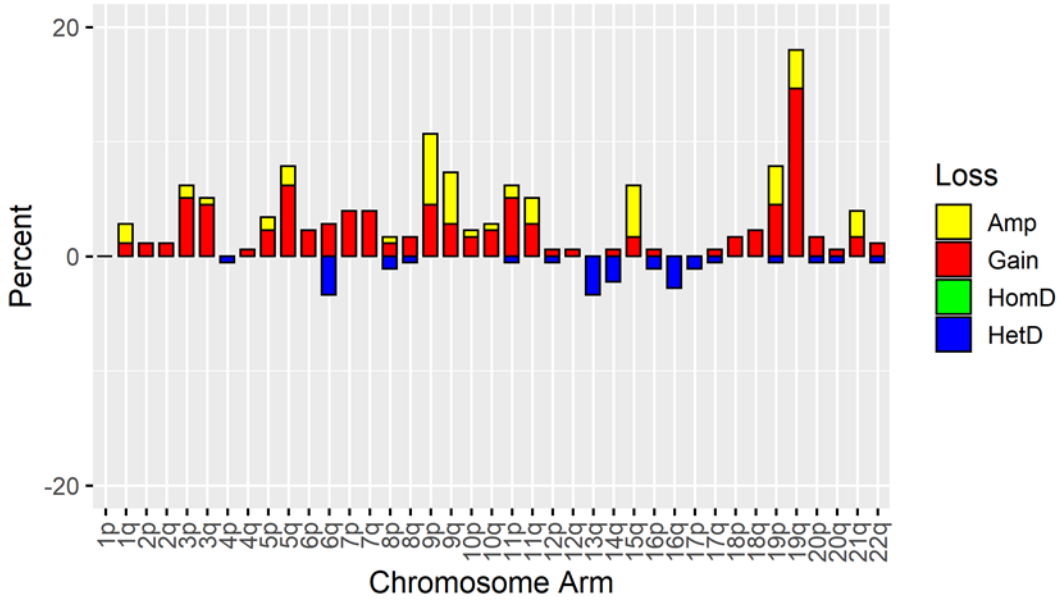

CNA	n	%
Gain/Amp(19q)	32	18
Gain/Amp(9p)	19	11
Gain/Amp(5q)	14	8
Gain/Amp(19p)	14	8
Gain/Amp(9q)	13	7
Gain/Amp(11p)	11	6
Gain/Amp(15q)	11	6
Gain/Amp(3p)	11	6

Figure 5-5 Frequency of interstitial CNA loss at relapse (Top). Table 5-3 Loss of interstitial CNA with a frequency of ≥5% (Bottom).

5.3.3 Net change in CNA

As a consequence of branching evolution, the frequency of some CNA appear relatively stable at relapse, despite evidence of evolution within matched samples. For example new del(16q) evolved in 12 tumors at relapse, but another 5 tumours with del(16q) at presentation reverted to diploid status at relapse. A stable net frequency of CNA at relapse points away from significance/driver potential of the lesion.

In contrast CNA with a clear net increase in frequency at relapse highlight those more likely to be drivers of disease progression. Within my cohort interstitial CNA with a net increase in frequency of >5% at relapse include gain/amp(1q), del(13q) and del(17p), each increasing from 79 to 100, 69 to 80 and 19 to 30, cases respectively (**Figure 5-6)**. The net change in gain/amp(1q) and gain/amp(19q) were statistically significant, increasing from 44% to 56% (*P*=0.034) and decreasing from 49% to 37% (*P*=0.024) respectively.

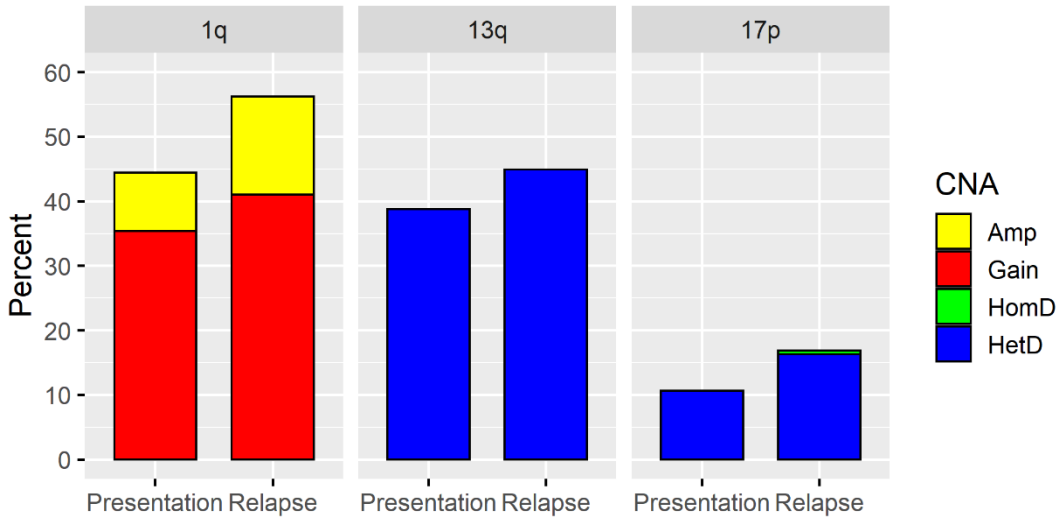

Figure 5-6 Frequency of 1q, 13q, and 17p CNA at sequential time points; Amp: amplification; HetD: heterozygous deletion; HomD: homozygous deletion.

5.4 Focal CNA

In contrast to 1q, where CNA involve the whole chromosome arm, focal CNA was more common in 1p. The contrast of evolving new CNA between 1p and 1q at relapse is demonstrated by Heatmap in **Figure 5-7.** Evolution of focal CNA was most common in 1p, 11q and 8q.

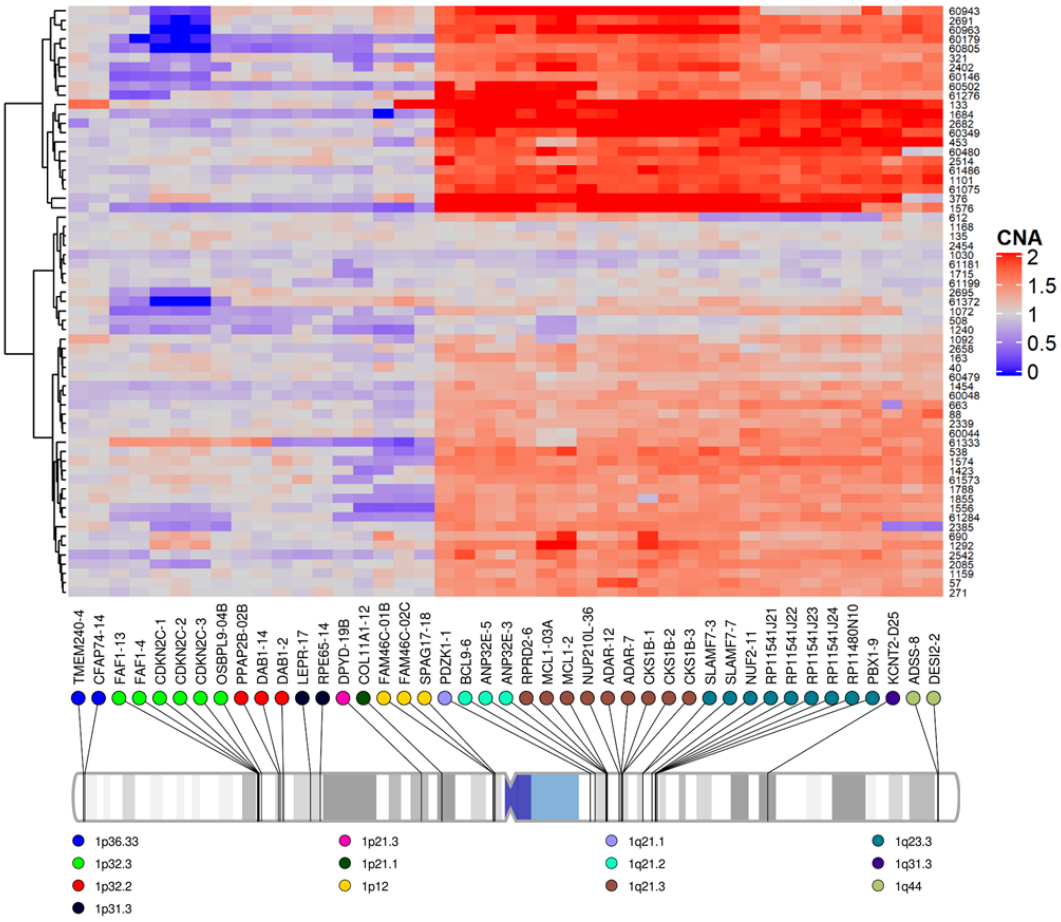

Figure 5-7 Heatmap of evolving chromosome 1 CNA at relapse. 63 tumours with new change in this region at relapse. On the left (y-axis) dendrogram representing unsupervised clustering analysis of emerging CNAs in areas interrogated by digitalMLPA probes, which are annotated with gene name and chromosomal location below (x-axis). Probe ratio colour coded as per scale representing normalised digitalMLPA copy number.

5.4.1 Focal 1p deletion

New focal deletion at relapse was most frequent in 1p seen in 16 (9.0%) tumours; 9 (5.1%) at 1p32.3 implicating *FAF1, CDKN2C* and 4 (2.1%) at 1p12 implicating *FAM46C.* Focal deletion of 1p32.3 and 1p21.1-1p12 were mutually exclusive in all cases except one patient who acquired both at relapse, suggesting divergent evolutionary trajectories.

Clonal evolution of 1p deletions found at presentation was also observed. There were 8 (4.5%) cases with focal 1p32.3 deletion at presentation (4 heterozygous and 4 homozygous). 3 of 4 (75%) heterozygous 1p32.3 deletions evolved to homozygous deletion at relapse. Whereas only 1 of 4 (25%) homozygous 1p32.3 deletions reverted to heterozygous status at relapse. Resolution of presentation CNA to diploid status at relapse was seen in 9 of 22 cases (41.0%) with focal 1p12 deletion, resulting in a net decrease of the aberration.

5.4.2 Focal 11q deletion

The second commonest new focal deletion at relapse involved 11q22.2-11q22.3 (*BIRC2/3, ATM*). Observed in 5 (2.8%) tumours; 3 heterozygous and 2 homozygous deletions.

Clonal evolution of 11q deletions found at presentation was also observed. There were 6/178 (3.4%) cases with deletion of 11q22.2-11q22.3 (*BIRC2/3, ATM*) at presentation; 2 heterozygous and 4 homozygous deletions. Of presenting heterozygous deletions; 1 (50%) evolved to homozygous at relapse and 1 (50%) reverted to diploid status. Of presenting homozygous deletions, 1 (25%) reverted to heterozygous deletion at relapse.

5.4.3 Focal 8q gain

The most frequent new focal increase in CNA at relapse involved 8q24.21 (*MYC*); with 6 (3.4%) and 4 (2.2%) new cases of gain or amplification respectively.

Clonal evolution of 8q24.21 gain or amplification identified at presentation was also observed. 15 (8.4%) tumours demonstrated gain of 8q24.21 at presentation, of which 2 (13.3%) gained a further copy at relapse resulting in

amplification. Conversely 3 (20%) lost a copy reverting to diploid status at relapse.

5.5 Evolution of High risk lesions

A particularly poor outcome has been demonstrated in patients with double-hit or triple-hit tumors, characterised by the simultaneous presence of ≥2 high risk aberrations t(4;14), t(14;16), t(14;20), gain(1q), del(1p) or del(17p) at presentation[7, 12, 17].

The frequency of high risk IgH translocations remained stable over time. However due to evolution of high risk CNA at relapse, I observed an increase of frequency of tumors with double-hit, triple-hit and even quadruple-hit at relapse (**Figure 5-8**). The frequency of each high risk combination per time point is summarised in **Figure 5-8**. Interestingly the frequency of single-hit tumors decreased at relapse, suggesting the evolution of high risk lesions occurs preferentially within tumors with at least 1 high risk lesion at baseline. This correlates with the findings reported by Keats et al. discussed in section 1.2.2.1.1 [28]

Amplification of 1q has been proposed to be an additional independent marker of high risk by some studies [41]. Approximately two thirds of amp(1q) tumors were “double-hit”, i.e. also carried t(4;14), t(14;16), t(14;20), or del(17p). Of all 178 relapsed tumors, nearly 10% carried both amp(1q) and at least 1 more high risk lesion. (**Figure 5-8**).

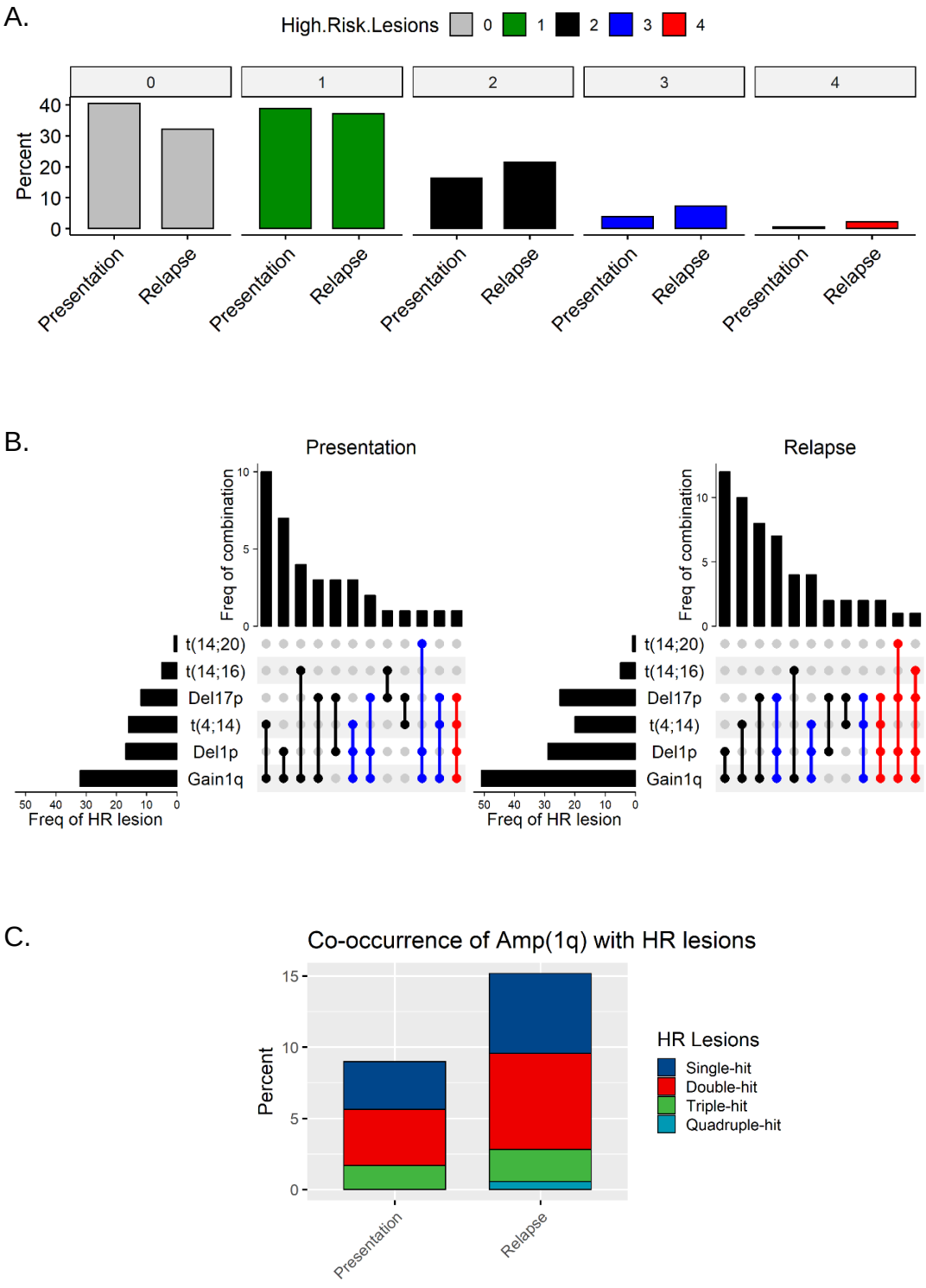

Figure 5-5-8 (A) Co-occurrence of high risk lesions at sequential time point; (B) Upset plots of presentation (left) and relapse (right) tumours, each showing the frequency of individual high risk lesions (left), combination of lesions (centre lines with dots indicating presence of lesion) and frequency of specific combination (top); (C) Overall frequency of amp(1q) at presentation and relapse with proportion of amp(1q) tumours showing 1q as the only high risk aberration (single hit) or in combination other high risk lesions (double, triple or quadruple hit).

5.6 Discussion

As previously reported branching linear and stable patterns of clonal evolution were observed at relapse, with non-stable evolution the predominant finding. The high proportion of non-stable evolution supports my hypothesis that changes in the molecular landscape of myeloma in response to therapy are central to emergence of disease progression and treatment resistance.

Digital MLPA uses a targeted approach to provide a virtual karyotype. I suspect non stable evolution could be even higher using genome wide techniques due to increased capture of focal CNA. However, Whole Genome Sequencing (WGS) by Next-Generation Sequencing (NGS) would require significant resources in terms of cost and high performance computing, placing it beyond the limits of this project. Importantly, dMLPA probes are highly curated for myeloma specific CNA based on published genome wide CNA data. Furthermore, dMLPA works with a fraction of the DNA input required for WGS, which is particularly relevant since DNA quality from myeloma tumours is often limited in comparison to other haematological cancers. Due to these factors, dMLPA is clinically relevant and the results generated here can be readily applied in a resource limited setting.

Disease progression within this cohort was characterised by emergence of clones with new interstitial CNA in the majority of tumours. New CNA most commonly involved gain or amplification of 1q highlighting its key role in disease progression. Other common new CNA included del(13q) and del(17p).

5.6.1 Gain (1q)

Genomic instability has been described as a hallmark feature of gain(1q). A potential mechanisms termed “jumping 1q syndrome” was described by Sawyer et al, in which tumours with gain(1q) were demonstrated to have unstable pericentromeric chromatin leading to recurrent translocations or segmental duplications; with increasing 1q copy number noted to correlate with worsening genomic instability[42]. More recently, whole genome sequencing data has demonstrated an association of gain/amp(1q) with

chromothripsis which involves catastrophic chromosomal shattering and random re-joining [43].

The association with genomic instability was demonstrated within my cohort with gain or amplification of 1q frequently co-evolving with other CNA. All tumours with new amp(1q) at relapse co-evolved with at least 2 other new CNA (range 2 to 12). Furthermore amp(1q) frequently co evolved with other high risk CNA. Previous description of the jumping 1q syndrome reported frequent deletions of the receptor chromosome which commonly involved 1p and 17p, providing a potential explanation for the high level of co evolution[42]. This finding either implicates gain/amp(1q) directly in the generation of CNA as per the “jumping 1q” hypothesis or highlights 1q as a driver region that provides a synergistic advantage for genetically unstable tumours. The mechanistic details of chromosome instability in myeloma are still under investigation.

Following my majority rule to identify CNA, focal CNA in 1q was rare. This correlates with findings from the CoMMpass study, which examined over a 1000 myeloma tumours and noted whole arm CNA to be most common in 1q[44]. While other studies have attempted to implicate specific driver genes form 1q, here a lack of focal 1q CNA prevents such differentiation. However it is important to note that no study has been able to identify a consistently deregulated pathway in gain(1q).

Examining my results in retrospect, potential areas of focal amplification (tandem duplications) within tumours that also have whole arm gain of 1q would not be identified using my majority rule. **Figure 5-7** shows that some tumours with new gain(1q) also have added focal amplification, for example of *MCL1* or *CKS1B*. I therefore re-examined the evolution of new gain or amplification at relapse per chromosome band (regardless of the presence or absence of whole arm CNA). The frequency of CNA in 1q21.2 and 1q21.3 was higher in comparison to other 1q bands **(Table 5-9),** suggesting a potential location for key genes driving the effects of gain(1q). The dMLPA 1q21.2 and 1q21.3 probes specifically map to *MCL1, CKS1B, ADAR, BCL9, ANP32E, RPRD2* and *NUP210L.*

Chromosome band	New Amp	New Gain	Total New
1q21.1	14	17	31
1q21.2	16	20	36
1q21.3	19	16	35
1q23.3	12	18	30
1q31.3	13	19	32
1q44	9	20	29

Table 5-4 Frequency of CNA per 1q chromosome band.

MCL-1 belongs to the *BCL2* family of anti-apoptosis proteins, expression of this gene is required for survival of normal plasma cells and myeloma cells[44]. Increased expression of *MCL1* in myeloma cells leads to apoptosis resistance associated with disease progression and shorter OS[45]. Increased expression has been shown to correlate with increasing copy number of 1q [44]. The dependency of myeloma cells on *MCL1* for survival is enhanced through expression of IL-6 from the bone marrow microenvironment. The IL-6 receptor gene (*IL6R*) is also located on 1q21, increased expression correlates with increasing 1q copy number [44, 46]. Binding of IL-6 to its receptor activates JAK2/STAT3, increasing *MCL1* transcription.

CKS1B belongs to the cyclin kinase subunit 1 protein family and is known to play an important role in cell proliferation[47]. Increased expression of *CKS1B* has been associated with worse clinical outcome in myeloma and shown to increase multidrug resistance in myeloma cell lines. It facilitates myeloma cell growth through; activation of cyclin-dependent kinases, SKP2-mediated ubiquitination of the tumor suppressor gene $p27^{Kip1}$ and upregulation of the STAT3 and MEK/ERK pathways [20, 48, 49].

ADAR1 is responsible for RNA editing, overexpression leads to abnormal hyper-editing and proliferation in myeloma cells which has been associated with inferior survival. Increased expression of *IL6R* and *ADAR1* have been demonstrated in amp(1q21), resulting in myeloma cell proliferation through the hyper-activation of the STAT3 pathway[44]

BCL9 is a component of the Wnt pathway, playing an important role in the transcriptional activity of β-catenin, dysregulation of this pathway has been

implicated in a number of cancers including myeloma. Increased expression has been associated with increased tumour proliferation[47] and overexpression was observed in 60% late stage myeloma patients and cell lines by Van Andel et al [50].

ANP32E is a histone acetyltransferase inhibitor involved in chromatin remodeling and transcription regulation. Increased expression has been demonstrated in gain(1q) tumours and associated with worse OS [51].

The dMLPA 1q21 probes provide a focused list genes associated with myeloma proliferation/progression and highlight potential therapeutic targets. Furthermore the majority of these genes are implicated in JAK/STAT3 activation providing a unifying pathway that could widen therapeutic targets/exploration. Investigations into the role of JAK inhibitors in treating myeloma are in early stages; one group reporting a clinical response to JAK2 inhibitor Ruxolitinib in combination with lenalidomide and dexamethasone for relapsed refractory patients[52].

5.6.2 Del(13q)

Del(13q) is frequently observed in MGUS and therefore thought to be an early event in clonal evolution[11]. As the second most common new CNA to evolve at relapse it continues to provide clonal advantage at later stages of progression. Frequent co-occurrence with gain/amp(1q) suggests a synergistic relationship of the aberrations. The majority of deletions were interstitial making identification of key genes challenging.

Focal homozygous deletion of *RB1* was observed within heterozygous 13q deletions; 3 tumours at presentation and newly acquired in another 2 tumours at relapse. *RB1* was the first tumour suppressor gene identified. RB (the protein encoded by *RB1*) plays a pivotal role in negative control of the cell cycle, deletions facilitates tumour proliferation. A previous study has also reported an increased prevalence of *RB1* homozygous deletion at relapse supporting its role in disease progression, it was also shown to have an independent association with worse prognosis [53].

DIS3 is also located on 13q, as one of the most frequently mutated genes in myeloma it has also been implicated in pathogenesis [54]. While focal deletions of *DIS3* were not observed in my cohort a high prevalence of *DIS3* mutations means bi allelic inactivation of the gene is possible [54].

Attributable to del(13q), deletion of *MIR15A*/*MIR16-1* has also been demonstrated to accelerate clonal proliferation of plasma cells and promote extramedullary disease in mouse models[55]. The study also suggests loss of *MIR15A*/*MIR16-1* expression could drive the clonal selection of del(13q) tumours[55]. In my cohort focal homozygous deletion of *MIR15A* was observed in one tumour from presentation. Del(13q) is also common in chronic lymphocytic leukaemia (CLL) and results in loss of expression of *MIR15A/MIR16-1* which leads to upregulation of *BCL2[56].* While this suggests a potential role for the BCL2 inhibitor venetoclax in del(13q) tumours, the drug was shown to have inferior OS in non t(11;14) tumours [57] where the frequency of del(13q) would have been higher.

5.6.3 Del(17p)

New del(17p) was also common at relapse, this aberration results in loss of *TP53*, a tumour suppressor gene with a critical role in cell cycle control and apoptosis. Cellular stress including DNA damaging drugs activate cellular p53 which induces cell cycle arrest and apoptosis. Disruption of *TP53* expression through deletion or mutation therefore facilitates chemotherapy resistance and early relapse. For this reason it is well established as adverse prognostic marker in a number of cancers. In CLL the adverse prognostic effects of *TP53* disruption have been successfully by-passed through the use of targeted molecular therapies such as tyrosine kinase inhibitor Ibrutinib and *BCL2* inhibitor Venetoclax[58]. This highlights the need for targeted novel agents in myeloma.

5.6.4 New focal CNA

Although observed at a lower frequency than interstitial, recurrent new focal CNA highlight specific genes that can be directly implicated in myeloma progression. Their importance further signified through evidence of clonal

evolution; for example evolution of focal heterozygous deletion at presentation to focal homozygous deletion at relapse.

Deletion of 1p32.3 (*CDKN2C*, *FAF1)* was the most common new focal CNA at relapse. The protein expressed by *CDKN2C* interacts with CDK4 and CDK6 to inhibit progression through the cell cycle, deletion therefore facilitating proliferation. *FAF1* mediates apoptosis, deletion therefore also facilitating uncontrolled tumour proliferation[11]. The second most common was focal del(11q22.2-11q22.3) (*BIRC2/3, ATM*). ATM is responsible for sensing DNA damage at the G1/S checkpoint, deletion would therefore allow tumours to proliferate in the presence of DNA damage, providing a mechanism of chemotherapy resistance and molecular evolution. Walker et al demonstrated worse prognosis in tumours with ATM disruption [59].

Gain/amp of 8q24.21 (*MYC*) was the most common new focal copy number increase at relapse. Dysregulation of *MYC* has been shown to play an important role in development and progression of myeloma. Signified by the numerous mechanisms of dysregulation observed in myeloma; translocations, copy number gain and mutations e.g. *NRAS and KRAS* [60]. *MYC* has a direct role in DNA replication, over expression can be linked to genomic instability, proliferation and immune evasion. The numerous mechanisms of this oncogene make it an important candidate for therapeutic targeting. There has been substantial work to target MYC through direct and indirect inhibition with a number of agents in early clinical trials [60].

5.6.5 Loss of CNA

Evolution of CNA also resulted in loss of aberrations at relapse. Recurrent loss of a CNA could suggest a survival advantage to clones without the aberration. From my data it is not clear if loss of CNA results from proliferation of an earlier sub-clone lacking said CNA or as a result of chromosome instability (CIN) leading to new deletions. I suspect linear loss reflects the former and branching the latter. Previous studies have demonstrated resolution of homozygous deletion to diploid status, which can only occur through proliferation of a previous sub-clone without the deletion. Within my data, resolution of homozygous focal deletion to heterozygous at relapse was only

observed in 2 tumours, of which one evolved with branching evolution and another with linear loss.

Gain(19q) was by far the most common CNA to be lost at relapse. Increased copy number of 19q at baseline is frequently observed in the context of HRD tumours with trisomy 19. HRD tumours are considered standard risk, with better clinical outcomes when compared to non HRD tumours. A literature search did not reveal any targets that would provide survival advantage with loss of gain(19q), however the jumping 1q syndrome could explain this observation. Sawyer et al reported frequent deletions in the receptor chromosomes of jumping 1q; 36 out of 50 tumours which most commonly involved 1p, 19q, 6q, 16q or 17p[42]. 32 tumours within my cohort demonstrated loss of gain(19q) at relapse, of these 9 had gain/amp(1q) from baseline and a further 9 acquired new gain/amp(1q) at relapse.

5.6.6 Conclusion

Evolution of CNA is common at relapse with new gain/amp(1q) the most dominant feature. The interstitial nature of CNA observed makes deciphering molecular dysregulation challenging, with multiple candidate genes described. Using sequential gene expression analysis I will attempt to clarify this matter in later chapters.

Gain(1q), del(1p) and del(17p) are recognised as independent adverse prognostic markers at diagnosis with a cumulative detrimental effect when they coexist. Jumping 1q syndrome may provide a viable explanation for their co-evolution with an increasing frequency of double, triple and quadruple hit tumours observed at relapse. However, other mechanisms of genomic instability that may underlie the CNA evolution observed are currently under investigation. New long-read sequencing technology such as Oxford Nanopore sequencing may also improve the characterisation of CNA changes over time.

Evolution of CNA likely contributes to a change in clinical behaviour but data is lacking regarding prognostic value of CNA acquired at later stages of disease. With increasing choice of treatment intensities at relapse, longitudinal genetic profiling could potentially help guide regime choice. I will therefore

investigate the prognostic significance of acquiring new CNA at relapse in later chapters.

Chapter 6: CNA evolution results- cytogenetic subgroups

6.1 Introduction

Variation in clinical outcome of patients despite uniform treatment reflects the molecular heterogeneity of myeloma. Early events such as IGH translocations or hyperdiploidy, shape the molecular structure and are associated with clinical outcomes. Molecular subgroups based on early events can therefore be used to predict clinical course, with t(4;14), t(14;16) and t(14;20) tumours associated with worse outcome. Constellations of secondary genetic events are also known to co-segregate within the specific molecular subgroups; for example gain(1q) and del(13) within t(4;14) tumours. These observations suggest differing evolutionary trajectories within molecular subgroups.

I have demonstrated that molecular evolution is a predominant feature of relapse, with change in copy number profile seen in 87.1% of tumours. Through description of sequential CNA within molecular subgroups I hope to identify specific pathways of tumour evolution, potential mechanisms of relapse and rationalised treatment plans.

I have used 2 different methods to classify molecular subgroups. The first based on tumour cytogenetics, the results per cytogenetic subgroup will be discussed in this chapter. The second method used hierarchical clustering to group tumours based on cyclin D1 and cyclin D2 expression, results per subgroup will be discussed in chapter 7. A summary of molecular subgroups and number of patients within each subgroup is shown in **Table 6-1.**

Classification	Sub-group	n	(%)
Cytogenetic (178 patients)	t(4;14)	19	(10.7)
	t(6;14)	0	(0.0)
	t(11;14)	21	(11.8)
	t(14;16)	2	(1.1)
	t(14;20)	1	(0.6)
	HRD with gain(11)	62	(34.8)
	HRD without gain(11)	34	(19.1)
	HRD & Translocation	13	(7.3)
	Other	26	(14.6)
Cyclin D expression (159 patients)	D1	78	(49.4)
	D2	55	(34.8)
	D1+D2	25	(15.8)

Table 6-1 Table to summarise molecular sub-grouping

6.2 Cytogenetic subgroups

Initiating genetic events are mutually exclusive in the majority of patients providing a useful basis to define molecular subgroups within this study. They also remain clonal over time facilitating accurate comparison between time points.

26 patients within the CNA evolution cohort had no evidence of HRD or common IgH translocation. I suspect these patients have IgH translocations with a less common chromosome partners not tested for in the taqman translocation assay, their sub group will be labelled as “Other”.

13 patients within the CNA evolution cohort had co-occurrence of HRD and IgH translocation. This phenomenon has previously been reported to occur at a frequency of approximately 4% [61]. Distinct molecular subgroups are required to facilitate recognition of evolutionary trajectories, this group was therefore labelled as “HRD & translocation".

94 patients within the CNA evolution cohort were identified as HRD. Within this large subgroup there will still be considerable molecular heterogeneity, which will likely impede recognition of specific patterns of evolution. Shah et al.

recently described molecular subgroups within the HRD group characterised by the presence or absence of gain(11)[12]. I have therefore investigated molecular change within two HRD groups; HRD with gain(11) and HRD without gain(11).

6.2.1 Evolution pattern per cytogenetic subgroup

Pattern of evolution was notably different between subgroups as shown in **Figure 6-1.** Change in CNA profile at relapse was most common in HRD tumours with 91.7% evolving in a branching or linear pattern. The majority of HRD tumours showed branching evolution; observed in 61.8% of HRD without gain(11) and 54.8% of HRD with gain(11). In contrast there was a higher frequency of stable tumours at relapse within the t(11;14) group; observed in 33.3%. Synonymous to the work previously reported by Bolli et al in section 1.2.2.1.3, linear evolution dominated t(4;14); observed in 36.8%.

The “Other” subgroup, represents patients with no evidence of HRD or common IgH translocation. It demonstrated a more varied distribution in pattern of evolution; with less branching when compared to HRD subgroups and less stable disease when compared to t(4;14) and t(11;14).

The “HRD & Translocation” subgroup was not included in **figure 6-1,** with a mixture of all major cytogenetic subgroups (HRD with gain(11), HRD without gain(11), t(4;14) and t(11;14)) the comparison of evolution pattern was limited. Within this subgroup branching, linear and linear loss were observed in 38.5%, 23.0% and 38.5% of tumours respectively. There was no stable evolution observed.

As expected, the number of patients within the t(14;16) and t(14;20) subgroups was low; 2 and 1 patient respectively. Therefore no meaningful comparison of evolution pattern could be made.

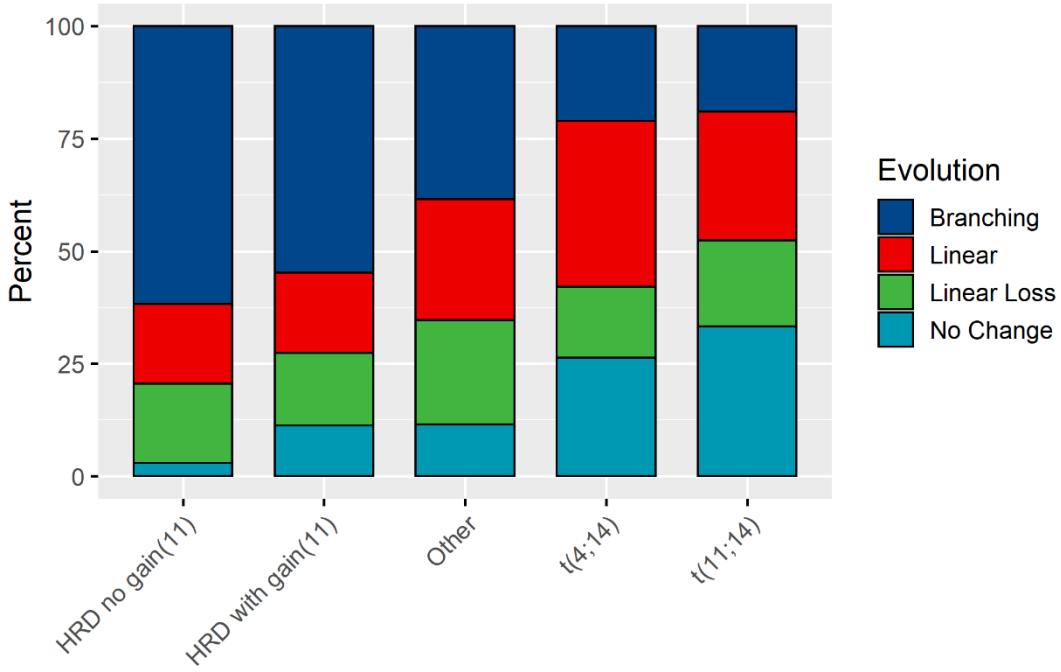

Figure 6-1 Frequency of evolutionary patterns per cytogenetic subgroups

6.2.2 t(4;14)

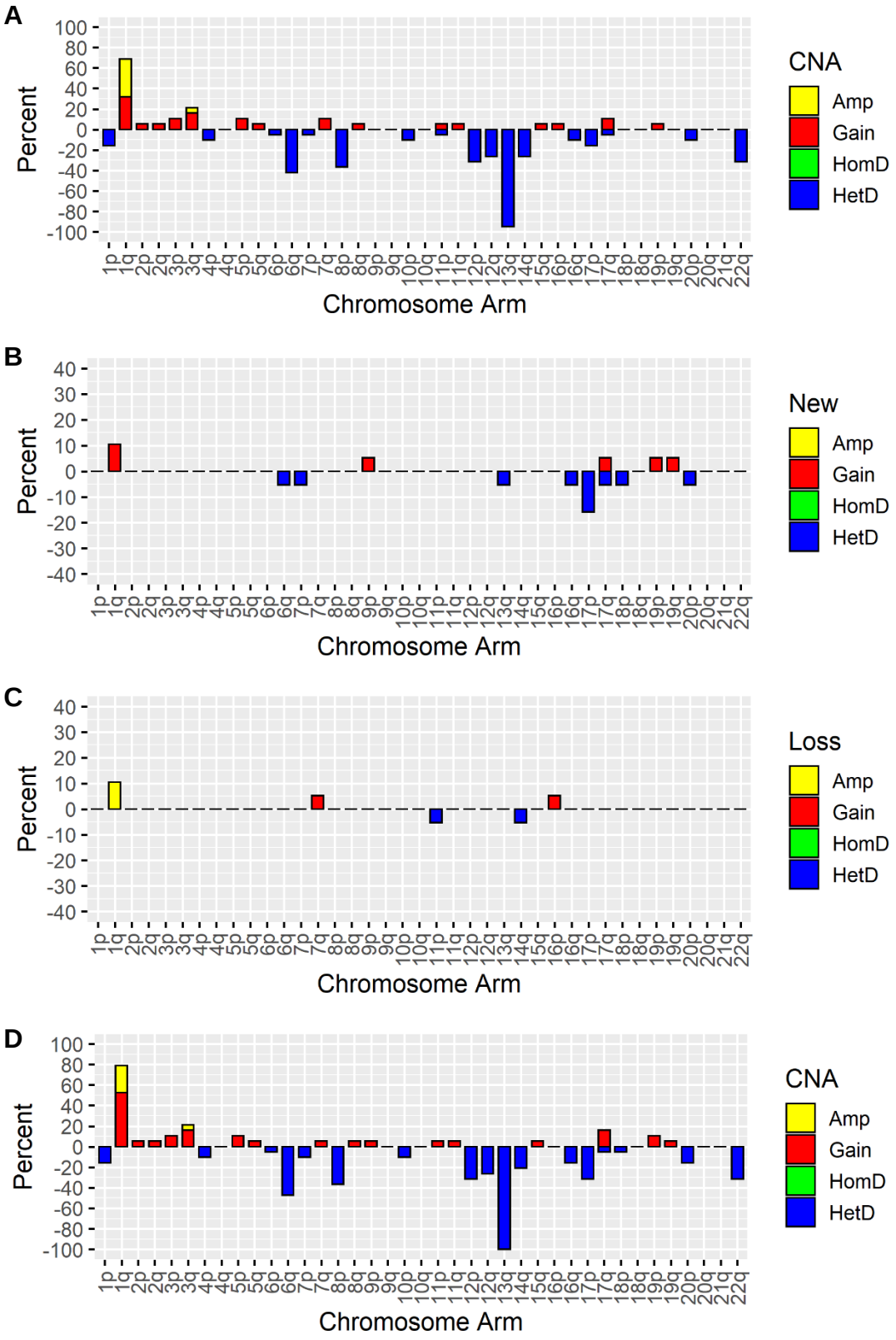

Figure 6-2 CNA evolution in the t(4;14) subgroup: (A) Frequency of interstitial CNA at presentation (B) Frequency of new interstitial CNA observed at relapse (C) Loss of interstitial CNA at relapse (D) Net frequency of interstitial CNA at relapse.

The t(4;14) subgroup contained 19 patients. **Figure 6-2** summarises frequency of interstitial CNA:

- CNA at presentation **(A)**
- New CNA at relapse **(B)**
- Loss of CNA at relapse **(C)**
- Net CNA at relapse **(D)**

6.2.2.1 Whole arm CNA in t(4;14)

There was a clear association of del(13q) and gain/amp(1q) with t(4;14) tumours. Demonstrated by the high frequency of del(13q) and gain/amp(1q) at presentation; observed in 18 (94.7%) and 13 (68.4%) tumours respectively, which at relapse increased to 19 (100%) and 15 (79.0%) respectively.

The most common new CNA to evolve at relapse was del(17p); observed in 3 (15.8%) tumours, as a consequence 6 (31.6%) tumours had del(17p) at relapse. The second most common new CNA to evolve was gain(1q); observed in 2 (10.5%) tumours. Interestingly the frequency of tumours with 1q amplification decreased from 7 (36.8%) at presentation to 5 (26.3%) at relapse.

6.2.2.2 Focal CNA in t(4;14)

At presentation the most common focal CNA involved del(11q.22.2) (*BIRC2/3*) observed in 7 (36.8%) tumours; 4 heterozygous and 3 homozygous. Of which 2 also involved deletion of 11q22.3 (*ATM*). Deletion of 1p12(*FAM46*) was observed in 3 (15.8%) of tumours at presentation.

Evolution of focal CNA was observed in 12 (63.2%) tumours at relapse; new CNA seen in 7 (36.8%) and loss of CNA in 5 (26.3%). New focal CNA per tumour ranged from 0-3. Loss of CNA per tumour ranged from 0-2.

The most common new focal CNA at relapse was del(11q22.2) (*BIRC*) observed in 3 (15.8%) tumours; 2 heterozygous and 1 homozygous. Loss of del(11q22.2) was also observed in 3 (15.8%) tumours; resulting in resolution of heterozygous deletion to diploid status at relapse (2 tumours) and homozygous to heterozygous deletion at relapse (1 tumour). The second

most common new focal CNA was gain(20q12) (*MAFB)* observed in 2 (10.5%) tumours.

6.2.2.3 Overall change in t(4;14)

Difference in average number of CNA per patient between time points approached significance: 5 (range 2-13) at presentation vs. 6 (range 3-12) at relapse (Wilcoxon Signed-Ranked *P* = 0.056). There were clonal changes in CNA from presentation to relapse in 73.7% of tumors. The proportion of Interstitial to focal was similar at 56.4% and 43.6% respectively.

6.2.3 t(11;14)

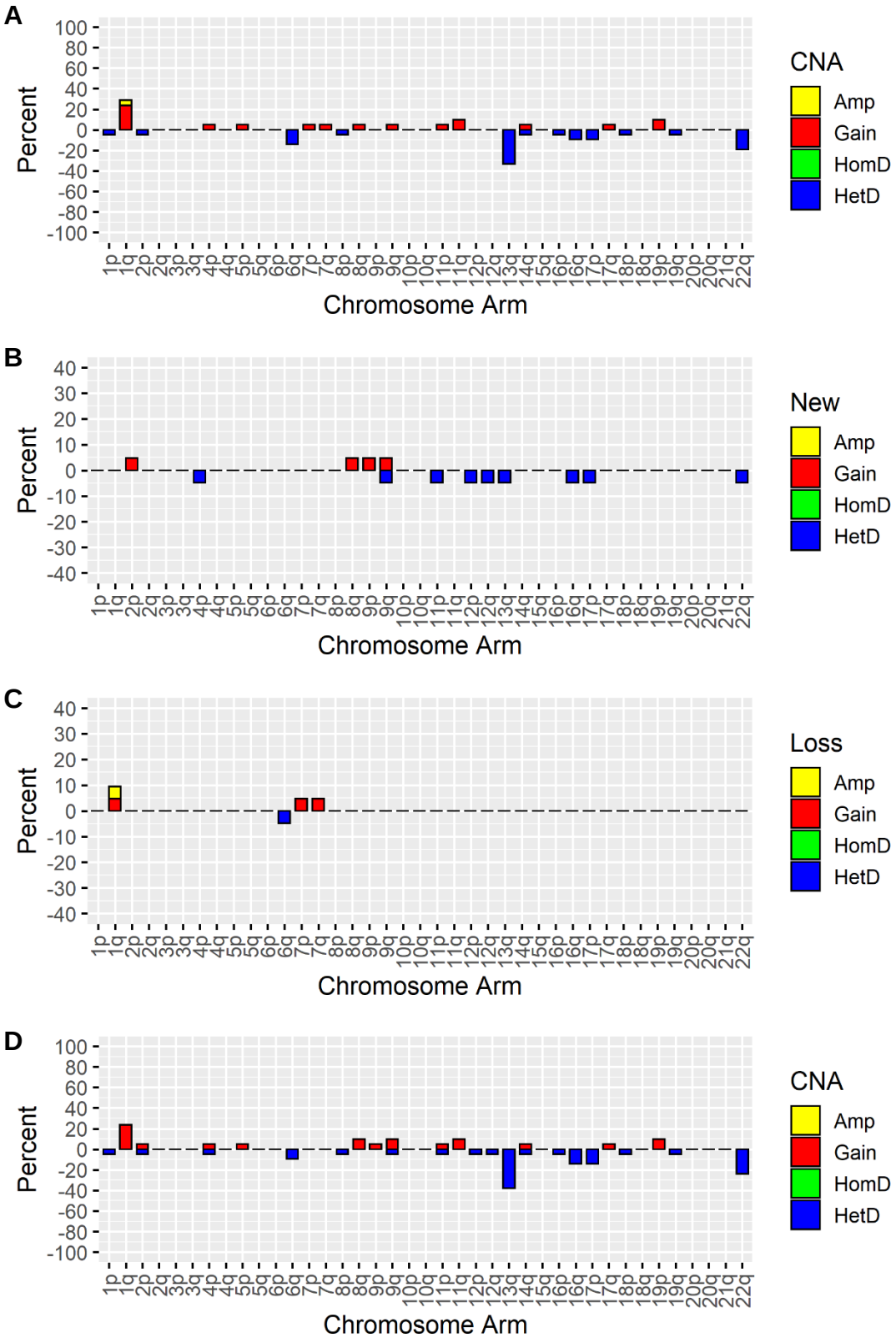

Figure 6-3 CNA evolution in the t(11;14) subgroup: (A) Frequency of interstitial CNA at presentation (B) Frequency of new interstitial CNA observed at relapse (C) Loss of interstitial CNA at relapse (D) Net frequency of interstitial CNA at relapse.

The t(11;14) subgroup contained 21 patients. **Figure 6-3** summarises frequency of interstitial CNA:

- CNA at presentation **(A)**
- New CNA at relapse **(B)**
- Loss of CNA at relapse **(C)**
- Net CNA at relapse **(D)**

6.2.3.1 Whole arm CNA in t(11;14)

CNA was relatively infrequent within this group at presentation and relapse. This was paralleled by a high frequency of stable evolution; observed in 33.3% of tumours.

Del(13q) and gain/amp(1q) were again the most common CNA observed at presentation; observed in 7 (33.3%) and 6 (28.6%) tumours respectively. However their frequencies were comparatively low to that of other subgroups.

Evolution of new CNA was observed, each occurring in <5% of tumours. One tumour with gain(1q) reverted to diploid status at relapse and another reverted to gain from amplification, resulting in a net decrease in gain/amp(1q).

6.2.3.2 Focal CNA in t(11;14)

At presentation the most common focal CNA involved gain/amp(11q13.3) (*CCND1*) observed in 8 (38.1%) tumours; 6 gain and 2 amplification. Del(11q.22.2) (*BIRC2/3*) and del(1p12)(FAM46C) were also frequent at presentation, observed in 5 (23.8%) and 3 (14.3%) tumours respectively.

Evolution of focal CNA was observed in 12 (57.1%) tumours at relapse; new CNA seen in 8 (38.1%) and loss of CNA seen in 4 (19.1%). New focal CNA per tumour ranged from 0-3. Loss of CNA per tumour ranged from 0-2.

The most common new focal CNA at relapse was gain(11q13.3)(*CCND1)* and gain(14q32.32)(*TRAF3*) each observed in 2 (9.5%) tumours. Recurrent new focal deletions were not observed at relapse. Recurrent loss of focal CNA at relapse was not observed. One tumour acquired new homozygous del(1p32.3) at relapse from diploid status.

6.2.3.3 Overall change in t(11;14)

There was no significant difference in the average number of CNA between time points; 2 (range 0-12) at presentation vs. 2 (range 0-17) at relapse (Wilcoxon Signed-Ranked *P* = 0.14). There were clonal changes in CNA from presentation to relapse in 66.7% of tumors. The proportion of Interstitial to focal was similar at 43.9% and 56.1% respectively.

6.2.4 HRD without gain(11)

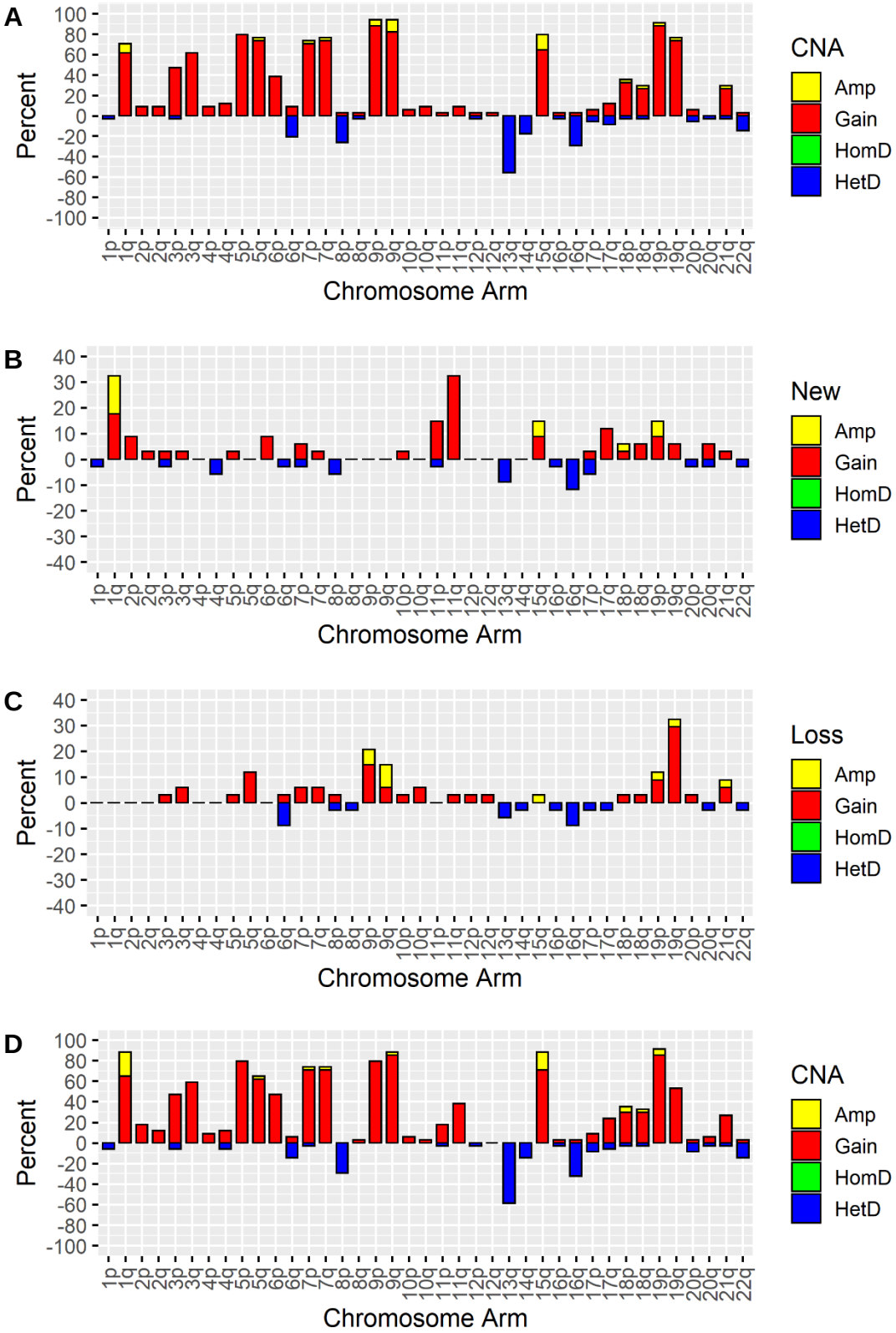

Figure 6-4 CNA evolution in the HRD without gain(11) subgroup: (A) Frequency of interstitial CNA at presentation (B) Frequency of new interstitial CNA observed at relapse (C) Loss of interstitial CNA at relapse (D) Net frequency of interstitial CNA at relapse.

The HRD without gain(11) subgroup contained 34 patients. **Figure 6-4** summarises frequency of interstitial CNA:

- CNA at presentation **(A)**
- New CNA at relapse **(B)**
- Loss of CNA at relapse **(C)**
- Net CNA at relapse **(D)**

6.2.4.1 Whole chromosome CNA in HRD without gain(11)

At presentation, 3 or 4 copies of chromosomes 9, 15, 7, 5, 19, 3, and 21 were observed in 91.2%, 79.4%, 73.5%, 73.5%, 70.6%, 44.1% and 29.4% of tumours respectively.

Evolution of new whole chromosome gain involved chromosome 15 in 5 (14.7%), chromosome 11 in 4 (11.8%) and chromosomes 7, 19 and 21 in 1 (2.9%) tumours respectively. 2 cases of new amp(15) evolved from trisomy status at presentation **(Table6-2)**.

Loss of a whole chromosome copy was also observed at relapse; resulting in resolution of gain to diploid status or amplification to gain. This was most frequent in chromosomes 9 and 21, each observed in 3 (8.8%) tumours respectively. Whole chromosome loss was also observed in chromosomes 3, 7, 15 and 19 **(Table6-2)**.

	New CNA		**Loss of CNA**	
Chr	**Diploid to Gain**	**Gain to Amp**	**Amp to Gain**	**Gain to Diploid**
3	0	0	0	1 (2.9%)
5	0	0	0	0
7	1 (2.9%)	0	0	2 (5.9%)
9	0	0	2 (5.9%)	1 (2.9%)
11	4 (11.8%)	0	0	0
15	3 (8.8%)	2 (5.9%)	1 (2.9%)	0
19	1 (2.9%)	0	1 (2.9%)	1 (2.9%)
21	1 (2.9%)	0	1 (2.9%)	2 (5.9%)

Table 6-2 Evolution of whole chromosome CNA at relapse within the HRD without gain(11) sub group. Chr: Chromosome.

6.2.4.2 Whole arm CNA in HRD without gain(11)

Synonymous to t(4;14) tumours, the most common secondary CNA at presentation was gain/amp(1q) and del(13q) observed in 24 (70.6%) and 19 (55.9%) tumours respectively. Conversely the frequency of gain/amp(1q) was higher than del(13q).

The most common new CNA at relapse was also gain/amp(1q) seen in 11 (32.4%) tumours. Of which 5 (14.7%) tumours demonstrated clonal evolution of the CNA, transitioning from gain(1q) at presentation to amp(1q) at relapse. This resulted in a net frequency of 88.2% at relapse.

Other frequent areas of new CNA included gain(11q) observed in 7 (20.6%) and gain/amp(19p), gain(17q) and del(16q) in 4 (11.8%) tumours.

With a high proportion of branching evolution noted. Resolution of baseline CNA to diploid status at relapse was most frequently observed with gain/amp(19q) and gain(5q); observed in 9 (26.5%) and 4 (11.8%) tumours respectively.

6.2.4.3 Focal CNA in HRD without gain(11)

At presentation the most common focal CNA involved gain(20q12) (*MAFB*) observed in 7 (20.6%) tumours. Del(1p32.3) (*CDKN2C, FAF1*) was also frequent at presentation, observed in 5 (14.7%); 2 heterozygous, 3 homozygous. Del(11q22.2) (*BIRC*), del(14q32.32) (*TRAF3*) and gain(8q24.21) (*MYC*) were each observed in 4 (11.8%) tumours at relapse.

Evolution of focal CNA was observed in 26 (76.5%) tumours at relapse; new CNA seen in 15 (44.1%) and loss of CNA seen in 14 (41.2%). New focal CNA per tumour ranged from 0-3. Loss of CNA per tumour ranged from 0-4.

The most common new focal CNA was gain(6q12) (*EYS*) observed in 3 (8.8%) tumours. The most common loss of CNA was gain(20q12) (*MAFB)* observed in 5 (14.7) tumours. Evolution of del(14q32.32)(*TRAF3*) from heterozygous to homozygous deletion was observed in 2 (5.9%) tumours. New homozygous deletion of 16q21.1 (*CYLD)* at relapse was seen in 1 (2.9%) tumour.

6.2.4.4 Overall change in HRD without gain(11)

By virtue of the high frequency in branching evolution, there was no significant difference in the average number of CNA per tumour between time points: 14 (range 6-26) at presentation vs. 15 (range 4-24) at relapse (*P*=0.34).

There were clonal changes in CNA from presentation to relapse in nearly all tumors (97.1%). The majority of CNA changes were interstitial (78.9%) compared to focal CNA which occurred in 21.1%).

6.2.5 HRD with gain(11)

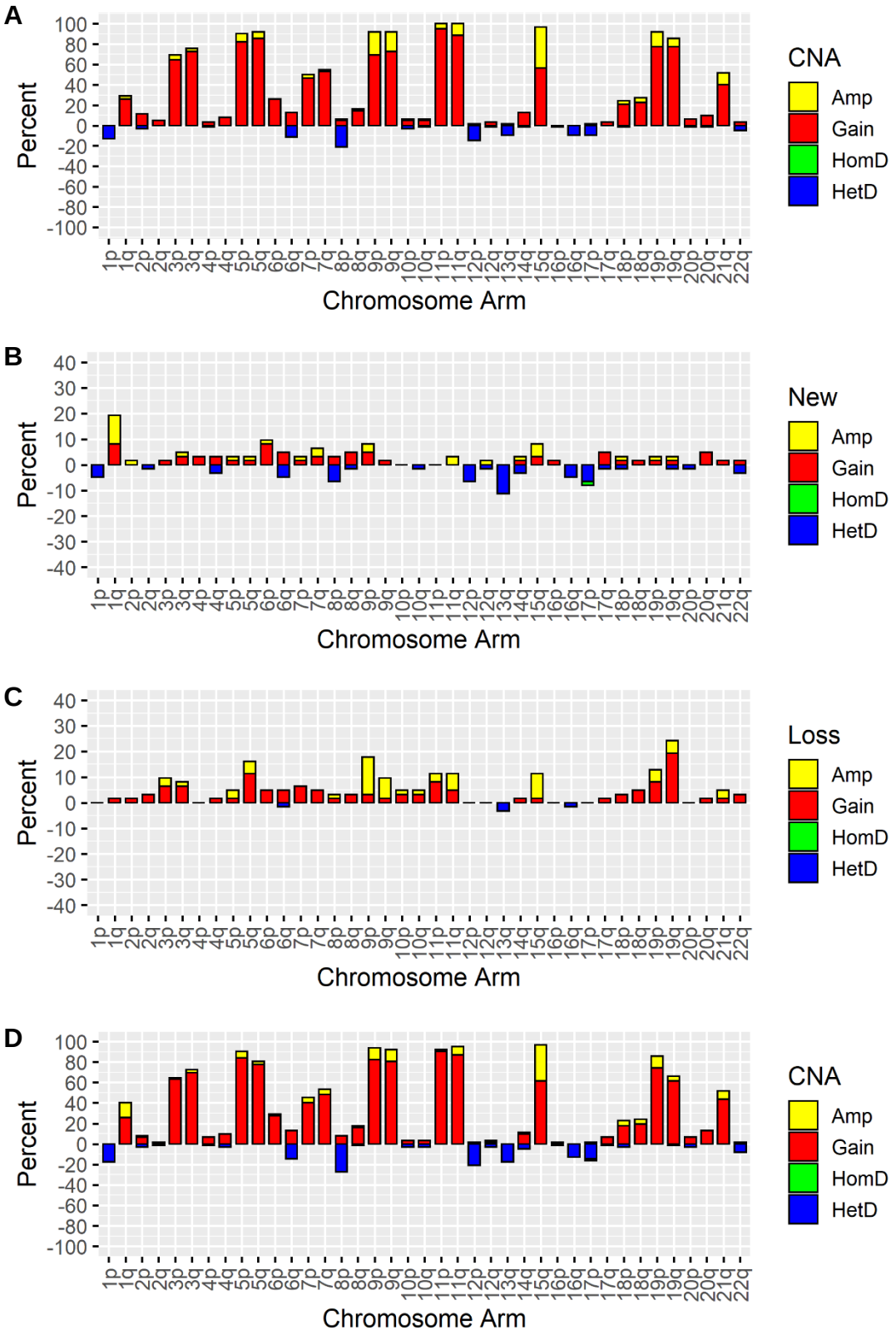

Figure 6-5 CNA evolution in the HRD with gain(11) subgroup: (A) Frequency of interstitial CNA at presentation (B) Frequency of new interstitial CNA observed at relapse (C) Loss of interstitial CNA at relapse (D) Net frequency of interstitial CNA at relapse

The HRD with gain(11) subgroup contained 62 patients. **Figure 6-5** summarises frequency of interstitial CNA:

- CNA at presentation **(A)**
- New CNA at relapse **(B)**
- Loss of CNA at relapse **(C)**
- Net CNA at relapse **(D)**

6.2.5.1 Whole chromosome CNA in HRD with gain(11)

At presentation, 3 or 4 copies of chromosomes 11, 15, 9, 5, 19, 3, 21 and 7 were observed in 100%, 96.8%, 88.7%, 87.1%, 82.3%, 69.4%, 51.6% and 48.4% of tumours respectively. In comparison to the HRD without gain(11) group, there was a higher frequency of gain(21) and lower frequency of gain(7).

Evolution of new whole chromosome gain occurred in chromosomes 3, 5, 9, 19 and 21 at a frequency of 1.6%, new copies of chromosome 15 evolved in 5 (8.1%) tumours, 3 (4.8%) of which were amplification evolving from trisomy status at presentation **(Table 6-3)**.

Loss of a whole chromosome copy was also observed at relapse; resulting in resolution of gain to diploid status, amplification to diploid status or amplification to gain. This was most frequent in chromosome 15 observed in 7 (11.3%) tumours; of which 5 (8.1%) reverted to gain from amplification and 1 (1.6%) reverted to diploid status from amplification **(Table 6-3)**.

	New CNA		**Loss of CNA**	
Chr	**Diploid to Gain**	**Gain to Amp**	**Amp to Gain**	**Gain to Diploid**
3	1 (1.6%)	0	1 (1.6%)	2 (3.2%)
5	0	1 (1.6%)	1 (1.6%)	2 (3.2%)
7	0	0	0	1 (1.6%)
9	1 (1.6%)	0	4 (6.5%)	0
11	0	0	1 (1.6%)	2 (3.2%)
15	2 (3.2%)	3 (4.8%)	5 (8.1%)	1 (1.6%)
19	1 (1.6%)	0	1 (1.6%)	2 (3.2%)
21	1 (1.6%)	0	2 (3.2%)	1 (1.6%)

Table 6-3 Evolution of whole chromosome CNA at relapse within the HRD with gain(11) sub group. Chr: Chromosome

6.2.5.2 Focal CNA in HRD with gain(11)

At presentation the most common focal CNA involved del(1p12) (*FAM46C*) observed in 9 (14.5%) tumours; 8 heterozygous and 1 homozygous. Del(6p25.3)(*IRF4)* and gain(8q24.21)(*MYC)* were each observed in 6 (9.7%) tumours at presentation. Heterozygous del(1p32.3) (*CDKN2C, FAF1*) was observed in 2 tumours at presentation.

Evolution of focal CNA was observed in 36 (58.1%) tumours at relapse; new CNA seen in 24 (38.7%) and loss of CNA seen in 17 (27.4%). New focal CNA per tumour ranged from 0-3. Loss of CNA per tumour ranged from 0-3.

The most common new focal gain/amplification at relapse involved 8q24.21 (*MYC)* observed in 4 (6.5%) tumours, 2 each respectively. The most common new focal deletion at relapse involved 1p32.3 (*CDKN2C* and *FAF1*) observed in 5 (8.1%), of which 2 were homozygous deletions, 1 evolving from heterozygous deletion at presentation. New del(6p25.3) at relapse was observed in 2 (3.2%) tumours. New homozygous deletion of 16q21.1 (*CYLD)* at relapse was seen in 1 (1.6%) tumour, evolving from heterozygous deletion at presentation. The most common loss of CNA at relapse involved del(1p12) (*FAM46C*) observed in 4 (6.5%) tumours.

Interestingly focal deletions of 6p25.3 (*IRF4*) were almost exclusive to the HRD with gain(11) sub group; at presentation 6 (85.7%) del(6p25.3) were observed in HRD with gain(11) tumours, the other observed in a t(11;14) tumour. All new del(6p25.3) at relapse were found within the HRD with gain(11) subgroup. *IRF4* is implicated in the mechanism of action of IMiDs.

6.2.5.1 Whole arm CNA in HRD with gain(11)

While molecular change within this group was observed in 88.7% of tumors, recurrent change was less frequent with chromosomal distribution more varied when compared to the HRD group without gain(11).

The most frequent new CNA to evolve at relapse was gain or amplification of 1q; observed in 5 (8.1%) and 7 (11.3%) tumours respectively. Of which 4 (6.5%) demonstrated clonal evolution of CNA, transitioning from gain(1q) at presentation to amp(1q) at relapse. New heterozygous deletion of 13q was

observed in 7 (11.3%) tumours at relapse. One tumour demonstrated clonal evolution of del(17p); transitioning from heterozygous deletion at presentation to homozygous deletion at relapse.

Loss of CNA was also observed at relapse; resolution of gain to diploid status, amplification to diploid or amplification to gain. Loss most frequently involved 19q, observed in 12 (19.4%) tumours, of which 2 reverted to gain from amplification and 1 tumour reverted to diploid status from amplification. Loss of CNA in 5q was observed in 10 (16.1%) tumours; of which 2 reverted to gain from amplification and 1 tumour reverted to diploid status from amplification.

6.2.5.2 Overall change in HRD with gain(11)

Consistent with the high frequency in branching evolution, there was no significant difference in the average number of CNA per tumour between time points: 15 (range 6-34) at presentation vs. 15 (range 8-29) at relapse (*P*=0.40).

There were clonal changes in CNA from presentation to relapse in nearly all tumors (88.7%). The majority of CNA changes were interstitial (80.1%) compared to focal CNA which occurred in 19.9%).

6.2.6 t(14;16)

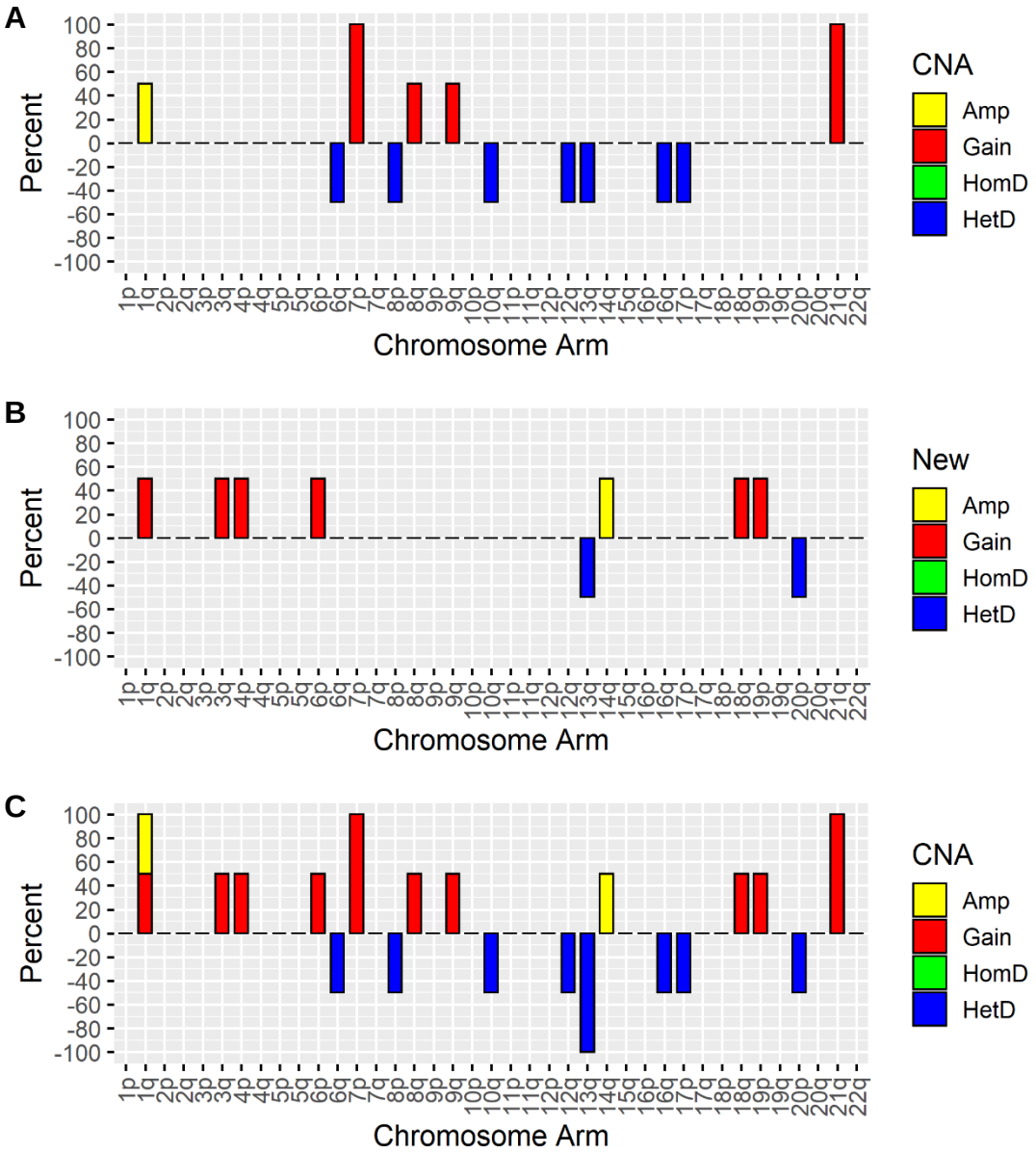

Figure 6-6 CNA evolution in the t(14;16) subgroup: (A) Frequency of interstitial CNA at presentation (B) Frequency of new interstitial CNA observed at relapse (C) Net frequency of interstitial CNA at relapse.

The t(14;16) subgroup contained 2 patients. **Figure 6-6** summarises frequency of interstitial CNA:

- CNA at presentation **(A)**
- New CNA at relapse **(B)**
- Net CNA at relapse **(C)**

Due to the low frequency of t(14;16) (two patients) sequential CNA analysis provided limited information regarding subgroup evolutionary trajectory.

There was no significant difference in the average number of CNA per tumour between time points; 8.5 (range 5-12) at presentation vs 13 (range 7-19) at relapse (*P*=0.5).

There were clonal changes in CNA from presentation to relapse in both tumors. The majority of CNA changes were interstitial (60%) compared to focal CNA which occurred in 40%.

New gain(1q) and del(13q) at relapse was observed in 1 tumour resulting in a net frequency at relapse of 100% for both CNA.

New focal gain(20q12)(*MAFB*) was observed in 1 tumour. New focal del(1p12)(*FAM46C*) was 1 tumour.

6.2.7 t(14;20)

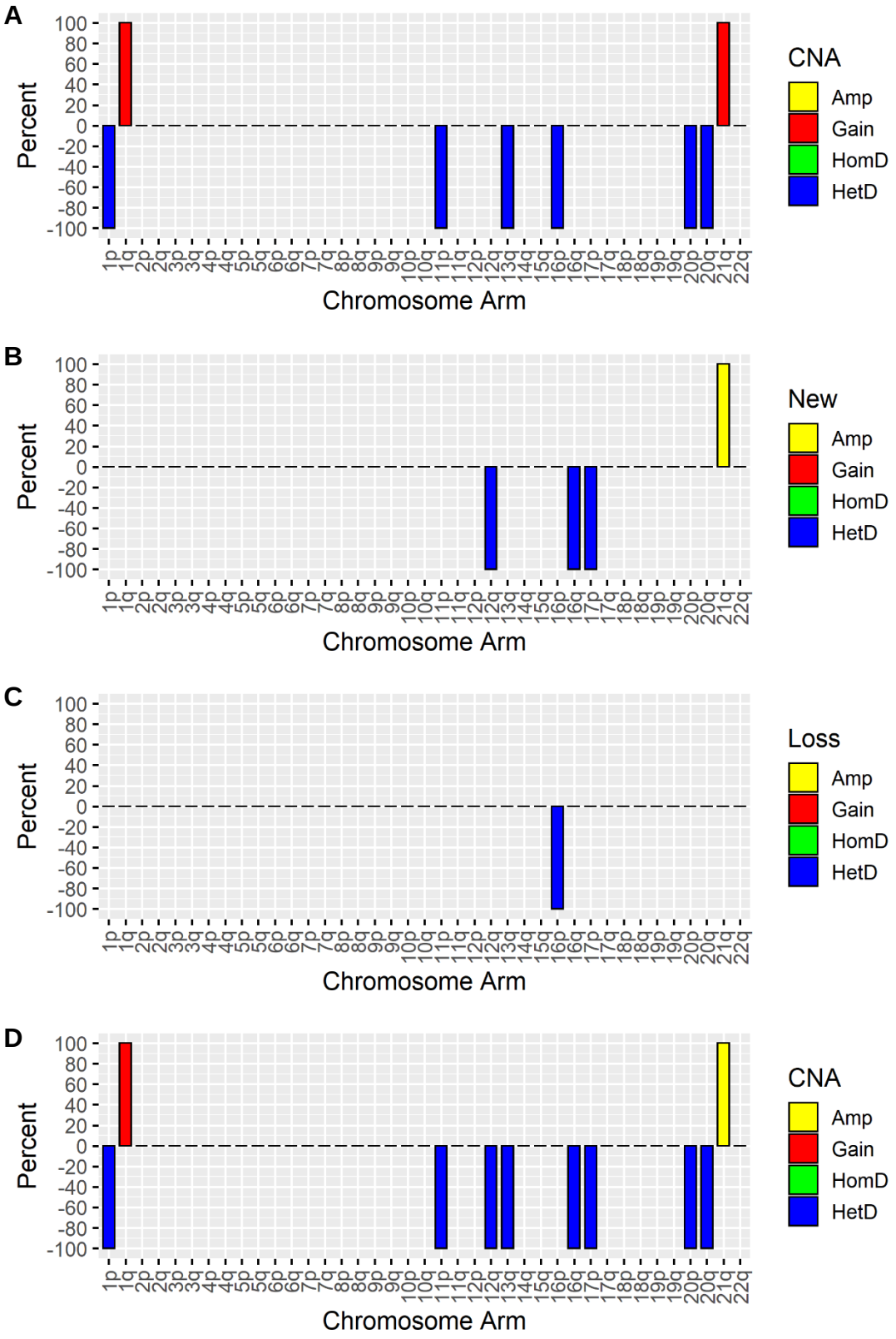

Figure 6-7 CNA evolution in the t(14;20) subgroup: (A) Frequency of interstitial CNA at presentation (B) Frequency of new interstitial CNA observed at relapse (C) Loss of interstitial CNA at relapse (D) Net frequency of interstitial CNA at relapse

The t(14;16) subgroup contained 1 patients. **Figure 6-7** summarises frequency of interstitial CNA:

- CNA at presentation **(A)**
- New CNA at relapse **(B)**
- Loss of CNA at relapse **(C)**
- Net CNA at relapse **(D)**

Due to the low frequency of t(14;20) (1 patient) sequential CNA analysis provided limited information regarding subgroup evolutionary trajectory.

The number of CNA within the tumour increased form 8 at presentation to 13 at relapse, evolving with a branching pattern, 62.5% of changes involved interstitial and 37.5% focal CNA.

Evolution of new del(17p) at relapse resulted in the tumour becoming quadruple hit for high risk lesions at relapse.

6.2.8 Other

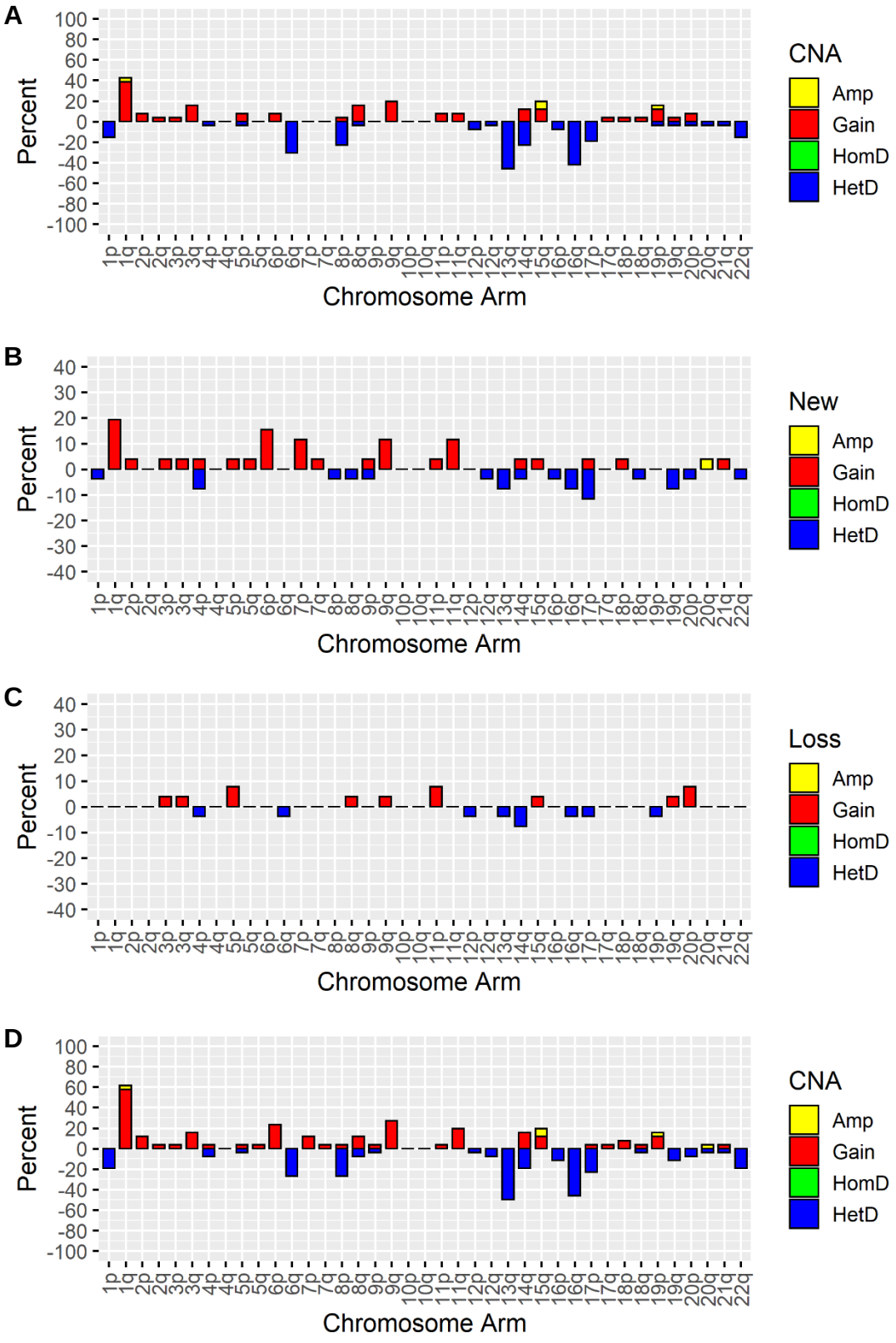

Figure 6-8 CNA evolution in the "Other" subgroup: (A) Frequency of interstitial CNA at presentation (B) Frequency of new interstitial CNA observed at relapse (C) Loss of interstitial CNA at relapse (D) Net frequency of interstitial CNA at relapse

The “Other” subgroup contained 26 patients. **Figure 6-8** summarises frequency of interstitial CNA:

- CNA at presentation **(A)**
- New CNA at relapse **(B)**
- Loss of CNA at relapse **(C)**
- Net CNA at relapse **(D)**

6.2.8.1 Whole arm CNA in “Other” subgroup

At presentation recurrent deletions were more common than gain:

- del(13q), del(16q), de(6q), del(14q), del(8p), del(17(p), del(1p) and del(22q) observed in 46.2%, 42.3%, 30.8%, 23.1%, 23.1%, 19.2%, 15.4% and 15.4% of tumours respectively.
- Gain/amp(1q), gain(9q) and gain(8q) observed in 38.5%, 19.2% and 15.4% of tumours respectively.

Evolution of new CNA was more common than loss of CNA. The most frequent new CNA to evolve at relapse was gain(1q) observed in 5 (19.2%) tumours. New gain(6p) was observed in 4 (15.4%) and new gain(11q), gain(9q) and del(17p) was observed in 3 (11.5%) tumours at relapse.

The net frequency of gain/amp(1q) and del(17p) at relapse was 61.5% and 23.1% respectively.

6.2.8.2 Focal CNA in “Other” subgroup

At presentation the most common focal CNA was gain(11q22.2)(BIRC), gain(8q24.21)(*MYC*) and del(16q.32.1)(WWOX) observed in 8 (30.8%), 4 (15.4%) and 3 (11.5%) tumours respectively.

Evolution of focal CNA was observed in 22 (84.6%) tumours at relapse; new CNA seen in 15 (57.7%) and loss of CNA seen in 13 (50.0%). New focal CNA per tumour ranged from 0-3. Loss of CNA per tumour ranged from 0-2.

The most common new focal CNA were gain/amp(8q24.21)(*MYC*) and del(1p12)(FAM46C) each observed in 2 (7.7%) tumours. Of which one tumour demonstrated evolution of gain(8q24.21) to amplification at relapse.

6.2.8.3 Overall change in “Other” subgroup

Clonal changes in CNA from presentation to relapse was observed in the majority of tumours (88.5%). Interstitial CNA changes (65.8%) were more common than focal CNA changes (34.2%).

There was no significant difference in the average number of CNA per tumour between time points; 5 (range 0-14) at presentation vs 6.5 (range 0-19) at relapse (*P*=0.15).

6.2.9 HRD & translocation

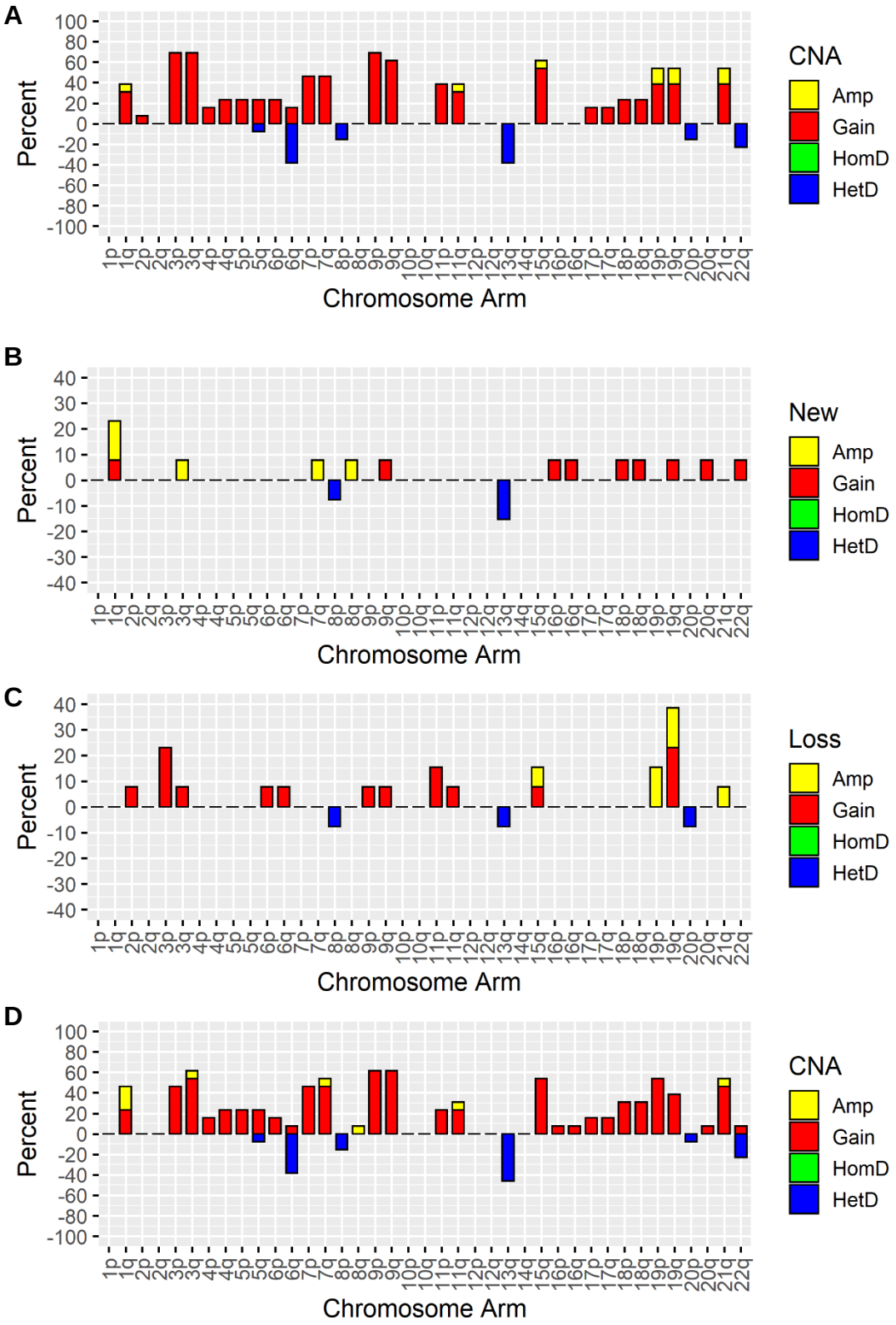

Figure 6-9 CNA evolution in the IgH translocation and HRD subgroup: (A) Frequency of interstitial CNA at presentation (B) Frequency of new interstitial CNA observed at relapse (C) Loss of interstitial CNA at relapse (D) Net frequency of interstitial CNA at relapse.

The HRD and translocation subgroup contained 13 patients. **Figure 6-9** summarises frequency of interstitial CNA:

- CNA at presentation **(A)**
- New CNA at relapse **(B)**
- Loss of CNA at relapse **(C)**
- Net CNA at relapse **(D)**

6.2.9.1 Whole chromosome CNA in HRD & translocation

Table 6-4 summarises the combination of IgH translocation and trisomies observed at presentation for each tumour. 3/4 of t(11;14) tumours also had gain(11) and the final t(11;14) tumour had amplification of the 11q arm.

There was no evolution of new trisomies at relapse. Loss of trisomy to diploid status was observed in chromosomes 3 and 15 in 1 tumour respectively. Loss of amplification to gain was observed chromosomes 19 and 21, for 2 and 1 tumours respectively.

IgH translocation	Trisomies
t(4;14)	3, 9, 15, 19, 21
t(4;14)	3, 6, 9, 11, 15
t(4;14)	15, 19
t(4;14)	3, 6, 7, 9, 15
t(4;14)	3, 15
t(6;14)	4, 7, 9, 18
t(11;14)	5, 18, 21
t(11;14)	5, 7, 11, 15, 19, 21
t(11;14)	3, 5, 7, 11, 15, 19, 21
t(11;14)	4, 9, 11, 18
t(14;16)	3, 7, 9, 17, 19, 21
t(14;16)	3,7, 9, 15, 17, 19, 21
t(14;16)	3, 9, 21

Table 6-4 Combination of IgH translocations and trisomies.

6.2.9.2 Whole arm CNA in HRD & translocation

The most frequent new CNA to evolve at relapse was gain/amp(1q) observed in 3 (23.1%) tumours. Of which, 2 showed evolution of gain to amplification at relapse. The second most frequent new CNA at relapse was del(13q) observed in 2 (15.4%) tumours. Loss of del(13q) at relapse was also observed in 1 (7.7%) tumour. The most frequent loss of CNA at relapse was gain(11p) demonstrated in 2 (15.4%) tumours.

6.2.9.3 Focal CNA in HRD & translocation

At presentation focal CNA was most frequent in del(11q22.2)(BIRC) and gain(8q24.21)(*MYC*) observed in 3 (23.1%) and 2 (15.4%) tumours respectively.

Evolution of focal CNA was observed in 8 (61.5%) tumours at relapse; new CNA seen in 6 (46.2%) and loss of CNA seen in 5 (38.5%). New focal CNA per tumour ranged from 0-3. Loss of CNA per tumour ranged from 0-5.

New focal del(1p32.3) was observed in 2 tumours at relapse, of which one demonstrated evolution of CNA from heterozygous to homozygous deletion.

6.2.9.4 Overall change in HRD & translocation

Clonal changes in CNA from presentation to relapse was observed in all tumours (100%). Interstitial CNA changes (67.7%) were more common than focal CNA changes (32.3%).

There was no significant difference in the average number of CNA per tumour between time points; 12 (range 7-18) at presentation vs 12 (range 2-16) at relapse (P=1).

6.3 High risk CNA

Differences in the frequency of high risk CNA at presentation and relapse for each major cytogenetic subgroup are demonstrated in **Figure 6-10**.

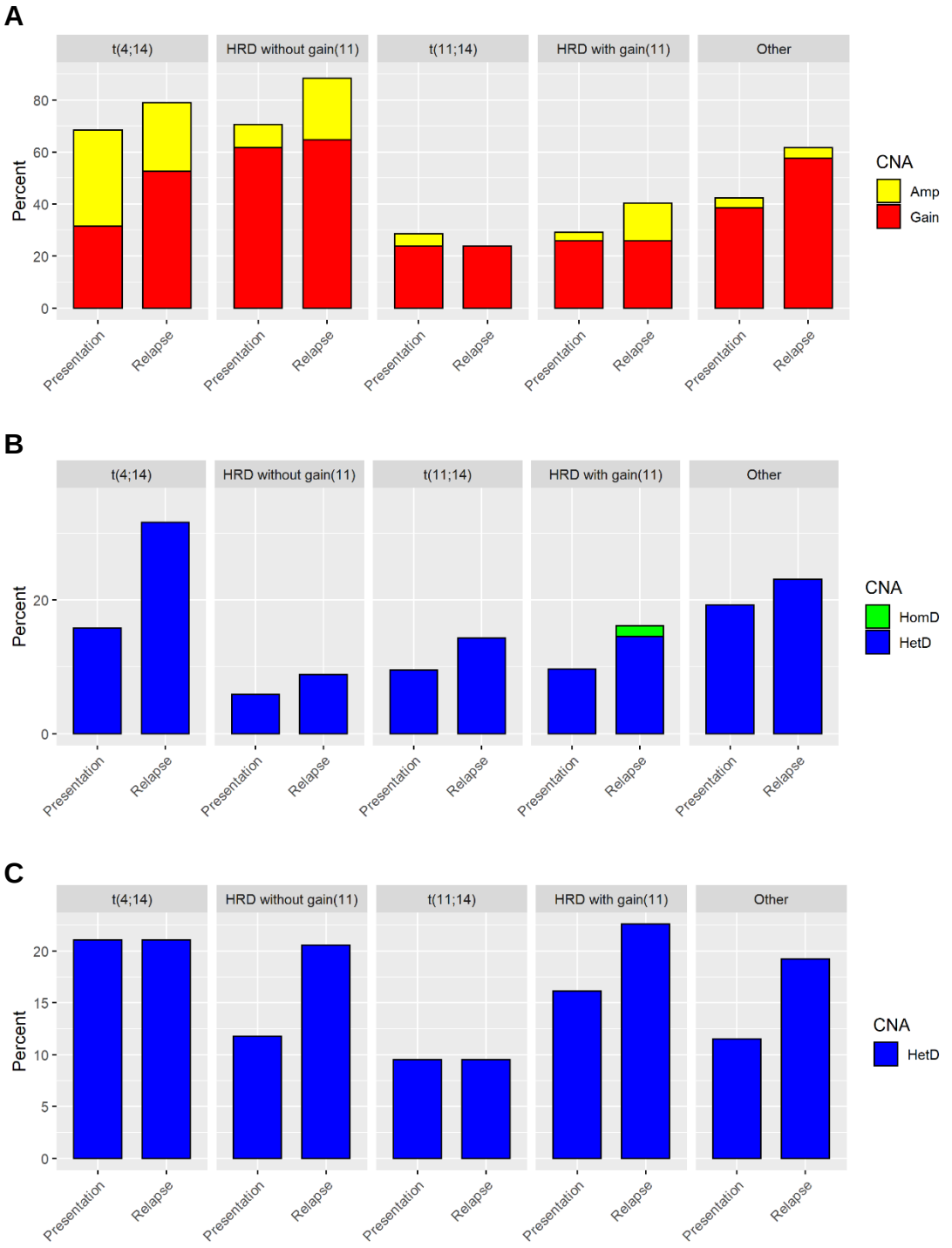

Figure 6-10 Frequency of high risk CNA per major molecular subgroup A: Gain/amp(1q); B: Del(17p); C: Del(1p) +Focal del(1p32.3).

6.3.1 Multiple hit tumours

The proportions of tumours with co-existing high risk lesions per cytogenetic subgroup are demonstrated in **Figure 6-11**. All subgroups contained tumours with more than 1 high risk lesion. Double, triple and quadruple hits were more common in the t(4;14), t(14;16) and t(14;20) subgroups. Tumours with 0-1 high risk lesions were most common in t(11;14) and HRD with gain(11). Clonal evolution of high risk lesions at relapse was observed in all subgroups resulting in a net increase of double hit or higher tumours. Interpretation of t(14;16) and t(14;20) subgroups should be taken with caution given the low frequency of patients in each.

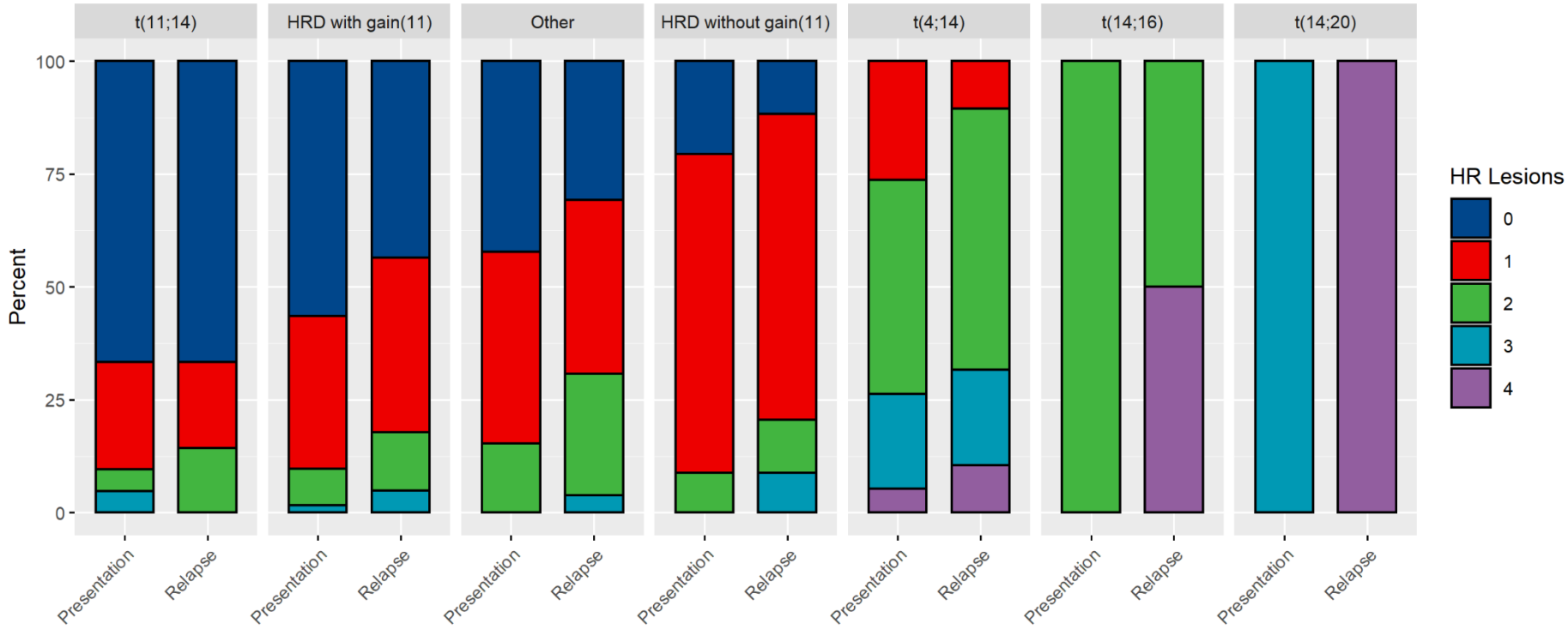

Figure 6-11 Co-existing high risk lesions per cytogenetic subgroup at sequential time points.

6.4 Discussion

This analysis has identified distinct evolutionary trajectories between cytogenetic subgroups. Most apparent between the 4 major subgroups; t(4;14), t(11;14), HRD with gain(11) and HRD without gain(11).

The t(4;14) subgroup was defined by a high proportion of tumours with del(13q), gain(1q), del(17p) and del(11q22.22)(BIRC), which increases from presentation to relapse. Such high frequencies of del(13q) and gain(1q) suggests a synergistic relationship and a clear survival advantage for clones carrying the aberrations, also reflected in the paucity of branching evolution observed at relapse **Figure 6-12**. The evolution of a clearly dominant clone with little variation between tumours correlates with the poor outcome associated with the t(4;14) translocation.

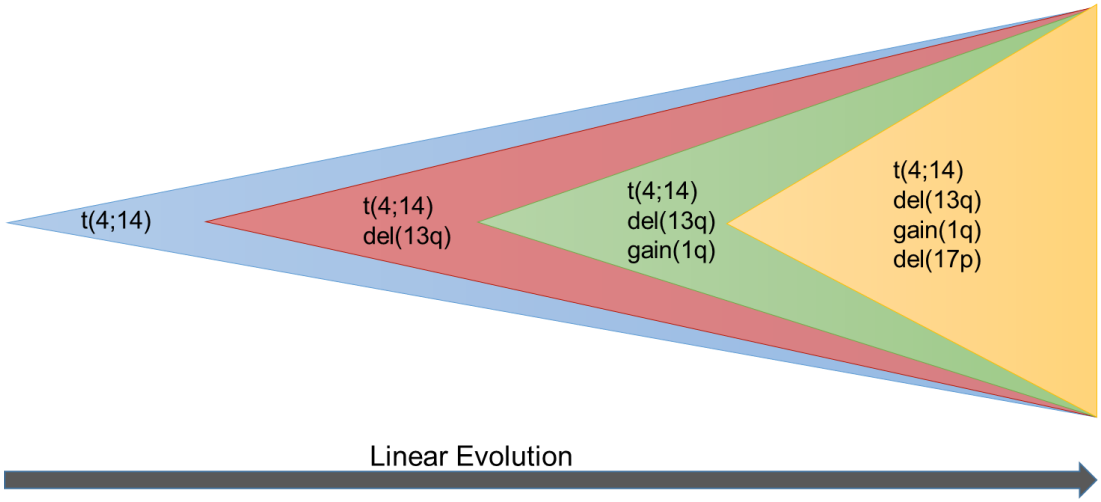

Figure 6-12 Example of linear evolution observed in a t(4;14) tumour

Conversely CNA was infrequent in t(11;14) tumours, with a high proportion demonstrating a stable pattern of evolution at relapse. This suggests a relative lack of chromosome instability which would correlate with the low frequency of gain(1q) observed and better clinical outcomes often associated with t(11;14) patients.

Unlike t(4;14) and t(11;14), branching evolution was a predominant feature of HRD tumours. The broad variation in acquisition and loss of CNA reflecting the diversity in competing clones. Interestingly the branching pattern of CNA evolution also involved whole chromosomes. While HRD is an initiating event,

this observation suggests that archetypal HRD trisomies are not all obtained as a single first hit. This observation correlates with work recently published by Aktas Samur et al [62].

Focal gain of *MYC* was more common in HRD tumours. Previous studies have also shown *MYC* dysregulation to be more common in HRD tumours [63]. *MYC* activates DNA replication, increased expression could lead to chromosome instability and help explain the level of branching evolution observed in these tumours [60]. The heterogeneity of clonal evolution in HRD makes it difficult to identify distinct pathways. Examining HRD tumours based on the presence or absence of gain(11) has helped to clarify the issue.

The evolutionary pathway of HRD without gain(11) tumours mirrored that of t(4;14) tumours with the predominant feature of gain(1q) and del(13q). Interestingly the frequency of gain(1q) was higher than del(13q) in the tumours suggesting a difference in the temporal acquisition of each CNA compared to t(4;14) tumours. A common feature to both HRD without gain(11) and t(4;14) tumours is overexpression of *CCND2* [7, 12], this could be the overarching mechanism that facilitates evolution/survival of clones containing gain(1q) and del(13).

Conversely, HRD with gain(11) tumours mirrored the evolutionary pathway of t(11;14) tumours with a relative lack of recurrent secondary CNA. Most notable in the lower frequency of gain(1q) and del(13q). Overexpression of *CCND1* is a common feature in HRD with gain(11) and t(11;14) tumours [12, 27]. *CCND1* expression appears to protect tumours against chromosome instability; stable evolution being more common in HRD with gain(11) when compared to HRD without gain(11). Overexpression of *CCND1* could provide a survival advantage to clones without gain(1q) therefore reducing chromosome instability associated with jumping 1q syndrome. *CCND1* expression is known to be highest in t(11;14) and I observed loss of gain(1q) at relapse in two t(11;14) tumours resulting in a net reduction in frequency of the CNA.

High risk CNA; gain(1q), del(17p) and del(1p) were observed in all subgroups. By virtue of their association with poor clinical outcome, these aberrations must provide a survival advantage to harbouring clones, resulting in treatment

resistance and early relapse. As discussed above, the evolution of gain(1q) was disproportionate across subgroups, favouring the CCND2 dysregulated groups; t(4;14) and HRD without gain(11). The chromosome instability associated with gain(1q) provides rationale for its coevolution with other high risk CNA. This was certainly observed in the t(4;14) subgroup. However, despite the high frequency of gain(1q) in HRD without gain(11) tumours, del(17p) was relatively infrequent. Suggesting other factors contribute to chromosome stability for example *MMSET/FGFR3* dysregulation in t(4;14) tumours or alternatively the level *CCND2* expression.

6.4.1 Conclusion

The clear differences noted in evolutionary trajectories of cytogenetic subgroups demonstrates differing mechanisms of relapse/progression, which suggests myeloma treatments could be rationalised to improve outcomes. Evidence to support this can be drawn from recent studies of Venetoclax, where superior responses were noted in t(11;14) tumours. This was attributed to higher *BCL2:BCL2L1* and *BCL2:MCL1* mRNA expression ratios in t(11;14) tumours [57]. *MCL1* is located on 1q and this finding likely correlates with the lower frequency of gain/amp (1q) observed in t(11;14) tumours. Perhaps HRD with gain(11) tumours would also have a better response to Venetoclax over HRD without gain(11) tumours.

The proportion of tumours with multiple high risk lesions appears to correlate to perceived CCND1: CCND2 expression, with the highest frequency of double, triple and quadruple hits noted in CCND2 dysregulated tumours **(Figure 6-11)**. Further investigation of evolutionary trajectories based on D group cyclin expression will therefore be presented in the next chapter.

While I have identified divergent evolutionary trajectories, precise understanding of associated molecular dysregulation is challenging due to the interstitial nature of the CNA observed. As previously stated in chapter 5, I hope to use sequential gene expression data to clarify this problem in later chapters.

Chapter 7: CNA evolution results- cyclin D subgroups

7.1 Introduction

After investigation of CNA evolution at relapse within cytogenetic subgroups, parallels were noted between the t(4;14) and HRD without gain(11) tumours and between t(11;14) and HRD with gain(11) tumours. Similarities between these groups may be attributed to *CCND1* and *CCND2* expression.

The TC classification previously demonstrated a relative overexpression of *CCND2* within t(4;14) and CCND1 expression within t(11;14) tumours. Assignment of HRD to D1 and D2 groups was also based on *CCND1* and *CCND2* expression respectively [13, 34]. Shah et al. later described relative overexpression of *CCND1* in HRD tumours with gain(11) and *CCND2* in HRD without gain(11), similar to the D1 and D2 subgroups[12].

I have therefore utilised expression data from the Taqman translocation assay to define subgroups based on unsupervised clustering of *CCND1* and *CCND2* expression at presentation. As there was only 1 case with t(6;14), *CCND3* expression was not considered.

Taqman data was available for 158 cases from the CNA evolution cohort at presentation. Unsupervised clustering produced 3 distinct groups based on tumor biology which I have labelled D1, D2 and D1+2, while similar, it is important to note that these groups are not synonymous to the TC classification system, which uses the expression of 8 genes to define groups. The distribution of initiating events and presentation CNA within each group is summarised in **Figure 7-1** and **Table 6-1.**

In this analysis I have only considered evolution of interstitial CNA between presentation and relapse. Focal CNA were not included.

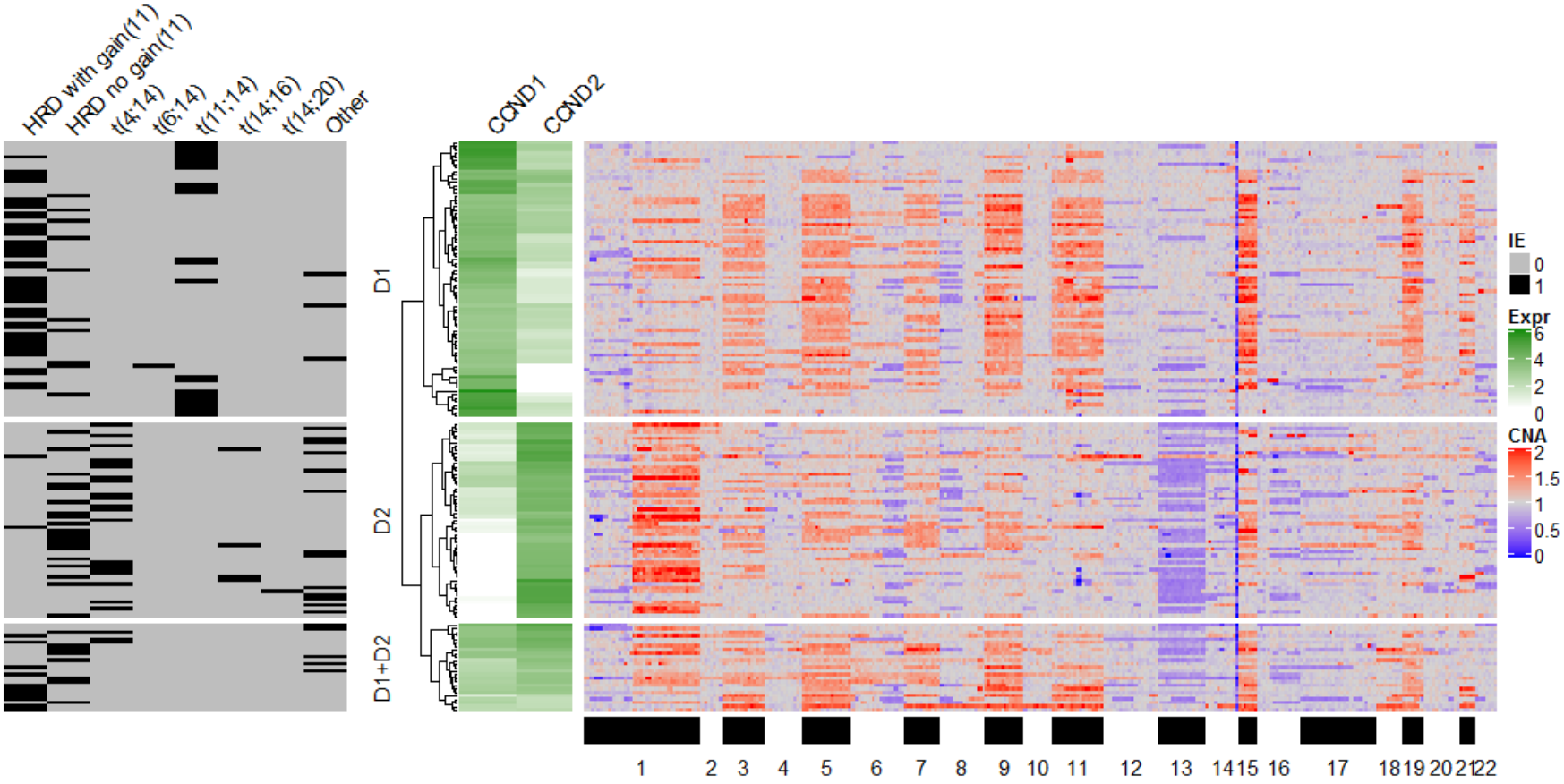

Figure 7-1 Heatmap demonstrating subgroups based on cyclin D1 and cyclin D2 expression (middle) and corresponding CNA at presentation (right). Legend on left side provides context on cytogenetic subgroups (dark bar = present, grey = absent). Legend at bottom: black and white bands representing chromosomal mapping of digitalMLPA probes chr1-22 from left to right in ascending order of genomic position.

7.1.1 Evolution of CNA at relapse

Distribution in pattern of evolution per cyclin D expression subgroup is shown in **Figure 7-2**. Clonal evolution of CNA at relapse was highest in the D1+D2 group observed in 25 (96%) of tumours; the majority (65%) were branching. The proportion of evolution patterns was similar between the D1 and D2 groups with evolution of CNA observed in 66 (84.6%) and 46 (83.6%) of tumours respectively.

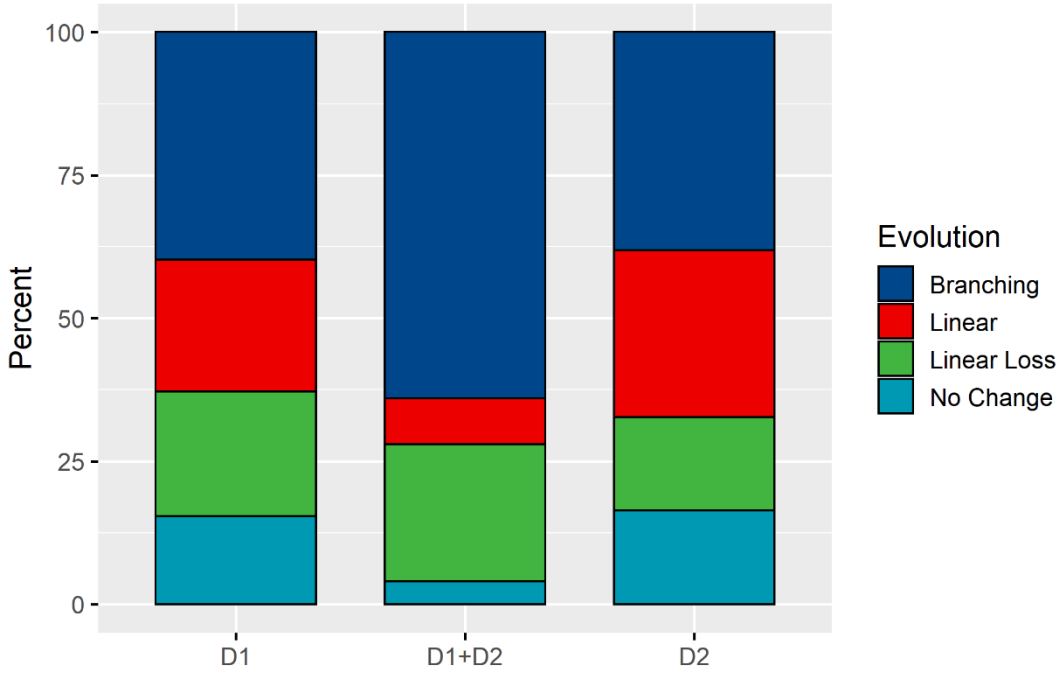

Figure 7-2 Frequency of evolutionary patterns per cyclin D cluster.

7.1.2 D1 Subgroup

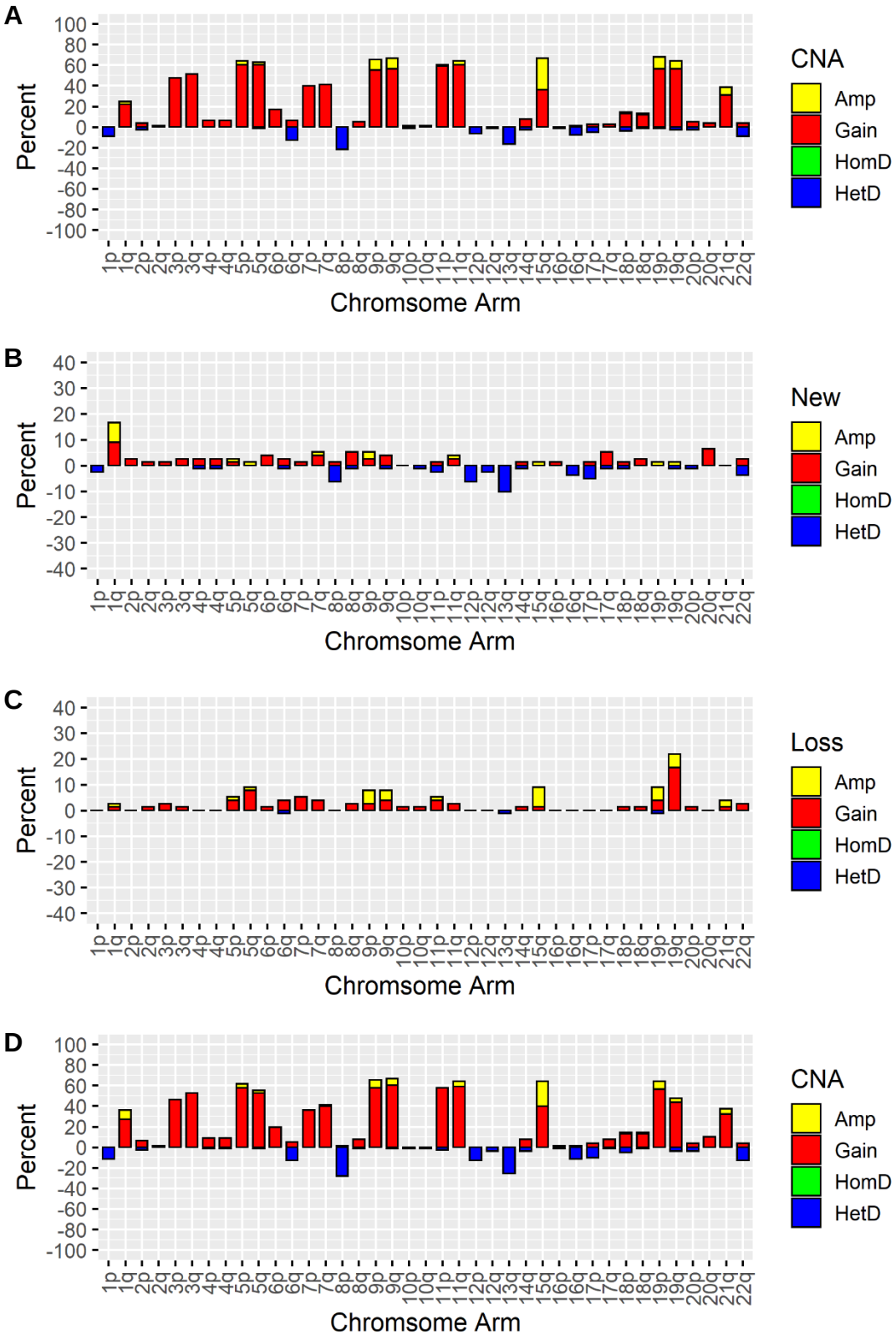

Figure 7-3 CNA evolution in the D1 subgroup (A) Frequency of interstitial CNA at presentation (B) Frequency of new interstitial CNA observed at relapse (C) Loss of interstitial CNA at relapse (D) Net frequency of interstitial CNA at relapse.

The D1 subgroup contained 78 patients. **Figure 7-3** summarises frequency of interstitial CNA:

- CNA at presentation **(A)**
- New CNA at relapse **(B)**
- Loss of CNA at relapse **(C)**
- Net CNA at relapse **(D)**

This group is characterised by high ratio of *CCND1:CCND2* expression. All t(11;14) and the majority (79.0%) of HRD with gain(11) tumors were clustered into this group. Of note there was an absence of high risk IgH translocations.

At presentation, 3 or 4 copies of chromosomes 3, 5, 7, 9, 11, 15, 19 and 21 were seen in 46.2%, 60.3%, 38.5%, 62.8%, 57.7%, 66.7%, 60.3% and 38.5% of tumours respectively.

The most frequent (non HRD) CNA at presentation involved gain/amp(1q), del(8p), del(13q), gain(6p) and del(6q); observed in 19 (24.4%), 15 (21.8%), 13 (16.7%), 13 (16.7%) and 10 (12.8%) tumours respectively.

The most common new CNA to evolve at relapse were gain/amp(1q) and del(13q); observed in 15(19.2%) and 8 (10.3%) tumours. New del(12p) and del(8p) at relapse was seen in 5 (6.4%) tumours.

Loss of CNA at relapse was most commonly involved gain(19q) observed in 9 (11.5%) of tumours, followed by gain(15) observed in 6 (7.7%) tumours.

Overall there was a significant increase in the average number of CNA per tumour between time points; 10.4 (range 0-20) at presentation vs 10.9 (range 0-23) at relapse (P=0.010). Branching, linear, linear loss and stable evolution were observed in 39.7%, 23.1%, 21.8% and 15.5% of tumours respectively.

7.1.3 D2

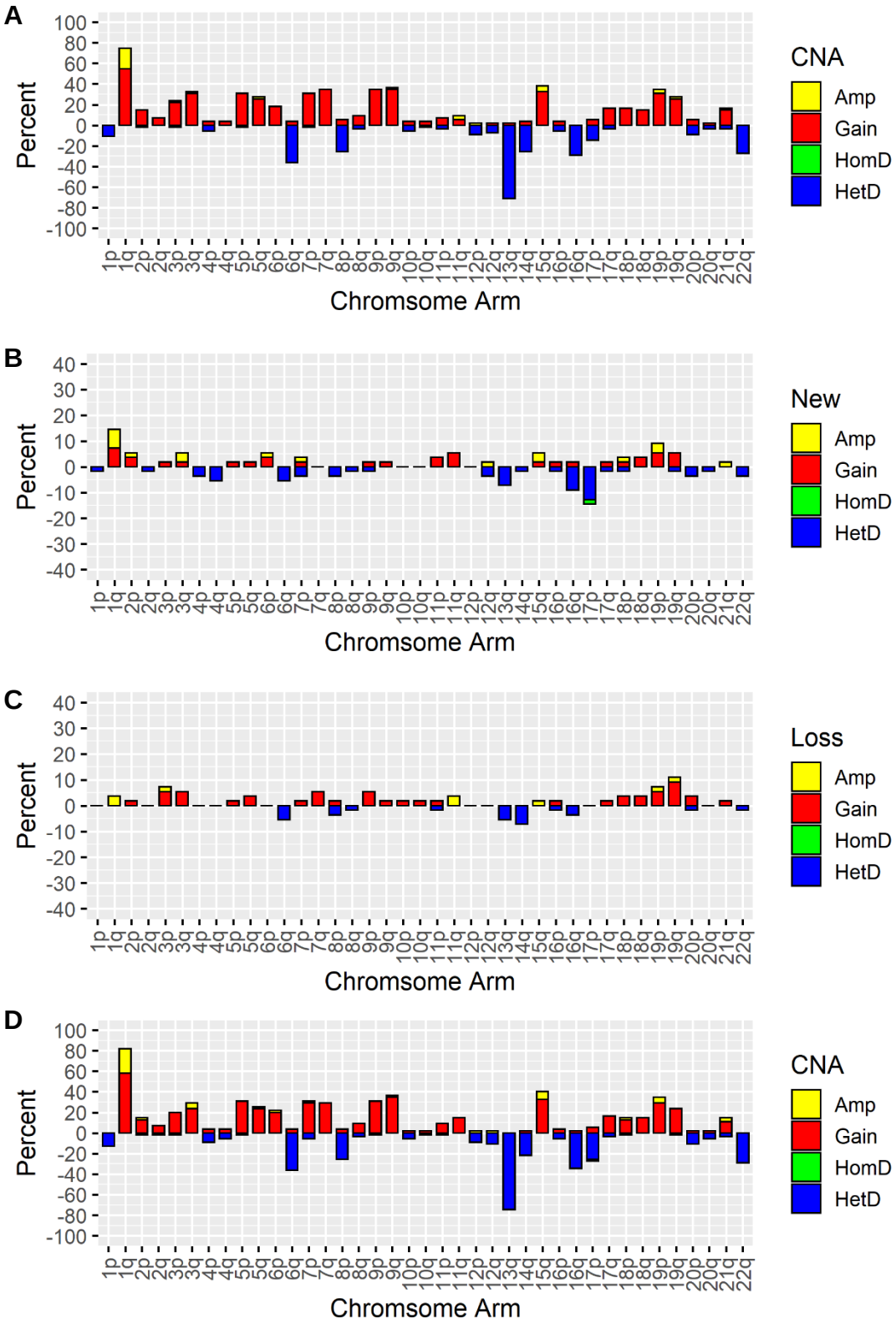

Figure 7-4 CNA evolution in the D2 subgroup (A) Frequency of interstitial CNA at presentation (B) Frequency of new interstitial CNA observed at relapse (C) Loss of interstitial CNA at relapse (D) Net frequency of interstitial CNA at relapse.

The D2 subgroup contained 55 patients. **Figure 7-4** summarises frequency of interstitial CNA:

- CNA at presentation **(A)**
- New CNA at relapse **(B)**
- Loss of CNA at relapse **(C)**
- Net CNA at relapse **(D)**

This group is characterised by a high ratio of *CCND2:CCND1* expression. The majority (89.3%) of tumours with high risk IgH translocations were clustered to this group. It also contains over half (52.6%) of tumours with HRD without gain(11) in comparison to just 3.5% of HRD with gain(11) tumours.

At presentation, 3 or 4 copies of chromosomes 3, 5, 7, 9, 11, 15, 19 and 21 were seen in 21.8%, 23.6%, 29.1%, 30.9%, 3.6%, 38.2%, 23.6% and 16.4% of tumours respectively.

The most frequent non HRD CNA at presentation involved gain/amp(1q) and del(13q) observed in 41 (74.6%) and 39 (70.9%) tumours respectively. Recurrent deletions were a predominant feature at presentation, the most frequent involving 6q, 16q, 22q, 14q, 8p, 17p, and 1p; observed in 36.4%, 29.1%, 27.3%, 25.6%, 25.6%, 14.6% and 10.9% of tumours respectively.

The most common new CNA to evolve at relapse involved gain/amp(1q), del(17p), del(16q) and del(13q) observed in 8 (14.6%), 7 (12.7%), 5 (9.1%) and 4 (7.3%) tumours respectively.

Recurrent loss of CNA at relapse was uncommon, the highest frequency observed involved del(14q) seen in 4 (7.3%) of tumour.

There was no significant difference in the mean number of CNA per tumour between time points; 9.12 (range 1-34) at presentation vs 9.44 (range 0-29) at relapse (P=0.14). Branching, linear, linear loss and stable evolution were observed in 38.2%, 29.1%, 16.4% and 16.4% of tumours respectively

7.1.4 D1+D2

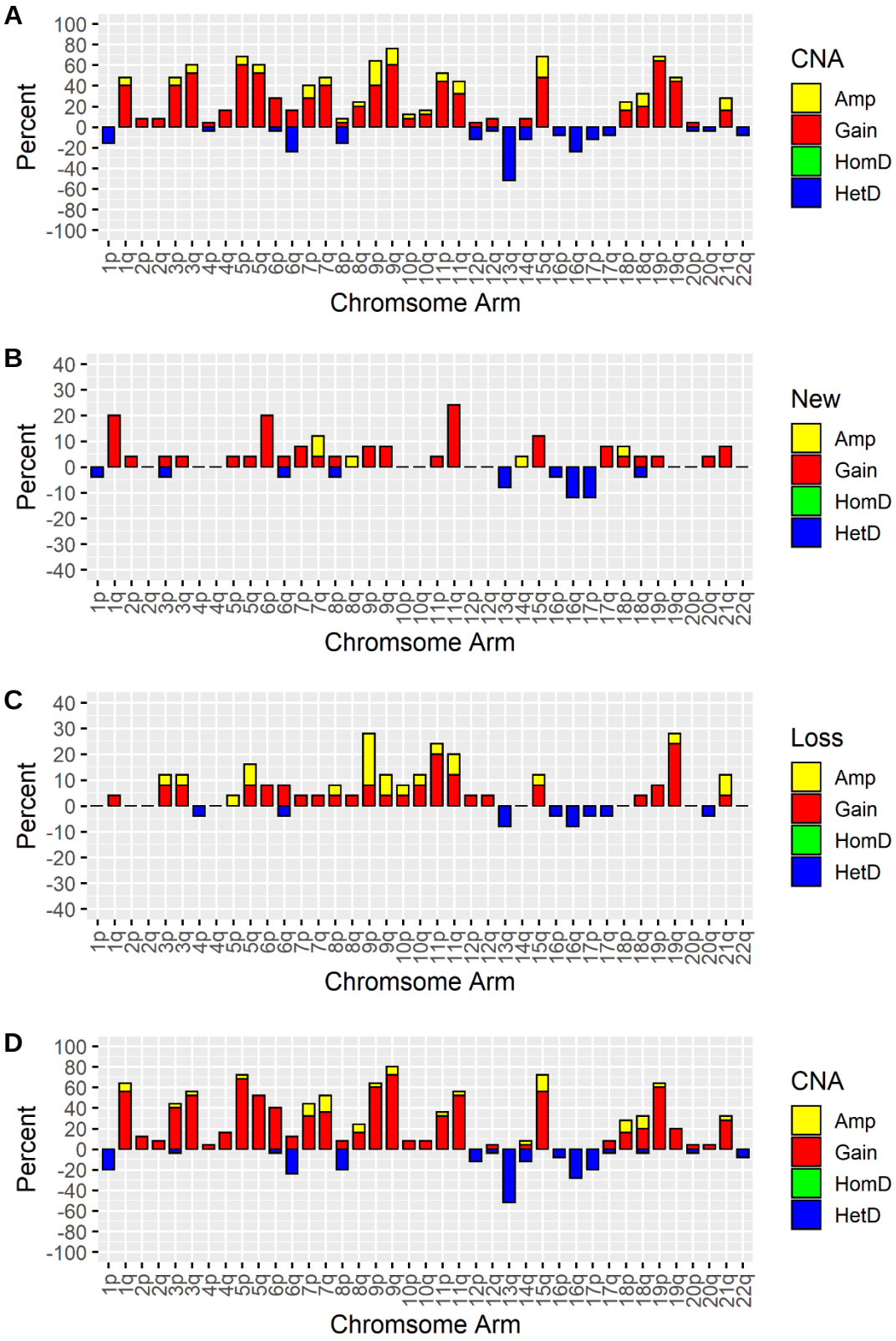

Figure 7-5 CNA evolution in the D1+D2 subgroup (A) Frequency of interstitial CNA at presentation (B) Frequency of new interstitial CNA observed at relapse (C) Loss of interstitial CNA at relapse (D) Net frequency of interstitial CNA at relapse.

The D1+D2 subgroup contained 25 patients. **Figure 7-5** summarises frequency of interstitial CNA:

- CNA at presentation **(A)**
- New CNA at relapse **(B)**
- Loss of CNA at relapse **(C)**
- Net CNA at relapse **(D)**

This group is characterised by an equal ratio of *CCND1: CCND2* expression at presentation. 19 (76%) tumours within the group are HRD; 8 (32%) HRD without gain(11) and 11 (44%) HRD with gain(11). Only 3 (12%) tumours harbour high risk IgH translocations.

At presentation, 3 or 4 copies of chromosomes 3, 5, 7, 9, 11, 15, 19 and 21 were seen in 48.0%, 60.0%, 40.0%, 64.0%, 44.0%, 68.0%, 44.0% and 28.0% of tumours respectively.

The most frequent new CNA to evolve at relapse involved gain(11q) observed in 6 (25%) tumours. Gain(1q) and gain(6p) were each observed in 5 (20%) tumours and gain(15), del(16q) and del(17p) in 3 (12%) tumours.

Recurrent loss of CNA at relapse was also observed. Loss of a whole chromosome resulting in resolution of trisomy to diploid or tetrasomy to trisomy occurred in chromosomes 3, 7, 9, 11, 15 and 21; observed in 1 (4%), 1 (4%), 2(8%), 3 (12%), 2 (8%) and 3 (12%) tumours respectively. Loss of gain/amp (19q), gain/amp(9p), gain(11p) and del(13q) was observed in 6 (24%), 4 (16%), 3 (12%) and 3 (12%) tumours respectively. Resulting in resolution of gain to diploid status, deletion to diploid status or amplification to gain.

There was no significant difference in the mean number of CNA per tumour between time points; 12.52 (range 0-22) at presentation vs 12.64 (range 0-24) at relapse (P=0.61). Branching, linear, linear loss and stable evolution were observed in 64%, 8%, 24% and 4% of tumours respectively

7.2 Evolution of high risk lesions

There was marked difference in the frequency of high risk initiating events between cyclin D groups, with the majority of t(4;14), t(14;16) and t(14;20) tumours in the D2 cluster.

Gain/amp(1q) and del(17p) followed a similar pattern; with highest frequencies observed in D2 cluster and lowest in the D1 cluster. Change in frequency of gain/amp(1q) between presentation and relapse for clusters D1, D1+D2 and D2 was 24.4% to 35.9%, 48.0% to 64.0% and 75.6% to 81.8% respectively. Change in frequency of del(17p) between presentation and relapse for clusters D1, D1+D2 and D2 was 5.1% to 10.3%, 12% to 20% and 14.6% to 27.3% respectively **Figure 7-6 (A, B)**. Del(1p) was more common in the D1+D2 and D2 clusters, with the largest increase at relapse seen in D1+D2 **(Figure 7-6C)**.

The proportion of tumours with single, double, triple or quadruple hit also correlated with *CCND2:CCND1* expression ratio, with a higher proportion of tumours with 1 or more high risk lesions seen in in the D2 cluster. All clusters demonstrated clonal evolution acquiring new high risk lesions at relapse. As a result, 51 (92.7%) tumours from the D2 group had at least 1 high risk lesion at relapse and 32 (58.2%) had at least 2. Conversely, 41 (52.6%) tumours from the D1 group had no high risk lesions at relapse **(Figure 7-7)**.

7.3 Association with overall survival

Univariate cox regression analysis was used to compare OS between cyclin D clusters. Survival data was available for 147 patients; D1 cluster: 75 patients; D1+D2 cluster: 21 patients and D2 cluster: 51 patients.

The D1+2 and D2 clusters were both associated with a shorter OS when compared to D1 (HR 2.28; *P*=0.013 and HR 1.58; *P*=0.094 respectively). Median OS was 32.7, 47.9 and 67 months for D1+2, D2 and D1 clusters respectively (log-rank *P*=0.03) **(Figure 7-8)**.

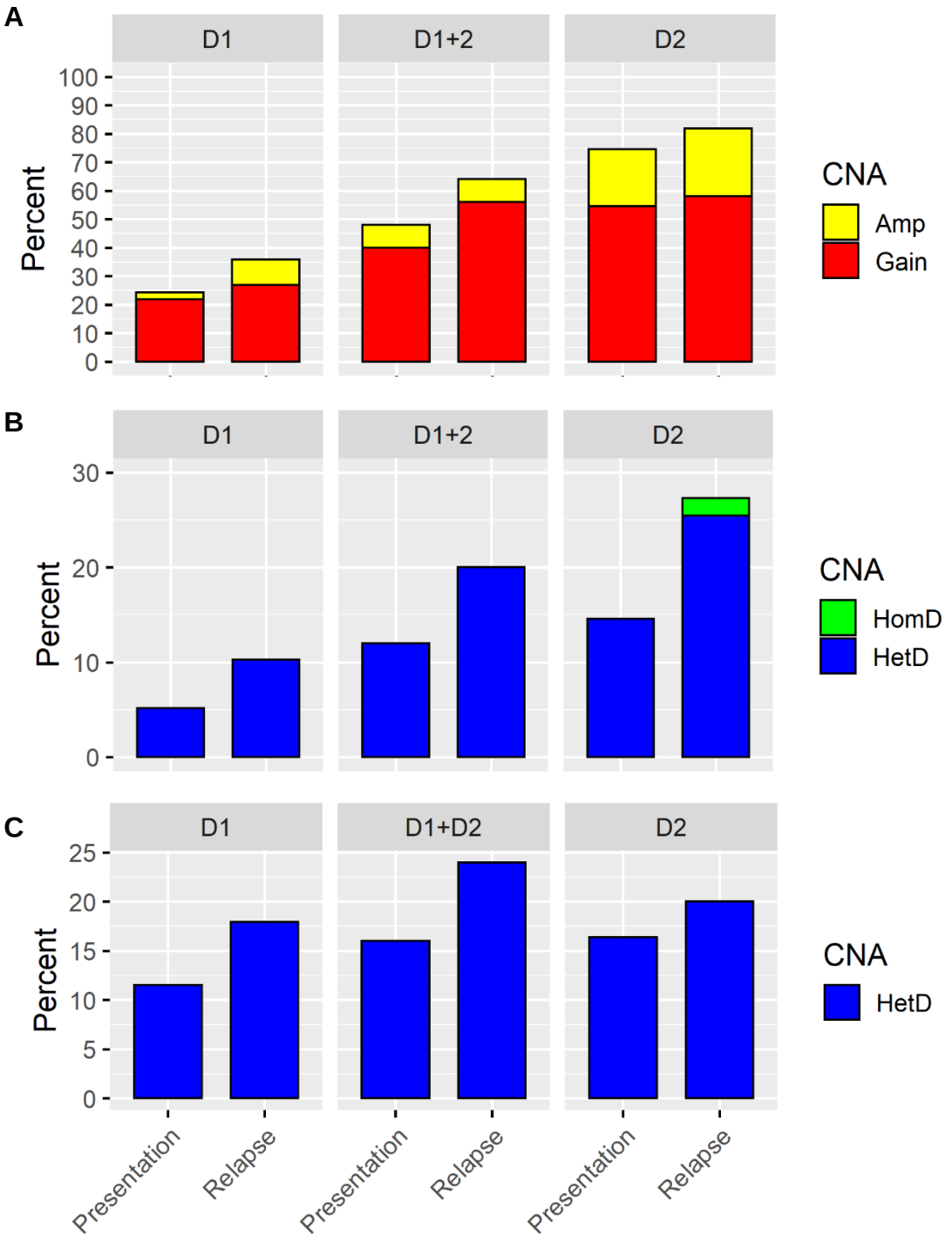

Figure 7-6 High risk CNA per cyclin D cluster at sequential time points; (A) gain/amp(1q); (B) del(17p); (C) del(1p32.3)/del(1p).

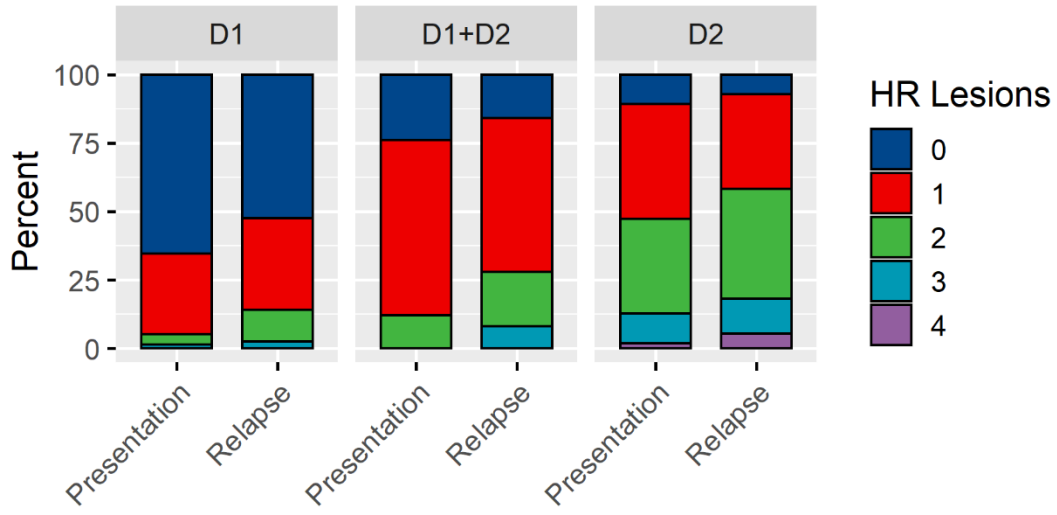

Figure 7-7: Co-existing high risk lesions per cyclin D cluster

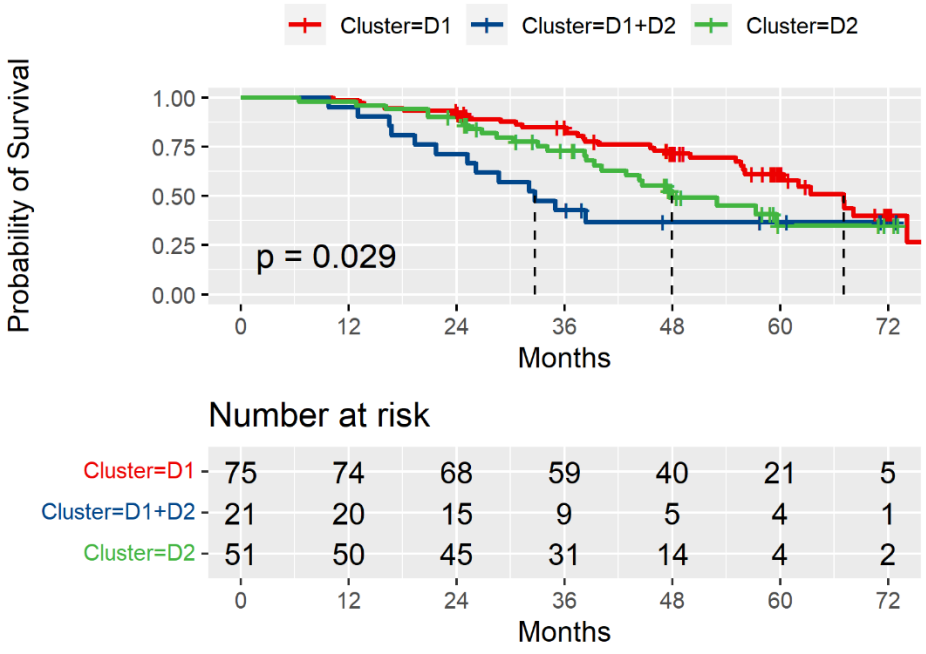

Figure 7-8: Kaplan-Meier for OS in relation to cyclin D cluster.

7.4 Discussion

Dysregulation of D group cyclins is well established as a universal characteristic of myeloma. Over expression of *CCND1* directly caused by translocation or increased copy number of 11q and overexpression of *CCND2* due to the downstream effects of t(4;14), t(14;16), t(14;20) and HRD. The distribution of initiating events within each cluster was therefore expected.

Correlation of high risk CNA at presentation with increasing *CCND2:CCND1* expression was the predominant feature of this analysis; mirrored by increased acquisition of new high risk CNA at relapse. Particularly with a striking enrichment for acquisition of del(17p) at relapse in the D2 group.

The high proportion of 1q amplification in the D2 group supports its association with chromosome instability and highlights its dependency on *CCND2* expression. While overexpression of *CCND2* has previously been attributed to high risk disease, better understanding of its dysregulation and downstream effects could provide insight into the evolution of high risk disease and reveal therapeutic targets.

CCND2 and *CCND1* expression in the D1+D2 group was relatively equal. This cluster could represent tumours with 2 major competing clones; one with high *CCND1* expression and the other with high *CCND2* expression. A change in dominant clone at relapse reflected by the high proportion of branching evolution observed at relapse within this group. Interestingly the D1+D2 group had a shorter median survival than the D2 group. It is important to note that clustering was based on expression at presentation. Given the potential switch of dominant clones at relapse within the D1+D2 group, it would be interesting to reassess clusters using cyclin D expression at relapse.

7.4.1 Conclusion

CCND2:CCND1 expression can be used to predict evolutionary trajectory, in particular tumours that will acquire high risk cytogenetic lesions. This could be of particular benefit for HRD tumours where cytogenetic molecular subgrouping was less informative. As discussed in Chapter 5, identification of

divergent evolutionary pathways provides scope for rationalised targeted therapies.

Chapter 8: CNA evolution results- in relation to treatment

8.1 Introduction

To investigate whether molecular changes in response to therapy are central to the emergence of disease progression and treatment resistance. I have looked for differences in CNA evolution between treatment pathways of the MXI trial.

Treatment pathways and randomisations of the 178 patients are summarised in **Figure 4-1** and **Table 4-1**. I have compared patients who received high dose melphalan vs none (TE vs TNE) and those who received lenalidomide maintenance vs observation. Comparisons of individual induction regimes were not pursued due to small patient numbers.

8.2 High dose melphalan

Within the CNA evolution cohort, 100 (56.2%) patients were transplant eligible and received high dose melphalan, 78 (43.8%) patients did not. The ratio of treatment intensities reflected that of whole MXI population. Of note this was not a randomisation step within the trial but instead a decision based on clinical criteria and clinician discretion.

Sub-group	Melphalan n (%)	No Melphalan n (%)
t(4;14)	16 (16.0)	3 (3.8)
t(11;14)	12 (12.0)	9 (11.5)
t(14;16)	1 (1.0)	1 (1.3)
t(14;20)	1 (1.0)	0 (0.0)
HRD with gain(11)	34 (34.0)	28 (35.9)
HRD without gain(11)	15 (15.0)	19 (24.4)
IgH t & HRD	8 (8.0)	5 (6.4)
Other	13 (13.0)	13 (16.7)

Table 8-1: Cytogenetic subgroups per treatment arm: Transplant eligibility.

Given the differences in CNA evolution noted between molecular sub-groups, I first considered the frequency of each cytogenetic subgroup within each treatment arm (**Table 8-1**). The frequency of each molecular subgroup was similar in patients treated with or without melphalan, with the exception of t(4;14). The number of patients with t(4;14) within TE and TNE groups was 16 (16.0%) and 3 (3.8%) respectively.

Both groups showed a net increase in the average number of CNA per patient between presentation and relapse. The increase was significant in both treatment arms. Melphalan treatment: Average CNA was 10.5 (range 0-34) at presentation vs. 11.5 (range 0-29) at relapse (Wilcoxon Signed-Ranked *P* = 0.0078). No Melphalan treatment: average CNA was 12.5 (range 0-26) at presentation vs. 13.0 (range 0-24) at relapse (Wilcoxon Signed-Ranked *P* = 0.0024)

There was no significant difference in the proportion of evolution patterns per treatment arm (Chi square *P*= 0.73). In patients who received melphalan, branching, linear, linear loss and stable patterns of evolution were observed in 44.9%, 21.8%, 17.9% and 15.4% of cases respectively. In patients who did not receive melphalan branching, linear, linear loss and stable patterns of evolution were observed in 46.0%, 23.0%, 20.0% and 11.0% of cases respectively (**Figure 8-1**).

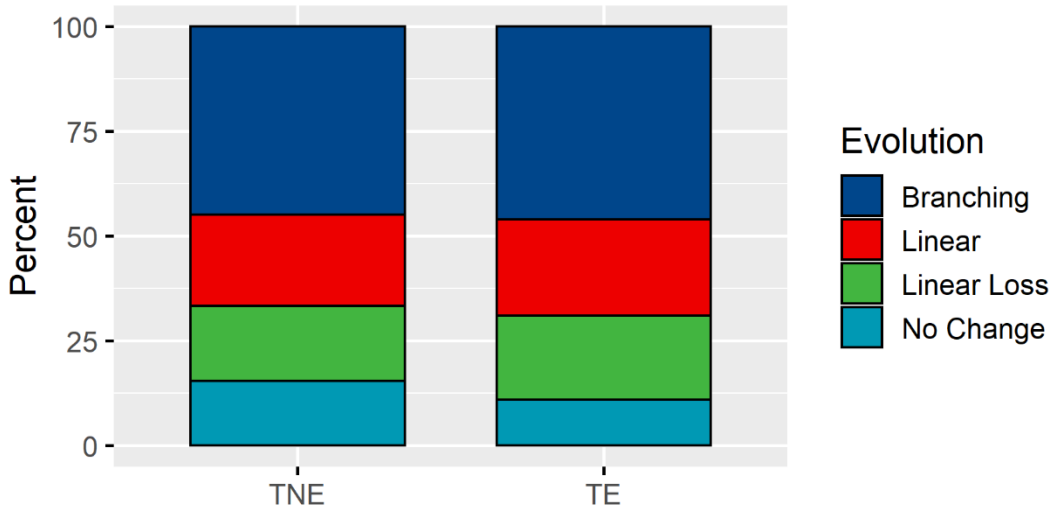

Figure 8-1 Evolutionary patterns based on treatment intensity; TE: Transplant eligible; TNE: Transplant non-eligible.

The frequency of new CNA acquisition at relapse was compared between treatment arms per chromosome arm. No significant difference was found. While not statistically significantly the largest variation in CNA evolution involved gain(8p), del(13q), del(17p) and gain(1q);

- New gain(8p) observed in 1.3% of tumours in TNE arm vs 7.0% of tumours in the TE arm
- New del(13q) observed in 6.4% of tumours in the TNE arm vs 12.0% tumours in the TE arm
- New del(17p) and gain(1q) observed in 5.1% of tumours in the TNE arm vs 10.0% of tumours in the TE arm.

Figure 8-2 shows all new interstitial and focal CNA per patient at relapse, split by TNE and TE patients, demonstrating a similar frequency of CNA evolution between both groups.

8.2.1 Change per cytogenetic subgroup

For each cytogenetic subgroup, the frequency of new CNA acquisition at relapse was compared between treatment arms per chromosome arm. No significant difference was found.

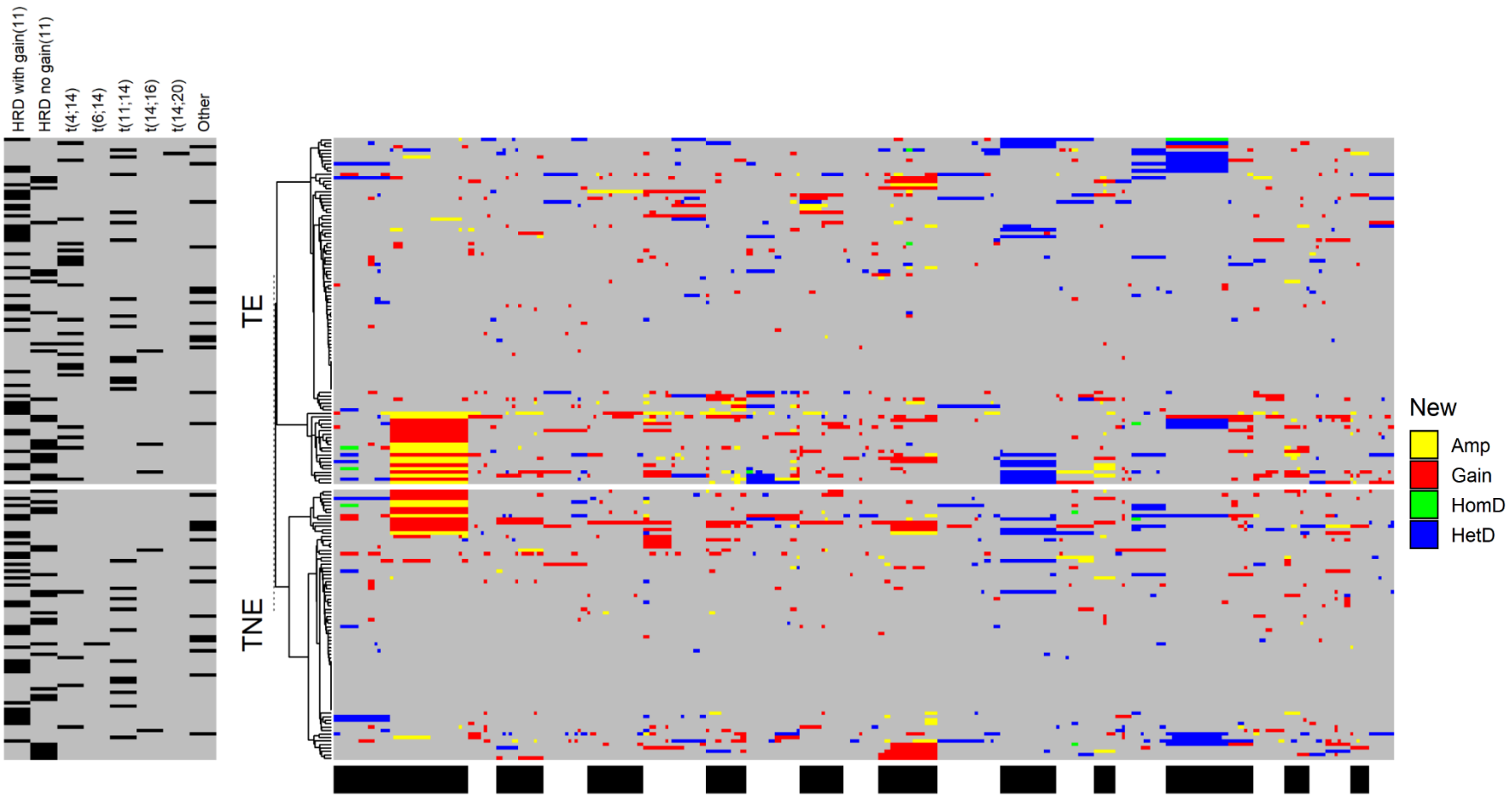

Figure 8-2 Heatmap of CNA evolution based on treatment intensity; TE: transplant eligible; TNE: transplant non-eligible. Legend on left side provides context on cytogenetic subgroups (dark bar = present, grey = absent). Legend at bottom: black and white bands representing chromosomal mapping of digitalMLPA probes chr1-22 from left to right in ascending order of genomic position.

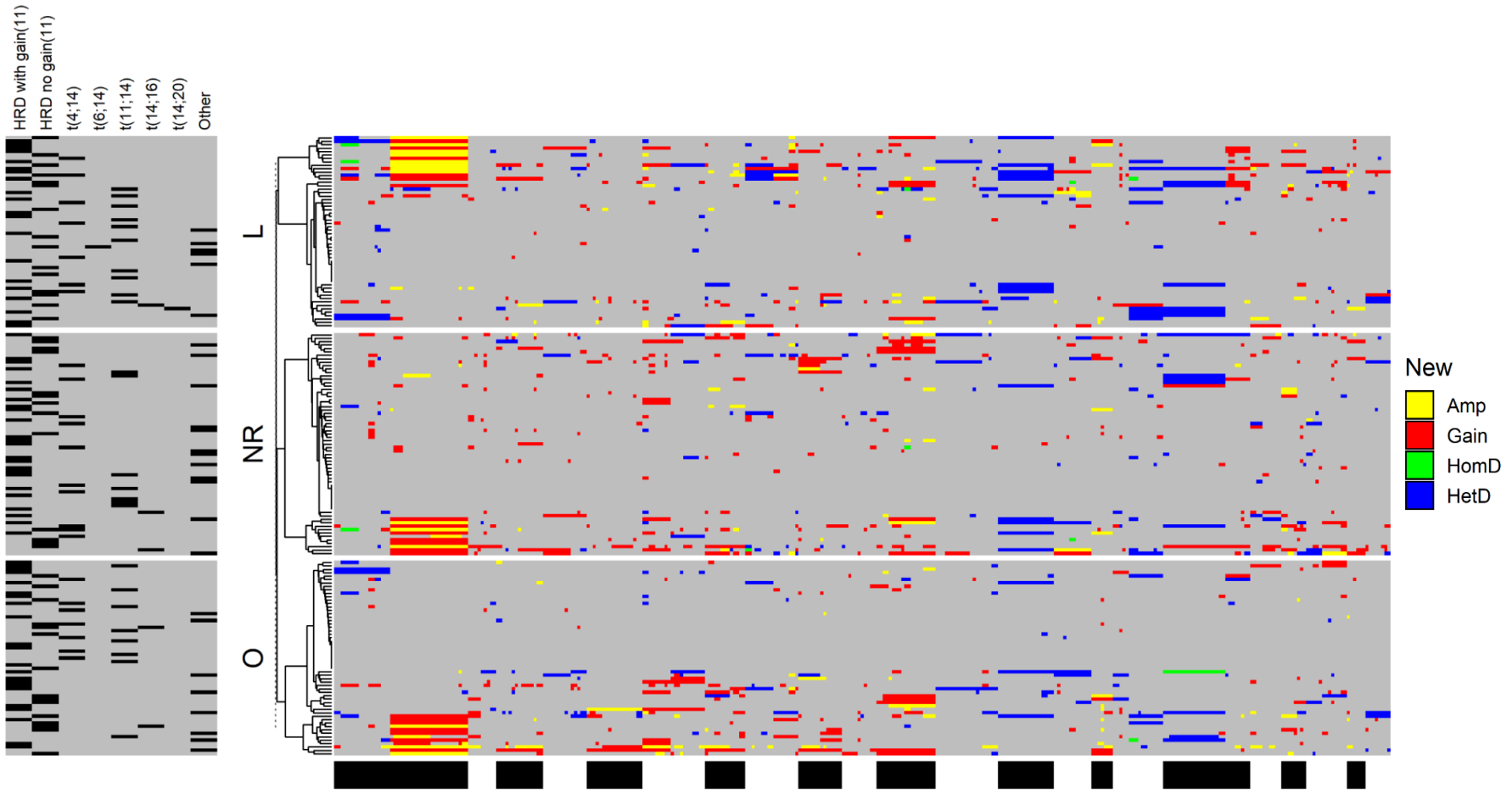

Figure 8-3 Heatmap of CNA evolution based on maintenance; L: lenalidomide; O: observation; NR: not randomised. Legend on left side provides context on cytogenetic subgroups (dark bar = present, grey = absent). Legend at bottom: black and white bands representing chromosomal mapping of digitalMLPA probes chr1-22 from left to right in ascending order of genomic position.

8.3 Lenalidomide maintenance

Within the CNA evolution cohort, 113 (63.5%) patients underwent randomisation; 57 randomised to observation and 56 randomised to lenalidomide based maintenance after completion of induction treatment. Within the lenalidomide maintenance randomisation, 42 were assigned lenalidomide monotherapy and 14 assigned lenalidomide with vorinostat. Since addition of vorinostat to lenalidomide did not result in a difference in outcome I have considered these patients as one group. Through clinician discretion 65 (36.5%) patients were not deemed suitable to enter the maintenance randomisation and were therefore not included in this comparison. As per trial protocol, treatment with lenalidomide maintenance continued until there was evidence of disease progression at which point the relapse bone marrow was performed. This provides useful data to look for molecular changes emerging under the ongoing selection pressure of lenalidomide.

Given the differences in CNA evolution noted between molecular sub-groups in chapter 6, I first considered the frequency of each subgroup per maintenance arm; lenalidomide vs observation (**Table 8-2**), frequencies were similar.

Group	Len Maintenance n (%)	Observation n (%)
t(4;14)	5 (8.9)	5 (8.7)
t(11;14)	9 (16.1)	7 (12.3)
t(14;16)	0 (0.0)	0 (0.0)
t(14;20)	1 (1.8)	0 (0.0)
HRD with gain(11)	20 (35.7)	20 (35.1)
HRD without gain(11)	10 (17.9)	12 (21.1)
IgH t & HRD	5 (8.9)	5 (8.8)
Other	6 (10.7)	8 (14.0)

Table 8-2 Cytogenetic subgroups per treatment arm: Maintenance randomisation.

Evolution of CNA at relapse was similar in each treatment group; Lenalidomide maintenance vs observation, suggesting that there is no relationship between the acquisition of CNAs and lenalidomide maintenance:

Both groups showed a net increase in the average number of CNA per patient between presentation and relapse. Lenalidomide maintenance arm: average CNA was 11.1 (range 0-23) at presentation vs. 11.7 (range 0-24) at relapse (Wilcoxon Signed-Ranked *P* = 0.050). Observation arm: average CNA was 12.1 (range 0-34) at presentation vs. 12.3 (range 0-29) at relapse (Wilcoxon Signed-Ranked *P* = 0.58).

There was no significant difference in distribution of evolution pattern between groups (Chi square *P*= 0.83) (**Figure 8-2**). Within the observation group branching, linear, linear loss and stable patterns of evolution were observed in 41.1%, 26.8%, 19.6% and 12.5% of patients respectively. Within the maintenance group branching, linear, linear loss and stable patterns of evolution were observed in 49.1%, 21.1%, 17.5%, and 12.3% of patients respectively.

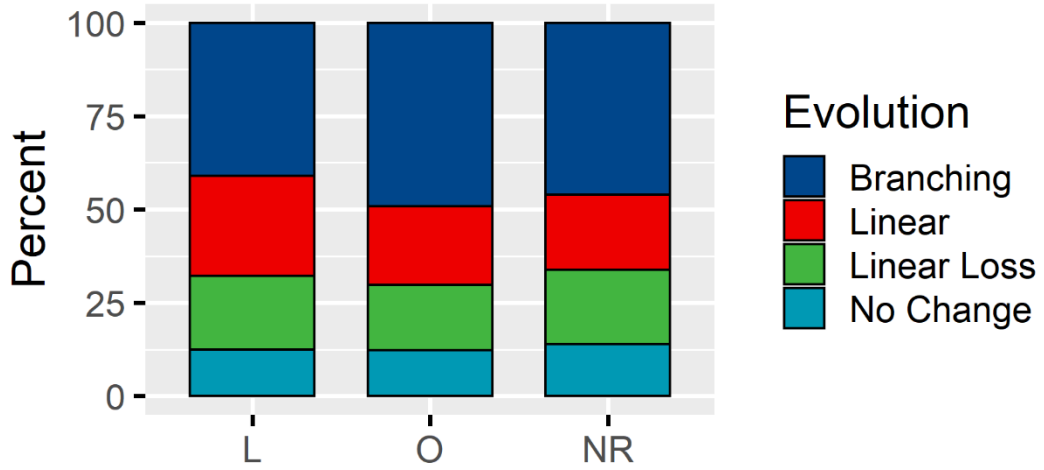

Figure 8-4: Evolutionary patterns based on maintenance randomisation; L: Lenalidomide; O: Observation; NR: Not randomised.

The frequency of new CNA acquisition at relapse was compared between treatment arms per chromosome arm. No significant difference was found. While not statistically significantly the largest variation in new CNA evolution involved del(13q), del(16q), amp(1q) and del(17p);

- New del(13q) was observed in 16.1% of tumours treated with lenalidomide maintenance vs 5.3% of tumours in the observation arm.
- New del(16q) was observed in 14.3% of tumours treated with lenalidomide maintenance vs 5.3% of tumours in the observation arm.
- New amp(1q) was observed in 14.3% of tumours treated with lenalidomide maintenance vs 5.3% of tumours in the observation arm.
- New del(17p) was observed in 12.5% of tumours treated with lenalidomide maintenance vs 3.5% of tumours in the observation arm.

Figure 8-4 shows all new interstitial and focal CNA per patient at relapse, split by maintenance arm. It demonstrates a similar frequency of CNA evolution between each group.

8.4 IMiD related genes

As discussed in section 1.1.5.2 the anti-myeloma effects of IMiDs include direct PC cytotoxicity, anti-angiogenesis and immune modulation[6]. IMiDs bind to cereblon, which acts as a substrate adaptor of the $CRL4^{CRBN}$E3 ubiquitin ligase complex. The binding of IMiDs leads to the selective ubiquitination and therefore proteasome degradation of PC transcription factors Ikaros *(IKZF1)* and Aiolos (*IKZF3). IKZF1* and *IKZF3* regulate a transcriptional network that is essential for malignant PC survival[26].

Probes for *CRBN, IRF4, IKZF1* and *IKZF3* are included within the dMLPA probe mix. I have therefore investigated focal CNA of these genes in relation to maintenance therapy with lenalidomide.

Evolution of focal CNA at relapse was observed, but uncommon for genes directly involved in IMiD mode of action (**Figure 8-5**). Out of all focal changes discussed below only 3 occurred in the presence of lenalidomide maintenance; new del(*CRBN*), new gain(*IRF4*) and loss of gain(*IRF4*).

8.4.1.1 *CRBN*

CRBN is located at 3p26.2. Gain of this gene is common in the context of HRD trisomy. At relapse, new gain(3p26.2) was observed in 3 (1.7%) tumours and new del(3p26.2) in 1 (0.6%) tumour.

8.4.1.2 *IRF4*

IRF4 is located at 6p25.3. For this gene CNA is common in the context interstitial gain(6p). At relapse new del (6p25.3) was observed in 1 (0.6%) and loss of del(6p25.3) to diploid status in 2 (1.1%) tumours. At relapse new gain(6p25.3) was observed in 2 tumours, resolution of the CNA to diploid status was observed in 3 tumours.

8.4.1.3 *IKZF1*

IKZF1 is located at 7p12.2. Gain of this gene is common in the context HRD trisomy. At relapse loss of del(7p12.2) was observed in 1 tumour. There was no new focal CNA in 7p12.2 at relapse.

8.4.1.4 *IKZF3*

IKZF3 is located at 17q12. At relapse loss of del(17q12) was observed in 1 tumour at relapse. There was no new focal CNA in 17q12 at relapse.

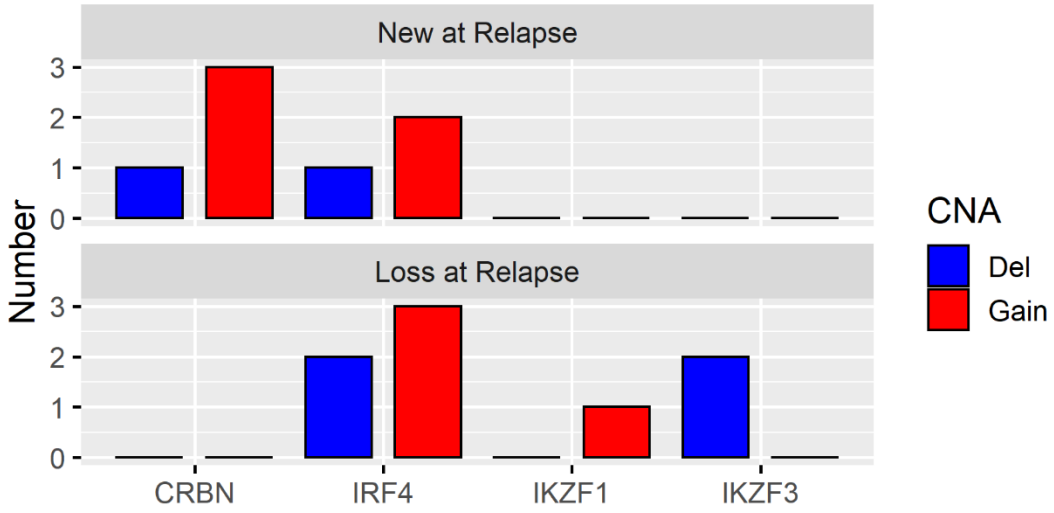

Figure 8-5: Focal CNA evolution in IMiD related genes

8.5 Discussion

In chapter 5 I demonstrated that clonal evolution occurs in the majority of tumours (87.1%) at relapse, with new gain/amp(1q) as the most prominent feature. I have also shown the trajectory of CNA evolution is affected by a tumours molecular subgroup.

This analysis aimed to see if treatment can be linked to specific CNA evolution and in doing so identify potential mechanisms of treatment resistance. There was no discernible difference in pattern of evolution at relapse in relation to treatments; transplant vs no transplant and lenalidomide maintenance vs observation. Jones et al previously described a difference in evolution pattern in relation to depth of treatment response; showing a higher frequency of branching evolution in patients who achieved CR and VGPR[14]. In future analysis it may be useful to compare treatment arms with patients also categorised by depth of response.

Importantly, there was no significant difference in the frequency of CNA change, per chromosome arm, in relation to treatment. Cytotoxic effects of myeloma treatment likely exert a degree of selection pressure on tumour clones; reflected by the majority of tumours demonstrating clonal evolution at relapse. While treatment may exert a selection pressure on tumours, these results do not demonstrate enrichment of any specific CNA profile. Therefore no CNA can be specifically implicated in mechanisms of treatment resistance.

A lack of specific CNA enrichment in relation to uniform treatment correlates with the work of Corre et al. (discussed in section 1.2.2.2.1) who suggested a heterogeneous result should be expected when applying a uniform pressure to an already heterogeneous population. To address this problem, my analysis has also examined CNA change in the context of cytogenetic subgroups per treatment arm. Again there was no enrichment for specific CNA in relation to treatment. Importantly, these results are unique to previous sequential studies as they allow direct comparison of evolution between randomised treatment arms, therefore providing stronger evidence for a lack of CNA enrichment.

Whilst not statistically significant, evolution of new del(17p) was more common in patients who received high dose melphalan suggesting a possible selection from treatment. Melphalan is a highly cytotoxic drug that causes significant DNA damage to tumours. It is therefore feasible that clones harbouring deletion of 17p/*TP53* would be resistant to melphalan treatment and would be positively selected for. Similarly evolution of new gain(1q) and del(17p) were also more common in patient who received lenalidomide maintenance. Without statistical significance the clinical relevance of this observation is unclear. Particularly when considering the bias selection of this cohort as I have only included relapsed patients from the MXI trial. Those relapsing in the TE and lenalidomide maintenance arms will be inherently high risk compared to the TNE and observation arms.

The lenalidomide vs observation arm of this cohort provided useful data to examine CNA of genes implicated in lenalidomide's mechanism of action. Focal CNA in these genes were rare and none were enriched by lenalidomide treatment, suggesting they are not a major determinant of acquired resistance to lenalidomide or other IMiDs. Furthermore, the lack of significant difference in CNA evolution in relation to lenalidomide supports outcomes reported by the MXI trial, where lenalidomide maintenance was shown to improve outcomes compared to observation. Dramatic changes to molecular landscape in relation to lenalidomide maintenance might put its clinical benefit into question.

8.5.1 Conclusion

With no enrichment of CNA in relation to treatment, sequential molecular profiling has not provided information regarding specific mechanisms of treatment resistance. Given the heterogeneity of myeloma, a larger cohort of tumours would be more informative. Further analysis with gene expression profiles in relation to treatment will be presented in later chapters. Of interest recent work from Rustad et al has reported mutational signature in relapsed myeloma specifically relating to melphalan therapy, it was not observed in newly diagnosed or melphalan naïve tumours [64]. Consistent with my hypothesis, this does demonstrate a selection pressures from treatment but highlights the difficulty in demonstrating associated clonal enrichment without

high resolution genetic profiling. Further work is required to establish how melphalan induced mutations will impact molecular evolution at relapse.

Chapter 9: CNA evolution results- clinical outcomes

9.1 Introduction

At diagnosis the presence of t(4;14), t(14;16), t(14;20), del(1p), gain(1q) or del(17p) are associated with shorter PFS and OS[12]. Due to molecular heterogeneity, investigating the impact of new CNA at relapse is challenging and data is limited.

To investigate the prognostic information obtained through evolutionary tracking of repeat tumor sampling, I have applied multivariate regression that includes time dependent covariates to consider high risk lesions observed from baseline and those evolving at relapse.

Before investigating time dependent covariates I used univariate analysis to confirm baseline variables associated with worse outcome within my cohort.

9.2 Univariate analysis of baseline variables

Cox regression analysis was used to estimate hazard ratios and respective 95% confidence intervals (CI) for each baseline molecular variable in relation to OS. OS was defined as time from date of randomisation to date of death of any cause. Variables investigated included, transplant eligibility (TE and TNE) molecular subgroups defined in section 6.2 and baseline interstitial CNA observed in ≥5% of tumours. 13 patients did not have OS data available and could not be included in the analysis, as a consequence risk associated with t(6;14) or t(14;20) could not be assessed.

A forest plot summarising univariate analysis of each variable is displayed in **Figure 9-1.** Del(17p) (HR 4.23; *P*=<0.001), t(14;16) (HR 2.77; *P*=0.029), del(1p) (HR2.73; *P*=0.003), gain(8q) (HR 2.16; *P*=0.032), del(12p) (HR 2.11; *P*=0.012), gain(1q) (HR 1.76; *P*=0.012) and TNE(HR 1.59; *P*=0.039) were all associated with a significantly shorter OS. These variables will be considered in the time dependent multivariate model. High risk lesion t(4;14) was not

found to be associated with a significantly shorter OS within this cohort. No CNA were found to have a significant association with longer OS.

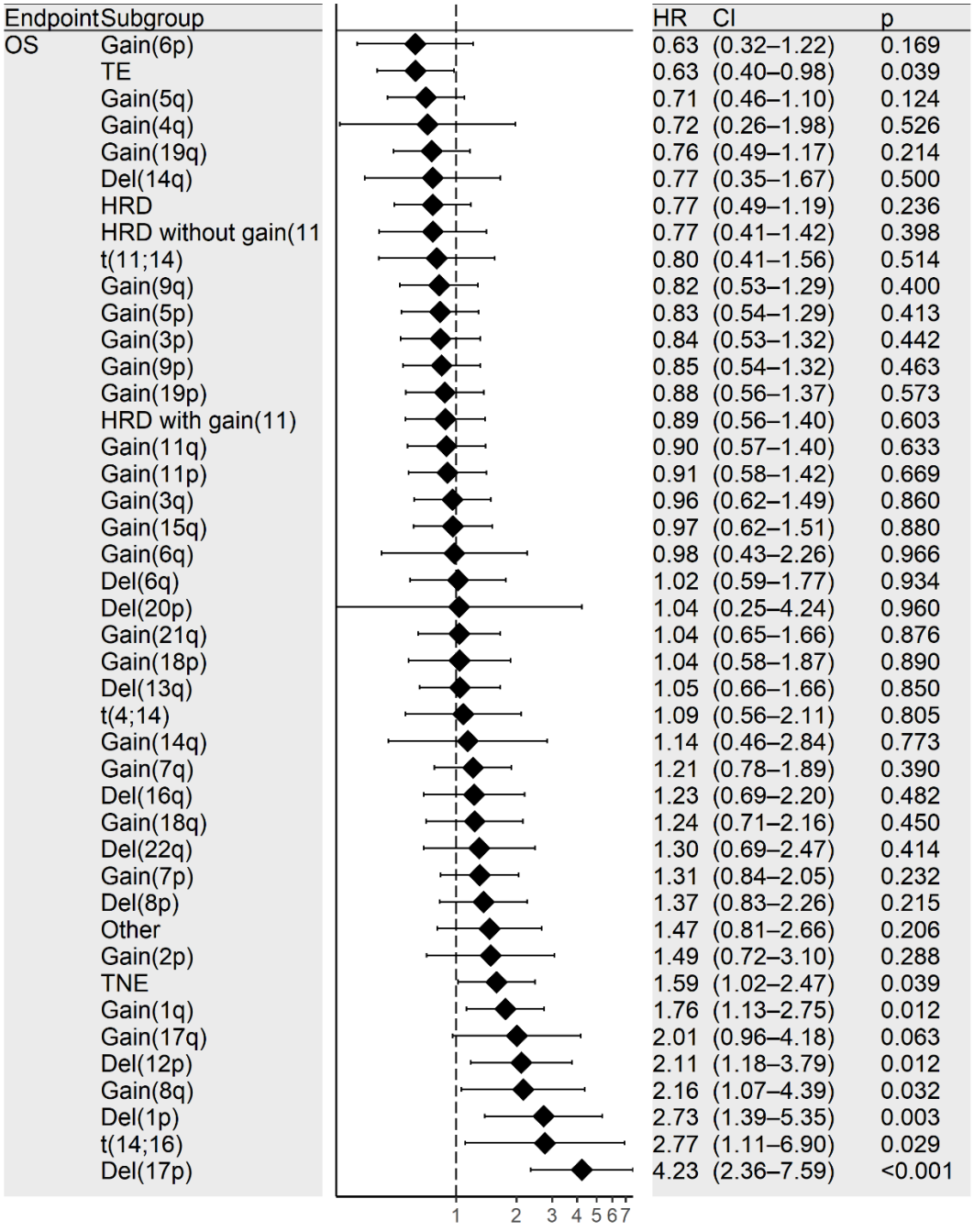

Figure 9-1 Forest plot summarising univariate analysis of baseline variables.

9.3 Multivariate analysis using time dependent variables

High risk variables from the univariate analysis in 9.2 were included in this analysis. OS was defined as time from date of randomisation to date of death of any cause, the presence/absence of CNA was considered over 2 time periods:

- Time period 1: time form presentation sample to first relapse sample
- Time period 2: time from first relapse sample to death.

High risk IgH translocations and transplant eligibility status were stable over both time intervals.

Within this model t(14;16), gain(1q), del(1p), gain(8q), del(17p) and transplant ineligibility were associated with a significantly shorter OS by multivariate analysis, respective HR were 2.79 for t(14;16) (*P*=0.036), 2.12 for gain(1q) (*P*=0.0020), 2.03 for del(1p) (*P*=0.039), 2.01 for gain(8q)(*P*=0.046), 2.20 for del(17p) (*P*=0.0076) and 2.15 (*P*=0.0012) for transplant ineligibility (**Table 9-1**). The results suggest that evolution of new gain(1q), del(1p), gain(8q) or del(17p) at relapse are associated with shorter OS.

Variable	**HR**	**95% CI**	***P value***
t(4;14)	1.19	(0.58-2.41)	0.64
t(14;16)	2.79	(1.07-7.25)	0.036
Gain(1q)	2.12	(1.32-3.41)	0.0020
Del(1p)	2.03	(1.04-3.96)	0.039
Gain(8q)	2.01	(1.01-4.00)	0.046
Del(17p)	2.20	(1.23-3.94)	0.0076
TNE	2.15	(1.35-3.42)	0.0012

Table 9-1 Multivariate analysis using time dependent variables; HR: hazard ratio; CI: confidence interval.

9.3.1 Hazard ratio over time

The model's cox proportional hazards assumption was also tested to demonstrate each covariate's risk over time (**Figures 9-2**). The plots demonstrate each covariate's log hazard ratio (HR) over time (depicted by the solid black line), each plot shows a relatively flat horizontal trajectory indicating stable HR regardless of time of CNA acquisition. Dashed black lines represent 95% confidence intervals (CI) of log HR over time and dashed green line average hazard ratio (HR) over time. The circles represent Schoenfeld's residuals. The proportional hazards assumption is upheld for each covariate, demonstrated by absence of significant correlation between residuals and time (**Table 9-2)**. Widening CIs to the right of plots reflect increasing uncertainty due to lower number of cases with respective follow-up.

	Chi squared	***p-value***
t(4;14)	0.0035	0.95
t(14;16)	7.61	0.0058
Gain(1q)	0.44	0.51
Del(1p)	0.92	0.34
Gain(8q)	0.063	0.80
Del(12p)	0.80	0.37
Del(17p)	0.35	0.56
TNE	0.25	0.62
Global	11.04	0.20

Table 9-2 Correlation of scaled Schoenfeld's residuals with time.

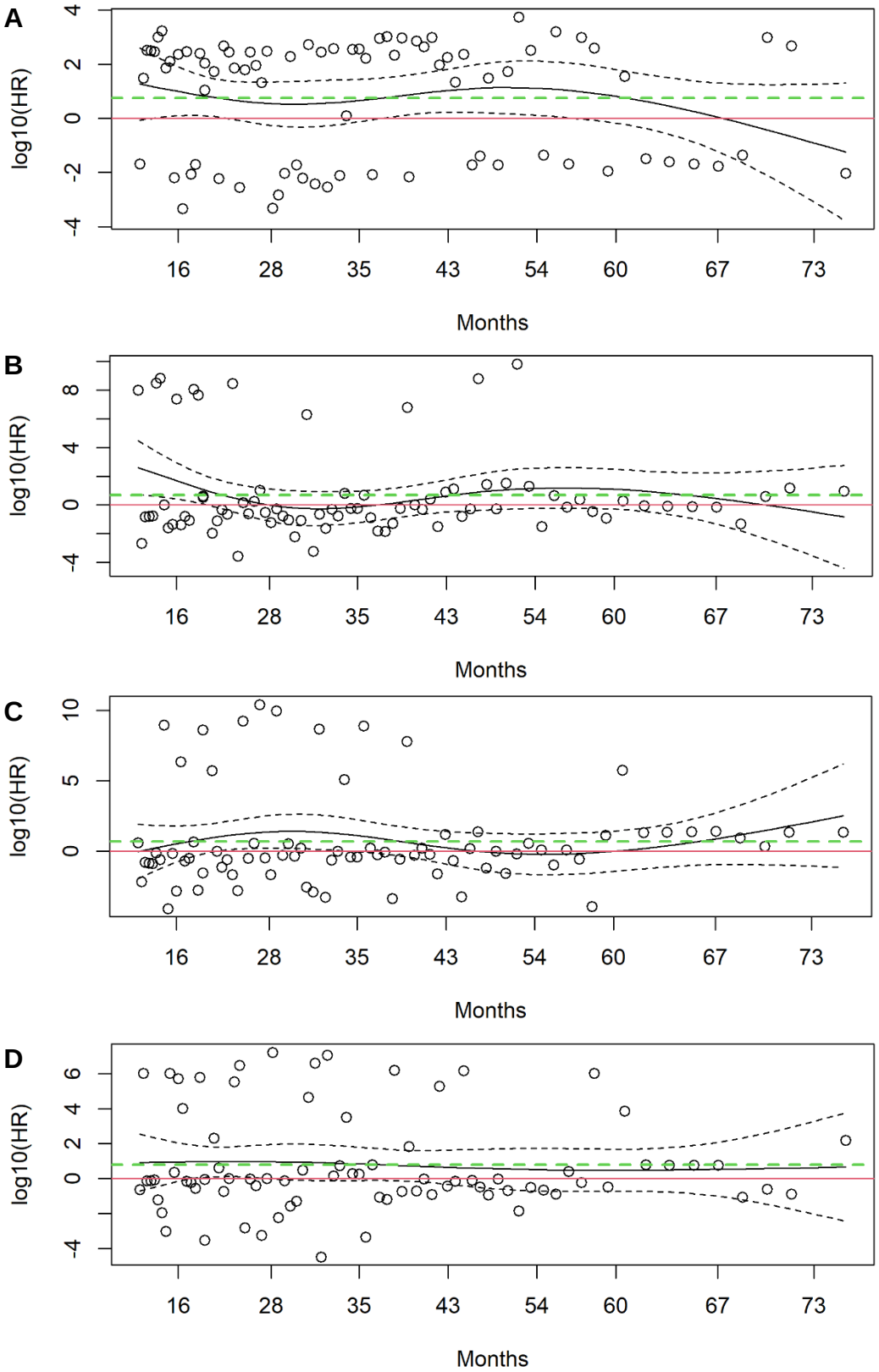

Figure 9-2 Graphical representation of proportional hazards assumption for each significant time dependent covariate. (A) gain(1q), (B) del(1p), (C) Gain(8q) and (D) del(17p).

9.3.2 Risk stratification by time point

High risk time dependant CNA were next stratified by time point of acquisition to enable construction of Kaplan-Meier curves. CNA were stratified as follows:

- CNA at both time points: "CNA-CNA"
- Evolution of novel CNA at relapse "Diploid-CNA"
- Normal copy number throughout "Diploid- Diploid"

9.3.2.1 Gain(1q)

Gain(1q) from baseline and evolution of new gain(1q) at relapse were both associated with significantly shorter OS when compared to normal 1q copy number (HR 2.11; *P*=0.0040 and HR 2.00; *P*=0.021 respectively). Median OS was 44.3 vs 47.9 vs 67.1 months for gain(1q) at presentation, evolution of new gain(1q) at relapse and normal 1q copy number respectively (log-rank *P* = 0.007) (**Figure 9-3**).

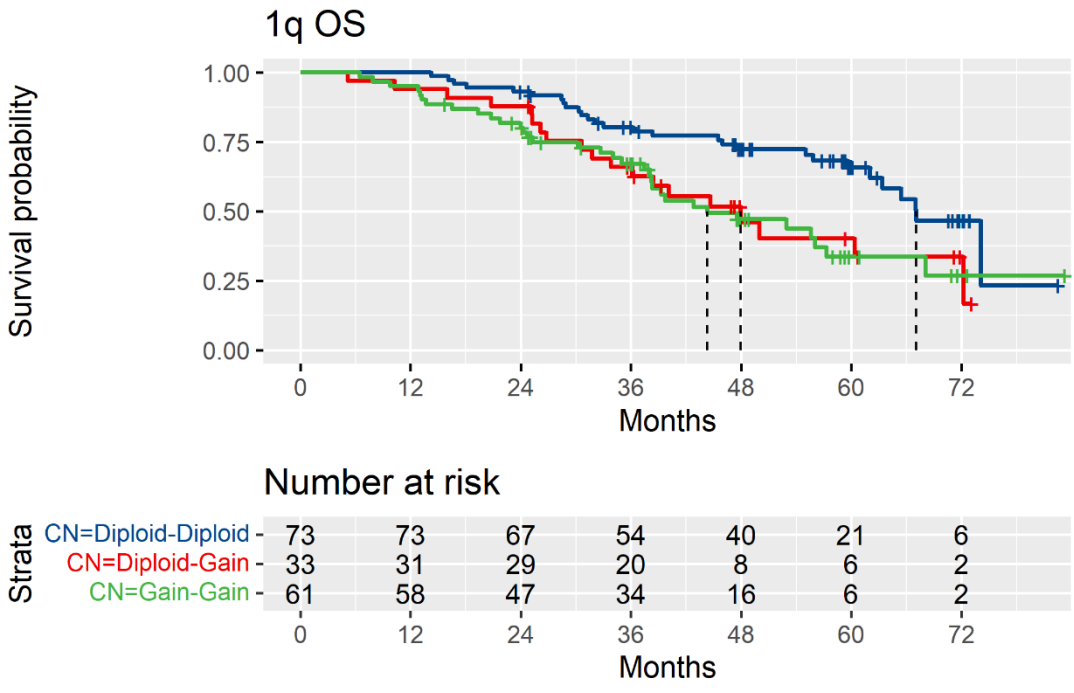

Figure 9-3 Kaplan-Meier for OS in relation to evolution of gain(1q).

9.3.2.2 Del(1p)

Evolution of interstitial del(1p) at relapse was not associated with a shorter OS when compared to normal copy number status, however the frequency of new CNA evolution was low making statistical assessment challenging. The median OS for evolution of del(1p) was not reached. Median OS was 31.5 vs 62.0 months for del(1p) at presentation and normal 1p copy number respectively (log-rank P =0.008) (**Figure 9-4**).

9.3.2.2.1 Del(1p32.3)(CDKN2C)

As discussed in chapter 5, CNA at 1p is often focal. My previous survival analyses have only considered whole arm deletion of 1p, of which new evolution at relapse is rare. The poor risk associated with del(1p) is often attribute to deletion of *CDKN2C*. I have therefore considered all tumours with del(1p32.3)(*CDKN2C)*; therefore capturing patients with del(1p) and focal del(1p32.3).

Evolution of new del(1p32.3) at relapse was not associated with a significantly shorter OS when compared to normal copy number status. Incorporating focal CNA did increase frequency of events and median survival was reached for all strata, although not statistically significant, evolution of new del(1p32.3) at relapse had a shorter median OS compared to tumours with normal copy number. Median OS was 38.3 vs 44.6 vs 63.4 months for del(1p32.3) at presentation, evolution of new del(1p32.3) from relapse and normal 1p32.3 copy number respectively (log-rank P =0.03) (**Figure 9-5**).

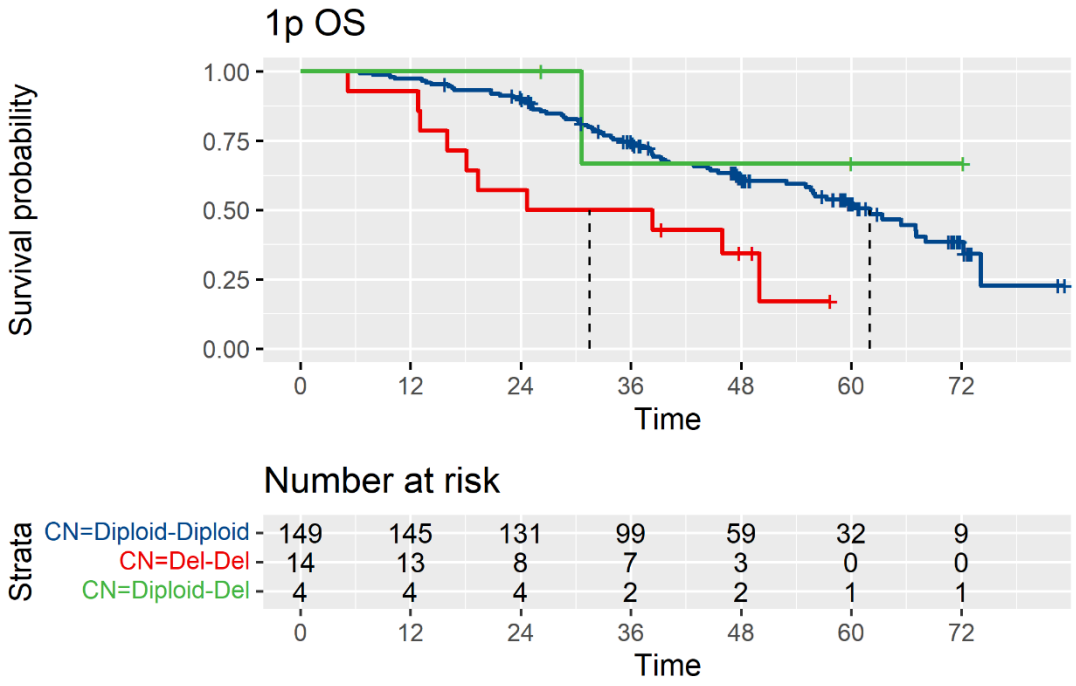

Figure 9-4 Kaplan-Meier for OS in relation to evolution of interstitial del(1p).

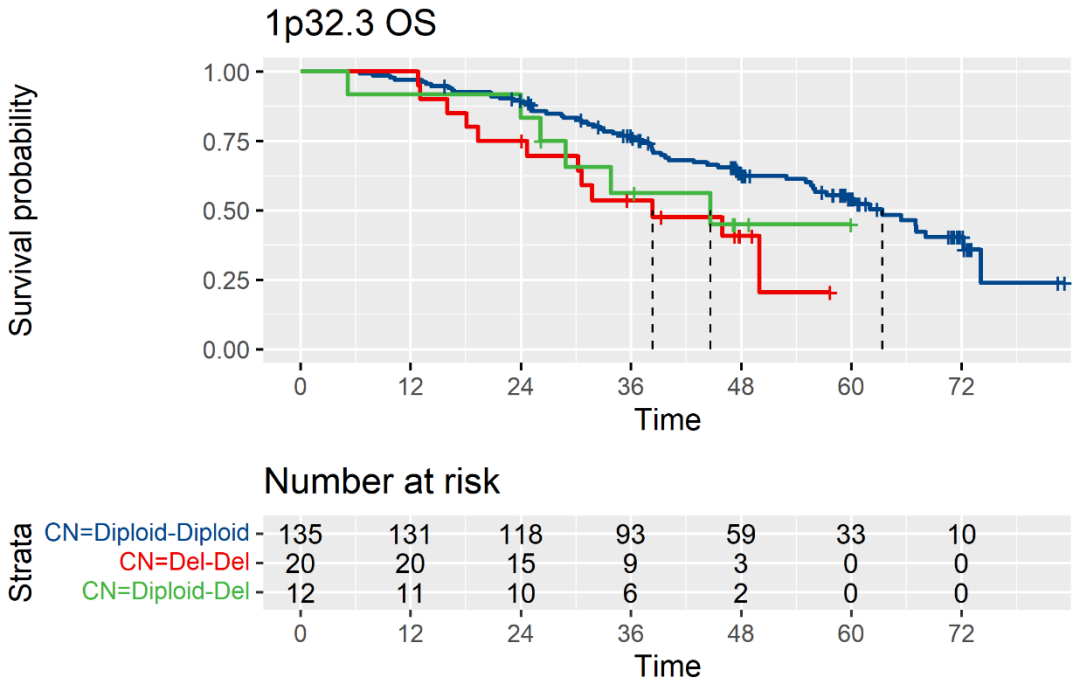

Figure 9-5 Kaplan-Meier for OS in relation to evolution of del(1p32.3).

9.3.2.3 Gain(8q)

Gain(8q) from baseline and evolution of new gain(8q) at relapse were each associated with significantly shorter OS when compared to normal 8q copy number (HR 2.32; *P*=0.021 and HR 4.00; *P*=0.0031 respectively). Median OS was 33.8 vs 26.2 vs 63.4 months for gain(8q) at baseline, evolution of new gain(8q) from relapse and normal 8q copy number respectively (log-rank *P*= 0.008) (**Figure 9-6**).

9.3.2.3.1 Gain(8q24.21)(MYC)

As demonstrated in chapter 5, focal CNA in 8q is also frequent, commonly involving *MYC*. My previous survival model only considered interstitial gain of 8q. I next considered all tumours with gain(8q24.21*)*; therefore capturing all patients with interstitial gain(8q) and focal gain(1q24.21)(*MYC*).

Interesting only new gain(8q24.21*)* at relapse was associated with a significantly shorter OS when compared to normal copy number status (HR 2.06; *P*=0.035). Although not significant, gain(8q24.21) at presentation had a shorter median OS compared to tumours with normal 8q copy number status. Median OS was 38.3 vs 36.2 vs 63.4 months for gain(8q24.21) at presentation, evolution of new gain(8q24.21) at relapse and normal 8q24.21 copy number respectively (log-rank *P*=0.07) (**Figure 9-7)**

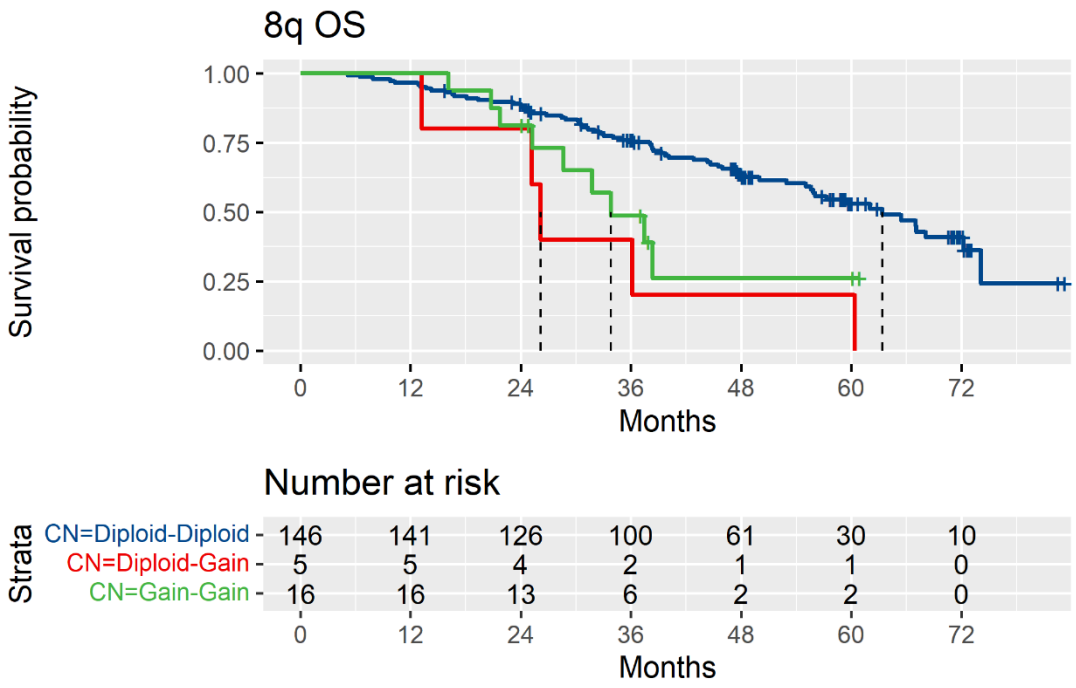

Figure 9-6 Kaplan-Meier for OS in relation to evolution of gain(8q).

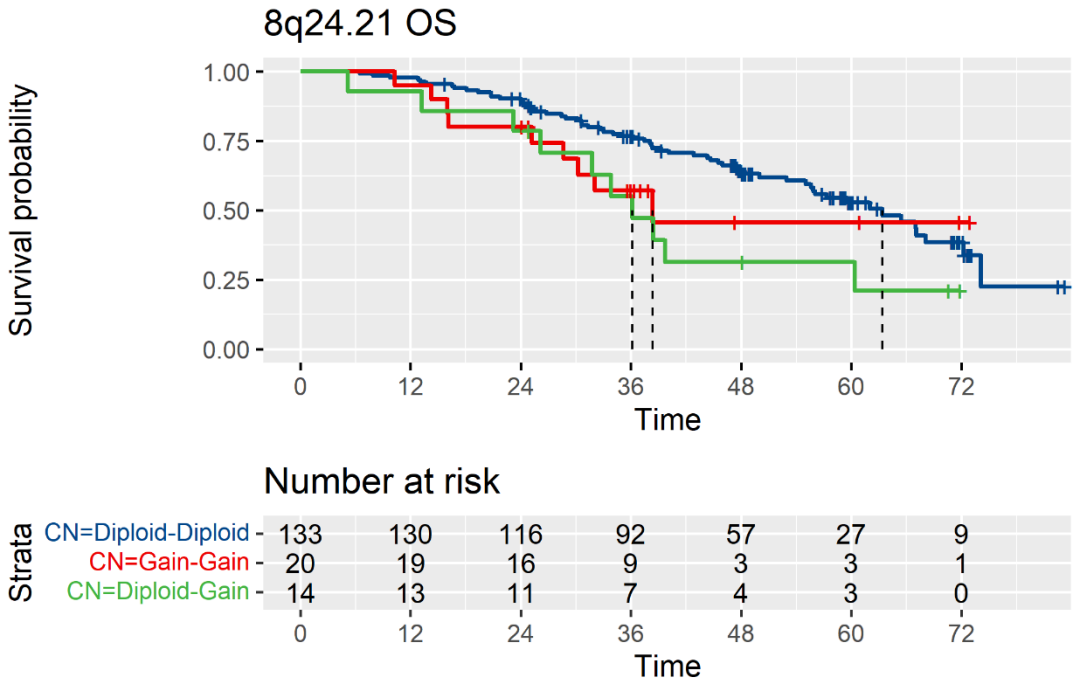

Figure 9-7 Kaplan-Meier for OS in relation to evolution of gain(8q24.21).

9.3.2.4 Del(17p)

Evolution of del(17p) at relapse was not associated with a significantly shorter OS when compared to normal copy number status, however the frequency of respective new CNA evolution was low making statistical assessment challenging. Median OS was 31.3 vs 60.5 vs 65.4 months for del(17p) at presentation, evolution of new del(17p) from relapse and normal 17p copy number respectively (log-rank P <0.001) (**Figure 9-8**).

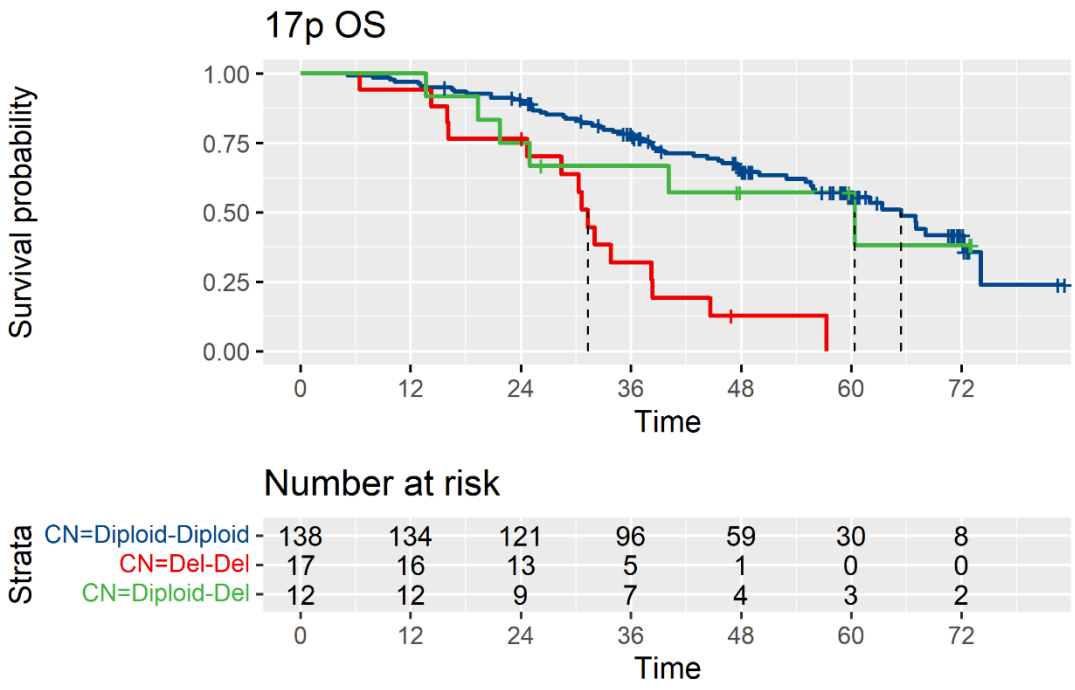

Figure 9-8 Kaplan-Meier for OS in relation to evolution of del(17p).

9.4 Risk assoicated with pattern of evolution

I also investigated the relationship evolution pattern at relapse with OS. Branching evolution at relapse was associated with the shortest survival, median OS was 44.6 vs 59.6 vs 62.0 vs 68.1 months for branching, linear, no change and linear loss respectively (log-rank *P*=0.02) (**Figure 9-9**). Branching evolution was associated with a significantly shorter OS when compared to linear loss (HR 2.61, *P*=0.0048).

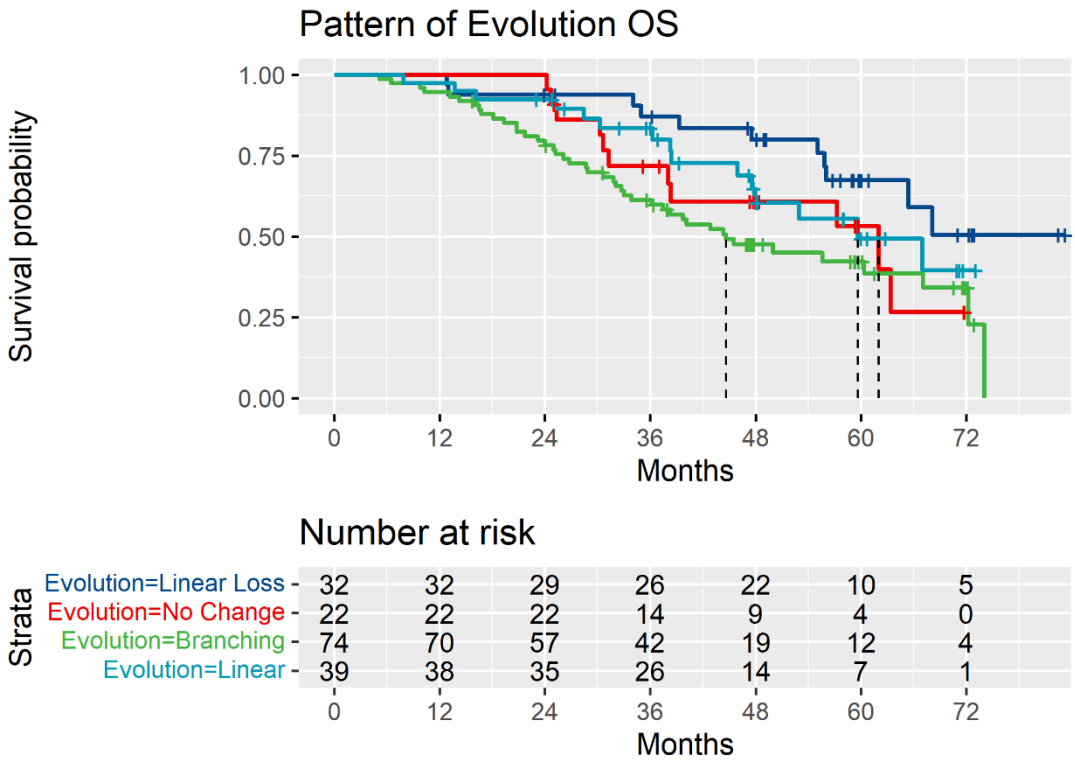

Figure 9-9 Kaplan-Meier for OS in relation to evolution pattern at relapse.

9.5 Discussion

Using time dependent variables to also consider CNA acquired at relapse t(14;16), gain(1q), del(1p) gain(8q) and del(17p) each had an independent association with significantly shorter OS. Tumours with t(4;14) were not associated with a significantly shorter OS, small sample size likely influencing this result. The cohort also has bias, selecting patients with earlier relapse than the whole trial population meaning some archetypal high risk lesions may not be able to demonstrate an independent association with shorter OS.

The presence of gain(1q) has been shown to increase risk of progression from smouldering to symptomatic myeloma[44]. Despite introduction of novel therapies in myeloma, gain(1q) at diagnosis continues to demonstrate an independent association with worse outcome in the majority of studies[44]. To the best of my knowledge, for the first time, I have demonstrated in a randomised controlled trial that acquisition of gain/amp(1q) at relapse is also independently associated with a shorter OS. Therefore providing further evidence that gain(1q) plays a key role in tumour progression and treatment resistance. With frequent new acquisition observed at relapse and a strong association with worse survival, it is clear that better understanding of the molecular dysregulation attributed to this CNA is required. Potential mechanisms attributed to gain(1q) were discussed in chapter 5 and will be explored using gene expression data in later chapters.

MYC dysregulation is recognised to play role in the development and progression of myeloma. While *MYC* translocations have been independently associated with worse outcome, gain/amp of *MYC* at baseline have previously only demonstrated a significant association in univariate analysis[60]. By examining the association of the gain(8q/*MYC*) in a time dependent model, acquisition of new gain(8q)/*MYC* at relapse was also associated with a significantly shorter OS. Interestingly the HR of new acquisition of gain(8q/*MYC*) was higher than tumours who demonstrated the CNA from baseline. This suggests the detrimental effects of the CNA require the presence of other secondary molecular aberrations. This correlates with

mouse models that demonstrated *MYC* dysregulation alone did not lead to the progression of MGUS to myeloma [65].

Although suggestive, a significant association with worse outcome relating to the acquisition of new del(1p) or del(17p) at relapse was not demonstrated. The power to robustly assert clinical relevance of these acquired lesions at relapse was limited by the lower frequency of new CNA observed.

I also demonstrated a relationship of evolution pattern with outcome; branching evolution at relapse associated with having a significantly shorter OS. HRD tumours have generally demonstrated better outcomes compared to non HRD tumours. However the HRD subgroup has marked molecular heterogeneity. With a large proportion of my HRD tumours demonstrating branching evolution at relapse, pattern of evolution could be used to help risk stratify this subgroup. Clinical relevance requires further investigation into the independent relationship of evolution pattern with outcome before it can be used to guide management decisions.

9.5.1 Conclusion

Acquisition of gain/amp(1q) at relapse is independently associated with a shorter OS providing further evidence that gain(1q) plays a key role in tumour progression and treatment resistance. This highlights the need for therapies that target genes associated with this CNA. While technically feasible, re-evaluation of high risk lesions at relapse is not standard practice outside of the trial setting. Treatment options for relapsed myeloma are increasing dramatically, with a range of intensities and modalities. Decisions regarding next line of therapy could be facilitated through repeat genetic profiling at relapse, where identification of high risk markers would influence choice.

Chapter 10: GEP evolution results-patient demographics

10.1 Introduction

Of the 178 patients from the CNA evolution cohort, those with adequate RNA at both time points also had sequential gene expression profiling using Affymetrix U133 Plus 2.0 Arrays. After QC checks discussed in sections 2.4.3 and 3.2.1, there were 67 patient with matched presentation relapse GEP. They will be referred to as the GEP evolution cohort.

10.2 Baseline Demographics

Baseline demographics are summarised in **Table 10-2**, they were similar to that of the overall MXI population.

10.3 Baseline Cytogenetics

The frequency of high risk cytogenetic lesions within the GEP evolution cohort was compared to the overall MXI population and summarised in **Table 10-1**. Frequency of baseline gain(1q) and del(1p) was higher than observed in overall MXI population; 49.3% vs 34.5% and 14.9% vs 10.3% respectively. Frequency of t(4;14) was lower than the overall MXI population; 6.0% vs 15.7%.

10.4 Treatment

Treatment pathway and randomisations of the 67 patients are summarised in **Figure 10-1.** There was equal ratio of TE to TNE patients with 34 (50.7%) and 33 (49.3%) patients within each group respectively. 46 (68.7%) patients underwent maintenance randomisation; 18 (26.9%) patients receiving lenalidomide based maintenance; 28 (41.8%) patients were randomised to observation. This ratio is inverted to one would be expect in the trial the randomisation was 2:1 in favour of Lenalidomide. This is likely associated with a higher likelihood of early relapse for patients on observation over maintenance.

10.5 Follow up

Overall median time to progression was 19.2 months (range 7.4-71.9 months) and median follow up 48.7 months (range 12.9 – 83.3 months).

		67 GEP Evolution cohort		All MXI (Shah et al.)	
HR lesion, n (%)	t(4;14)	4	(6.0)	163	(15.7)
	t(14;16)	1	(1.5)	38	(3.7)
	t(14;20)	1	(1.5)	13	(1.3)
	Gain/Amp (1q)	33	(49.3)	357	(34.5)
	Del(1p)	10	(14.9)	107	(10.3)
	Del 17p	6	(9.0)	96	(9.3)

Table 10-1 GEP evolution cohort: comparison of high risk cytogenetic lesions with overall MXI population.

		67 sequential GEP cohort		4242 non sequential cohort	
Sex, n (%)	F	20.0	(29.9)	1788.0	(42.1)
	M	47.0	(70.1)	2454.0	(57.9)
Age, mean (SD)	mean	67.2	(8.3)	65.7	(10.3)
n (%)	≤75	60.0	(89.5)	3470.0	(81.8)
	76-80	5.0	(7.5)	530.0	(12.5)
	>80	2.0	(3.0)	242.0	(5.7)
WHO, n (%)	0	27.0	(40.3)	1512.0	(35.6)
	1	27.0	(40.3)	1665.0	(39.3)
	2	8.0	(11.9)	630.0	(14.9)
	3	4.0	(6.0)	196.0	(4.6)
	NA	1.0	(1.5)	217.0	(5.1)
PP, n (%)	IgA	23.0	(34.3)	1034.0	(24.4)
	IgD	1.0	(1.5)	35.0	(0.8)
	IgG	37.0	(55.2)	2608.0	(61.5)
	IgM	0.0	(0.0)	15.0	(0.4)
	LCO	6.0	(9.0)	516.0	(12.2)
LC, n (%)	Kappa	43.0	(64.2)	2785.0	(65.7)
	Lambda	24.0	(35.8)	1410.0	(33.2)
Hb, mean (SD)		104.5	(17.6)	108.4	(19.4)
Creat, mean (SD)		106.7	(67.2)	102.0	(58.3)
Ca, mean (SD)		2.5	(0.3)	2.4	(0.3)
Albumin, mean (SD)		35.3	(5.6)	35.2	(6.7)
LDH, mean (SD)		357.1	(412.4)	302.4	(175.7)
B2M, mean (SD)		5.4	(3.3)	5.4	(5.0)
ISS, n (%)	I	14.0	(20.9)	1055.0	(24.9)
	II	30.0	(44.8)	1631.0	(38.4)
	III	22.0	(32.8)	1229.0	(29.0)
	NA	1.0	(1.5)	327.0	(7.7)
TE, n (%)		34.0	(50.7)	2468.0	(58.2)
Induction, n (%)	CRD	12.0	(35.3)	-	
	CTD	19.0	(55.9)	-	
	KCRD	3.0	(8.8)	-	
Maintenance, n (%)	Len	8.0	(23.5)	707.0	(28.6)
	Len + Vor	2.0	(5.9)	185.0	(7.5)
	Observation	13.0	(38.2)	489.0	(19.8)
	NR	11.0	(32.4)	1087.0	(44.0)
TNE, n (%)		33.0	(49.3)	1774.0	(41.8)
Induction, n (%)	CRDa	20.0	(60.6)	-	
	CTDa	13.0	(39.4)	-	
Maintenance, n (%)	Len	8.0	(24.2)	385.0	(21.7)
	Len + Vor	0.0	(0.0)	108.0	(6.1)
	Observation	15.0	(45.5)	292.0	(16.5)
	NR	10.0	(30.3)	989.0	(55.7)

Table 10-2 GEP evolution cohort baseline demographics; PS: performance status; PP: paraprotein; LC: light chain; LDH: lactate dehydrogenase; B2M: beta2 macroglobulin; ISS: International staging system; TE: transplant eligible; TNE: transplant non-eligible; Len: Lenalidomide; Vor: Vorinostat; NR Not randomised.

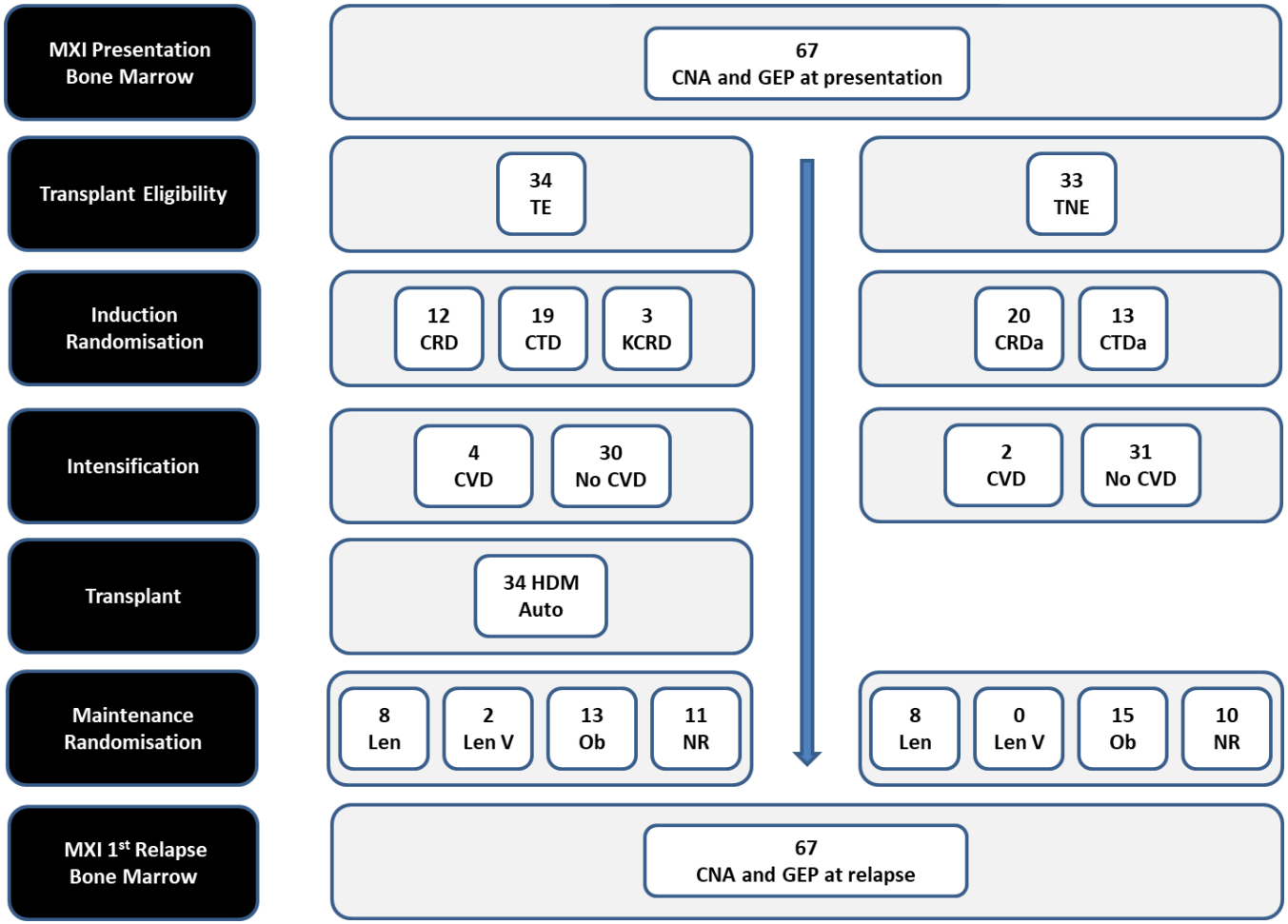

Figure 10-1: Summary of treatment randomisations for the GEP evolution cohort. MXI: Myeloma XI; TE: transplant eligible; TNE: Transplant non-eligible; C: Cyclophosphamide; R: lenalidomide; D: dexamethasone; T: thalidomide; K: carfilzomib; V: velcade; HDM: high dose melphalan; Len: lenalidomide; V: vorinostat; Ob: observation; NR; not randomised; a: attenuated.

Chapter 11: GEP evolution results-differential gene expression

11.1 Introduction

Differential gene expression (DGE) can be used to compare and contrast the biology of tumours. Comparison of myeloma tumours has identified distinct molecular subgroups and comparison at various stages of plasma cell dyscrasia have also provided insight to mechanisms of disease pathogenesis and progression[18].

Data regarding the differential expression of sequential myeloma tumours, from the same patient, is limited. Given the heterogeneous molecular landscape of myeloma, investigation of differential expression in sequential samples after uniform treatment has great potential to provide insight into specific mechanisms of treatment resistance.

Using gene expression data for 67 MXI patients at presentation and first relapse, I have investigated differential expression between the sequential time points using a linear regression model. The model uses each patient's unique trial ID to ensure only sequential samples are compared. A log fold increase in expression reflects increased expression at relapse and log fold decrease reflects decreased expression at relapse. Differential expression was considered significant in genes with a FDR of ≤0.05. Genes were ranked as described in methods and biological relevance investigated using GSEA from the broad institute. An FDR of ≤0.25 was used to identify gene sets with significant enrichment. Leading edge analysis of gene sets with significant enrichment was used to highlight specific genes of interest.

Differential expression between time points will be considered for all patients, per molecular subgroup and by treatment arm.

11.2 All patients

Significant differential expression at relapse was identified in 548 probe sets, 277 upregulated and 271 down regulated **(Supplementary Tables 14-3 and 14-4)**. Input data for Broad Institute GSEA requires a list of pre-ranked, unique gene, therefore duplicate genes were removed leaving 491 in the pre ranked list. Significant positive enrichment of 5 gene sets was observed at relapse; G2M checkpoint, E2F targets, *MYC* targets V1, Mitotic spindle and MTORC1 signalling **(Table11-1).** There were no gene sets with significant negative enrichment.

Gene set	SIZE	ES	NES	p-value	FDR q-value
HALLMARK_G2M_CHECKPOINT	32	0.57	3.51	0.000	0.000
HALLMARK_E2F_TARGETS	35	0.55	3.49	0.000	0.000
HALLMARK_MYC_TARGETS_V1	26	0.53	2.97	0.000	0.000
HALLMARK_MITOTIC_SPINDLE	15	0.41	1.84	0.017	0.020
HALLMARK_MTORC1_SIGNALING	21	0.33	1.71	0.025	0.031

Table 11-1 Positively enriched gene sets; ES: enrichment score; NES: normalised enrichment score; FDR: false discovery rate.

Leading edge analysis found *MCM2* to overlap 4 gene sets. *XPO1, MCM6, MAD2L1, TOP2A, SMC1A, BIRC5, CCNB2* and *CDK1* overlap 3 gene sets **(Figure 11-2)** suggesting upregulation of these genes could play an important role in disease progression. Of note multiple proteasomes genes were also observed in the leading edge analysis; *PSM4A, PSMC4* and *PSMD1.*

Enrichment plots for each gene set are shown in **Figure 11-1**. The top portion of each plot represents the running enrichment score (ES) as the analysis moves down the pre-ranked gene list, the score at the peak of the plot is the ES for the gene set. The middle portion of each plot shows where gene set members appear in the ranked list of genes. The leading edge genes are those that contribute most to the ES, appearing in the ranked list prior to the peak ES. The bottom portion of a plot shows the value of the ranking metric as you move down the pre-ranked genes, reflecting correlation with a phenotype. Information taken from GSEA user guide. (https://www.gsea-msigdb.org/gsea/doc/GSEAUserGuideFrame.html).

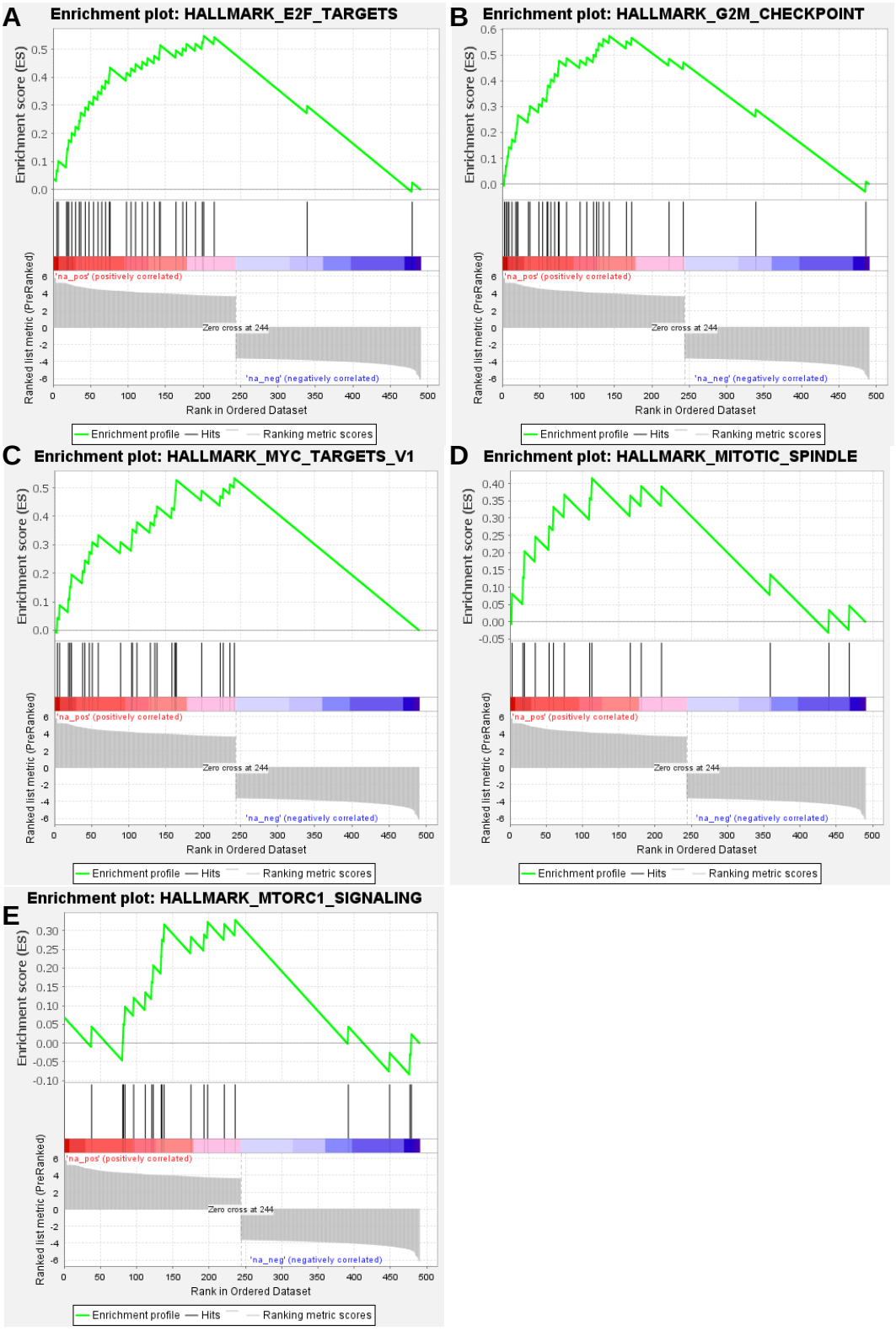

Figure 11-1 Enrichment plots: (A) G2M checkpoint; (B) E2F targets; (C) MYC targets V1; (C) mitotic spindle; (E) MTORC1 signaling.

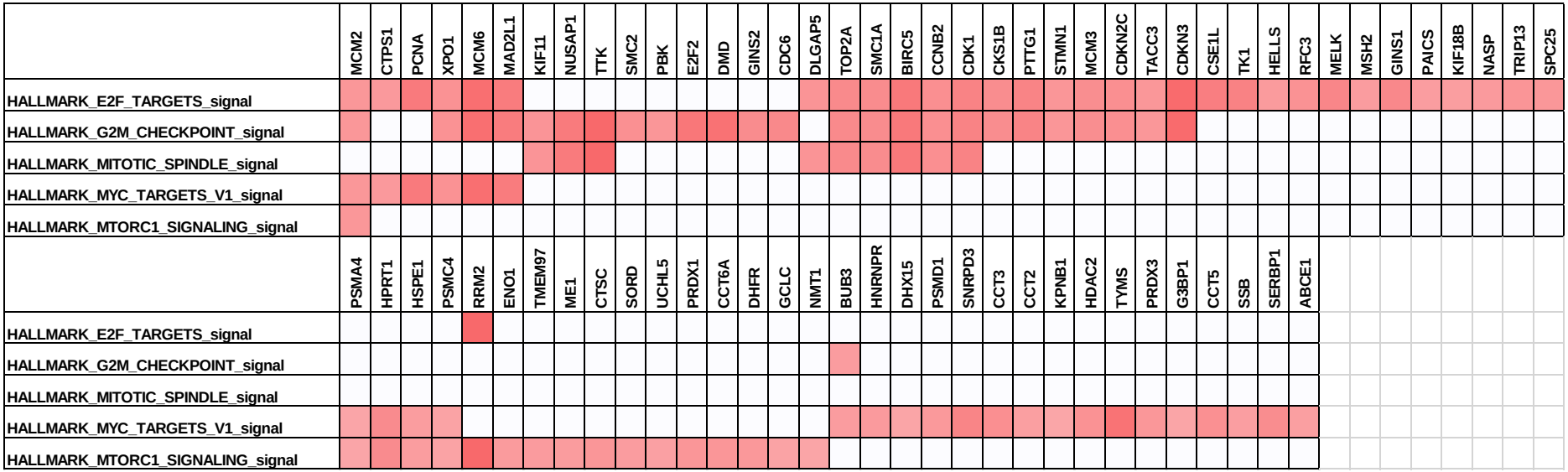

Figure 11-2 Leading edge analysis demonstrating clustered genes. Intensity of square colour representing high (red) to moderate (pink) expression. To facilitate review/printing the Heatmap has been split as two rows.

11.3 Molecular Subgroups

Investigation of differential gene expression between sequential tumours within each molecular subgroup was limited by the small number of patients per subgroup. When considering all probesets, no significant differential expression (FDR<0.05) between time-points was observed in any of the molecular subgroups and GSEA could not be applied.

Filtering of probesets using the “panp” package in R to only include those with stringent “present” calls rationalised expression data to 9202 probesets. Investigation of differential expression between sequential tumour samples within each molecular subgroup was repeated. As the largest subgroup, only HRD with gain(11) tumours demonstrated significant differential expression at relapse, observed in 7 genes; down regulation of *LDOC1, KCNMB2, CISH, MPHOSPH8, ZNF331* and *COPZ2,* and upregulation of *SERBP1*. The gene list was too small to apply GSEA. There was no significant differential expression in any other sub-groups

Probeset	Gene	Log FC	Ave Expr	Adj P Val
217724_at	*SERBP1*	0.58	12.38	0.048
227026_at	*MPHOSPH8*	-0.64	9.48	0.048
235897_at	*COPZ2*	-0.77	7.76	0.048
204454_at	*LDOC1*	-1.00	7.32	0.048
221223_x_at	*CISH*	-1.14	8.41	0.048
223377_x_at	*CISH*	-1.16	8.91	0.006
227613_at	*ZNF331*	-1.19	8.54	0.048
221097_s_at	*KCNMB2*	-1.50	7.33	0.048
223823_at	*KCNMB2*	-1.62	6.33	0.048

Table 11-2: Significant DGE in sequential HRD with gain(11) tumours.

Filtering probesets to only include those with the highest co-efficient of variation did not facilitate discovery of any genes with significant differential expression at relapse in any of the molecular subgroups.

11.4 Treatment arms

Investigation of differential gene expression between sequential tumours samples within each treatment arm was limited by the number of patients per arm.

11.4.1 Transplant eligible (TE)

34 patients in the transplant eligible arm had sequential GEP. Considering all probesets there was significant differential expression at relapse in 3 genes; down regulation of *CALR* (LFC -0.73; FDR 0.027) and *CISH* (LFC -1.13; FDR 0.048), upregulation of *PLCB1* (LFC 1.46; FDR 0.045). The gene list was too small to apply GSEA.

After filtering probesets to only include those with “present” calls (9202 probesets) linear regression demonstrated significant differential expression at relapse in 54 genes; 31 down regulated and 23 upregulated **(Supplementary Table 14-5)**. The largest log fold increase observed in *IGLV1-44* (1.77; FDR 0.02), *PLCB1* (1.46; FDR <0.01), *FAM133A* (1.07; FDR 0.05), *PHF19* (0.98; FDR 0.02). The largest log fold decrease observed in *TCEAL2* (-1.57; FDR 0.03), *TLL2* (-1.26; FDR 0.03), *KCNMB2* (-1.24; 0.01), *TGM6* (-1.15; 0.01), *CISH* (-1.13; <0.01). Due to size of gene list GSEA was unsuccessful.

11.4.2 Transplant non eligible (TNE)

33 patients in the transplant non eligible arm had sequential GEP. When considering all probesets there was significant differential expression at relapse in 3 genes; down regulation of *ALCAM* (LFC -1.34; FDR 0.026) and *PPBPP2* (LFC -1.66; FDR 0.040), upregulation of *SKA1* (LFC 1.61; FDR 0.0077). The gene list was too small to apply GSEA.

Filtering of probesets prior to application of the linear regression model did not increase the yield of genes with significant differential expression.

11.4.3 Maintenance: Lenalidomide arm

18 patients who were randomised to lenalidomide maintenance had sequential GEP. Examining all probesets, there was no significant differential expression (FDR<0.05) between time-points. Filtering of probesets for genes prior to application of the linear regression model did not increase the yield of genes with significant differential expression. No differential gene expression was observed when specifically filtering for genes which have been implicated in IMiD mechanism of action.

11.4.4 Maintenance: Observation arm

28 patients who were randomised to the observation arm had sequential GEP. Examining all probesets, there was no significant differential expression (FDR<0.05) between time-points. Filtering of probesets prior to application of the linear regression model did not increase the yield of genes with significant differential expression.

11.5 Discussion

Sequential expression profiling has demonstrated evolution of tumour biology at relapse, which correlates with frequent CNA evolution described in earlier chapters. Relapsed tumours were positively enriched for genes involved in the cell cycle; E2F transcription factor response, G2/M checkpoint and mitotic spindle assembly. Also for genes regulated by *MYC* and mTORC1 complex activation. All of which facilitate progression through the cell cycle resulting in tumour proliferation and therefore relapse. Importantly it highlights specific mechanisms of proliferation/relapse to facilitate development of targeted therapies that could overcome current drug resistance.

11.5.1 E2F transcription factor response

The cell cycle is tightly regulated via cyclin dependent kinases (CDK) which are activated by cyclins D, E, A and B and repressed by CDK inhibitors. The cell cycle is also regulated by checkpoints between phases which utilise physiological CDK inhibitors to halt transition[66].

Progression from G1 to S phase requires activation of CDK2 and CDK4 by cyclin D, resulting in the phosphorylation of retinoblastoma (Rb) protein and release of active E2F transcription factor leading to transcription of E2F responsive genes[66]. The positive enrichment of E2F responsive genes in my analysis highlights a role for drugs that can inhibit CDKs. Therapeutic CDK inhibitors have been used successfully in solid organ cancers, early studies have also demonstrated their potential in myeloma when combined with other anti-myeloma agents[67]. Palbociclib inhibits CDK4 and CDK6, it has been shown to induce G1 arrest and enhance bortezomib susceptibility in myeloma mouse models. A clinical trial of Palbociclib combined with bortezomib and dexamethasone for relapsed refractory disease demonstrated an overall response rate (ORR) of 20% and stable disease in 44% of patients, suggesting CDK inhibition could re-sensitise tumours to bortezomib[67]. Other potential CDK inhibitors with pre-clinical evidence include abemaciclib (CDK4/6), THZ (CDK7/12/13), Dinaciclib (CDK1/2/5/9), AT7519M (CDK4)[67].

11.5.2 G2/M checkpoint

DNA damage response (DDR) pathways act as checkpoints to ensure mitosis does not occur before DNA is repaired. Checkpoint inhibitors have therefore been developed with the aim of altering a tumours response to DNA damaging chemotherapy to enhance its effects[68]. G1/S and G2/M checkpoints are sensed by ATM and ATR respectively[66]. My analysis highlights the significance of the G2/M checkpoint at relapse. This correlates with work from Bortrugno et al who recently reported addiction of myeloma tumours to ATR but not ATM. They demonstrated ATR inhibition, using compound VX-970, to be strongly synergistic with melphalan. Resulting in reduced tumour proliferation, increased apoptosis and prolonged survival in animal models[69].

11.5.3 Mitotic spindle assembly

G2/M transition is also controlled by the spindle assembly checkpoint (SAC) and mitotic spindle checkpoint complex (MCC), which ensure effective attachment of chromosomes to spindles before mitosis can proceed[66]. I observed enrichment for genes associated with spindle assembly at relapse.

Vincristine is a microtubule agent that disrupts spindle formation and was previously used in myeloma. It is no longer used due to lack of efficacy when compared to PI and IMiDs. Newer microtubule targeting agents have also not been successful[66]. Targeting kinesin spindle proteins (KSP) is an alternative approach in assembly disruption, inhibition resulting in mono-polar spindle formation and SAC dependent mitotic arrest. A phase Ib/II clinical trial of Filanesib (KSP inhibitor), combined with pomalidomide and dexamethasone in relapsed refractory patients was recently reported to show ORR of 51% [70].

11.5.4 mTOR activation

The mTOR is a protein kinase belonging to the PI3K family which is involved in the regulation of cell growth, differentiation and proliferation. It is activated in many cancers including myeloma [71]. My analysis also showing it to play a key role in relapse and treatment resistance. With numerous mechanisms of mTOR activation described in myeloma it is an attractive therapeutic target. Early phase clinical trials of mTORC1 inhibitors in relapsed refractory disease have shown some success. Most recently the use of evorolimus in combination with lenalidomide resulted in ORR of 59% [72]. While numerous mTOR inhibitors have been developed, further clinical studies of their use in myeloma appear to be lacking and could be a focus of future work.

11.5.5 MYC

As discussed in chapter 5 the dysregulation of *MYC* has been shown to play an important role development and progression of myeloma. Signified by the numerous mechanisms of dysregulation observed in myeloma; translocations, copy number gain and mutations for example *NRAS and KRAS[60]*. Expression of *MYC* has a direct role in DNA replication, cell proliferation and immune evasion. My analysis demonstrates enrichment of MYC targets, signifying its role in relapse and treatment resistance. As an oncogene that contributes to numerous cancers, there has been substantial work to target MYC through direct and indirect inhibition[60].

DCR-MYC is a small interfering RNA (siRNA) which binds directly to MYC mRNA to inhibit translation, an early phase clinical trial of its use in myeloma

is currently in progress[60]. In order to bind to promoters of target genes, MYC requires dimerization with MAX. An alternative approach of direct MYC inhibition has focused on impeding MYC/MAX binding, however adequate bioavailability of inhibitors has been challenging so they are still in development[60].

BET proteins (BRD2, BRD3, and BRD4) regulate the transcription of *MYC*, providing an indirect target for MYC inhibition. A number of small molecule BET inhibitors have shown anti-proliferative effect in myeloma preclinical studies, early phase clinical trials are ongoing[60].

Translation of *MYC* mRNA is regulated by the eIF4F complex which is controlled via mTOR signalling, MYC also activates eIF4F expression providing a positive feedback loop[60]. The significance of this pathway in proliferation highlighted by the enrichment of both mTORc1 and MYC targets at relapse in my analysis. Targeting mTOR signalling via PI3K inhibition has been attempted with the aim of inhibiting *MYC* expression. TGR-1202 is a novel PI3Kδ inhibitor shown to disrupt the eIF4F/MYC axis providing an anti-tumours effect in myeloma cell lines. It is currently being trialled clinically in combination with carfilzomib[60]. Therapeutic translation inhibition through disruption of eIF4A has also been studied using Rocaglates. Rocaglate compound CMLD010509 has been shown to inhibit translation of oncogenes specifically involved in myeloma pathogenesis including *MYC, MDM2, CCND1, MCL-1,* and *MAF*, its use has shown promising results in preclinical studies of myeloma cells and mouse models[60].

As discussed in section 1.1.5.2, IMiD mechanism of action relies on CRBN mediated ubiquitination and subsequent proteasome degradation of IKZF1 and IKZF3, which results in downregulation of *IRF4.* There is a positive feedback loop between *IRF4* and *MYC* expression, for this reason IMiDs have been nominated as indirect inhibitors of MYC [60]. Conversely my analysis suggests increased expression of *MYC* is a mechanism of IMiD resistance, therefore targeting MYC could re-sensitise resistant tumours.

Based on enriched cellular processes at relapse I have discussed a number of targeted therapies that have potential in treating relapsed myeloma. Most are in preclinical or early clinical phase trials and further work is needed.

11.5.6 Leading edge analysis

The leading edge analysis from my analysis demonstrated 8 genes that overlap multiple enriched cellular processes, highlighting them as potential therapeutic targets; *MCM2, XPO1, MCM6, MAD2L1, TOP2A, SMC1A, BIRC5, CCNB2* and *CDK1.*

MCM2 and MCM6 proteins belongs to the mini chromosome maintenance (MCM) family which are involved in DNA replication, they are dysregulated in a number of cancers. Overexpression of *MCM2* was previously demonstrated to be an independent adverse prognostic biomarker in myeloma [73]. Trichostatin A, a classical histone deacetylase inhibitor has been shown to down regulate MCM2 expression inducing cell cycle arrest and apoptosis in colorectal carcinoma cell lines, therefore highlighting a potential novel agent in myeloma [73].

Upregulation of *XPO1* is of particular interest as this protein already has an FDA approved direct inhibitor named Selinexor which has shown therapeutic benefit in myeloma clinical trials. XPO1 is a known oncoprotein that controls the nuclear export and inactivation of tumour suppressors, it has also been shown to increase the translation of oncoproteins including MYC. Correlating with my analysis, *XPO1* overexpression has been associated with treatment resistance to bortezomib and IMiDs in myeloma [74]. Most relevant to my analysis, Bhutani et al described the IMID-14 gene expression score which predicted poor response to IMIDs, in which *XPO1* had the highest HR associated with PFS[75]. The use of Selinexor combined with dexamethasone in relapsed refractory myeloma demonstrated an ORR of 26% with median PFS of 3.7 months [76]. Preclinical studies have also demonstrated a synergistic effects of XPO1 inhibitors combined with proteasome inhibitors leading to the BOSTON phase 3 clinical trial which demonstrated superior PFS

in relapsed patients treated with weekly Selinexor bortezomib and dexamethasone versus twice weekly bortezomib dexamethasone [74].

TOP2A is a topoisomerase enzyme involved in chromosome segregation. A recent preclinical study demonstrated high expression of *TOP2A* to be associated with PI resistance in myeloma cells and that combination of carfilzomib and topoisomerase inhibitor had a synergistic anti myeloma effect [77]. Only 9.6% of patients in this analysis were treated with PI, suggesting high *TOP2A* expression has a broader role in proliferation and treatment resistance, supporting further investigation of the use of topoisomerase inhibitors in myeloma.

BIRC5 belongs to the inhibitor of apoptosis protein (IAP) family and plays a dual role in mitosis and apoptosis. It is known to be upregulated in a number of cancers including myeloma, with high expression implicated in stroma-mediated drug resistance [78]. Pre-clinical evidence was recently reported on the use of small molecule FL118 as a BIRC5 inhibitor, interestingly it was more effective on relapsed refractory vs newly diagnosed cells. It demonstrated promising anti myeloma effects, particularly in combination with melphalan and bortezomib [78]. A direct interaction of miR-101-3p with BIRC5 has also been described, highlighting another potential therapeutic target [79]. Finally, the number of proteasome genes observed at leading edge analysis also highlights the role of PI in relapsed myeloma.

11.5.7 Subgroup analysis

Despite having 67 sequential samples, attempts to investigate significant differential expression at relapse within molecular and treatment subgroups was impeded by small sample size. This demonstrates the difficulty in identifying consistent patterns of change within a heterogeneous group of tumours. It also suggests a persistent degree of tumour heterogeneity within molecular subgroups. The results highlight the difficulty in analysing sequential samples, where change in expression between time points of one tumour is more subtle than differential expression between two different tumours. This was reflected in the relatively small LFC observed in genes with significant

DGE in section 11.2 **(Appendix table 14-4)**. With thousands of genes compared, adjusted p values are required to minimise the false discovery rate. Coupled with subtle changes in expression, sequential tumour analysis clearly requires a much larger cohort size to ensure adequate power.

Although GSEA was not possible, filtering probesets prior to regression analysis did provide a list of probesets with significant differential expression at relapse in the TE (melphalan treated) subgroup. Interestingly IGLV1-44 demonstrated the largest log fold increase. IgL translocations have been described in ~10% of newly diagnosed myeloma and are associated with poor prognosis. They are often found at a sub-clonal level, demonstrating them to be later/secondary events in myeloma progression. The majority are also associated with focal amplifications of the IgL enhancer [80]. Significant increase in IgLV1-44 at relapse could reflect new IgL translocations at relapse, facilitating overexpression of oncogenes to provide mechanisms of melphalan treatment resistance. Furthermore, IgL translocations commonly juxtapose with *MYC* highlighting a potential mechanism of *MYC* upregulation at relapse in my cohort [80]. *HDAC2* was also significantly overexpressed, it is involved in DNA damage response [81], therefore providing a potential mechanism of melphalan resistance. HDAC inhibitors are already in clinical use with Panobinostat, a pan HDAC inhibitor, used in relapsed refractory myeloma. Investigation of HDAC inhibitors to potentiate melphalan might be interesting. *PHF19* was also significantly upregulated, overexpression in myeloma cell lines has been shown to mediate EZH2 phosphorylation as a mechanism of drug resistance [82]. Furthermore the myeloma DREAM challenge identified *PHF19* expression as a novel high risk biomarker [83].

With no significant differential expression identified at relapse in patients treated with lenalidomide maintenance, specific mechanisms of IMiD resistance cannot be described.

11.5.8 Conclusion

Through sequential expression analysis I have highlight a number of cellular processes and genes involved in relapse and treatment resistance.

Therapeutic targeting for many are already being investigated, these results adding further weight to their exploration. Targeting XPO1 shows particular promise with clinical evidence from the BOSTON phase 3 clinical trial which demonstrated superior PFS in relapsed patients treated with weekly selinexor bortezomib and dexamethasone [74]. While selinexor is associated with significant side effects, in particular nausea and cachexia. Clinical proof of efficacy paired with this data provides a strong rationale to further pursue XPO1 targeting as a biological mechanism involved in relapse. Development of better tolerated inhibitors may potentially open opportunities for targeting relapse earlier.

With multiple mechanisms of dysregulation and clear enrichment at relapse, I believe successful targeting of MYC will be key in the treatment of relapsed myeloma and could play a vital role in overcoming IMiD resistance.

Unfortunately this DGE analysis does not provide evidence to help rationalise treatment based on molecular subgroup. Larger sample size may and novel approaches to probeset filtering may facilitate future sequential analysis. Also molecular subgroups were based on cytogenetics, consensus clustering of baseline expression to identify molecular subgroups could be considered in future analysis.

Chapter 12: GEP evolution results- high risk signatures

12.1 Introduction

Examination of tumour transcriptome in relation to outcome data has allowed the creation of gene expression risk scores used to help prognosticate myeloma patients. A variety of scores have been demonstrated to provide independent prognostic value to the already established high risk cytogenetic lesions. The most widely accepted signatures include the EMC92 and UAMS70 scores. A summary of published risk scores can be seen in **Table 1-4** in section 1.1.4.3.

Risk scores provide a manageable sized pool of genes on which to focus attention for further translational research. While their expression is known to correlate with aggressive clinical behaviour and therefore early relapse, knowledge of how their expression changes from presentation to relapse is lacking. Review of sequential scores could reveal specific genes implicated in relapse.

For patients in the GEP evolution cohort, I have calculated EMC92 and UAMS70 risk score at each time point and examined change in expression of individual genes.

12.2 EMC92 score

The EMC92 score is based on the expression profiles of 290 patients within the HOVON-65/GMMG-HD4 trial. Univariate cox regression and principal component analysis was used to assess the relationship of probe sets with outcome, resulting in a 92 gene signature. The score is calculated as the sum of weighted expression, patients with a score above 0.827 are considered high risk which reflects an OS of less than 2 years [19]. The signature was also validated within the Total Therapy (TT) 2, TT3 and Myeloma IX trial cohorts of newly diagnosed myeloma patients and finally within the relapsed APEX trial cohort. The Myeloma IX cohort also provided data on the presence high risk

cytogenetics, tumours considered high risk by EMC92 had a higher proportion of del(17p), Gain(1q), t(4;14) and t(14;16) when compared to standard risk. However multivariate cox regression within the myeloma IX cohort demonstrated the EMC92 score to remain prognostically independent of del(17p), B2M >3.5 mg/l and PS >1[19].

12.2.1 Change in score

In my analysis of the GEP evolution cohort, EMC92 score increased at relapse in the majority (67.2%) of tumours and there was a significant increase in the median score of all patients at relapse: -0.27 (range -1.84 to 1.83) at presentation vs. -0.04 (range -1.59 to 3.57) at relapse (Wilcoxon Signed-Ranked *P* = 0.0018) (**Figure 12-1**). There was a change in risk status for 11 (16.4%) tumours; 8 (11.9%) transitioning from standard risk to high risk and 3 (4.5%) returning to standard risk from high. The net frequency of cases with high risk EMC92 score increased from 10 (14.9%) at presentation to 15 (22.4%) at relapse (**Figure 12-1**).

12.2.2 Association with OS

The association of EMC92 score with overall survival was investigated using univariate cox regression. Patients were stratified by their sequential risk status to produce 4 groups; “High-High”, “High-Standard”, “Standard-High” and “Standard-Standard”. A sustained high risk score at presentation and relapse (“High-High”) was associated with a significantly shorter OS (HR 5.16, *P*=0.0045) when compared to “Standard- Standard” risk tumours. Evolution of new high risk at relapse (“Standard-High”) was also associated with a significantly shorter OS (HR 3.38, *P*=0.018) when compared to “Standard-Standard”. Patients who lost high risk status at relapse (“High-Standard”) had shorter OS compared to those with standard risk “Standard-Standard”, the difference was not significant suggesting the score can also identify improvement in risk, this should be interpreted with caution given the small numbers within this group. Median OS was 26.8, 28.0, 32.7 and 74.1 months for Standard-High, High-High, High-Standard and Standard-Standard respectively (log-rank *P*=0.0023) (**Figure 12-2)**.

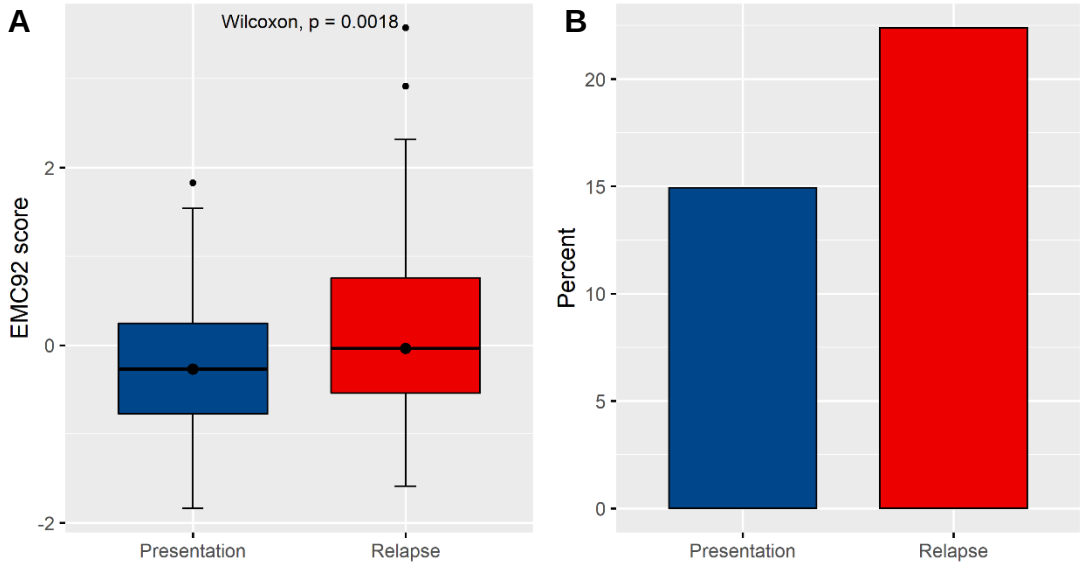

Figure 12-1 Sequential EMC92 scores: (A) boxplots of EMC92 scores; (B) bar graphs showing frequency of high risk tumours.

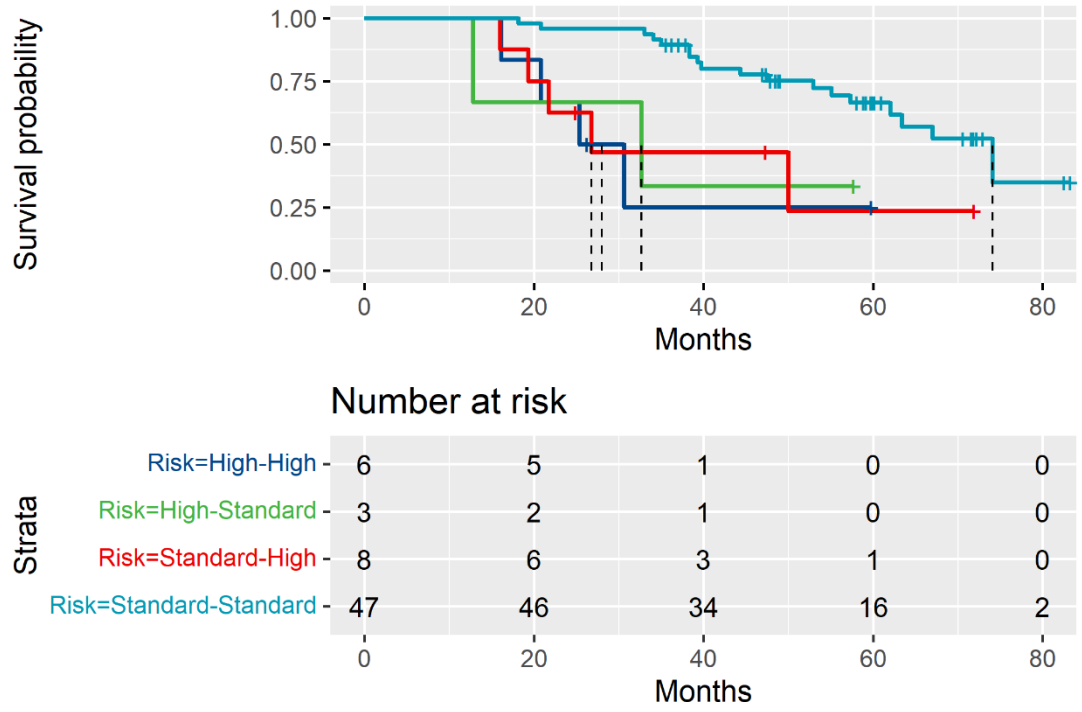

Figure 12-2: Kaplan-Meier for OS in relation to sequential EMC92 risk status.

12.2.3 Change per probe set

Change in expression of the 92 probesets was examined between time points. Using the limma linear regression model, 25 probesets demonstrated significant differential gene expression at relapse (FDR <0.05); 21 upregulated and 4 downregulated **(Table 12-1)**.

Probesets with a significant increase in expression at relapse and LFC of >0.5 included *MAGEA6, TOP2A, MCM2, FANCI, KIF4A, PGM2, ZWINT, MCM3, MCM6, SEPTIN11, PPP2R1B, BIRC5* and *SPAG5.* Probesets with a significant decrease in expression at relapse and LFC of >0.5 include *FAM49A* and *DHRS9*.

Probeset	Gene	Log FC	Av. Exp	FDR
214612_x_at	*MAGEA6*	1.24	8.55	0.001
201292_at	*TOP2A*	0.78	7.59	0.027
202107_s_at	*MCM2*	0.77	8.74	0.002
213007_at	*FANCI*	0.74	8.14	0.009
218355_at	*KIF4A*	0.70	6.70	0.037
225366_at	*PGM2*	0.68	7.80	0.002
204026_s_at	*ZWINT*	0.65	9.72	0.000
201555_at	*MCM3*	0.64	9.35	0.001
201930_at	*MCM6*	0.60	10.48	0.000
201307_at	*SEPTIN11*	0.59	9.51	0.000
202884_s_at	*PPP2R1B*	0.57	8.12	0.018
210334_x_at	*BIRC5*	0.56	8.56	0.009
203145_at	*SPAG5*	0.51	8.26	0.007
218662_s_at	*NCAPG*	0.50	7.94	0.028
212282_at	*TMEM97*	0.48	10.11	0.003
211963_s_at	*ARPC5*	0.46	11.63	0.009
222680_s_at	*DTL*	0.46	8.52	0.012
221826_at	*ANGEL2*	0.45	8.34	0.032
201795_at	*LBR*	0.40	10.68	0.009
202532_s_at	*DHFR*	0.39	9.55	0.013
222154_s_at	*SPATS2L*	0.36	11.65	0.009
208967_s_at	*AK2*	0.28	11.30	0.040
221677_s_at	*DONSON*	0.27	9.83	0.018
209026_x_at	*TUBB*	0.27	12.42	0.018
211714_x_at	*TUBB*	0.25	12.81	0.027
202542_s_at	*AIMP1*	0.19	12.04	0.031
200775_s_at	*HNRNPK*	0.18	14.10	0.009
200933_x_at	*RPS4X*	-0.18	17.35	0.037
208904_s_at	*RPS28*	-0.22	16.93	0.007
213350_at	*RPS11*	-0.41	11.67	0.000
209683_at	*FAM49A*	-0.65	9.77	0.028
224009_x_at	*DHRS9*	-0.96	8.81	0.003

Table 12-1: EMC92 probesets with significant differential genes expression at relapse.

12.2.4 Change in score per molecular subgroup

Mean EMC92 score was highest in t(4;14) and lowest in t(11;14) tumours at both time points. The frequency of high risk scores at presentation for t(4;14), t(11;14) and HRD tumours was 50.0%, 14.3% and 7.1% respectively (**Figure 12-3**).

Mean scores increased from presentation to relapse in t(4;14) and HRD tumours but decreased in t(11;14) tumours. Increase in EMC92 score at relapse was most common in HRD tumours, observed in 82.1% of HRD with gain(11) and 57.1% of HRD without gain(11). The largest increase in score was 3.57, observed in a HRD with gain(11) tumour (**Figure 12-4)**. High risk status only changed in HRD tumours, with a net increase in frequency of high risk tumours at relapse. (**Figure 12-3**).

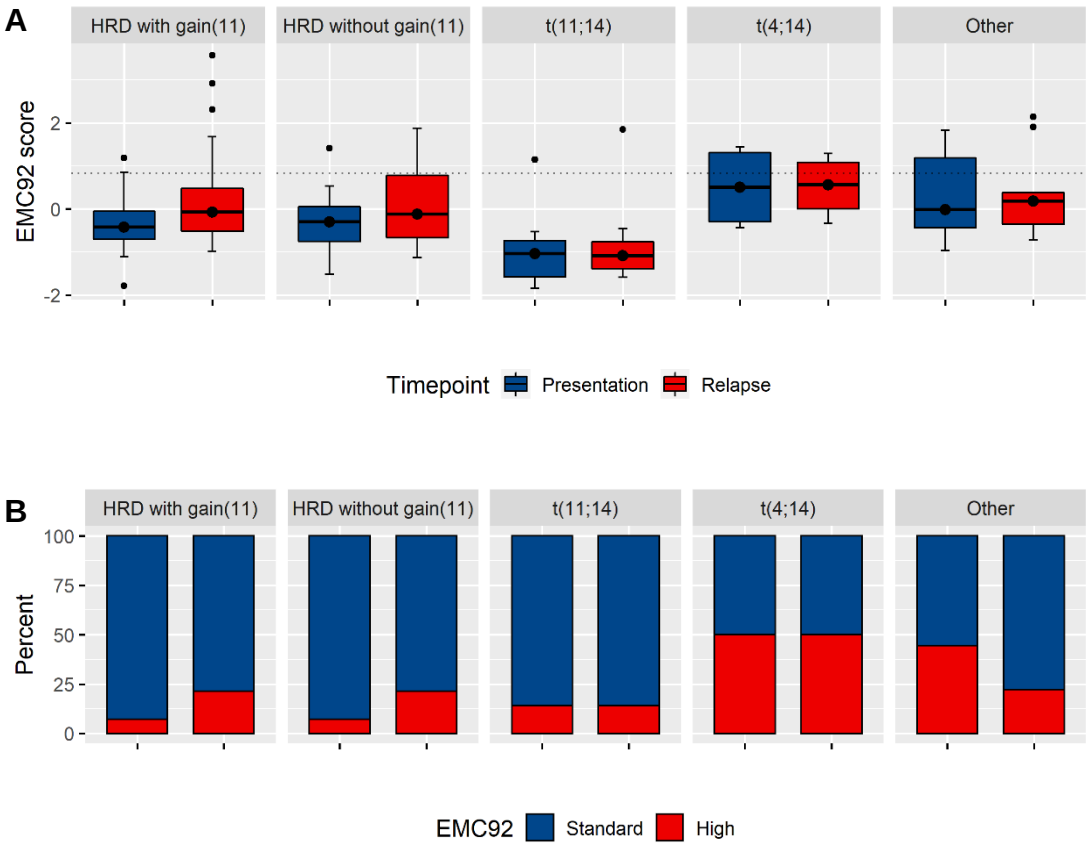

Figure 12-3 Sequential EMC92 scores per cytogenetic subgroup: (A) boxplots comparing EMC92 scores between time points (dotted line shows EMC92 high risk threshold); (B) bar graphs showing frequency of EMC92 high risk tumours at each time point.

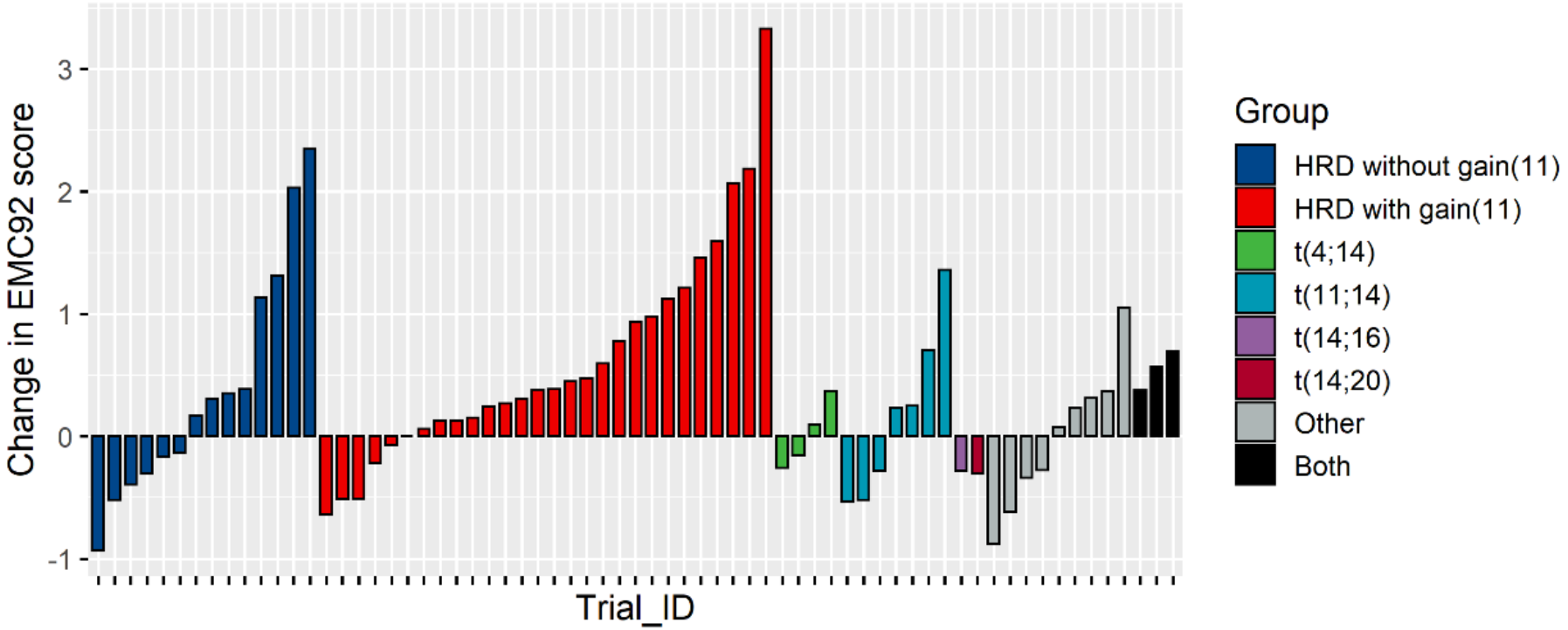

Figure 12-4: Change in EMC92 per cytogentic subgroup.

12.3 UAMS70 score

The UAMS70 score is based on the expression profiles of 351 newly diagnosed myeloma patients treated on the UARK 98-026 trial. Data was split into quartiles to identify highest and lowest expressed genes, univariate regression analysis was then used to see which were associated with shortest survival. 51 genes with high expression and 19 genes with low expression were identified. Difference in the mean log2 expression of high and low genes was calculated per patient to provide the UAMS70 score. K mean clustering of the score identified distinct groups resulting in a cut off of >0.66 to identify high risk scores. Patients with scores >0.66 were associated with a significantly poorer event free survival and OS. The signature was also validated using expression data from 181 newly diagnosed myeloma patients from the UARK 03-033 trial. Multivariate analysis of OS showed the UAMS70 score to retain significance after adjustment for ISS, gain(1q), t(4;14) and LDH [20].

12.3.1 Change in score

Surprisingly only 2 of 67 (3.0%) patients had a high risk UAMS70 score at presentation. UAMS70 scores increased in the majority (71.6%) of patients, with a significant increase in the median UAMS70 score at relapse: -0.28 (range -1.23 to 0.98) at presentation vs. -0.00073 (range -0.91 to 1.70) at relapse (Wilcoxon Signed-Ranked *P* <0.001) (**Figure 12-5**). Change in score translated to a change in risk status for 7 (10.1%) tumours; all transitioning from standard risk to high. The net frequency of tumours with a high risk UAMS70 score increased to 9 (13.4%) at relapse (**Figure 12-5**).

12.3.2 Association with OS

The association of UAMS70 score with overall survival was investigated using univariate cox regression. Patients were stratified by their sequential risk status to produce 3 groups; “High-High, “Standard-High” and “Standard-Standard”. Sustained high risk scores at presentation and relapse (“High-High”) were associated with a shorter OS (HR 7.49, *P*=0.061) when compared to “Standard-Standard” risk, while this did not reach significance this group only accounted for 2 patients. Evolution of a high risk score at relapse

("standard-high") was associated with a significantly shorter OS (HR 5.33, *P*=0.0012) when compared to "Standard-Standard" risk. Median OS was 16.1, 25.7 and 74.1 months for High-High, Standard-High and Standard-Standard respectively (log-rank *P*<0.001) (**Figure 12-6**).

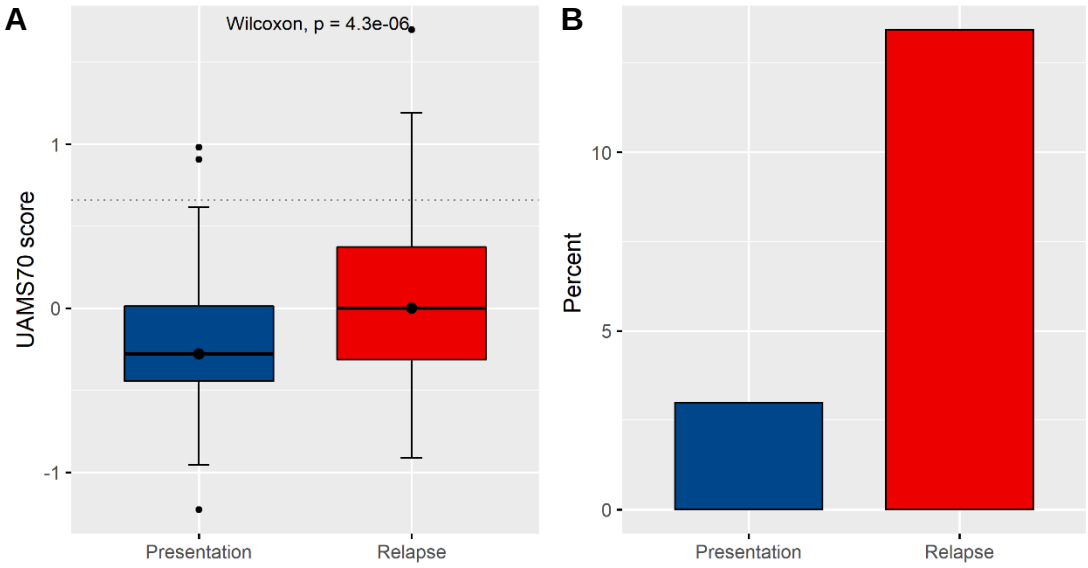

Figure 12-5 Sequential UAMS70 scores: (A) boxplots of UAMS70 scores; (B) bar graphs showing frequency of high risk tumours.

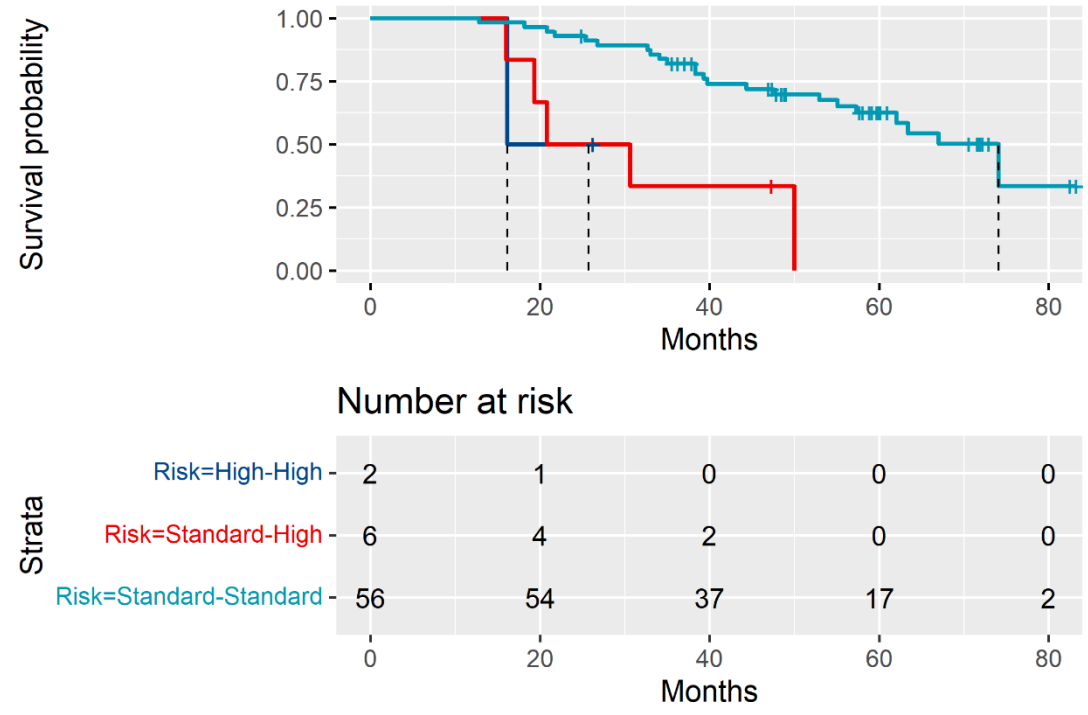

Figure 12-6 Kaplan-Meier for OS in relation to sequential UAMS70 risk status.

12.3.3Change per probeset

24 probesets demonstrated significant differential expression at relapse (FDR <0.05); 22 of the signatures highly expressed genes were upregulated and 2 of the signatures genes with low expression were downregulated **(Table 12-2)**.

Genes with significant upregulation and LFC of >0.5 include *FABP5, ASPM, CENPW, AURKA, TRIP13, SLC19A1, LARS2, RUVBL1, BIRC5* and *CKS1B*. Significant down regulation with LFC >0.5 included *ITPRIP* and "237964_at" (location unknown)

Probeset	Gene	log FC	Av. Exp	FDR
202345_s_at	*FABP5*	0.80	10.84	<0.001
219918_s_at	*ASPM*	0.80	7.08	0.016
226936_at	*CENPW*	0.71	9.56	<0.001
204092_s_at	*AURKA*	0.63	7.30	0.040
204033_at	*TRIP13*	0.62	8.28	0.001
211576_s_at	*SLC19A1*	0.62	8.10	0.006
204016_at	*LARS2*	0.57	6.03	0.020
201614_s_at	*RUVBL1*	0.57	9.10	0.005
210334_x_at	*BIRC5*	0.56	8.56	0.006
201897_s_at	*CKS1B*	0.56	10.96	<0.001
218947_s_at	*MTPAP*	0.46	9.02	0.006
201231_s_at	*ENO1*	0.39	12.37	0.001
225082_at	*CPSF3*	0.35	10.23	0.001
201947_s_at	*CCT2*	0.32	12.40	0.003
210460_s_at	*PSMD4*	0.30	11.85	0.002
203432_at	*TMPO*	0.30	9.57	0.009
204023_at	*RFC4*	0.29	10.43	0.016
222417_s_at	*SNX5*	0.29	10.86	0.006
224523_s_at	*CMSS1*	0.29	10.85	0.015
200750_s_at	*RAN*	0.28	13.12	0.020
201091_s_at	*CBX3*	0.27	12.38	0.006
1555864_s_at	*PDHA1*	0.22	10.96	0.008
225582_at	*ITPRIP*	-0.68	10.48	0.000
237964_at	NA	-0.93	5.81	0.008

Table 12-2: UAMS70 probes with significant differential gene expression at relapse.

12.3.4 Change in score per molecular subgroup

At presentation mean scores per subgroup were highest in the t(4;14) and "Other" sub-groups and lowest in the t(11;14) sub-group. Only 2 tumours were classified as high risk at presentation both were observed in the "other" sub-group (**Figure 12-7)**.

Mean UAMS70 score increased at relapse in all sub-groups, an increase in score was observed in the majority of patients for all subgroups, with the highest proportion observed in the "Other" subgroup. The largest increase in score per patient was observed in an HRD tumours (**Figure 12-8**).

Evolution of new high risk status at relapse was seen in 14.3% of patients within the HRD with gain(11), HRD without gain(11) and t(11;14) subgroups respectively. Frequency of high risk tumours remained stable in all other subgroups (**Figure 12-7)**.

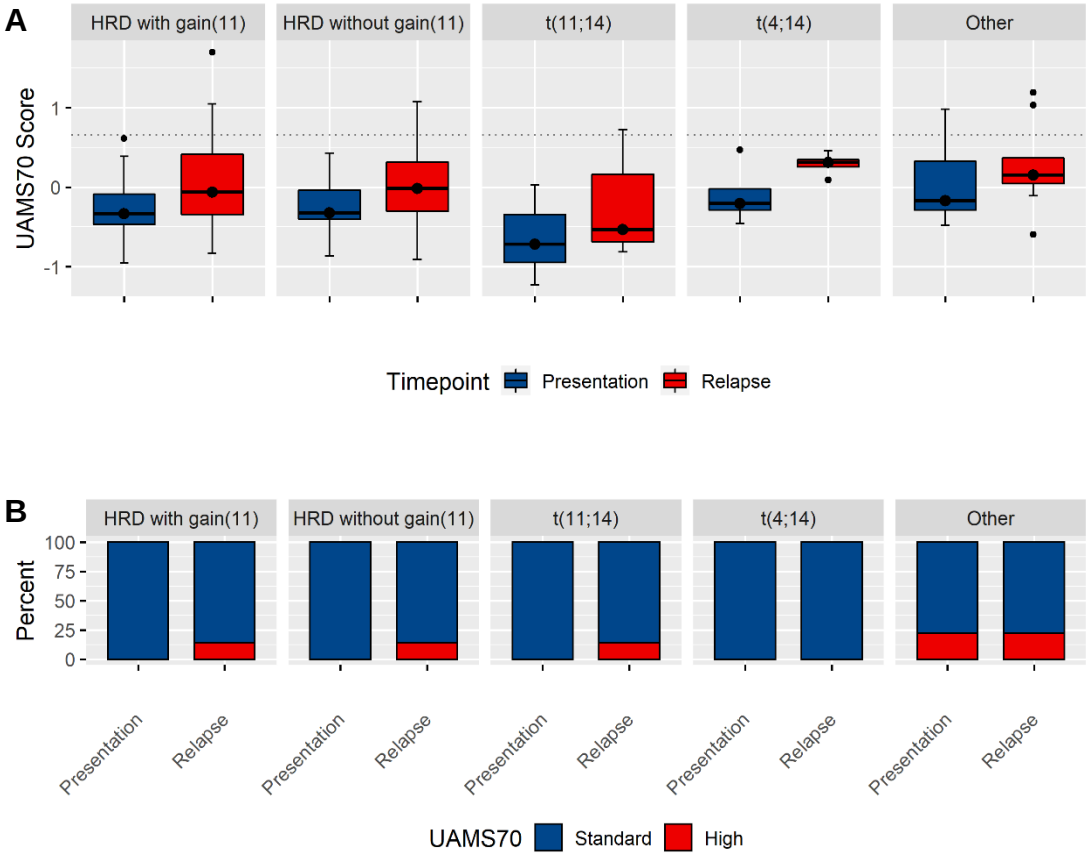

Figure 12-7 Sequential UAMS70 scores per cytogenetic subgroups: (A) boxplots comparing UAMS70 scores between time points (dotted line shows high risk threshold); (B) bar graphs showing frequency of UAMS70 high risk tumours at each time point.

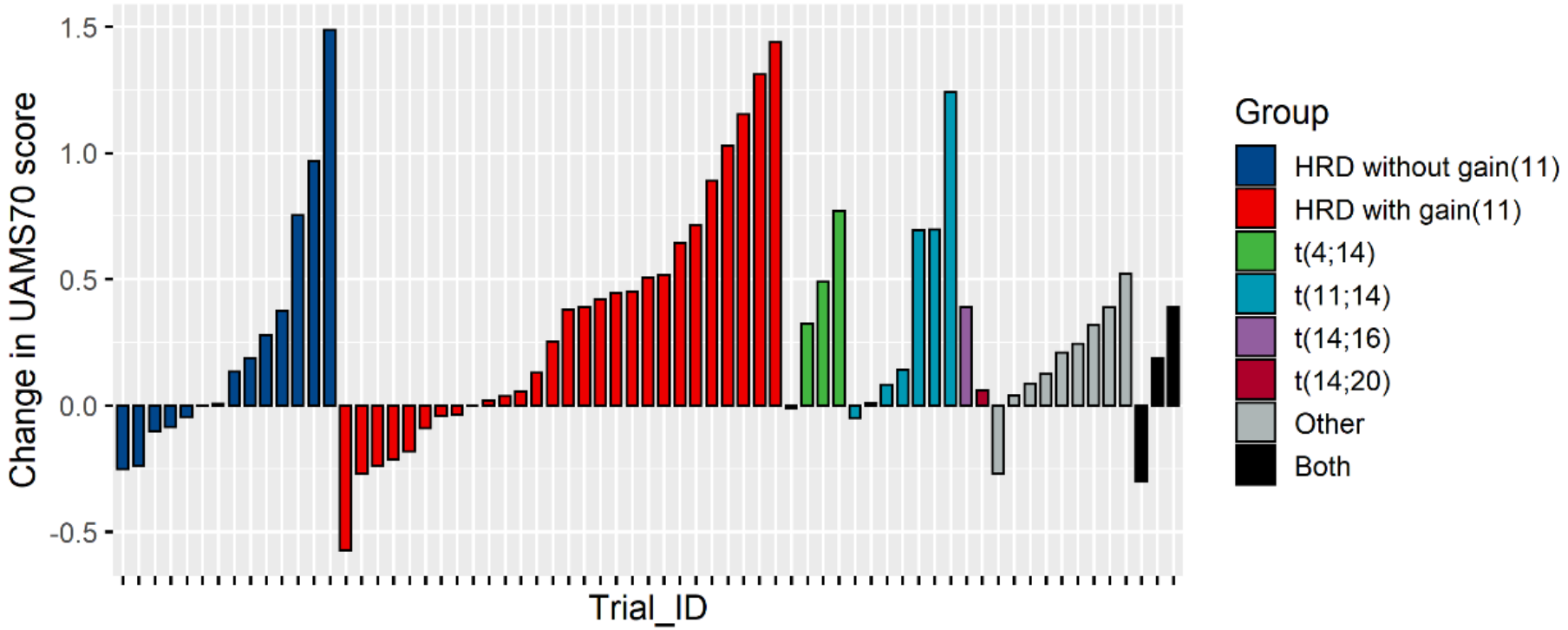

Figure 12-8: Change in UAMS70 score per cytogentic subgroup.

12.4 Pattern of evolution and risk score

Each of the 67 patients were grouped based on CNA evolution patterns at relapse. Branching, linear, linear loss and stable evolution patterns were observed in 29 (43.3%), 10 (14.9%), 15 (22.4%), and 13 (19.4%) of tumours respectively. EMC92 and UAMS70 scores per evolution group were compared at presentation and relapse.

12.4.1 EMC92

Non stable patterns of evolution were associated with an increase in median EMC92 score at relapse, whereas median score at relapse was similar in patients with stable evolution. There was a significant increase in median EMC92 score at relapse in tumours that evolved with a branching pattern; -0.159 (range -1.79 to 1.41) at presentation vs. 0.179 (range -1.13 to 3.57) at relapse (Wilcoxon Signed-Ranked P = 0.00045).

At relapse the proportion of high risk EMC92 scores increased in tumours that demonstrated branching and linear evolution; from 10.3% to 31.0% and 20% to 30% respectively. The proportion of high risk scores decreased at relapse in tumours demonstrating linear loss; from 13.3% to 0%. The proportion of high risk scores did not change in tumours with stable evolution **(Figure 12-9)**.

12.4.2 UAMS70

Median UAMS70 score was seen to increase at relapse in all patterns of evolution, there was a significant increase within branching, linear and stable groups, suggesting that the score is not dependent on CNA. At relapse the proportion of high risk scores increased within tumours demonstrating branching and stable evolution groups, from 0% to 20.7% and 0% to 7.7% respectively. Proportion of high risk scores at relapse did not change in tumours demonstrating patterns of linear and linear loss evolution **(Figure 11-9)**.

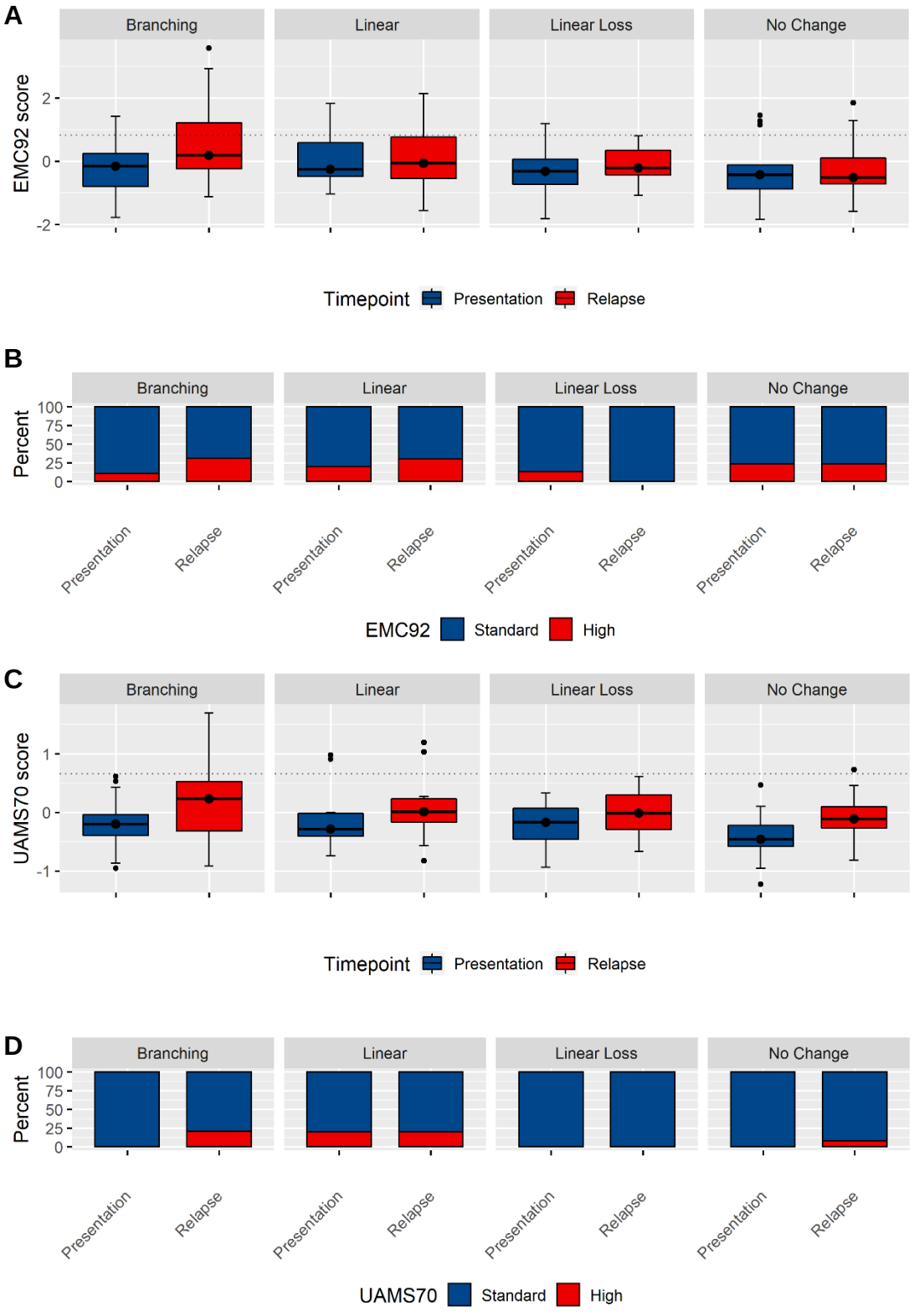

Figure 12-9 Compairson of EMC92 (A+B) and UAMS70 (C+D) scores between time points based on CNA evolution pattern at relapse. Boxplots of scores (A+C), bargraphs of high risk frequency (B+D)

12.5 Discussion

This analysis demonstrates evolution of transcriptional high risk tumour biology at relapse. While only some tumours did transition into high risk status, the majority demonstrated an increase in risk score suggesting emergence of a more aggressive/proliferative clone. This would correlate with natural history of myeloma, where response and remission times are reduced at each relapse.

Association of high risk GEP signatures with inferior outcomes in relapsed disease has previously been demonstrated, but it was less clear whether acquisition of high risk status at relapse in tumours with non-high risk status at presentation also had inferior outcome. My work demonstrates within a randomised controlled trial that evolution of high risk GEP signature is clearly associated with inferior subsequent outcome. Similar in analogy to the CNA results, this supports the need to re-evaluate genetic profiles at relapse to help guide treatment decisions.

The EMC92 score appeared to correlate more closely with evolutionary trajectories of cytogenetic subgroups described in Chapters 5 and 6. This was surprising as the UAMS70 score is defined by dysregulated genes mapping to chromosome 1. The EMC92 score also identified a higher proportion of high risk tumours at each time point.

12.5.1EMC92

Using gene ontology (GO), common biological processes relating to EMC92 probesets with significant dysregulation at relapse were considered. Upregulated genes were associated with DNA replication (*MCM3, MCM6, MCM2, DONSON* and *DTL*), cell division (*TUBB, SPAG5, ZWINT, NCAPG* and *BIRC5*), G1/S transition of mitotic cell cycle, double-strand break repair via break-induced replication and DNA replication initiation (*MCM3, MCM6, and MCM2),* chromosome segregation (*TOP2A, SPAG5* and *BIRC5*) and apoptotic process (*AIMP1, BIRC5* and *MCM2*). Down regulated genes were associated with translation (*RPS4X, RPS11* and *RPS28*).

Genes with the largest LFC at relapse were next considered. *MAGEA6* demonstrated the largest increase in expression at relapse (LFC 1.24, FDR 0.001). Dysregulation of the MAGEA gene family has previously been reported in myeloma, inhibiting apoptosis and causing chemotherapy resistance, Mei et al have recently highlighted it as a potential therapeutic target [84]. *TOP2A* (LFC 0.78; FDR 0.027) and *MCM2* (LFC0.77; FDR 0.002) were also significantly upregulated in my overall DGE analysis in section 11.2 and highlighted in the leading edge analysis. Their presence in the EMC92 score provides validation of my results, their potential role in relapse and treatment resistance discussed was chapter 11.

12.5.2 UAMS70

Using gene ontology (GO), common biological processes relating to UAMS70 probesets with significant dysregulation at relapse were considered. Upregulated genes were associated with cell division (*RAN*, *RUVBL1*, *CKS1B*, *AURKA*, *BIRC5* and *CENPW*), negative regulation of apoptotic process (*AURKA, BIRC5, RUVBL1, PSMD4*), negative regulation of transcription, DNA-templated (*CBX3, ENO1* and *BIRC5*), mitotic cell cycle (*RAN, AURKA* and *CENPW*), and chromosome segregation (*BIRC5* and *CENPW*).

Boyle et al also recently completed GEP analysis of sequential tumour samples, they reported 18 probesets from the UAMS70 score to show significant differential gene expression at relapse (FDR <0.001), of which 10 were also significantly dysregulated in my analysis; *FABP5, ASPM, CENPW, AURKA, TRIP13, SLC19A1, BIRC5, CKS1B, RFC4* and *ITPRIP* [85].

The largest log fold increase at relapse was observed in *FABP5* (LFC 0.8; FDR <0.001), a gene that plays an instrumental role in adipocyte biology. Studies have demonstrated increased expression in myeloma, it is thought to facilitate cellular interaction/survival within the bone marrow microenvironment and has been suggested as potential therapeutic target [86].

12.5.3 Conclusion

As expected features of high risk disease increase at relapse in the majority of patients, the increase of high risk scores at relapse was consistent with

previous studies looking at sequential GEP signatures [15, 85]. Both signatures remained prognostic at relapse supporting the role for repeat genetic profiling at relapse to guide treatment strategies. Evolution of expression provided insight into mechanisms of relapse. A handful of genes identified in the DGE analysis from chapter 11 were also significantly upregulated here highlighting their significance in myeloma relapse and the potential benefit of therapeutic targeting. In particular, *BIRC5* stands out as the only gene found in both the EMC2 and UAMS70 signatures and was significantly upregulated at relapse in DGE analysis of all patients (section 11.2, section 12.2.3 and 12.3.3).

Chapter 13: GEP evolution results- 1q CNA

13.1 Introduction

The CNA analysis highlighted the significance of gain/amp(1q) in myeloma progression and relapse. While recognised as an adverse prognostic marker in myeloma, identification of consistently deregulated genes associated with this CNA is challenging [47]. To look for potential driver genes I have examined gene expression in relation gain/amp(1q).

13.2 Frequency of 1q CNA

67 patients with sequential gene expression data were examined, at presentation 27 (40.3%) and 6 (9.0%) tumours demonstrated gain or amplification of 1q respectively. At relapse, acquisition of new gain or amplification(1q) was observed in 3 (4.5%) and 4 (6.0%) tumours respectively, 3 out of 4 new amplifications evolved from gain(1q) at presentation. Resolution of gain(1q) at presentation to diploid status at relapse was observed in 1 tumour **(Table 13-1)**. Of note, new gain/amp(1q) at relapse was less common than that observed in the overall cohort of 178 patients in chapter 5; 10.5% versus 19% respectively.

Presentation	Relapse	Frequency	%
Diploid	Diploid	30	44.8
Diploid	Gain	3	4.5
Diploid	Amplification	1	1.5
Gain	Diploid	1	1.5
Gain	Gain	23	34.3
Gain	Amplification	3	4.5
Amplification	Amplification	6	9.0

Table 13-1: GEP evolution cohort: Frequency of 1q copy number evolution.

13.3 New gain/amp(1q) at relapse

Linear regression was applied to investigate differential gene expression between sequential tumour samples of patient who acquired new gain/amp(1q) at relapse (7 patients). Significant differential expression required an FDR of ≤0.05. The analysis was limited by the small number of patients.

Looking at all probesets, there was no significant differential expression at relapse. Filtering of probesets prior to application of the linear regression model did not increase the yield of genes with significant differential expression.

13.4 Gain/amp(1q) vs diploid tumours

Sequential differential expression was limited by small sample size. In order to identify potential driver genes associated with 1q CNA, I next investigated differential expression between tumours with gain/amp(1q) versus diploid status at presentation.

Significant differential expression (FDR <0.05) was found in 146 probesets; 111 upregulated, 35 downregulated **(Supplementary Tables 14-6 and 14-7)**. 95 probesets (65.1%) were located on 1q with the highest density found at 1q21. GSEA of C1 positional gene sets demonstrated significant positive enrichment at 1q21 (NES 1.31; FDR 0.165), no other C1 gene sets were enriched. Due to the small number of genes, GSEA of hallmark gene sets was not successful.

To identify clinically relevant genes, relationship of expression with OS was examined. To do so, expression at presentation was categorised as high or low in relation to mean probeset expression.

Of significantly upregulated probesets, high expression at presentation was associated with a significantly shorter OS in 21 genes **(Table 13-2)**. The majority (95.2%) located on 1q, with the highest proportion (33.3%) at 1q21. The strongest HR was observed in *CKS1B* (HR 3.15, p<0.001), *NTPCR* (2.98,

<0.001), *CHD1L* (HR 2.89, p<0.001), *MRPL55* (2.84, <0.001) and *BROX* (2.77, <0.001).

Of the significantly down regulated probesets, low expression at presentation was associated with a significantly shorter OS in 12 genes **(Table 13-3)**. The strongest HR was observed in *CCND1* (3.81, <0.001), *IL6* (3.69, <0.001), *STAP1* (3.19, <0.001), *CD44* (2.95, <0.001) and *SIDT1* (2.78, <0.001).

Of the genes with a significant association to OS, I next filtered for those with a corresponding change in expression in tumours that acquire new gain/amp(1q) at relapse.

Sequential increase in mean expression for tumours with acquisition of new gain/amp of 1q at relapse was observed in *CKS1B, CHD1L, MRPL55, BROX, RNF115, RNPEP, PSMD4, TIMM17A, UHMK1, POLR3C, MTX1, TFB2M, ARPC5* and *TIPRL.* Survival curves and expression based on copy number for *CKS1B, CHD1L, RNPEP* and *PSMD4* are demonstrated in **Figure 13-2 and 13-3.**

Sequential mean decrease in expression for tumours with acquisition of new gain/amp of 1q at relapse was observed in *CCND1, STAP1, ASAP1, TNFRSF14* and *FBXW7*, examples demonstrated in **Figure 13-4.**

Gene	Chr band	HR	95% CI	*P* value
CHD1L	1q21.1	2.89	(1.68-4.98)	<0.001
RNF115	1q21.1	2.04	(1.20-3.48)	0.009
POLR3C	1q21.1	1.99	(1.37-2.88)	<0.001
ANP32E	1q21.2	2.62	(1.80-3.81)	<0.001
CKS1B	1q21.3	3.15	(1.83-5.45)	<0.001
PSMD4	1q21.3	2.24	(1.66-3.03)	<0.001
SNAPIN	1q21.3	1.71	(1.01-2.91)	0.046
MTX1	1q22	1.93	(1.14-3.27)	0.014
UHMK1	1q23.3	2.01	(1.17-3.44)	0.011
TIPRL	1q24.2	1.50	(1.03-2.17)	0.034
PIGC	1q24.3	2.74	(1.58-4.76)	<0.001
ARPC5	1q25.3	1.62	(1.12-2.36)	0.011
RNPEP	1q32.1	2.38	(1.39-4.08)	0.002
TIMM17A	1q32.1	2.04	(1.40-2.99)	<0.001
FLVCR1-DT	1q32.3	2.74	(1.59-4.74)	<0.001
BROX	1q41	2.77	(1.63-4.69)	<0.001
MRPL55	1q42.13	2.84	(1.65-4.89)	<0.001
NTPCR	1q42.2	2.98	(1.71-5.19)	<0.001
OPN3	1q43	1.90	(1.32-2.76)	0.001
TFB2M	1q44	1.75	(1.02-3.01)	0.042
COX5B	2q11.2	2.73	(1.58-4.72)	<0.001

Table 13-2 Upregulated probesets in gain/amp(1q) associated with significantly shorter OS.

Gene	Chr band	HR	95% CI	*P* value
TNFRSF14	1p36.32	2.66	(1.54-4.62)	<0.001
SIDT1	3q13.2	2.78	(1.59-4.85)	<0.001
STAP1	4q13.2	3.19	(2.16-4.72)	<0.001
FBXW7	4q31.3	1.52	(1.12-2.06)	0.007
IL6	7p15.3	3.69	(2.14-6.38)	<0.001
KIF13B	8p12	2.22	(1.31-3.77)	0.003
ASAP1	8q24.21-22	2.68	(1.84-3.91)	<0.001
CD44	11p13	2.95	(1.67-5.21)	<0.001
CCND1	11q13.3	3.81	(2.59-5.60)	<0.001
SLC35F2	11q22.3	2.14	(1.23-3.72)	0.007
APOL3	22q12.3	2.21	(1.29-3.78)	0.004
P2RY8	Xp22.33	2.45	(1.43-4.20)	0.001

Table 13-3 Downregulated probesets in gain/amp(1q) associated with significantly shorter OS.

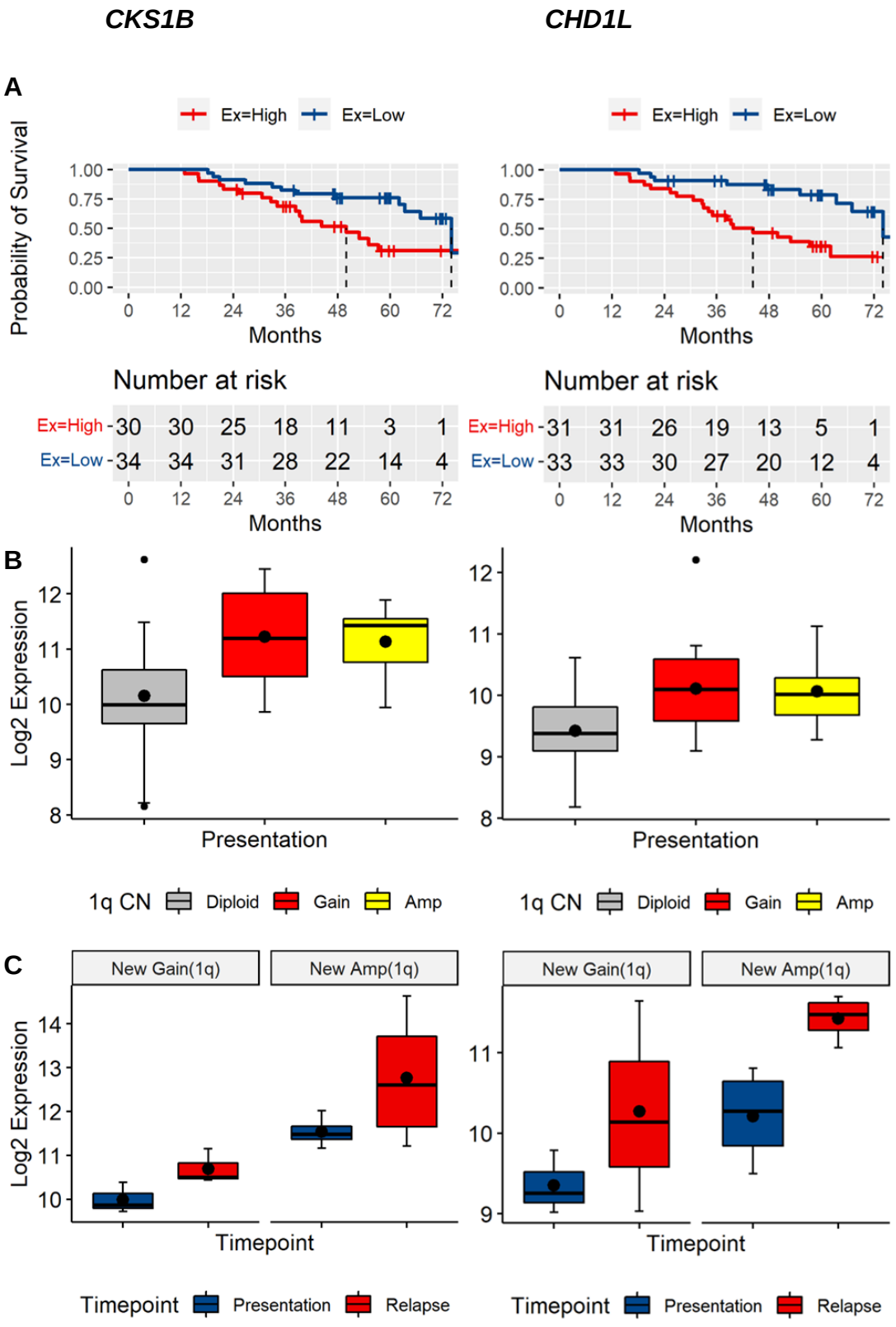

Figure 13-1 *CKS1B* (Left) and *CHLD1* (Right): Kaplan Meier survival curves of high vs low expression at presentation (A). Comparison of expression at presentation based on 1q copy number status (B). Change in expression between time points for tumours with acquisition of new 1q gain/ amplification at relapse (C).

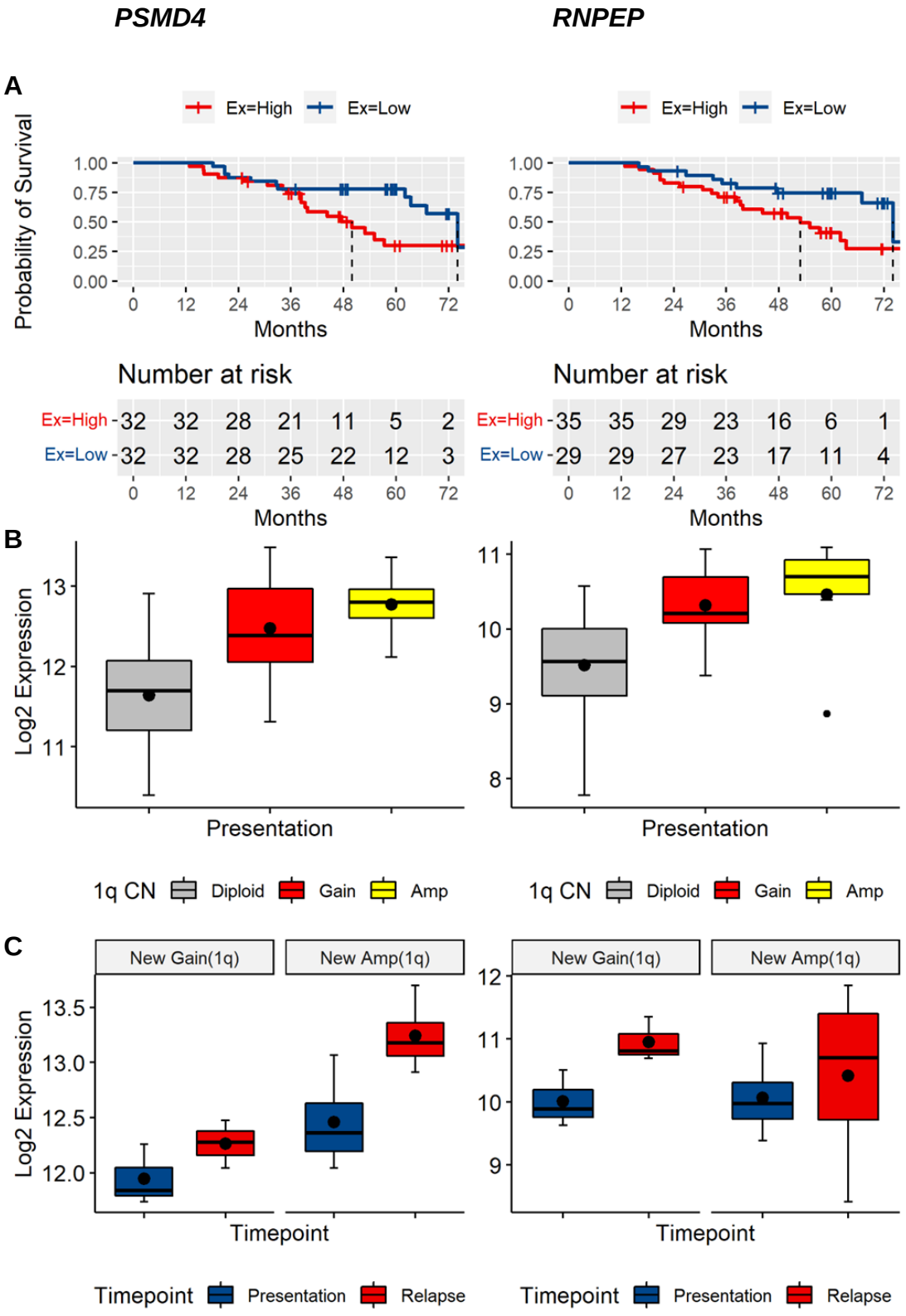

Figure 13-2 *PSMD4* (Left) and *RNPEP* (Right): Kaplan Meier survival curves high vs low expression at presentation (A). Comparison of expression at presentation based on 1q copy number status (B). Change in expression between time points for tumours with acquisition of new 1q gain/ amplification at relapse (C).

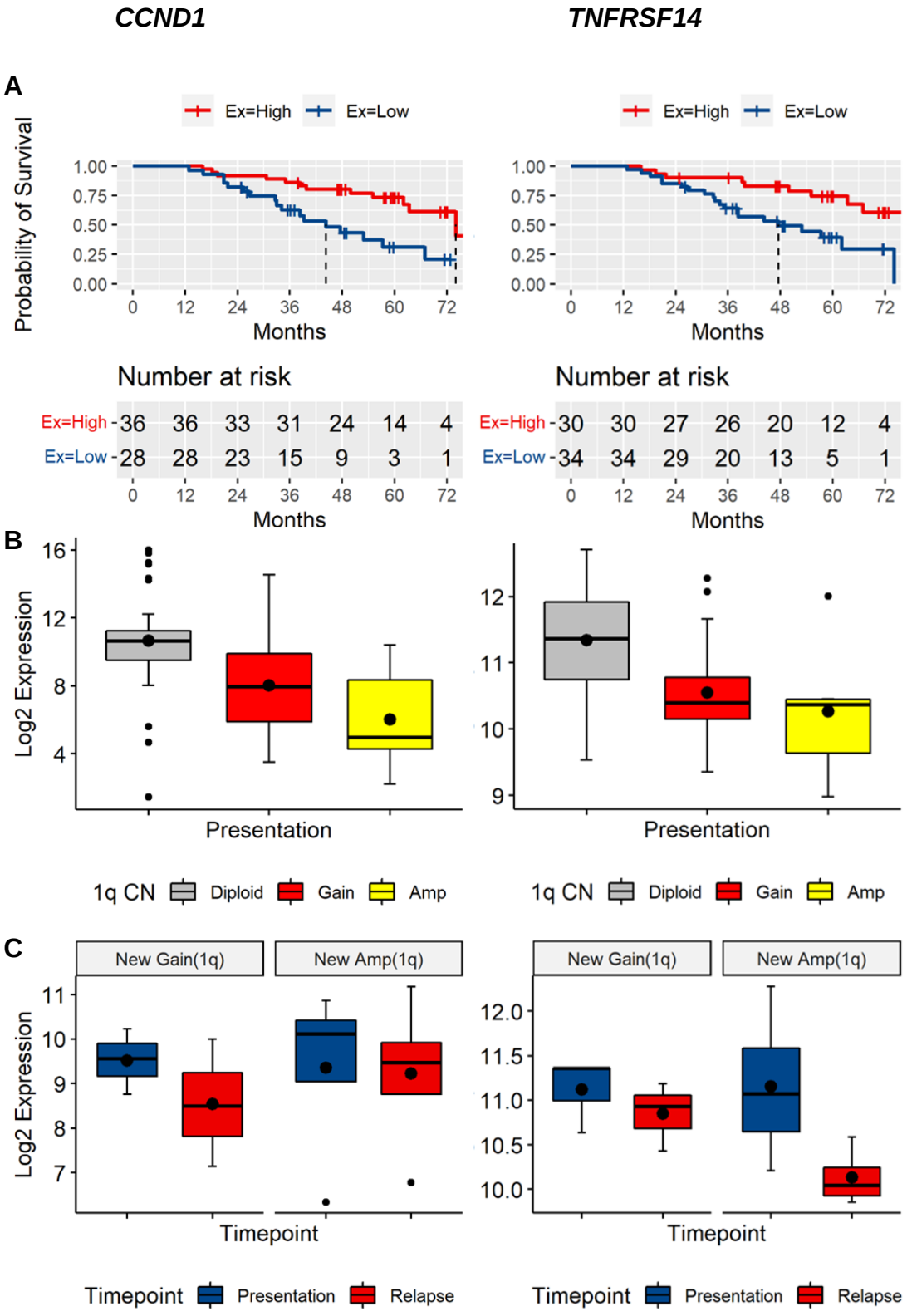

Figure 13-3 *CCND1* (Left) and *TNFRSF14* (Right): Kaplan Meier survival curves high vs low expression at presentation (A). Comparison of expression at presentation based on 1q copy number status (B). Change in expression between time points for tumours with acquisition of new 1q gain/ amplification at relapse (C).

13.5 Monoclonal antibody targets

Evidence supports the use of monoclonal antibodies in treatment of myeloma, with therapeutic targeting of cell surface proteins SLAMF7 (elotuzumab) and CD38 (daratumumab and isatuximab). Clinical trials have also considered their efficacy in treating patients with high risk lesions such as gain(1q). Expression of *SLAMF7* and *CD38* at presentation was similar regardless of 1q copy number status. Mean sequential expression of *SLAMF7* decreased at relapse in tumours that acquired new gain or amp(1q) suggesting a potential corresponding loss of elotuzumab efficacy. Sequential expression of *CD38* varied at relapse with a mean decrease observed in tumours with new gain(1q) at relapse but no change in tumours that acquire amp(1q) **(Figure 13-5).**

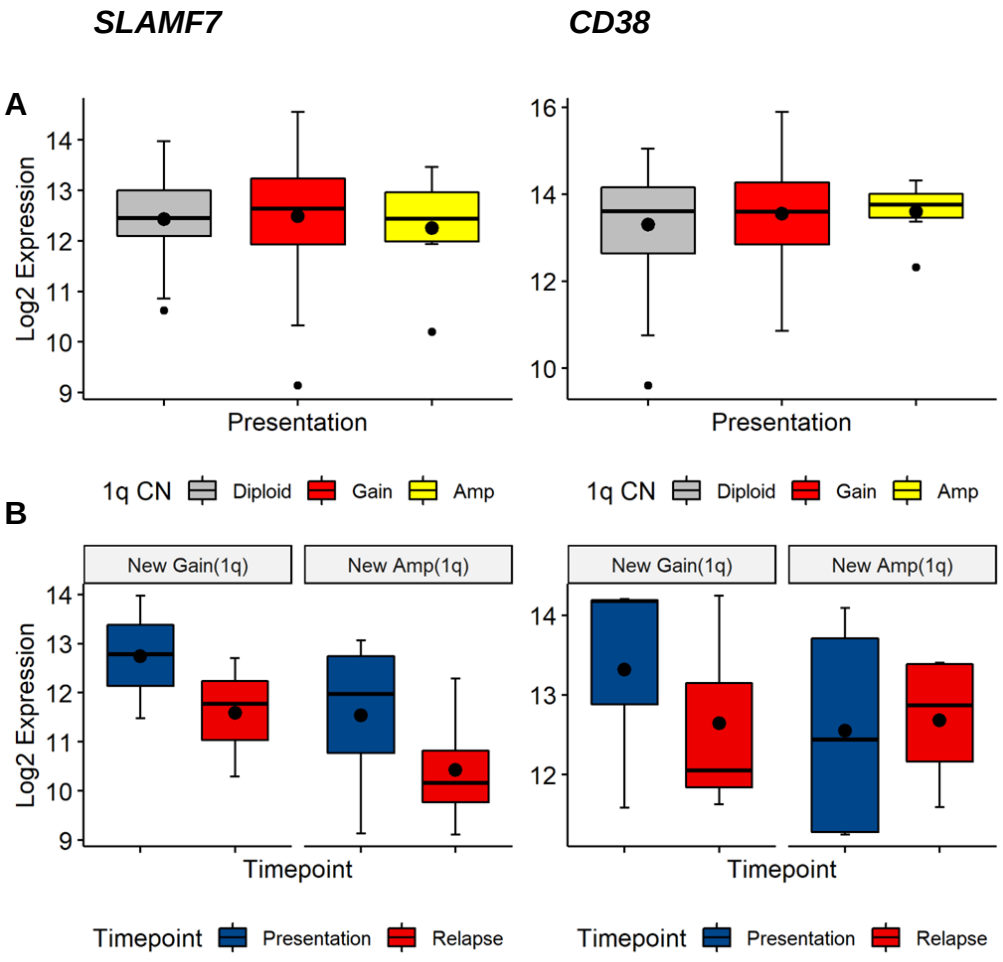

Figure 13-4 *SLAMF7* (Left) and *CD38* (Right): Comparison of expression at presentation based on 1q copy number status (A). Change in expression between time points for tumours with acquisition of new 1q gain/ amplification at relapse (B).

13.6 Discussion

Analysis in chapter 5 demonstrated 1q CNA to be interstitial in the majority of cases. As the largest chromosome, there are over 900 genes located on 1q highlighting the complexity of this CNA. Unfortunately sequential differential expression analysis of tumours that acquire new gain/amp(1q) at relapse was not informative, limited by small sample size. However, comparison of tumours with or without gain/amp(1q) did reveal significantly upregulated genes. Furthermore there was significant enrichment for genes located at 1q21, this correlates with previous reports and allows focus for future studies[44].

Examining sequential expression for tumours that acquire new gain/amp(1q) at relapse helped to identify those genes associated with worse OS that show a dynamic change with CNA evolution, genes of interest are discussed in more detail below.

CKS1B was discussed in chapter 5, it facilitates myeloma cell growth through activation of cyclin-dependent kinases, SKP2-mediated ubiquitination of the tumor suppressor gene $p27^{Kip1}$ and upregulation of the STAT3 and MEK/ERK pathways [20, 48, 49]. A handful of pre-clinical trials using small molecules to inhibit the actions of CKS1B have been reported, each successfully reducing myeloma cell proliferation, highlighting its potential as a therapeutic target [47]. However, none of the recently developed cell cycle inhibitors have demonstrated clinical efficacy in early myeloma trials, demonstrating the need to better understand the specific role of CKS1B in driving myeloma tumour survival.

RNPEP codes aminopeptidase B which contribute to proteolysis down steam from the ubiquitin-proteasome pathway and is known to be overexpressed in myeloma [87]. Upregulation in my analysis is of particular interest as there is a clinically trialled drug that can utilise *RNPEP* expression. Melflufen is a novel peptide-drug conjugate that, once absorbed by cells, is hydrolysed by aminopeptidase to release an alkylating agent inside the tumour. *RNPEP* expression has been linked to bortezomib resistance, with higher expression in resistant cell lines which were successfully treated with Melflufen[88]. The phase III OCEAN study has directly compared Melflufen dexamethasone

versus pomalidomide dexamethasone in relapsed refractory patients, results were recently presented at the 18th IMWG meeting and are not yet published. Although median PFS was longer in the Melflufen arm, there was an inferior OS compared to the pomalidomide arm. As a consequence the drug has been discontinued and will therefore not likely to play a role. Nonetheless, increased expression of *RNEP* at relapse in relation to gain(1q) supports the development of other therapeutic agents that utilise aminopeptidase activity to target the high risk tumour biology.

PSMD4 encodes a proteasome subunit and is therefore a target of PI in myeloma. The positive correlation of *PSMD4* expression and 1q copy number has previously been described, with increased expression attributed to bortezomib resistance [21]. It also contributes to the high risk GEP70 signature discussed in chapter 12 [20], my analysis showing significant upregulation at relapse when sequential scores were examined. A previous study suggested that carfilzomib might be able to overcome the negative effects of *PSMD4* overexpression, however evidence from head to head studies of carfilzomib and bortezomib regimes in relation to 1q CNA is lacking [44]. Of interest Song et al provide preclinical evidence for therapeutic targeting of ubiquitin receptor Rpn10/PSMD4 in PI resistance[89].

CHD1L also shows potential therapeutic targeting, it is a known oncogene with anti-apoptotic effects demonstrated in myeloma cell lines and it has also been shown to facilitate cell adhesion mediated drug resistance [90].

Significant down regulation of *CCND1* in gain/amp(1q) tumours was consistent with CNA results presented in chapters 6 and 7. Where gain/amp(1q) was less common in tumours with high *CCND1* expression. Better understanding of this inverse relationship could reveal potential therapeutic targets.

Based on literature searches, other potential driver genes reported at 1q21 include *MCL1, IL6R, ADAR, PDZK1* and *ILF2* [44]. *MCL1, ADAR* and *IL2* expression did appear to correlate with 1q copy number however high expression was not associated with worse OS in my analysis. Of note their mean expression was relatively high, regardless of copy number, which could

explain the lack of association with OS. *IL6R* and *PDZK1* expression did not correlate with copy number or survival.

Elotuzumab is a monoclonal antibody that targets SLAMF7, a glycoprotein expressed on the surface of PC and natural killer (NK) cells, *SLAMF7* gene is located on 1q [91]. While the addition of elotuzumab to pomalidomide and dexamethasone has demonstrated clinical benefit in RR myeloma [92]. Clinical trials have not been able to demonstrate a better response in gain(1q) tumours versus those without the CNA [91]. In my analysis there was no significant differential expression of *SLAMF7* between tumours with or without gain/amp(1q) at presentation. Furthermore, expression decreased at relapse in tumours that acquired new gain/amp(1q) at relapse **(Figure 13-5)**. This could explain why tumours with gain(1q) have not been more vulnerable to elotuzumab in clinical trials, assuming that there is a direct correlation of gene and cell surface expression.

Daratumumab is a CD38 monoclonal antibody with efficacy in treating high risk myeloma, demonstrated by meta-analysis of several clinical trials [93]. However, evidence to specifically show daratumumab efficacy in gain/amp(1q) tumours is lacking [44, 91]. Furthermore, a single prospective observational study reported worse outcome in daratumumab treated patients with gain(1q). The authors suggested high expression of *CD55* (complement inhibitory protein) in gain(1q) tumours as a potential mechanism of daratumumab resistance [94]. In my analysis *CD55* was significantly upregulated in gain/amp(1q) tumours at presentation compared to those without the CNA.

Conversely, CD38 monoclonal antibody isatuximab, has demonstrated efficacy in treating gain(1q) tumours in RR myeloma; ICARIA-MM trial demonstrating efficacy when combined with pomalidomide and dexamethasone [95], IKEMA trial demonstrating efficacy when combined with carfilzomib and dexamethasone [91]. In my analysis, *CD38* expression did not correlate with 1q copy number at presentation. However there was a decrease in *CD38* expression in tumours that acquired new gain(1q) at relapse **(Figure 13-5)**. In chapter 5 I discussed JAK-STAT3 activation as a potential unifying pathway of dysregulated genes in gain(1q). JAK-STAT3 activation from bone

marrow stromal cells has been shown to down regulate CD38 on myeloma cells. The use of JAK inhibitor, ruxolitinib, was also shown to upregulate *CD38* expression in myeloma cell lines to enhance daratumumab mediated cytotoxicity. The efficacy of CD38 monoclonal antibody in overcoming the high risk biology of gain/amp(1q) needs further investigation and the potential enhancing effects of JAK inhibition make this an interesting focus for future work.

Conclusion

Sequential genetic profiling of myeloma tumours before and after first line treatment has demonstrated frequent and heterogeneous molecular evolution at relapse. The high proportion of non-stable evolution in response to therapy supporting my hypothesis that molecular changes are central to disease progression and treatment resistance.

Evolution of gain/amp(1q) was the dominant feature of relapse, highlighting its significance in disease progression. Furthermore, acquisition at relapse was also shown to retain prognostic significance. Deciphering the specific mechanisms through which gain/amp(1q) drives high risk biology remains difficult. Results from this project supports evidence that associates the CNA with chromosome instability. This finding either implicates gain/amp(1q) directly in the generation of CNA or highlights 1q as a driver region that provides a synergistic advantage for unstable tumours. Importantly using CNA and expression data this project has highlighted a number of potential driver genes/therapeutic targets relating to gain/amp(1q), providing focus for future translational research.

In support of my hypothesis, I have also demonstrated distinct evolutionary trajectories between molecular subgroups based on cytogenetics and cyclin D expression. This suggests differing mechanism of disease progression and highlights the potential for rationalised treatments. However, further work is needed to allow identification of targeted treatments relevant to the biology of subgroups.

Although molecular evolution was observed in the majority of tumours at relapse, I did not identify enrichment of any specific CNA in relation treatment. Applying uniform treatment pressures to a heterogeneous landscape could produce heterogeneous results, thus explaining the lack of enrichment observed. However CNA evolution in the context of cytogenetic subgroups per treatment arm also failed to identify enrichment. This project was therefore

unable to use sequential CNA assessment to identify specific mechanisms of treatment resistance. Future investigations may benefit form larger cohorts with longer follow up and the addition of higher resolution analysis such as sequencing data.

The use of time dependent variables ensured cox regression analysis also considered CNA acquired at relapse and showed t(14;16), gain(1q), del(1p) gain(8q) and del(17p) each to have an independent association with significantly shorter OS. To my knowledge, for the first time, I have demonstrated in a randomised controlled trial that acquisition of gain/amp(1q) at relapse is also independently associated with a shorter OS. This is of particular clinical relevance as it supports a change in current UK practice where repeat bone marrow sampling is uncommon. Identifying high risk lesions on repeat genetic profiling could influence subsequent treatment choice and improve outcomes in relapsed myeloma. I also demonstrated an association of branching evolution with worse OS, supporting the role for repeat molecular profiling at relapse and a potential mechanism of identifying high risk HRD tumours.

Consistent with changes observed in CNA at relapse, sequential GEP has also demonstrated evolution of tumour biology and provided insight into mechanisms of relapse. Relapsed tumours were positively enriched for genes involved in the cell cycle progression and for those regulated by *MYC* and mTORC1 activation, all of which facilitate tumour proliferation. The results highlighting focus for future translational research and the potential efficacy of current targeted therapies under early investigation. Leading edge analysis was of particular interest highlighting the role of XPO1 in relapsed disease and also the important role of PI. With phase 3 clinical evidence supporting the role of selinexor in the treatment of relapsed refractory myeloma, development of a better tolerated XPO1 inhibitor could facilitate it use earlier in relapse and improve outcomes.

Attempts to investigate significant differential expression at relapse within molecular and treatment subgroups was impeded by small sample size. I was therefore unable to identify specific mechanisms treatment resistance or

progression within subgroups. The results highlight the difficulty in analysing sequential samples, where change in expression between time points of one tumour is more subtle than differential expression between two different tumours. It highlights the need for even larger cohorts in future sequential studies and consideration of less statistically stringent analysis to enable identification of dysregulation.

This project focused on sequential tumour sampling, which caused a number of challenges. Particularly that small differences in sequential tumour quality had the potential to produce false positive results. Rigorous QC steps were therefore required. As a result my initial cohort size diminished and the large cohort size planned for adequate subgroup analysis was compromised. This was particularly challenging in the sequential GEP analysis. Differences in tumour quality were likely compounded by the IMWG definition of relapse, where tumour burden is often lower than that observed at presentation, increasing chance of contamination with non-malignant CD138 cells higher. In future analysis perhaps bone marrow sampling prior to next treatment would help resolve the matter.

The process of myeloma tumour sampling should also be considered. Myeloma tumour samples are obtained from bone marrow biopsies of the iliac crest bone. There may be spatial differences in clones throughout the bone marrow, it is therefore not known whether clonal evolution at relapse predominantly reflects genomic instability or a sub-clone previously residing outside iliac crest before treatment. Future studies could utilise circulating tumour DNA profiling to overcome limitations of spatial heterogeneity in myeloma, although their sensitivity and clinical relevance still requires validation in myeloma.

While appropriate to the time and cost limitations of this project, dMLPA only provided a targeted view of myeloma CNA. Sequential sequencing data would provide a more in depth review of molecular evolution. Consideration of changes to the tumour microenvironment could also provide insight into the mechanisms of relapse and treatment resistance.

Supplementary tables

Table 13-4 dMLPA D006-X2 probes; T: Target; K: Karyotype; R: Reference (pages 214-217)

hg19 location	gene (probe number)	type	hg19 location	gene (probe number)	type	hg19 location	gene (probe number)	type	hg19 location	gene (probe number)	type
1p36.33	TMEM240 (S013173)	K	5q31.3	PCDHAC1 (S011408)	T	11p15.5	DEAF1 (S013410)	K	16q23.2	MAF (S011443)	T
1p36.33	CFAP74 (S013039)	K	5q31.3	PCDHAC2 (S011474)	T	11p14.3	ANO5 (S011081)	K	16q24.3	ANKRD11 (S013330)	K
1p32.3	*FAF1* (S011387)	T	5q31.3	PCDHB2 (S011475)	T	11p14.3	ANO5 (S011497)	K	16q24.3	GAS8 (S013152)	K
1p32.3	*FAF1* (S011458)	T	5q31.3	PCDHB10 (S011409)	T	11q12.3	BEST1 (S011082)	K	17p13.3	VPS53 (S013064)	K/R
1p32.3	*CDKN2C* (S011456)	T	5q31.3	SLC25A2 (S011476)	T	11q13.3	CCND1 (S011498)	T	17p13.3	NXN (S013141)	K/R
1p32.3	*CDKN2C* (S013428)	T	5q31.3	PCDHGA11 (S011407)	T	11q13.3	CCND1 (S011423)	T	17p13.1	*TP53* (S010576)	T
1p32.3	*CDKN2C* (S011457)	T	5q32	SH3TC2 (S011477)	T	11q13.3	CCND1 (S011422)	T	17p13.1	*TP53* (S010577)	T
1p32.3	OSBPL9 (S011024)	K	5q35.3	COL23A1 (S013387)	K	11q22	MTMR2 (S011083)	K	17p13.1	*TP53* (S010578)	T
1p32.2	PPAP2B (S011023)	K	5q35.3	MAPK9 (S012993)	K	11q22.2	BIRC3 (S011499)	T	17p13.1	*TP53* (S010580)	T
1p32.2	DAB1 (S011454)	T	6p25.3	*IRF4* (S013429)	T	11q22.2	BIRC2 (S011424)	T	17p13.1	*TP53* (S010581)	T
1p32.2	DAB1 (S011453)	T	6p25.3	*IRF4* (S011412)	T	11q22.3	ATM (S010241)	T	17p13.1	*TP53* (S010582)	T
1p31.3	LEPR (S011451)	T	6p25.2	SERPINB6 (S013346)	K/R	11q22.3	ATM (S011500)	T	17p13.1	*TP53* (S010583)	T
1p31.3	RPE65 (S011452)	T	6p25.2	ECI2 (S013200)	K/R	11q22.3	ATM (S010284)	T	17p13.1	*TP53* (S010584)	T
1p21.3	DPYD (S011450)	T	6p22.3	JARID2 (S011479)	T	11q22.3	ATM (S010293)	T	17p13.1	*TP53* (S010585)	T
1p21.1	COL11A1 (S011449)	T	6p22.3	JARID2 (S011480)	T	11q25	NTM (S013142)	K	17p13.1	*TP53* (S010586)	T
1p12	FAM46C (S011448)	T	6p22.3	KIAA0319 (S011411)	T	11q25	JAM3 (S011426)	T	17p13.1	*TP53* (S010587)	T
1p12	FAM46C (S011386)	T	6p22.1	ZFP57 (S011051)	K/R	11q25	NCAPD3 (S011425)	T	17p13.1	*TP53* (S010588)	T
1p12	SPAG17 (S011022)	K	6p21.33	TNF (S011410)	K/R	11q25	NCAPD3 (S013089)	K	17p13.1	*TP53* (S010589)	T
1q21.1	PDZK1 (S011388)	T	6p12.3	PKHD1 (S011478)	K/R	12p13.33	WNK1 (S013063)	K	17p13.1	*TP53* (S010590)	T
1q21.2	*BCL9* (S011389)	T	6p11.2	PRIM2 (S011050)	K/R	12p13.33	CACNA2D4 (S013116)	K	17p13.1	PIK3R6 (S011104)	K/R

hg19 location	gene (probe number)	type	hg19 location	gene (probe number)	type	hg19 location	gene (probe number)	type	hg19 location	gene (probe number)	type
1q21.2	*ANP32E* (S011391)	T	6q12	EYS (S011481)	T	12p13.33	TSPAN9 (S011505)	K	17p13.1	USP43 (S011103)	K/R
1q21.2	*ANP32E* (S011390)	T	6q13	COL19A1 (S011052)	K	12p13.31	LTBR (S011432)	T	17p11.2	RAI1 (S011102)	K/R
1q21.3	RPRD2 (S011025)	K	6q13	RIMS1 (S011053)	K	12p13.31	LTBR (S011431)	T	17p11.2	MIR33B (S011522)	T
1q21.3	MCL1 (S011394)	T	6q22.33	LAMA2 (S011054)	K	12p13.31	CD27 (S011503)	T	17q11.2	PSMD11 (S011105)	K/R
1q21.3	MCL1 (S011396)	T	6q23.3	TNFAIP3 (S011482)	T	12p13.31	VAMP1 (S011428)	T	17q12	*IKZF3* (S011444)	T
1q21.3	NUP210L (S011026)	K	6q25.3	TFB1M (S011414)	T	12p13.31	NCAPD2 (S011429)	T	17q12	*IKZF3* (S011523)	T
1q21.3	ADAR (S011392)	T	6q25.3	WTAP (S011483)	T	12p13.31	NCAPD2 (S011427)	T	17q21.31	MAP3K14 (S011446)	T
1q21.3	ADAR (S011393)	T	6q25.3	IGF2R (S011413)	T	12p13.31	CHD4 (S011430)	T	17q21.31	MAP3K14 (S011445)	T
1q21.3	*CKS1B* (S011459)	T	6q26	PARK2 (S011484)	T	12p13.31	CHD4 (S011504)	T	17q23.2	MED13 (S011106)	K/R
1q21.3	*CKS1B* (S011460)	T	6q26	PARK2 (S011415)	T	12p13.2	ETV6 (S011502)	T	17q25.3	CCDC57 (S013115)	K/R
1q21.3	*CKS1B* (S011395)	T	6q27	SMOC2 (S013056)	K	12p13.1	CDKN1B (S011501)	T	17q25.3	CSNK1D (S013157)	K/R
1q23.3	SLAMF7 (S011399)	T	6q27	ERMARD (S013199)	K	12p12.3	AEBP2 (S011086)	K	18p11.31	LPIN2 (S011109)	K/R
1q23.3	SLAMF7 (S011398)	T	7p22.1	RADIL (S013184)	K	12p11.22	FAR2 (S011084)	K/R	18p11.31	TGIF1 (S011525)	K/R
1q23.3	NUF2 (S011397)	T	7p15.3	RAPGEF5 (S011057)	K	12p11.22	TMTC1 (S011085)	K/R	18p11.21	GNAL (S011108)	K/R
1q23.3	RP11 (S011463)	T	7p15.3	STK31 (S011058)	K	12q12	KIF21A (S010040)	K/R	18p11.21	SPIRE1 (S011107)	K/R
1q23.3	RP11 (S011466)	T	7p12.3	ADCY1 (S011055)	K	12q12	NELL2 (S014297)	K/R	18p11.21	RNMT (S011524)	K/R
1q23.3	RP11 (S011465)	T	7p12.3	ABCA13 (S011056)	K	12q23.1	NEDD1 (S011088)	K/R	18q11.2	NPC1 (S011526)	K/R
1q23.3	RP11 (S011464)	T	7p12.2	*IKZF1* (S013432)	T	12q23.1	SLC17A8 (S011087)	K/R	18q11.2	NPC1 (S011110)	K/R
1q23.3	RP11 (S011462)	T	7p12.2	*IKZF1* (S011485)	T	12q24.22	NOS1 (S011507)	K/R	18q21.1	LOXHD1 (S011111)	K/R
1q23.3	PBX1 (S011461)	T	7p12.2	*IKZF1* (S011486)	T	12q24.33	GALNT9 (S013154)	K/R	18q21.1	LIPG (S011112)	K/R
1q31.3	KCNT2 (S011027)	K	7p11.2	LANCL2 (S014303)	K	12q24.33	PGAM5 (S013304)	K/R	18q23	CTDP1 (S013109)	K/R
1q44	ADSS (S013049)	K	7q11.22	WBSCR17 (S011059)	K	13q12.3	KATNAL1 (S011089)	K	18q23	TXNL4A (S013126)	K/R
1q44	DESI2 (S013025)	K	7q31.1	PNPLA8 (S011060)	K	13q14.11	ENOX1 (S011537)	T	19p13.3	PPAP2C (S013083)	K
2p25.3	TMEM18 (S012958)	K/R	7q31.1	IFRD1 (S011061)	K	13q14.2	*RB1* (S011434)	T	19p13.3	CDC34 (S013220)	K
2p25.3	COLEC11 (S013217)	K/R	7q34	BRAF (S011487)	T	13q14.2	*RB1* (S011509)	T	19p13.2	GCDH (S011115)	K
2p22.3	SPAST (S011029)	K/R	7q36.3	RBM33 (S013182)	K	13q14.2	RCBTB2 (S011510)	T	19p13.2	STX10 (S011114)	K

hg19 location	gene (probe number)	type	hg19 location	gene (probe number)	type	hg19 location	gene (probe number)	type	hg19 location	gene (probe number)	type
2p16.1	PEX13 (S011400)	K/R	7q36.3	WDR60 (S012950)	K	13q14.2	DLEU2 (S011508)	T	19p13.11	GMIP (S011113)	K
2p11.2	REEP1 (S011028)	K/R	8p23.3	FBXO25 (S013012)	K	13q14.2	KCNRG (S011538)	T	19q13.11	SLC7A9 (S011116)	K
2q11.1	PROM2 (S011030)	K/R	8p23.3	CLN8 (S013029)	K	13q14.2	*MIR15A* (S011539)	T	19q13.42	DNAAF3 (S013156)	K
2q24.3	SCN1A (S011031)	K/R	8p23.1	GATA4 (S011489)	T	13q14.2	DLEU1 (S011435)	T	19q13.43	SLC27A5 (S013344)	K
2q32.2	COL3A1 (S011467)	K/R	8p21.3	GFRA2 (S011065)	K	13q14.2	DLEU1 (S011541)	T	20p13	RSPO4 (S013131)	K/R
2q37.3	CAPN10 (S013042)	K/R	8p21.3	TNFRSF10B (S011418)	T	13q14.3	DLEU7 (S011543)	T	20p13	TGM6 (S013070)	K/R
2q37.3	KIF1A (S012999)	K/R	8p21.3	TNFRSF10A (S011417)	T	13q14.3	RNASEH2B (S011511)	T	20p12.3	TRMT6 (S011121)	K/R
3p26.2	TRNT1 (S012953)	K	8p21.2	NEFL (S011416)	T	13q14.3	ATP7B (S011540)	T	20p12.2	PLCB4 (S011120)	K/R
3p26.2	*CRBN* (S011401)	T	8p21.2	CDCA2 (S011064)	K	13q14.3	VPS36 (S014299)	T	20p11.23	RIN2 (S011119)	K/R
3p26.1	SUMF1 (S013175)	K	8p12	RBPMS (S011063)	K	13q14.3	PCDH8 (S011542)	T	20q11.22	ACSS2 (S011123)	K/R
3p24.2	NR1D2 (S011035)	K	8p12	GSR (S011062)	K	13q21.33	KLHL1 (S012572)	K	20q11.22	EDEM2 (S011122)	K/R
3p24.1	NEK10 (S011034)	K	8p11.23	ZNF703 (S011488)	T	13q22.1	*DIS3* (S011436)	T	20q11.23	SAMHD1 (S011527)	K/R
3p12.3	CNTN3 (S011033)	K	8q12.2	CHD7 (S011490)	K/R	13q22.1	*DIS3* (S011437)	T	20q12	MAFB (S011447)	T
3p11.1	HTR1F (S011032)	K	8q12.2	CHD7 (S011066)	K/R	13q34	ARHGEF7 (S013121)	K	20q13.12	SLC13A3 (S011124)	K/R
3q12.1	CPOX (S011036)	K	8q21.3	RMDN1 (S011068)	K/R	13q34	GRK1 (S013151)	K	20q13.13	STAU1 (S011125)	K/R
3q23	CLSTN2 (S011037)	K	8q21.3	CPNE3 (S011067)	K/R	14q11.2	CHD8 (S011090)	K/R	20q13.33	OSBPL2 (S013088)	K/R
3q23	ATR (S011469)	T	8q22.3	RRM2B (S011491)	T	14q22.1	DDHD1 (S011091)	K/R	20q13.33	UCKL1 (S013125)	K/R
3q23	ATR (S013431)	T	8q24.21	*MYC* (S011492)	T	14q22.2	SAMD4A (S011092)	K/R	21q11.2	RBM11 (S013183)	K
3q23	ATR (S011468)	T	8q24.21	*MYC* (S011493)	T	14q24.3	NPC2 (S011512)	K/R	21q11.2	HSPA13 (S011126)	K
3q24	SLC9A9 (S011038)	K	8q24.21	*MYC* (S010805)	T	14q32.31	DYNC1H1 (S013378)	K/R	21q22.11	ITSN1 (S011127)	K
3q29	ACAP2 (S013332)	K	8q24.3	SLC39A4 (S012965)	K/R	14q32.32	TRAF3 (S011513)	T	21q22.2	PSMG1 (S011528)	K
3q29	KIAA0226 (S013000)	K	9p24.3	DOCK8 (S013022)	K	14q32.32	TRAF3 (S013430)	T	21q22.3	PDE9A (S013140)	K
4p16.3	FGFR3 (S011404)	T	9p24.1	JAK2 (S011494)	T	14q32.33	APOPT1 (S013391)	K/R	21q22.3	PWP2 (S011128)	K
4p16.3	FGFR3 (S011405)	T	9p24.1	GLDC (S013009)	K	14q32.33	CEP170B (S011440)	T	21q22.3	TSPEAR (S013172)	K
4p16.3	FGFR3 (S011403)	T	9p22.3	FREM1 (S011072)	K	14q32.33	MTA1 (S011439)	T	22q11.1	GAB4 (S014304)	T
4p16.3	LETM1 (S013364)	K/R	9p22.2	BNC2 (S011071)	K	14q32.33	MTA1 (S011514)	T	22q11.21	CECR2 (S014302)	T

hg19 location	gene (probe number)	type	hg19 location	gene (probe number)	type	hg19 location	gene (probe number)	type	hg19 location	gene (probe number)	type
4p16.3	WHSC1 (S011402)	T	9p13.2	FBXO10 (S011069)	K	14q32.33	IGHD (S011441)	T	22q11.21	HIRA (S011529)	T
4p16.3	WHSC1 (S011406)	T	9p13.2	DCAF10 (S011070)	K	15q12	GABRB3 (S011515)	K	22q11.23	SMARCB1 (S011530)	T
4p16.3	ADD1 (S013059)	K/R	9q21.12	TRPM3 (S011073)	K	15q12	GABRB3 (S011093)	K	22q11.23	SMARCB1 (S011531)	T
4p15.32	LDB2 (S000062)	K/R	9q31.1	ALDOB (S011074)	K	15q22.2	VPS13C (S011094)	K	22q12.2	NF2 (S011532)	T
4p15.31	KCNIP4 (S011039)	K/R	9q34.3	COL5A1 (S011495)	T	15q22.31	USP3 (S011095)	K	22q12.2	ZMAT5 (S014300)	K
4p13	ATP8A1 (S011470)	K/R	9q34.3	TRAF2 (S011419)	T	15q26.3	IGF1R (S011516)	T	22q12.2	SFI1 (S014298)	K
4q13.1	TECRL (S011040)	K/R	9q34.3	TRAF2 (S011420)	T	15q26.3	CHSY1 (S013163)	K	22q12.3	LARGE (S011533)	T
4q13.2	UGT2A1 (S011041)	K/R	9q34.3	GRIN1 (S013195)	K	15q26.3	TM2D3 (S013299)	K	22q13.2	EP300 (S011534)	T
4q25	CFI (S011471)	K/R	9q34.3	EHMT1 (S013020)	K	16p13.3	DECR2 (S013415)	K/R	22q13.31	TRMU (S013069)	K
4q31.22	ZNF827 (S011042)	K/R	10p15.3	DIP2C (S013412)	K/R	16p13.3	IFT140 (S013104)	K/R	22q13.33	BRD1 (S013118)	K
4q35.2	CYP4V2 (S013202)	K/R	10p15.2	PFKP (S013187)	K/R	16p13.13	TXNDC11 (S011098)	K/R			
4q35.2	TRIML1 (S012955)	K/R	10p14	UPF2 (S011496)	K/R	16p13.12	CPPED1 (S011097)	K/R			
5p15.33	IRX4 (S013194)	K	10p13	NMT2 (S011076)	K/R	16p11.2	HIRIP3 (S011096)	K/R			
5p15.31	NSUN2 (S013190)	K	10p13	ITGA8 (S011077)	K/R	16q11.2	GPT2 (S010065)	K			
5p15.2	DNAH5 (S011046)	K	10p11.1	ZNF25 (S011075)	K/R	16q12.1	LONP2 (S011099)	K			
5p13.3	NPR3 (S011045)	K	10q11.21	MARCH8 (S011078)	K/R	16q12.1	CYLD (S011442)	T			
5p13.2	TTC23L (S011044)	K	10q11.22	ARHGAP22 (S011079)	K/R	16q12.1	CYLD (S011517)	T			
5q11.2	IL31RA (S011048)	K	10q22.2	KAT6B (S011080)	K/R	16q13	SLC12A3 (S011518)	T			
5q11.2	MIER3 (S011047)	K	10q25.1	ADD3 (S011421)	K/R	16q22.1	SLC12A4 (S011100)	K			
5q31.2	MYOT (S011049)	T	10q26.3	INPP5A (S013003)	K/R	16q22.1	DUS2 (S011101)	K			
5q31.2	CTNNA1 (S011472)	T	10q26.3	KNDC1 (S012996)	K/R	16q23.1	WWOX (S011520)	T			
5q31.3	PCDHA1 (S011473)	T	11p15.5	RIC8A (S013302)	K	16q23.1	WWOX (S011521)	T			

Table 13-5 Taqman translocation assay primers.

MMSET:	**CCND3:**
for: gagaaggacagtttgaaaaattatgc	for: ccatcgaaaaactgtgcatctaca
rev: cccacatagagaaaggtgaacttg	rev: cctcccagtcccgcaact
probe: VIC-cagggaaattgagggcccagtgg-MGB	probe: VIC-cgaccacgctgtctctccccg-MGB
MAF:	**ITGB7:**
for: gcttccgagaaaacggctc	for: ctcagccttaccctccctct
rev: tgcgagtgggctcagttatg	rev: gactccagcaacgtggtaca
probe: FAM-cgacaacccgtcctctcccgagttt-MGB	probe VIC-caagggtcacggtggaagacaggct-MGB
FGFR3:	**CX3CR1:**
for: acggcacaccctacgttacc	for: ataggtacctggccatcgtc
rev: ctcaaaggtgacgttgtgcaa	rev: ggtagtcaccaaggcattca
probe: VIC-caccaccgacaaggagctagaggttctct-MGB	probe FAM-accgtgcagcatggcgtcac-MGB
MAFB:	**AURKA:**
for: gcccgaccgaacagaagac	for: gcctggccactatttacagg
rev: ctcgggcgtcaggttgag	rev: gcatcatggaccgatctaaag
probe: FAM-agcagatgaacccc-MGB	probe: FAM- cgttttggacctccaactggagc-MGB
CCND1:	**GAPDH:**
for: ccgtccatgcggaagatc	for: gaaggtgaaggtcggagtc
rev: gaagacctcctcctcgcact	rev: gaagatggtgatgggatttc
probe: VIC-tctgttcctcgcagacctccagca-MGB	probe: NED-caagcttcccgttctcagcc-MGB
CCND2:	
for: caccaacacagacgtggattgt	
rev: cggtactgctgcaggctattg	
probe: FAM-caaagcttgccaggagcagattgagg-MGB	

Table 13-6 All patients DGE at relapse: Probesets with significant log fold increase (Pages 219-224)

Probeset	Symbol	Log FC	Ex	FDR	Band	Probeset	Symbol	Log FC	Ex	FDR	Band
217724_at	SERBP1	0.52	12.26	0.010	1p31.3	224436_s_at	NIPSNAP3A	0.51	9.76	0.031	9q31.1
217725_x_at	SERBP1	0.39	11.66	0.029	1p31.3	223559_s_at	INIP	0.36	10.65	0.044	9q32
227369_at	SERBP1	0.31	9.66	0.047	1p31.3	227211_at	PHF19	0.97	8.82	0.002	9q33.2
204159_at	CDKN2C	1.06	8.99	0.018	1p32.3	225533_at	PHF19	0.87	7.09	0.012	9q33.2
208680_at	PRDX1	0.43	12.98	0.019	1p34.1	227212_s_at	PHF19	0.76	9.25	0.005	9q33.2
201970_s_at	NASP	0.36	9.82	0.036	1p34.1	203447_at	PSMD5	0.35	9.34	0.048	9q33.2
202613_at	CTPS1	0.78	8.04	0.033	1p34.2	220865_s_at	PDSS1	0.62	8.30	0.021	10p12.1
210502_s_at	PPIE	0.47	9.82	0.031	1p34.2	222962_s_at	MCM10	1.22	5.06	0.027	10p13
210371_s_at	RBBP4	0.51	12.23	0.008	1p35.1	218006_s_at	ZNF22	0.29	10.35	0.049	10q11.21
200783_s_at	STMN1	0.54	9.45	0.028	1p36.11	204026_s_at	ZWINT	0.65	9.72	0.008	10q21.1
228361_at	E2F2	0.72	8.87	0.004	1p36.12	203213_at	CDK1	1.22	8.24	0.009	10q21.2
208766_s_at	HNRNPR	0.28	13.22	0.026	1p36.12	224461_s_at	AIFM2	0.97	7.07	0.027	10q22.1
224578_at	RCC2	0.39	9.74	0.031	1p36.13	201807_at	VPS26A	0.32	11.35	0.040	10q22.1
37012_at	CAPZB	0.34	11.36	0.046	1p36.13	226896_at	CHCHD1	0.44	11.20	0.029	10q22.2
201231_s_at	ENO1	0.39	12.37	0.026	1p36.23	201847_at	LIPA	0.61	12.52	0.016	10q23.31
208002_s_at	ACOT7	0.52	8.21	0.035	1p36.31	234040_at	HELLS	1.22	4.87	0.046	10q23.33
214113_s_at	RBM8A	0.41	9.90	0.043	1q21.1	204444_at	KIF11	1.10	7.07	0.026	10q23.33
212539_at	CHD1L	0.33	9.92	0.049	1q21.1	227350_at	HELLS	0.99	7.44	0.038	10q23.33
209268_at	VPS45	0.61	8.71	0.043	1q21.2	1566363_at	DNTT	0.87	7.31	0.033	10q24.1
201897_s_at	CKS1B	0.56	10.96	0.015	1q21.3	202441_at	ERLIN1	0.60	9.29	0.014	10q24.31
226455_at	CREB3L4	0.52	8.76	0.012	1q21.3	209045_at	XPNPEP1	0.39	10.54	0.004	10q25.1
211609_x_at	PSMD4	0.32	12.09	0.038	1q21.3	201619_at	PRDX3	0.61	11.62	0.020	10q26.11
210460_s_at	PSMD4	0.30	11.85	0.049	1q21.3	220275_at	CUZD1	0.74	6.41	0.047	10q26.13
200910_at	CCT3	0.42	12.58	0.011	1q22	209974_s_at	BUB3	0.44	12.25	0.029	10q26.13
201707_at	PEX19	0.48	9.48	0.018	1q23.2	201456_s_at	BUB3	0.38	10.86	0.032	10q26.13
210243_s_at	B4GALT3	0.32	12.25	0.037	1q23.3	222403_at	MTCH2	0.43	9.52	0.049	11p11.2

Probeset	Symbol	Log FC	Ex	FDR	Band	Probeset	Symbol	Log FC	Ex	FDR	Band
209568_s_at	RGL1	0.82	8.48	0.036	1q25.3	225340_s_at	CAPRIN1	0.42	12.20	0.013	11p13
223405_at	NPL	0.82	9.04	0.015	1q25.3	205413_at	MPPED2	1.06	5.59	0.044	11p14.1
219960_s_at	UCHL5	0.44	10.60	0.037	1q31.2	217980_s_at	MRPL16	0.31	10.64	0.044	11q12.1
224581_s_at	NUCKS1	0.39	10.82	0.031	1q32.1	201487_at	CTSC	0.55	11.39	0.023	11q14.2
222250_s_at	INTS7	0.66	8.47	0.028	1q32.3	225647_s_at	CTSC	0.55	10.88	0.019	11q14.2
209484_s_at	NSL1	0.50	10.38	0.049	1q32.3	222209_s_at	TMEM135	0.40	9.76	0.031	11q14.2
219481_at	TTC13	0.33	10.22	0.034	1q42.2	218357_s_at	TIMM8B	0.50	12.54	0.028	11q23.1
219032_x_at	OPN3	0.44	10.01	0.032	1q43	212568_s_at	DLAT	0.45	10.00	0.035	11q23.1
214768_x_at	IGKC	1.03	11.51	0.022	2p11.2	226154_at	DNM1L	0.28	11.38	0.031	12p11.21
226751_at	CNRIP1	1.01	6.74	0.029	2p14	227711_at	GTSF1	0.97	9.05	0.010	12q13.13
208775_at	XPO1	0.49	11.65	0.022	2p15	201946_s_at	CCT2	0.43	11.64	0.033	12q15
209421_at	MSH2	1.00	7.55	0.041	2p21	212585_at	OSBPL8	0.39	10.29	0.022	12q21.2
215000_s_at	FEZ2	0.63	9.44	0.002	2p22.2	208892_s_at	DUSP6	0.73	10.11	0.046	12q21.33
201007_at	HADHB	0.31	11.51	0.049	2p23.3	222466_s_at	MRPL42	0.44	10.28	0.034	12q22
222192_s_at	LDAH	0.60	8.37	0.046	2p24.1	217919_s_at	MRPL42	0.39	11.24	0.044	12q22
201890_at	RRM2	1.15	10.76	0.001	2p25.1	227928_at	PARPBP	1.10	6.47	0.044	12q23.2
209773_s_at	RRM2	0.93	10.49	0.002	2p25.1	220060_s_at	PARPBP	0.69	7.66	0.015	12q23.2
225082_at	CPSF3	0.35	10.23	0.030	2p25.1	223114_at	COQ5	0.39	9.45	0.048	12q24.31
224877_s_at	MRPS5	0.50	8.89	0.029	2q11.1	204127_at	RFC3	0.61	8.50	0.022	13q13.2
212949_at	NCAPH	0.92	6.35	0.033	2q11.2	215096_s_at	ESD	0.32	11.62	0.049	13q14.2
201930_at	MCM6	0.60	10.48	0.002	2q21.3	203386_at	TBC1D4	0.95	6.51	0.046	13q22.2
217388_s_at	KYNU	1.28	6.42	0.020	2q22.2	225585_at	RAP2A	0.42	9.44	0.041	13q32.1
209891_at	SPC25	0.91	7.14	0.030	2q24.3	226747_at	TXNDC16	0.49	9.47	0.030	14q22.1
201138_s_at	SSB	0.33	10.62	0.032	2q31.1	1555758_a_at	CDKN3	0.73	9.90	0.002	14q22.2
225114_at	AGPS	0.49	9.17	0.010	2q31.2	209714_s_at	CDKN3	0.62	9.74	0.003	14q22.2
1553956_at	TMEM237	0.60	8.16	0.008	2q33.1	203764_at	DLGAP5	1.05	7.82	0.026	14q22.3
205133_s_at	HSPE1	0.36	11.77	0.029	2q33.1	202309_at	MTHFD1	0.43	10.53	0.019	14q23.3

Probeset	Symbol	Log FC	Ex	FDR	Band	Probeset	Symbol	Log FC	Ex	FDR	Band
236356_at	NDUFS1	0.95	8.02	0.025	2q33.3	202411_at	IFI27	1.25	9.91	0.020	14q32.12
235931_at	METTL21A	0.82	7.17	0.046	2q33.3	216491_x_at	IGHM	1.38	10.16	0.015	14q32.33
235177_at	METTL21A	0.45	8.74	0.023	2q33.3	219978_s_at	NUSAP1	0.75	9.45	0.006	15q15.1
203039_s_at	NDUFS1	0.30	9.99	0.045	2q33.3	218039_at	NUSAP1	0.70	10.09	0.004	15q15.1
202020_s_at	LANCL1	0.42	10.33	0.012	2q34	201563_at	SORD	0.59	9.03	0.029	15q21.1
208642_s_at	XRCC5	0.32	12.33	0.016	2q35	216733_s_at	GATM	0.54	10.50	0.048	15q21.1
229779_at	COL4A4	0.57	8.60	0.048	2q36.3	223077_at	TMOD3	0.48	9.48	0.020	15q21.2
218726_at	HJURP	1.03	6.37	0.022	2q37.1	202705_at	CCNB2	0.75	9.29	0.018	15q22.2
201198_s_at	PSMD1	0.38	10.45	0.022	2q37.1	202503_s_at	PCLAF	0.80	11.74	0.004	15q22.31
226355_at	POC1A	0.65	7.24	0.044	3p21.2	222606_at	ZWILCH	0.49	9.59	0.011	15q22.31
217745_s_at	NAA50	0.38	12.19	0.035	3q13.31	201931_at	ETFA	0.36	12.46	0.029	15q24.2
202107_s_at	MCM2	0.77	8.74	0.029	3q21.3	201486_at	RCN2	0.38	12.72	0.049	15q24.3
212694_s_at	PCCB	0.37	10.95	0.031	3q22.3	203396_at	PSMA4	0.42	12.38	0.049	15q25.1
1555501_s_at	RSRC1	0.54	8.86	0.019	3q25.32	225210_s_at	RAMAC	0.49	10.54	0.029	15q25.2
225158_at	GFM1	0.52	9.57	0.050	3q25.32	206420_at	IGSF6	0.93	7.90	0.047	16p12.2
219787_s_at	ECT2	0.74	8.02	0.039	3q26.31	212600_s_at	UQCRC2	0.28	12.58	0.049	16p12.2
225366_at	PGM2	0.68	7.80	0.030	4p14	219493_at	SHCBP1	0.79	8.50	0.021	16q11.2
201385_at	DHX15	0.39	12.10	0.048	4p15.2	221521_s_at	GINS2	0.87	8.10	0.015	16q24.1
218663_at	NCAPG	1.00	7.58	0.011	4p15.31	228868_x_at	CDT1	0.52	8.36	0.046	16q24.3
218308_at	TACC3	0.97	6.55	0.030	4p16.3	202053_s_at	ALDH3A2	0.36	10.50	0.019	17p11.2
201014_s_at	PAICS	0.44	11.05	0.044	4q12	212281_s_at	TMEM97	0.50	10.12	0.027	17q11.2
203302_at	DCK	0.58	9.15	0.046	4q13.3	212282_at	TMEM97	0.48	10.11	0.046	17q11.2
201307_at	SEPTIN11	0.59	9.51	0.004	4q21.1	212279_at	TMEM97	0.45	9.77	0.050	17q11.2
208848_at	ADH5	0.72	8.70	0.016	4q23	208777_s_at	PSMD11	0.32	11.28	0.038	17q11.2
201036_s_at	HADH	0.56	10.57	0.004	4q25	32128_at	CCL18	0.97	9.05	0.024	17q12
201035_s_at	HADH	0.54	9.76	0.031	4q25	201291_s_at	TOP2A	1.25	8.39	0.013	17q21.2
211569_s_at	HADH	0.50	9.69	0.010	4q25	220565_at	CCR10	0.89	10.47	0.004	17q21.2

Probeset	Symbol	Log FC	Ex	FDR	Band	Probeset	Symbol	Log FC	Ex	FDR	Band
1554768_a_at	MAD2L1	0.71	9.49	0.017	4q27	203968_s_at	CDC6	0.59	8.51	0.012	17q21.2
203362_s_at	MAD2L1	0.67	10.66	0.005	4q27	224608_s_at	VPS25	0.47	10.06	0.017	17q21.2
204168_at	MGST2	0.75	9.06	0.029	4q31.1	222039_at	KIF18B	0.56	8.22	0.044	17q21.31
201872_s_at	ABCE1	0.41	10.95	0.033	4q31.21	222398_s_at	EFTUD2	0.51	10.42	0.018	17q21.31
201873_s_at	ABCE1	0.35	11.00	0.037	4q31.21	201157_s_at	NMT1	0.32	10.78	0.047	17q21.31
33494_at	ETFDH	0.40	8.47	0.022	4q32.1	208974_x_at	KPNB1	0.35	11.67	0.050	17q21.32
218883_s_at	CENPU	0.54	10.62	0.017	4q35.1	224330_s_at	MRPL27	0.54	10.11	0.034	17q21.33
202783_at	NNT	0.43	10.27	0.027	5p12	228273_at	PRR11	0.75	9.19	0.018	17q22
210757_x_at	DAB2	1.07	7.76	0.030	5p13.1	213009_s_at	TRIM37	0.38	9.61	0.041	17q22
202780_at	OXCT1	0.47	9.97	0.017	5p13.1	200614_at	CLTC	0.35	12.35	0.041	17q23.1
210567_s_at	SKP2	0.63	8.23	0.012	5p13.2	218014_at	NUP85	0.66	8.43	0.029	17q25.1
208696_at	CCT5	0.61	11.44	0.012	5p15.2	202095_s_at	BIRC5	1.19	8.71	0.004	17q25.3
203200_s_at	MTRR	0.34	11.16	0.020	5p15.31	202338_at	TK1	0.94	8.12	0.008	17q25.3
204033_at	TRIP13	0.62	8.28	0.027	5p15.33	1554408_a_at	TK1	0.71	8.55	0.046	17q25.3
214710_s_at	CCNB1	0.68	8.67	0.030	5q13.2	203931_s_at	MRPL12	0.31	11.20	0.047	17q25.3
203474_at	IQGAP2	0.72	9.85	0.030	5q13.3	202589_at	TYMS	0.93	11.07	0.002	18p11.32
202534_x_at	DHFR	0.50	10.80	0.021	5q14.1	1554696_s_at	TYMS	0.75	9.65	0.006	18p11.32
48808_at	DHFR	0.49	10.23	0.045	5q14.1	203344_s_at	RBBP8	0.39	10.80	0.008	18q11.2
203253_s_at	PPIP5K2	0.40	10.54	0.046	5q21.1	217640_x_at	SKA1	0.93	6.62	0.044	18q21.1
201506_at	TGFBI	1.05	8.18	0.040	5q31.1	232101_s_at	PIGN	0.77	7.75	0.026	18q21.33
203024_s_at	C5orf15	0.40	11.65	0.031	5q31.1	223180_s_at	TIMM21	0.58	10.31	0.028	18q22.3
207168_s_at	MACROH2A1	0.36	12.42	0.018	5q31.1	218105_s_at	MRPL4	0.31	10.46	0.038	19p13.2
201514_s_at	G3BP1	0.73	9.21	0.047	5q33.1	201252_at	PSMC4	0.33	10.80	0.044	19q13.2
1552280_at	TIMD4	0.88	9.52	0.040	5q33.3	206102_at	GINS1	1.16	7.10	0.012	20p11.21
203554_x_at	PTTG1	0.57	11.55	0.009	5q33.3	213222_at	PLCB1	1.10	7.37	0.008	20p12.3
209406_at	BAG2	0.91	8.20	0.009	6p12.1	201202_at	PCNA	0.87	10.94	0.004	20p12.3
202923_s_at	GCLC	0.35	9.93	0.043	6p12.1	200709_at	FKBP1A	0.45	9.91	0.029	20p13

Probeset	Symbol	Log FC	Ex	FDR	Band	Probeset	Symbol	Log FC	Ex	FDR	Band
201555_at	MCM3	0.64	9.35	0.017	6p12.2	210052_s_at	TPX2	0.84	8.04	0.034	20q11.21
206214_at	PLA2G7	0.99	7.45	0.047	6p12.3	210766_s_at	CSE1L	0.51	9.98	0.006	20q13.13
218106_s_at	MRPS10	0.28	10.50	0.043	6p21.1	201111_at	CSE1L	0.51	8.76	0.046	20q13.13
211656_x_at	HLA-DQB1	0.82	8.50	0.029	6p21.32	216560_x_at	IGLC1	1.56	10.04	0.006	22q11.22
223461_at	TBC1D7	0.35	9.53	0.046	6p24.1	217227_x_at	IGLV1-44	1.46	9.80	0.005	22q11.22
204822_at	TTK	1.44	7.20	0.002	6q14.1	217258_x_at	IGLV1-44	1.35	9.19	0.028	22q11.22
209377_s_at	HMGN3	0.38	13.48	0.019	6q14.1	216853_x_at	IGLJ3	1.29	9.47	0.004	22q11.22
204058_at	ME1	1.18	7.40	0.032	6q14.2	215214_at	IGLC1	1.18	10.06	0.008	22q11.22
204059_s_at	ME1	0.82	8.39	0.028	6q14.2	224342_x_at	BMS1P20	1.13	10.20	0.046	22q11.22
206854_s_at	MAP3K7	0.46	9.28	0.036	6q15	211881_x_at	IGLJ3	1.04	10.23	0.024	22q11.22
201833_at	HDAC2	0.40	11.47	0.014	6q21	211798_x_at	IGLJ3	0.94	10.91	0.030	22q11.22
226936_at	CENPW	0.71	9.56	0.006	6q22.32	202567_at	SNRPD3	0.48	12.03	0.006	22q11.23
201327_s_at	CCT6A	0.35	11.31	0.018	7p11.2	218190_s_at	UQCR10	0.33	13.48	0.025	22q12.2
212792_at	DPY19L1	0.52	9.36	0.050	7p14.2	203665_at	HMOX1	1.06	10.11	0.009	22q12.3
215380_s_at	GGCT	0.34	11.26	0.040	7p14.3	206632_s_at	APOBEC3B	0.77	10.26	0.002	22q13.1
201141_at	GPNMB	0.71	10.23	0.022	7p15.3	210250_x_at	ADSL	0.43	10.49	0.008	22q13.1
217809_at	BZW2	0.36	12.08	0.045	7p21.1	202144_s_at	ADSL	0.40	11.22	0.009	22q13.1
204766_s_at	NUDT1	0.83	7.65	0.014	7p22.3	218117_at	RBX1	0.46	12.08	0.026	22q13.2
209780_at	PHTF2	0.44	10.12	0.046	7q11.23	201589_at	SMC1A	0.64	9.84	0.014	Xp11.22
209095_at	DLD	0.39	11.28	0.045	7q31.1	203881_s_at	DMD	1.30	6.76	0.002	Xp21.2
204353_s_at	POT1	0.58	8.79	0.031	7q31.33	202043_s_at	SMS	0.40	9.60	0.013	Xp22.11
219148_at	PBK	0.75	8.15	0.028	8p21.1	231131_at	FAM133A	1.24	8.78	0.011	Xq21.32
214770_at	MSR1	1.39	6.79	0.004	8p22	239481_at	FAM133A	0.71	10.82	0.028	Xq21.32
218096_at	AGPAT5	0.70	9.47	0.006	8p23.1	219485_s_at	PSMD10	0.42	11.53	0.046	Xq22.3
200839_s_at	CTSB	0.42	12.43	0.046	8p23.1	209629_s_at	NXT2	0.57	8.93	0.027	Xq23
202345_s_at	FABP5	0.80	10.84	0.002	8q21.13	209628_at	NXT2	0.38	10.61	0.029	Xq23
202119_s_at	CPNE3	0.43	11.56	0.048	8q21.3	218499_at	STK26	0.42	10.50	0.020	Xq26.2

Probeset	Symbol	Log FC	Ex	FDR	Band	Probeset	Symbol	Log FC	Ex	FDR	Band
204825_at	MELK	0.90	8.35	0.010	9p13.2	202854_at	HPRT1	0.46	11.43	0.009	Xq26.2
219174_at	IFT74	0.52	8.51	0.043	9p21.2	205110_s_at	FGF13	0.78	8.03	0.040	Xq26.3
204240_s_at	SMC2	0.94	7.90	0.019	9q31.1	214612_x_at	MAGEA6	1.24	8.55	0.017	Xq28
224436_s_at	NIPSNAP3A	0.51	9.76	0.031	9q31.1	207325_x_at	MAGEA1	1.15	6.32	0.049	Xq28
223559_s_at	INIP	0.36	10.65	0.044	9q32	210467_x_at	MAGEA12	1.04	7.76	0.015	Xq28

Table 13-7 All patients DGE at relapse: Probesets with significant log fold increase (Pages 225-230)

Probeset	Symbol	Log FC	Ex	FDR	Band	Probeset	Symbol	Log FC	Ex	FDR	Band
221446_at	ADAM30	-0.90947	5.975593	0.033182	1p12	212614_at	ARID5B	-0.78301	11.45413	0.031054	10q21.2
230409_at	MAGI3	-0.62402	7.873248	0.044952	1p13.2	204716_at	CCDC6	-0.64498	9.984059	0.013381	10q21.2
213694_at	RSBN1	-0.58826	7.885142	0.046635	1p13.2	241996_at	RUFY2	-0.47911	7.967206	0.042311	10q21.3
205288_at	CDC14A	-0.99011	6.419036	0.031879	1p21.2	218878_s_at	SIRT1	-0.4346	9.52337	0.031054	10q21.3
1560101_at	SYDE2	-1.28284	4.670428	0.035054	1p22.3	225373_at	VSIR	-0.45592	10.55617	0.013919	10q22.1
227128_s_at	TACSTD2	-0.3739	3.668885	0.049686	1p32.1	219903_s_at	CYP2C8	-0.84765	4.583833	0.040239	10q23.33
224457_at	FOXD2-AS1	-0.67316	4.689822	0.043086	1p33	215843_s_at	TLL2	-0.96246	5.867333	0.029668	10q24.1
223622_s_at	HYI	-0.37272	9.783722	0.042867	1p34.2	213601_at	SLIT1	-0.53387	8.227896	0.023188	10q24.1
222842_at	AGO4	-0.96906	5.789844	0.046011	1p34.3	1553909_x_at	SLF2	-0.9279	6.020481	0.044315	10q24.31
235837_at	SNIP1	-0.79266	7.490986	0.010975	1p34.3	204465_s_at	INA	-0.9771	6.05621	0.017033	10q24.33
222961_at	SERINC2	-1.0717	6.091277	0.0277	1p35.2	225582_at	ITPRIP	-0.67798	10.47823	0.008623	10q25.1
209018_s_at	PINK1	-0.27854	9.774418	0.043678	1p36.12	1562831_a_at	WDR11-AS1	-0.758	7.082241	0.042498	10q26.12
219139_s_at	CROCCP3	-1.002	5.089359	0.044421	1p36.13	243143_at	FAM24A	-1.14416	4.562809	0.035852	10q26.13
1566105_at	MFN2	-0.60748	5.343621	0.049223	1p36.22	1570026_at	CPXM2	-0.66629	5.77527	0.008626	10q26.13
214521_at	HES2	-1.05527	4.629448	0.021562	1p36.31	222932_at	EHF	-1.03775	4.916765	0.049599	11p13
1566737_at	LINC01346	-1.13548	4.397672	0.023188	1p36.32	215323_at	LUZP2	-0.84494	5.968951	0.031054	11p14.3
206817_x_at	CELF3	-0.89292	6.255675	0.034802	1q21.3	223935_at	TRPM5	-0.86225	4.143414	0.047059	11p15.5
220090_at	CRNN	-0.71936	5.005958	0.044421	1q21.3	1569452_at	LMNTD2-AS1	-0.549	3.885197	0.039842	11p15.5
206181_at	SLAMF1	-0.90418	10.73033	0.029367	1q23.3	224559_at	MALAT1	-0.93132	10.47109	0.005926	11q13.1
211395_x_at	FCGR2C	-0.70598	11.11121	0.045792	1q23.3	229396_at	OVOL1	-0.56092	8.19031	0.039842	11q13.1
222871_at	KLHDC8A	-0.91078	6.98074	0.045552	1q32.1	43934_at	GPR137	-0.34627	8.440016	0.026112	11q13.1
244097_at	CR2	-1.20619	4.932954	0.045161	1q32.2	1555505_a_at	TYR	-0.9765	6.346714	0.048977	11q14.3
215161_at	CAMK1G	-0.64355	4.478755	0.040239	1q32.2	233923_at	ARHGAP42	-1.21058	4.629889	0.012205	11q22.1
224571_at	IRF2BP2	-0.42799	9.993307	0.045989	1q42.3	1561939_at	DYNC2H1	-1.1764	4.03271	0.038542	11q22.3
1565947_a_at	CHML	-0.73484	3.395284	0.043086	1q43	212524_x_at	H2AX	-0.91362	5.249479	0.037742	11q23.3
230390_at	LOC101928222	-0.77882	4.784462	0.037678	2p24.1	1553484_at	LINC00477	-1.047	5.825418	0.014724	12p12.1

Probeset	Symbol	Log FC	Ex	FDR	Band	Probeset	Symbol	Log FC	Ex	FDR	Band
208092_s_at	FAM49A	-0.73734	9.866836	0.02224	2p24.2	214989_x_at	PLEKHA5	-0.63998	9.703254	0.010609	12p12.3
228459_at	LRATD1	-1.36889	4.313917	0.012205	2p24.3	207101_at	VAMP1	-0.97992	6.055461	0.011712	12p13.31
216188_at	MYCNOS	-1.10359	4.65821	0.035852	2p24.3	216424_at	CD4	-0.74915	3.171508	0.049686	12p13.31
39548_at	NPAS2	-0.80939	6.02062	0.027185	2q11.2	205056_s_at	GPR162	-0.70828	5.366364	0.031702	12p13.31
225606_at	BCL2L11	-0.62645	11.4496	0.017082	2q13	232811_x_at	PRICKLE1	-0.45523	8.25455	0.048624	12q12
219496_at	SOWAHC	-0.61008	8.413864	0.026538	2q13	204255_s_at	VDR	-0.47775	9.267242	0.045552	12q13.11
217028_at	CXCR4	-0.89333	13.85931	0.007905	2q22.1	232732_at	LOC100652999	-0.83042	4.790488	0.032429	12q13.13
209201_x_at	CXCR4	-0.85222	12.84521	0.026195	2q22.1	212803_at	NAB2	-0.72755	6.811013	0.049223	12q13.3
211919_s_at	CXCR4	-0.8069	13.03752	0.012566	2q22.1	216974_at	KITLG	-1.13276	3.9276	0.032274	12q21.32
231376_at	UPP2	-1.21879	4.536855	0.006202	2q24.1	1559975_at	BTG1	-0.58031	10.73114	0.020177	12q21.33
223952_x_at	DHRS9	-1.34213	8.584777	0.010819	2q31.1	200920_s_at	BTG1	-0.4505	14.46959	0.042158	12q21.33
224009_x_at	DHRS9	-0.96362	8.812145	0.040239	2q31.1	243234_at	TBX3	-0.98858	4.137564	0.014378	12q24.21
219799_s_at	DHRS9	-0.92671	9.370176	0.012892	2q31.1	211296_x_at	UBC	-0.29169	17.58341	0.04651	12q24.31
227537_s_at	SP3	-0.84499	6.562578	0.049223	2q31.1	1555264_a_at	LINC00598	-0.93519	5.221572	0.048656	13q14.11
209508_x_at	CFLAR	-0.41172	10.2758	0.047272	2q33.1	212284_x_at	TPT1	-0.2958	17.77029	0.040332	13q14.13
204334_at	KLF7	-0.67198	9.192147	0.030361	2q33.3	212869_x_at	TPT1	-0.28499	17.73929	0.048953	13q14.13
207260_at	FEV	-0.56728	4.877768	0.027567	2q35	214327_x_at	TPT1	-0.28138	17.28813	0.047839	13q14.13
205476_at	CCL20	-0.9417	4.013197	0.006202	2q36.3	1559544_s_at	RB1-DT	-0.80225	6.843483	0.049686	13q14.2
207140_at	ALPI	-0.5734	3.745218	0.022818	2q37.1	1564561_at	LINC01442	-1.13021	4.30159	0.010975	13q21.2
1567378_x_at	DNAH1	-1.35715	4.552755	0.019179	3p21.1	1565602_at	PCDH9	-1.02763	4.829206	0.034802	13q21.32
223961_s_at	CISH	-1.11501	7.186524	0.024601	3p21.2	243928_s_at	ABCC4	-1.01723	5.223758	0.049377	13q32.1
223377_x_at	CISH	-0.95195	8.935442	0.001495	3p21.2	1552842_at	HS6ST3	-0.87161	4.524978	0.043969	13q32.1
221223_x_at	CISH	-0.80522	8.574014	0.004375	3p21.2	205727_at	TEP1	-1.27638	5.360151	0.022538	14q11.2
1553396_a_at	CCDC13	-1.13542	7.581778	0.012361	3p22.1	211667_x_at	TRAV12-2	-0.80958	7.19857	0.029625	14q11.2
231656_x_at	OSBPL10	-0.77715	7.833253	0.037964	3p23	204588_s_at	SLC7A7	-0.52695	10.53184	0.023234	14q11.2
208530_s_at	RARB	-1.02849	5.540531	0.047354	3p24.2	230800_at	ADCY4	-0.64496	5.200867	0.034802	14q12
234697_x_at	TAMM41	-1.03467	6.264576	0.043694	3p25.2	221200_at	ERVK3-2	-0.99147	4.940024	0.04081	14q24.2

Probeset	Symbol	Log FC	Ex	FDR	Band	Probeset	Symbol	Log FC	Ex	FDR	Band
1569362_at	ALCAM	-1.18002	7.645435	0.001495	3q13.11	226210_s_at	MEG3	-1.01724	4.475596	0.016442	14q32.2
201951_at	ALCAM	-0.80384	9.982592	0.023188	3q13.11	230677_at	EXOC3L4	-1.02593	5.096725	0.008626	14q32.32
201952_at	ALCAM	-0.61914	10.97925	0.021562	3q13.11	206673_at	GPR176	-0.99396	6.008399	0.028335	15q14
1563466_at	MYLK	-1.10316	4.911082	0.016988	3q21.1	227846_at	GPR176	-0.5965	8.347884	0.026938	15q14
229162_s_at	ABTB1	-0.96398	5.85767	0.019179	3q21.3	238742_x_at	SPINT1-AS1	-0.80524	7.052122	0.043678	15q15.1
239662_x_at	TMCC1	-0.58748	5.477319	0.043086	3q22.1	238845_at	SLC30A4	-1.1112	4.346268	0.035054	15q21.1
213554_s_at	CDV3	-0.36096	12.92244	0.026195	3q22.1	205398_s_at	SMAD3	-1.09138	7.890007	0.002094	15q22.33
206535_at	SLC2A2	-0.93261	3.102417	0.024233	3q26.2	200763_s_at	RPLP1	-0.27076	17.69144	0.047354	15q23
221097_s_at	KCNMB2	-0.90138	7.663876	0.021496	3q26.32	230345_at	SEMA7A	-0.7782	7.932373	0.047539	15q24.1
225140_at	KLF3	-0.5693	8.851539	0.021562	4p14	1562455_at	LOC101929586	-0.98994	6.290093	0.031054	15q25.1
222913_at	KLF3	-0.45445	8.495967	0.029542	4p14	231187_at	SLC28A1	-0.70558	4.283804	0.049407	15q25.3
235105_at	MED28	-0.60448	4.124477	0.029668	4p15.32	234576_at	ANPEP	-0.87051	4.38908	0.036044	15q26.1
208346_at	PPBPP2	-1.24166	5.185658	0.004682	4q13.3	207383_s_at	RHBDL1	-0.94742	4.280712	0.041521	16p13.3
216021_s_at	GLRA3	-1.4428	5.829024	0.002471	4q34.1	1569396_at	LOC101929280	-0.58995	8.143941	0.013919	16p13.3
242985_x_at	RNF180	-1.1443	4.606406	0.045872	5q12.3	219135_s_at	LMF1	-0.53827	9.84962	0.046011	16p13.3
224422_x_at	PMCHL2	-0.98493	5.433213	0.045772	5q13.2	236549_x_at	SNX20	-0.97244	6.477721	0.037964	16q12.1
206795_at	F2RL2	-0.84613	3.972115	0.03285	5q13.3	216611_s_at	SLC6A2	-0.78942	5.611644	0.044342	16q12.2
217335_at	LINC01949	-0.96462	5.569829	0.031054	5q14.3	228928_x_at	BANP	-0.36485	9.101452	0.041516	16q24.2
207906_at	IL3	-0.99591	4.025789	0.027442	5q31.1	223467_at	RASD1	-0.95266	9.731892	0.045872	17p11.2
202335_s_at	UBE2B	-0.50115	7.928101	0.002094	5q31.1	1559324_at	USP32P2	-0.87607	5.109915	0.033622	17p11.2
228588_s_at	UBE2B	-0.39141	11.13585	0.034307	5q31.1	1557986_s_at	SMCR8	-0.78909	7.022548	0.032518	17p11.2
216918_s_at	DST	-0.88919	5.295475	0.010772	6p12.1	207641_at	TNFRSF13B	-0.58115	9.831968	0.043969	17p11.2
202284_s_at	CDKN1A	-0.71871	11.95142	0.006449	6p21.2	210345_s_at	DNAH9	-0.82939	6.668078	0.028961	17p12
1553906_s_at	FGD2	-0.37448	11.82203	0.046635	6p21.2	201557_at	VAMP2	-0.58354	8.090259	0.046709	17p13.1
214404_x_at	SPDEF	-0.69987	6.197315	0.048394	6p21.31	214792_x_at	VAMP2	-0.40914	8.766473	0.025961	17p13.1
40446_at	PHF1	-0.30793	12.35079	0.015133	6p21.32	221426_s_at	OR3A3	-0.93082	6.605976	0.026979	17p13.2
208812_x_at	HLA-C	-0.29656	16.88033	0.031054	6p21.33	1562256_at	NLRP1	-0.46953	8.38251	0.018439	17p13.2

Probeset	Symbol	Log FC	Ex	FDR	Band	Probeset	Symbol	Log FC	Ex	FDR	Band
221875_x_at	HLA-F	-0.33811	14.58733	0.016988	6p22.1	1566171_at	RFFL	-0.74366	6.603769	0.04312	17q12
217436_x_at	HLA-J	-0.33131	12.91848	0.037678	6p22.1	1563945_at	YWHAEP7	-0.64818	7.661381	0.040239	17q12
204806_x_at	HLA-F	-0.31204	14.13093	0.029125	6p22.1	234880_x_at	KRTAP1-3	-0.51522	3.921669	0.04312	17q21.2
235084_x_at	TRIM38	-0.51206	9.237445	0.030372	6p22.2	211956_s_at	EIF1	-0.31327	16.88647	0.014079	17q21.2
202150_s_at	NEDD9	-0.58798	8.369266	0.033321	6p24.2	235897_at	COPZ2	-0.61947	8.096752	0.001952	17q21.32
213477_x_at	EEF1A1	-0.27683	17.66999	0.04136	6q13	233349_at	TLK2	-1.20322	5.405492	0.019125	17q23.2
242446_at	C6orf163	-1.31909	4.805433	0.020177	6q15	1553314_a_at	KIF19	-0.92579	6.281976	0.016988	17q25.1
210089_s_at	LAMA4	-0.7791	4.360135	0.039842	6q21	221943_x_at	RPL38	-0.30372	12.64906	0.029668	17q25.1
240460_at	LOC101929122	-1.323	4.852246	0.037343	6q25.3	206355_at	GNAL	-1.06285	6.47282	0.027881	18p11.21
1552542_s_at	TAGAP	-0.65031	10.37004	0.019179	6q25.3	217425_at	MC2R	-0.73145	3.463604	0.046026	18p11.21
229723_at	TAGAP	-0.61322	11.15925	0.021143	6q25.3	210917_at	YES1	-0.97504	4.314118	0.045556	18p11.32
227621_at	WTAP	-0.57295	9.488114	0.041067	6q25.3	233686_at	ASXL3	-0.74132	6.899746	0.047799	18q12.1
240033_at	PLG	-0.76637	5.130254	0.029367	6q26	215683_at	RBFADN	-0.91809	6.369028	0.023213	18q23
232722_at	RNASET2	-0.8509	6.578667	0.045872	6q27	206882_at	SLC1A6	-0.74868	4.789089	0.015047	19p13.12
231706_s_at	EVX1	-0.55491	4.243405	0.045529	7p15.2	212952_at	CALR	-0.40037	10.76081	0.015133	19p13.13
237449_at	SP8	-1.43601	4.165541	0.008623	7p21.1	204949_at	ICAM3	-0.33959	14.3706	0.020177	19p13.2
242420_at	PPP1R9A	-0.90582	6.514938	0.038914	7q21.3	1558400_x_at	ANKRD24	-1.16186	4.911764	0.019179	19p13.3
217700_at	CNPY4	-0.90896	6.1631	0.040239	7q22.1	209304_x_at	GADD45B	-1.11097	12.66149	0.010236	19p13.3
219815_at	GAL3ST4	-0.88225	5.670381	0.037964	7q22.1	209305_s_at	GADD45B	-1.09687	12.60766	0.011217	19p13.3
207883_s_at	TFR2	-0.85942	6.796238	0.038914	7q22.1	207574_s_at	GADD45B	-1.02407	13.25152	0.012419	19p13.3
224263_x_at	ZAN	-0.62795	4.288912	0.043086	7q22.1	220674_at	CD22	-1.37051	4.705042	0.009939	19q13.12
223982_s_at	PNPLA8	-0.51726	12.37958	0.047663	7q31.1	215326_at	PAK4	-0.8369	5.972089	0.029673	19q13.2
243171_at	LOC100128325	-1.16205	6.444779	0.004331	7q32.2	204815_s_at	DHX34	-0.53441	4.098768	0.045552	19q13.32
239055_at	LINC-PINT	-1.02871	5.974279	0.023159	7q32.3	217510_at	CRX	-0.83584	4.459911	0.046011	19q13.33
206806_at	DGKI	-1.23256	5.583132	0.014724	7q33	202014_at	PPP1R15A	-0.69381	11.7703	0.029125	19q13.33
228759_at	CREB3L2	-0.55926	11.81668	0.029367	7q33	213350_at	RPS11	-0.409	11.67437	0.008626	19q13.33
231830_x_at	RAB11FIP1	-0.45721	9.108917	0.048977	8p11.23	241957_x_at	LIN7B	-0.4051	8.795419	0.043086	19q13.33

Probeset	Symbol	Log FC	Ex	FDR	Band	Probeset	Symbol	Log FC	Ex	FDR	Band
212096_s_at	MTUS1	-0.57043	9.700005	0.024762	8p22	223897_at	ZNF765	-1.07635	4.673054	0.035997	19q13.42
218839_at	HEY1	-1.07028	7.199715	0.018978	8q21.13	229508_at	U2AF2	-0.89629	4.063371	0.029367	19q13.42
222863_at	ZBTB10	-0.94205	7.140059	0.031684	8q21.13	227613_at	ZNF331	-0.75112	8.806339	0.017504	19q13.42
228562_at	ZBTB10	-0.85843	9.568268	0.031054	8q21.13	232774_x_at	ZIK1	-0.94943	5.431462	0.047799	19q13.43
44783_s_at	HEY1	-0.61673	9.397295	0.024515	8q21.13	206004_at	TGM3	-0.90964	6.275531	0.033321	20p13
203501_at	CPQ	-0.64123	9.945644	0.04137	8q22.1	215707_s_at	PRNP	-0.39972	10.10723	0.048624	20p13
218273_s_at	PDP1	-0.51897	8.243487	0.044315	8q22.1	225091_at	ZCCHC3	-0.31175	9.585956	0.043086	20p13
1560011_at	JRK	-0.99265	5.96065	0.034361	8q24.3	218159_at	DDRGK1	-0.27148	11.20589	0.043969	20p13
1552799_at	TSNARE1	-0.62503	4.290879	0.037343	8q24.3	232209_x_at	HM13	-0.25422	11.04866	0.043086	20q11.21
237036_at	FBXO10	-0.7196	4.906701	0.021562	9p13.2	213171_s_at	MMP24	-0.78657	5.438662	0.042887	20q11.22
1556771_a_at	CNTFR-AS1	-0.86022	7.214332	0.026077	9p13.3	230533_at	ZMYND8	-0.39685	9.103577	0.03208	20q13.12
206549_at	INSL4	-0.90743	6.069774	0.0277	9p24.1	202716_at	PTPN1	-0.5266	10.78281	0.023188	20q13.13
1554708_s_at	SPATA6L	-0.88364	5.71874	0.031054	9p24.2	231801_at	NFATC2	-0.67142	4.626035	0.046085	20q13.2
1569555_at	GDA	-0.93415	5.882096	0.035054	9q21.13	237805_at	LOC729296	-0.8527	3.703496	0.043678	20q13.33
1562761_at	NMRK1	-0.60163	7.27774	0.029146	9q21.13	214750_at	PLAC4	-0.99526	5.883882	0.010975	21q22.2
216997_x_at	TLE4	-0.59153	8.684065	0.016988	9q21.31	203996_s_at	CFAP410	-0.5668	8.018982	0.021562	21q22.3
214688_at	TLE4	-0.51524	7.720505	0.033112	9q21.31	1560977_a_at	BCL2L13	-0.80663	6.728757	0.043086	22q11.21
205908_s_at	OMD	-1.1624	5.40219	0.033321	9q22.31	1563478_at	KIAA1671	-1.02777	4.078286	0.033701	22q11.23
216979_at	NR4A3	-1.05122	5.60095	0.011773	9q31.1	232340_at	MIATNB	-0.63761	7.702403	0.040239	22q12.1
210392_x_at	NR6A1	-0.89217	6.055337	0.0277	9q33.3	226051_at	SELENOM	-0.61606	12.6098	0.029668	22q12.2
1557867_s_at	CFAP157	-0.64722	6.963366	0.035411	9q34.11	230011_at	MEI1	-0.55456	12.13203	0.012892	22q13.2
1554787_at	STKLD1	-0.84289	4.986355	0.027088	9q34.2	1554208_at	MEI1	-0.47625	12.20259	0.014469	22q13.2
236744_at	AJM1	-0.79661	6.086823	0.022058	9q34.3	205050_s_at	MAPK8IP2	-0.6778	6.878192	0.045989	22q13.33
229473_at	MAMDC4	-0.72165	5.958631	0.02444	9q34.3	215884_s_at	UBQLN2	-0.4004	12.23099	0.030361	Xp11.21
219620_x_at	TOR4A	-0.3223	8.689815	0.031054	9q34.3	1555248_a_at	WNK3	-0.69395	7.160031	0.029424	Xp11.22
231035_s_at	OTUD1	-0.72426	11.94934	0.015324	10p12.2	1561352_at	LINC01204	-0.71991	4.425637	0.046026	Xp11.3
1553630_at	CABCOCO1	-1.13774	3.852209	0.007605	10q21.2	1553006_at	ADGRG4	-1.10367	4.337027	0.0277	Xq26.3

Probeset	Symbol	Log FC	Ex	FDR	Band	Probeset	Symbol	Log FC	Ex	FDR	Band
1558000_at	ARID5B	-1.07486	7.301566	0.018854	10q21.2	204454_at	LDOC1	-0.68275	7.481514	0.046497	Xq27.1
212614_at	ARID5B	-0.78301	11.45413	0.031054	10q21.2	215911_x_at	ATP2B3	-1.11361	4.385884	0.048953	Xq28

Table 13-8 Patient treated with melphalan: Probesets with significant DGE at relapse (Pages 231-232).

Probeset	Gene	Log FC	Ave Expr	FDR	Probeset	Gene	Log FC	Ave Expr	FDR
217227_x_at	IGLV1-44	1.77	9.9	0.02	218159_at	DDRGK1	-0.33	11.25	0.05
213222_at	PLCB1	1.46	7.43	0.00	221951_at	TMEM80	-0.4	9.92	0.03
239481_at	FAM133A	1.07	10.73	0.05	213619_at	HNRNPH1	-0.41	13.35	0.03
227211_at	PHF19	0.98	9.24	0.02	209057_x_at	CDC5L	-0.42	10.26	0.02
203474_at	IQGAP2	0.75	10.02	0.05	211956_s_at	EIF1	-0.42	16.88	0.01
225017_at	CCDC14	0.64	9.43	0.01	214116_at	BTD	-0.45	10.32	0.03
211945_s_at	ITGB1	0.63	11.86	0.03	227026_at	MPHOSPH8	-0.45	9.35	0.02
203362_s_at	MAD2L1	0.62	10.65	0.03	210633_x_at	KRT10	-0.48	11.89	0.02
208775_at	XPO1	0.53	11.7	0.04	222279_at	HLA-F-AS1	-0.54	10.65	0.03
203462_x_at	EIF3B	0.52	11.5	0.04	224606_at	KLF6	-0.54	14.28	0.05
211987_at	TOP2B	0.5	11.55	0.03	217608_at	SREK1IP1	-0.54	8.67	0.02
226154_at	DNM1L	0.49	11.36	0.00	227299_at	CCNI	-0.55	9.06	0.02
202567_at	SNRPD3	0.49	11.99	0.05	213350_at	RPS11	-0.57	11.58	0.01
203344_s_at	RBBP8	0.48	10.78	0.01	228588_s_at	UBE2B	-0.62	11.1	0.01
201833_at	HDAC2	0.47	11.54	0.03	229996_s_at	PCGF5	-0.63	8.76	0.01
222398_s_at	EFTUD2	0.46	10.57	0.03	214176_s_at	PBXIP1	-0.66	8.64	0.03
202053_s_at	ALDH3A2	0.42	10.59	0.02	1562836_at	DDX6	-0.67	9.16	0.01
201381_x_at	CACYBP	0.42	12.35	0.05	228638_at	FAM76A	-0.67	8.62	0.02
212287_at	SUZ12	0.41	12.01	0.02	204588_s_at	SLC7A7	-0.73	10.47	0.03
210250_x_at	ADSL	0.4	10.55	0.02	212952_at	CALR	-0.73	10.96	0.00
218190_s_at	UQCR10	0.39	13.37	0.01	204454_at	LDOC1	-0.75	7.78	0.03
201794_s_at	SMG7	0.38	10.26	0.02	221223_x_at	CISH	-0.82	8.47	0.02
203095_at	MTIF2	0.38	11.02	0.03	213694_at	RSBN1	-0.87	7.85	0.03
218159_at	DDRGK1	-0.33	11.25	0.05	229693_at	TMEM220	-0.97	8.92	0.04
221951_at	TMEM80	-0.4	9.92	0.03	224559_at	MALAT1	-1.02	10.65	0.04
213619_at	HNRNPH1	-0.41	13.35	0.03	203501_at	CPQ	-1.02	9.9	0.05

Probeset	Gene	Log FC	Ave Expr	FDR	Probeset	Gene	Log FC	Ave Expr	FDR
209057_x_at	CDC5L	-0.42	10.26	0.02	223377_x_at	CISH	-1.13	8.63	0.00
211956_s_at	EIF1	-0.42	16.88	0.01	233983_at	TGM6	-1.15	6.66	0.01
214116_at	BTD	-0.45	10.32	0.03	221097_s_at	KCNMB2	-1.24	7.84	0.01
227026_at	MPHOSPH8	-0.45	9.35	0.02	215843_s_at	TLL2	-1.26	6.04	0.03
210633_x_at	KRT10	-0.48	11.89	0.02	211276_at	TCEAL2	-1.57	5.95	0.03

Table 13-9 Gain/amp(1q) vs diploid copy number DGE at presentation: Probesets with significant log fold increase (Pages 233-235)

Probeset	Gene	LFC	Ave Expr	adj. P Val	Ch band	Probeset	Gene	LFC	Ave Expr	adj. P Val	Ch band
34210_at	CD52	2.04	10.38	0.043	1p36.11	225317_at	ACBD6	0.75	10.51	0.02	1q25.2
212742_at	RNF115	0.5	10.65	0.032	1q21.1	230257_s_at	TSEN15	0.91	10.73	0.007	1q25.3
209382_at	POLR3C	0.64	9.45	0.043	1q21.1	1555797_a_at	ARPC5	0.96	10.35	0.007	1q25.3
212539_at	CHD1L	0.68	9.76	0.041	1q21.1	211963_s_at	ARPC5	1.01	11.4	0.025	1q25.3
210573_s_at	POLR3C	0.72	8.98	0.028	1q21.1	225399_at	TSEN15	1.27	10.89	0.004	1q25.3
218389_s_at	APH1A	0.61	11.76	0.041	1q21.2	1552618_at	STX6	1.41	6.86	0.008	1q25.3
221505_at	*ANP32E*	0.86	12.02	0.032	1q21.2	225400_at	TSEN15	1.9	8.5	0.007	1q25.3
208103_s_at	*ANP32E*	0.97	10.68	0.004	1q21.2	220083_x_at	UCHL5	0.85	9.03	0.041	1q31.2
202244_at	PSMB4	0.6	14.11	0.025	1q21.3	219933_at	GLRX2	0.89	10.22	0.02	1q31.2
209609_s_at	MRPL9	0.62	12.33	0.014	1q21.3	212530_at	NEK7	0.91	11.25	0.022	1q31.3
229253_at	THEM4	0.67	10.01	0.041	1q21.3	1558508_a_at	C1orf53	1	9.68	0.026	1q31.3
202243_s_at	PSMB4	0.69	13.54	0.013	1q21.3	203316_s_at	SNRPE	0.7	13.97	0.028	1q32.1
222976_s_at	TPM3	0.7	13.78	0.042	1q21.3	215171_s_at	TIMM17A	0.8	12.37	0.019	1q32.1
212541_at	FLAD1	0.71	9.54	0.02	1q21.3	208270_s_at	RNPEP	0.82	9.92	0.008	1q32.1
222537_s_at	CDC42SE1	0.72	9.92	0.013	1q21.3	225068_at	KLHL12	0.83	9.89	0.007	1q32.1
222212_s_at	CERS2	0.75	11.82	0.035	1q21.3	201821_s_at	TIMM17A	0.85	11.75	0.022	1q32.1
210460_s_at	PSMD4	0.82	11.7	0.022	1q21.3	204478_s_at	RABIF	0.9	9.47	0.003	1q32.1
226455_at	CREB3L4	0.91	8.5	0.043	1q21.3	212135_s_at	ATP2B4	1.27	7.99	0.049	1q32.1
200882_s_at	PSMD4	0.92	12.09	0.004	1q21.3	1555950_a_at	CD55	1.09	12.44	0.014	1q32.2
211609_x_at	PSMD4	0.95	11.93	0.006	1q21.3	201926_s_at	CD55	1.11	12.04	0.013	1q32.2
223066_at	SNAPIN	0.98	10.35	0.032	1q21.3	218407_x_at	NENF	0.9	11.98	0.009	1q32.3
201897_s_at	*CKS1B*	1.07	10.68	0.007	1q21.3	228867_at	TATDN3	1.04	9.36	0.008	1q32.3
205945_at	*IL6R*	1.5	10.44	0.049	1q21.3	235126_at	FLVCR1-DT	1.11	8.58	0.007	1q32.3
217728_at	S100A6	1.65	12.88	0.007	1q21.3	226801_s_at	AIDA	0.82	13.06	0.031	1q41
203186_s_at	S100A4	1.88	12.05	0.016	1q21.3	226128_at	BROX	0.84	10.84	0.008	1q41
210386_s_at	MTX1	0.61	10.91	0.041	1q22	217900_at	IARS2	0.92	11.39	0.025	1q41

Probeset	Gene	LFC	Ave Expr	adj. P Val	Ch band	Probeset	Gene	LFC	Ave Expr	adj. P Val	Ch band
201771_at	SCAMP3	0.69	11.08	0.031	1q22	223993_s_at	CNIH4	0.78	12.23	0.038	1q42.11
208822_s_at	DAP3	0.83	12.43	0.007	1q22	225719_s_at	MRPL55	0.64	10.85	0.035	1q42.13
201275_at	FDPS	0.83	11.53	0.007	1q22	200075_s_at	GUK1	0.65	12.34	0.016	1q42.13
218291_at	LAMTOR2	0.84	11.25	0.007	1q22	201956_s_at	GNPAT	0.75	11.19	0.016	1q42.2
200910_at	CCT3	0.85	12.37	0.019	1q22	203073_at	COG2	0.77	10.1	0.009	1q42.2
219373_at	DPM3	0.98	11.74	0.046	1q22	219481_at	TTC13	0.78	10.06	0.025	1q42.2
225401_at	GLMP	1.09	10.25	0.019	1q22	223272_s_at	NTPCR	1.41	8.62	0.031	1q42.2
203550_s_at	FAM189B	1.1	8.58	0.041	1q22	214170_x_at	FH	0.98	11.08	0.009	1q43
1558693_s_at	GLMP	1.12	9.7	0.009	1q22	203033_x_at	FH	1	10.8	0.016	1q43
224233_s_at	MSTO1	1.17	8.65	0.007	1q22	219032_x_at	OPN3	1.21	9.79	0.009	1q43
218678_at	NES	2.59	7.16	0.007	1q23.1	226350_at	CHML	1.33	9.82	0.028	1q43
217797_at	UFC1	0.67	13.93	0.039	1q23.3	224392_s_at	OPN3	1.37	8.16	0.028	1q43
201966_at	NDUFS2	0.77	11.07	0.041	1q23.3	224824_at	COX20	0.59	11.12	0.043	1q44
216591_s_at	SDHC	0.83	10.47	0.045	1q23.3	218605_at	TFB2M	0.79	11.03	0.035	1q44
224691_at	UHMK1	0.85	11.95	0.036	1q23.3	212371_at	DESI2	0.85	11.03	0.043	1q44
210131_x_at	SDHC	0.91	11.18	0.032	1q23.3	202703_at	DUSP11	0.64	10.57	0.035	2p13.1
215088_s_at	SDHC	0.96	11.04	0.007	1q23.3	211025_x_at	COX5B	0.66	12.67	0.045	2q11.2
201612_at	ALDH9A1	0.81	11.96	0.009	1q24.1	220133_at	ODAM	1.72	5.23	0.009	4q13.3
1553677_a_at	TIPRL	0.68	9.42	0.02	1q24.2	225723_at	CCDC167	1.22	10.43	0.016	6p21.2
227669_at	MPC2	0.72	9.75	0.018	1q24.2	222392_x_at	PERP	1.7	12.38	0.005	6q23.3
1554351_a_at	TIPRL	0.79	10.56	0.02	1q24.2	217744_s_at	PERP	1.76	11.68	0.035	6q23.3
202846_s_at	PIGC	0.83	10.34	0.025	1q24.3	221909_at	RNFT2	1.94	5.51	0.035	12q24.22
201381_x_at	CACYBP	0.92	12.1	0.007	1q25.1	210321_at	GZMH	2.18	6.33	0.02	14q12
210691_s_at	CACYBP	0.98	11.44	0.01	1q25.1	213062_at	NTAN1	0.97	10.65	0.025	16p13.11
242458_at	RALGPS2	1.17	8.66	0.004	1q25.2	213061_s_at	NTAN1	1.19	10.83	0.01	16p13.11
227533_at	RALGPS2	1.36	10.58	0.009	1q25.2	209731_at	NTHL1	1.34	8.65	0.007	16p13.3
232112_at	RALGPS2	1.37	8.18	0.028	1q25.2	227949_at	PHACTR3	2.83	7.18	0.009	20q13.32

Probeset	Gene	LFC	Ave Expr	adj. P Val	Ch band	Probeset	Gene	LFC	Ave Expr	adj. P Val	Ch band
227224_at	RALGPS2	1.38	11.29	0.006	1q25.2	211198_s_at	ICOSLG	1.26	5.34	0.043	21q22.3
240310_at	TOR1AIP1	1.54	6.78	0.016	1q25.2	211471_s_at	RAB36	1.06	8.6	0.028	22q11.23
225317_at	ACBD6	0.75	10.51	0.02	1q25.2	205164_at	GCAT	1.86	6.54	0.044	22q13.1

Table 13-10 Gain/amp(1q) vs diploid copy number DGE at presentation: Probesets with significant log fold decrease.

Probeset	Gene	LFC	Ave Expr	adj. P Val	Ch band	Probeset	Gene	LFC	Ave Expr	adj. P Val	Ch band
204032_at	BCAR3	-1.34	8.85	0.032	1p22.1	208711_s_at	CCND1	-3	9.19	0.028	11q13.3
214453_s_at	IFI44	-1.81	8.24	0.042	1p31.1	240890_at	CASP17P	-1.85	9.38	0.035	11q22.3
209354_at	TNFRSF14	-0.82	10.94	0.038	1p36.32	218826_at	SLC35F2	-1.1	11.13	0.026	11q22.3
226702_at	CMPK2	-2.24	9.45	0.043	2p25.2	212079_s_at	KMT2A	-0.97	9.64	0.049	11q23.3
219734_at	SIDT1	-1.15	9.89	0.019	3q13.2	212067_s_at	C1R	-1.29	9.7	0.041	12p13.31
1554343_a_at	STAP1	-2.35	9.78	0.007	4q13.2	227609_at	EPSTI1	-1.24	9.22	0.031	13q14.11
220059_at	STAP1	-2.26	11.01	0.007	4q13.2	227228_s_at	CCDC88C	-0.97	10.2	0.044	14q32.11
218751_s_at	FBXW7	-1	11.38	0.016	4q31.3	217838_s_at	EVL	-1.25	8.78	0.007	14q32.2
229419_at	FBXW7	-1	12.23	0.008	4q31.3	228617_at	XAF1	-1.78	9.97	0.024	17p13.1
222729_at	FBXW7	-0.9	11.11	0.004	4q31.3	206133_at	XAF1	-1.53	10.16	0.015	17p13.1
201694_s_at	EGR1	-1.57	12.53	0.022	5q31.2	1557644_at	RUNDC3A-AS1	-1.98	4.98	0.035	17q21.31
205207_at	IL6	-1.82	7.64	0.032	7p15.3	201641_at	BST2	-0.93	12.1	0.009	19p13.11
202962_at	KIF13B	-0.64	9.16	0.04	8p12	216262_s_at	TGIF2	-0.88	8.69	0.035	20q11.23
224791_at	ASAP1	-0.95	10.25	0.032	8q24.21	204994_at	MX2	-1.66	9.09	0.019	21q22.3
224796_at	ASAP1	-0.66	9.8	0.013	8q24.21	221087_s_at	APOL3	-1.86	8.18	0.022	22q12.3
202145_at	LY6E	-1.63	8.52	0.043	8q24.3	209546_s_at	APOL1	-1.22	9.46	0.039	22q12.3
234411_x_at	CD44	-2.01	4.88	0.004	11p13	229686_at	P2RY8	-0.96	11.15	0.032	Xp22.33
208712_at	CCND1	-3.33	8.67	0.011	11q13.3						

References

1. Moreau, P., et al., *Multiple myeloma: ESMO Clinical Practice Guidelines for diagnosis, treatment and follow-up.* Ann Oncol, 2017. **28**(suppl_4): p. iv52-iv61.
2. UK, C.R. *Cancer-statistics*. Available from: https://www.cancerresearchuk.org/health-professional/cancer-statistics/statistics-by-cancer-type/myeloma#heading-Two, Accessed November 2018.
3. Rajkumar, S.V., *Updated Diagnostic Criteria and Staging System for Multiple Myeloma.* Am Soc Clin Oncol Educ Book, 2016. **35**: p. e418-23.
4. Kyle, R.A., et al., *Long-Term Follow-up of Monoclonal Gammopathy of Undetermined Significance.* N Engl J Med, 2018. **378**(3): p. 241-249.
5. Rajkumar, S.V., et al., *International Myeloma Working Group updated criteria for the diagnosis of multiple myeloma.* Lancet Oncol, 2014. **15**(12): p. e538-48.
6. *Multiple myeloma: 2018 update on diagnosis, risk-stratification, and management.* Am J Hematol, 2018. **93**(8): p. 981-1114.
7. Pawlyn, C. and G.J. Morgan, *Evolutionary biology of high-risk multiple myeloma.* Nat Rev Cancer, 2017. **17**(9): p. 543-556.
8. Morgan, G.J., B.A. Walker, and F.E. Davies, *The genetic architecture of multiple myeloma.* Nat Rev Cancer, 2012. **12**(5): p. 335-48.
9. González, D., et al., *Immunoglobulin gene rearrangements and the pathogenesis of multiple myeloma.* Blood, 2007. **110**(9): p. 3112-21.
10. Fonseca, R., et al., *Genetics and cytogenetics of multiple myeloma: a workshop report.* Cancer Res, 2004. **64**(4): p. 1546-58.
11. Manier, S., et al., *Genomic complexity of multiple myeloma and its clinical implications.* Nat Rev Clin Oncol, 2017. **14**(2): p. 100-113.
12. Shah, V., et al., *Prediction of outcome in newly diagnosed myeloma: a meta-analysis of the molecular profiles of 1905 trial patients.* Leukemia, 2018. **32**(1): p. 102-110.
13. Bergsagel, P.L., et al., *Cyclin D dysregulation: an early and unifying pathogenic event in multiple myeloma.* Blood, 2005. **106**(1): p. 296-303.
14. Jones, J.R., et al., *Clonal evolution in myeloma: the impact of maintenance lenalidomide and depth of response on the genetics and sub-clonal structure of relapsed disease in uniformly treated newly diagnosed patients.* Haematologica, 2019. **104**(7): p. 1440-1450.
15. Weinhold, N., et al., *Clonal selection and double-hit events involving tumor suppressor genes underlie relapse in myeloma.* Blood, 2016. **128**(13): p. 1735-44.
16. Munshi, N.C., et al., *Consensus recommendations for risk stratification in multiple myeloma: report of the International Myeloma Workshop Consensus Panel 2.* Blood, 2011. **117**(18): p. 4696-700.

17. Boyd, K.D., et al., *A novel prognostic model in myeloma based on co-segregating adverse FISH lesions and the ISS: analysis of patients treated in the MRC Myeloma IX trial.* Leukemia, 2012. **26**(2): p. 349-55.
18. Szalat, R., H. Avet-Loiseau, and N.C. Munshi, *Gene Expression Profiles in Myeloma: Ready for the Real World?* Clin Cancer Res, 2016. **22**(22): p. 5434-5442.
19. Kuiper, R., et al., *A gene expression signature for high-risk multiple myeloma.* Leukemia, 2012. **26**(11): p. 2406-13.
20. Shaughnessy, J.D., et al., *A validated gene expression model of high-risk multiple myeloma is defined by deregulated expression of genes mapping to chromosome 1.* Blood, 2007. **109**(6): p. 2276-84.
21. Shaughnessy, J.D., et al., *Pharmacogenomics of bortezomib test-dosing identifies hyperexpression of proteasome genes, especially PSMD4, as novel high-risk feature in myeloma treated with Total Therapy 3.* Blood, 2011. **118**(13): p. 3512-24.
22. Decaux, O., et al., *Prediction of survival in multiple myeloma based on gene expression profiles reveals cell cycle and chromosomal instability signatures in high-risk patients and hyperdiploid signatures in low-risk patients: a study of the Intergroupe Francophone du Myélome.* J Clin Oncol, 2008. **26**(29): p. 4798-805.
23. Dickens, N.J., et al., *Homozygous deletion mapping in myeloma samples identifies genes and an expression signature relevant to pathogenesis and outcome.* Clin Cancer Res, 2010. **16**(6): p. 1856-64.
24. Greipp, P.R., et al., *International staging system for multiple myeloma.* J Clin Oncol, 2005. **23**(15): p. 3412-20.
25. Rajkumar, S.V., et al., *Proteasome inhibition as a novel therapeutic target in human cancer.* J Clin Oncol, 2005. **23**(3): p. 630-9.
26. Fink, E.C. and B.L. Ebert, *The novel mechanism of lenalidomide activity.* Blood, 2015. **126**(21): p. 2366-9.
27. Jackson, G.H., et al., *Lenalidomide maintenance versus observation for patients with newly diagnosed multiple myeloma (Myeloma XI): a multicentre, open-label, randomised, phase 3 trial.* Lancet Oncol, 2019. **20**(1): p. 57-73.
28. Keats, J.J., et al., *Clonal competition with alternating dominance in multiple myeloma.* Blood, 2012. **120**(5): p. 1067-76.
29. Magrangeas, F., et al., *Minor clone provides a reservoir for relapse in multiple myeloma.* Leukemia, 2013. **27**(2): p. 473-81.
30. Bolli, N., et al., *Heterogeneity of genomic evolution and mutational profiles in multiple myeloma.* Nat Commun, 2014. **5**: p. 2997.
31. Kortüm, K.M., et al., *Longitudinal analysis of 25 sequential sample-pairs using a custom multiple myeloma mutation sequencing panel (M(3)P).* Ann Hematol, 2015. **94**(7): p. 1205-11.
32. Corre, J., et al., *Multiple myeloma clonal evolution in homogeneously treated patients.* Leukemia, 2018.
33. Durie, B.G., et al., *International uniform response criteria for multiple myeloma.* Leukemia, 2006. **20**(9): p. 1467-73.
34. Kaiser, M.F., et al., *A TC classification-based predictor for multiple myeloma using multiplexed real-time quantitative PCR.* Leukemia, 2013. **27**(8): p. 1754-7.

35. Benard-Slagter, A., et al., *Digital Multiplex Ligation-Dependent Probe Amplification for Detection of Key Copy Number Alterations in T- and B-Cell Lymphoblastic Leukemia.* J Mol Diagn, 2017. **19**(5): p. 659-672.
36. Kosztolányi, S., et al., *High-Throughput Copy Number Profiling by Digital Multiplex Ligation-Dependent Probe Amplification in Multiple Myeloma.* J Mol Diagn, 2018. **20**(6): p. 777-788.
37. Boyle, E.M., et al., *A molecular diagnostic approach able to detect the recurrent genetic prognostic factors typical of presenting myeloma.* Genes Chromosomes Cancer, 2015. **54**(2): p. 91-8.
38. Subramanian, A., et al., *Gene set enrichment analysis: a knowledge-based approach for interpreting genome-wide expression profiles.* Proc Natl Acad Sci U S A, 2005. **102**(43): p. 15545-50.
39. Xu, Z., et al., *Immunoglobulin class-switch DNA recombination: induction, targeting and beyond.* Nat Rev Immunol, 2012. **12**(7): p. 517-31.
40. Shah, V., et al., *Subclonal.* Blood, 2018. **132**(23): p. 2465-2469.
41. Walker, B.A., et al., *A high-risk, Double-Hit, group of newly diagnosed myeloma identified by genomic analysis.* Leukemia, 2019. **33**(1): p. 159-170.
42. Sawyer, J.R., et al., *An acquired high-risk chromosome instability phenotype in multiple myeloma: Jumping 1q Syndrome.* Blood Cancer J, 2019. **9**(8): p. 62.
43. Maclachlan, K.H., et al., *Copy number signatures predict chromothripsis and clinical outcomes in newly diagnosed multiple myeloma.* Nat Commun, 2021. **12**(1): p. 5172.
44. Schmidt, T.M., R. Fonseca, and S.Z. Usmani, *Chromosome 1q21 abnormalities in multiple myeloma.* Blood Cancer J, 2021. **11**(4): p. 83.
45. Wuillème-Toumi, S., et al., *Mcl-1 is overexpressed in multiple myeloma and associated with relapse and shorter survival.* Leukemia, 2005. **19**(7): p. 1248-52.
46. Gupta, V.A., et al., *Bone marrow microenvironment-derived signals induce Mcl-1 dependence in multiple myeloma.* Blood, 2017. **129**(14): p. 1969-1979.
47. Burroughs Garcìa, J., et al., *Role of 1q21 in Multiple Myeloma: From Pathogenesis to Possible Therapeutic Targets.* Cells, 2021. **10**(6).
48. Shi, L., et al., *Over-expression of CKS1B activates both MEK/ERK and JAK/STAT3 signaling pathways and promotes myeloma cell drug-resistance.* Oncotarget, 2010. **1**(1): p. 22-33.
49. Shaughnessy, J., *Amplification and overexpression of CKS1B at chromosome band 1q21 is associated with reduced levels of p27Kip1 and an aggressive clinical course in multiple myeloma.* Hematology, 2005. **10 Suppl 1**: p. 117-26.
50. van Andel, H., et al., *Aberrant Wnt signaling in multiple myeloma: molecular mechanisms and targeting options.* Leukemia, 2019. **33**(5): p. 1063-1075.
51. Walker, B.A., et al., *A compendium of myeloma-associated chromosomal copy number abnormalities and their prognostic value.* Blood, 2010. **116**(15): p. e56-65.

52. Ghermezi, M., T.M. Spektor, and J.R. Berenson, *The role of JAK inhibitors in multiple myeloma.* Clin Adv Hematol Oncol, 2019. **17**(9): p. 500-505.
53. Chavan, S.S., et al., *Bi-allelic inactivation is more prevalent at relapse in multiple myeloma, identifying RB1 as an independent prognostic marker.* Blood Cancer J, 2017. **7**(2): p. e535.
54. Boyle, E.M., et al., *and.* Clin Cancer Res, 2020. **26**(10): p. 2422-2432.
55. Chesi, M., et al., *Monosomic loss of MIR15A/MIR16-1 is a driver of multiple myeloma proliferation and disease progression.* Blood Cancer Discov, 2020. **1**(1): p. 68-81.
56. Rassenti, L.Z., et al., *dysregulation to identify therapeutic target combinations for chronic lymphocytic leukemia.* Proc Natl Acad Sci U S A, 2017. **114**(40): p. 10731-10736.
57. Kumar, S., et al., *Efficacy of venetoclax as targeted therapy for relapsed/refractory t(11;14) multiple myeloma.* Blood, 2017. **130**(22): p. 2401-2409.
58. Ahn, I.E., X. Tian, and A. Wiestner, *Ibrutinib for Chronic Lymphocytic Leukemia with.* N Engl J Med, 2020. **383**(5): p. 498-500.
59. Walker, B.A., et al., *Mutational Spectrum, Copy Number Changes, and Outcome: Results of a Sequencing Study of Patients With Newly Diagnosed Myeloma.* J Clin Oncol, 2015. **33**(33): p. 3911-20.
60. Jovanović, K.K., et al., *Targeting MYC in multiple myeloma.* Leukemia, 2018. **32**(6): p. 1295-1306.
61. Pawlyn, C., et al., *Coexistent hyperdiploidy does not abrogate poor prognosis in myeloma with adverse cytogenetics and may precede IGH translocations.* Blood, 2015. **125**(5): p. 831-40.
62. Aktas Samur, A., et al., *Deciphering the chronology of copy number alterations in Multiple Myeloma.* Blood Cancer J, 2019. **9**(4): p. 39.
63. Misund, K., et al., *MYC dysregulation in the progression of multiple myeloma.* Leukemia, 2020. **34**(1): p. 322-326.
64. Rustad, E.H., et al., *Timing the initiation of multiple myeloma.* Nat Commun, 2020. **11**(1): p. 1917.
65. Chesi, M., et al., *AID-dependent activation of a MYC transgene induces multiple myeloma in a conditional mouse model of post-germinal center malignancies.* Cancer Cell, 2008. **13**(2): p. 167-80.
66. Maes, A., et al., *The therapeutic potential of cell cycle targeting in multiple myeloma.* Oncotarget, 2017. **8**(52): p. 90501-90520.
67. Richter, A., et al., *Cyclin-Dependent Kinase Inhibitors in Hematological Malignancies-Current Understanding, (Pre-)Clinical Application and Promising Approaches.* Cancers (Basel), 2021. **13**(10).
68. Ghelli Luserna di Rora', A., I. Iacobucci, and G. Martinelli, *The cell cycle checkpoint inhibitors in the treatment of leukemias.* J Hematol Oncol, 2017. **10**(1): p. 77.
69. Botrugno, O.A., et al., *ATR addiction in multiple myeloma: synthetic lethal approaches exploiting established therapies.* Haematologica, 2020. **105**(10): p. 2440-2447.
70. Ocio, E.M., et al., *Filanesib in combination with pomalidomide and dexamethasone in refractory MM patients: safety and efficacy, and association with alpha 1-acid glycoprotein (AAG) levels. Phase Ib/II*

Pomdefil clinical trial conducted by the Spanish MM group. Br J Haematol, 2021. **192**(3): p. 522-530.
71. Feng, Y., et al., *The Role of mTOR Inhibitors in Hematologic Disease: From Bench to Bedside.* Front Oncol, 2020. **10**: p. 611690.
72. Günther, A., et al., *Activity of everolimus (RAD001) in relapsed and/or refractory multiple myeloma: a phase I study.* Haematologica, 2015. **100**(4): p. 541-7.
73. Quan, L., et al., *Prognostic role of minichromosome maintenance family in multiple myeloma.* Cancer Gene Ther, 2020. **27**(10-11): p. 819-829.
74. Grosicki, S., et al., *Once-per-week selinexor, bortezomib, and dexamethasone versus twice-per-week bortezomib and dexamethasone in patients with multiple myeloma (BOSTON): a randomised, open-label, phase 3 trial.* Lancet, 2020. **396**(10262): p. 1563-1573.
75. Bhutani, M., et al., *Investigation of a gene signature to predict response to immunomodulatory derivatives for patients with multiple myeloma: an exploratory, retrospective study using microarray datasets from prospective clinical trials.* Lancet Haematol, 2017. **4**(9): p. e443-e451.
76. Chari, A., et al., *Oral Selinexor-Dexamethasone for Triple-Class Refractory Multiple Myeloma.* N Engl J Med, 2019. **381**(8): p. 727-738.
77. Reale, A., et al., *TOP2A expression predicts responsiveness to carfilzomib in myeloma and informs novel combinatorial strategies for enhanced proteasome inhibitor cell killing.* Leuk Lymphoma, 2021. **62**(2): p. 337-347.
78. Holthof, L.C., et al., *Preclinical evidence for an effective therapeutic activity of FL118, a novel survivin inhibitor, in patients with relapsed/refractory multiple myeloma.* Haematologica, 2020. **105**(2): p. e80-e83.
79. Abdi, J., et al., *Ectopic expression of BIRC5-targeting miR-101-3p overcomes bone marrow stroma-mediated drug resistance in multiple myeloma cells.* BMC Cancer, 2019. **19**(1): p. 975.
80. Barwick, B.G., et al., *Multiple myeloma immunoglobulin lambda translocations portend poor prognosis.* Nat Commun, 2019. **10**(1): p. 1911.
81. Miller, K.M., et al., *Human HDAC1 and HDAC2 function in the DNA-damage response to promote DNA nonhomologous end-joining.* Nat Struct Mol Biol, 2010. **17**(9): p. 1144-51.
82. Yu, T., et al., *Polycomb-like Protein 3 Induces Proliferation and Drug Resistance in Multiple Myeloma and Is Regulated by miRNA-15a.* Mol Cancer Res, 2020. **18**(7): p. 1063-1073.
83. Mason, M.J., et al., *Multiple Myeloma DREAM Challenge reveals epigenetic regulator PHF19 as marker of aggressive disease.* Leukemia, 2020. **34**(7): p. 1866-1874.
84. Mei, A.H., et al., *MAGE-A inhibit apoptosis and promote proliferation in multiple myeloma through regulation of BIM and p21.* Oncotarget, 2020. **11**(7): p. 727-739.
85. Boyle, E.M., et al., *High-risk transcriptional profiles in multiple myeloma are an acquired feature that can occur in any subtype and more frequently with each subsequent relapse.* Br J Haematol, 2021. **195**(2): p. 283-286.

86. Jia, H., et al., *FABP5, a Novel Immune-Related mRNA Prognostic Marker and a Target of Immunotherapy for Multiple Myeloma.* Front Med (Lausanne), 2021. **8**: p. 667525.
87. Miettinen, J.J., et al., *Aminopeptidase Expression in Multiple Myeloma Associates with Disease Progression and Sensitivity to Melflufen.* Cancers (Basel), 2021. **13**(7).
88. Byrgazov, K., et al., *Novel Peptide-drug Conjugate Melflufen Efficiently Eradicates Bortezomib-resistant Multiple Myeloma Cells Including Tumor-initiating Myeloma Progenitor Cells.* Hemasphere, 2021. **5**(7): p. e602.
89. Song, Y., et al., *Preclinical Validation of Ubiquitin Receptor PSMD4 As Therapeutic Target in Multiple Myeloma.* Blood, 2019. **134**(Supplement_1): p. 4403-4403.
90. Xu, X., et al., *Cell adhesion induces overexpression of chromodomain helicase/ATPase DNA binding protein 1-like gene (CHD1L) and contributes to cell adhesion-mediated drug resistance (CAM-DR) in multiple myeloma cells.* Leuk Res, 2016. **47**: p. 54-62.
91. Bisht, K., et al., *Chromosomal 1q21 abnormalities in multiple myeloma: a review of translational, clinical research, and therapeutic strategies.* Expert Rev Hematol, 2021: p. 1-16.
92. Dimopoulos, M.A., et al., *Elotuzumab plus Pomalidomide and Dexamethasone for Multiple Myeloma.* N Engl J Med, 2018. **379**(19): p. 1811-1822.
93. Giri, S., et al., *Evaluation of Daratumumab for the Treatment of Multiple Myeloma in Patients With High-risk Cytogenetic Factors: A Systematic Review and Meta-analysis.* JAMA Oncol, 2020. **6**(11): p. 1759-1765.
94. Mohan, M., et al., *Daratumumab in high-risk relapsed/refractory multiple myeloma patients: adverse effect of chromosome 1q21 gain/amplification and GEP70 status on outcome.* Br J Haematol, 2020. **189**(1): p. 67-71.
95. Harrison, S.J., et al., *Subgroup analysis of ICARIA-MM study in relapsed/refractory multiple myeloma patients with high-risk cytogenetics.* Br J Haematol, 2021. **194**(1): p. 120-131.